The thermo-structural charaterisation of a main chain liquid crysal polymer

Gail Mclean

The Thermo-Structural Characterisation of a Main Chain Liquid Crystal Polymer

by

Gail McLean
B.Sc. (Hons) Applied Chemistry
University of Strathclyde 1988

Submitted for the degree of PhD
University of Durham, Department of Chemistry 1992

To Margaret: my sister

and my best mate

Table of Contents

Declaration

Abstract

Acknowledgements

Page No.

Chapter 1 : Introduction

1.1	*Historical introduction*	*1*
1.2	*Properties and applications of liquid crystal polymers*	*6*
1.3	*Experimental methods used in the thermo-structural characterisation of LCP*	*9*
1.3.1	*Introduction*	*9*
1.3.2	*Techniques applied*	*10*
a)	*Differential scanning calorimetry*	*10*
b)	*Polarising optical microscopy*	*11*
c)	*Wide angle x-ray scattering*	*12*
d)	*Small angle neutron scattering*	*13*
1.4	*Main-chain liquid crystal polymer studied*	*14*
1.5	*A synopsis of the aims of the present study*	*15*
1.6	*References*	*16*

Chapter 2 : Synthesis of Ordered LCP

2.1	*Introduction*	*19*
2.2	*Synthetic routes to main chain liquid crystalline polyesters and block copolymers*	*24*
2.3	*Synthetic routes to ordered LCP*	*27*
2.3.1	*Regioregular polymer: route 1*	*27*
2.3.2	*Sequentially ordered polymer: route 2*	*29*

		Page No.
2.4	*Experimental*	33
2.4.1	*Characterisation techniques*	33
2.4.2	*Preparation of regioregular polymer via route 1*	33
2.4.2.1	*Reagents*	33
a)	*Synthesis and purification of bis(4-formylphenyl) isophthalate (iii)*	34
2.4.2.2	*Reagents*	34
a)	*Preparation of tetrabutylammonium permanganate*	34
2.4.2.3	*Reagents*	35
a)	*Attempts to synthesise bis(4-carboxyphenyl)isophthalate (v)*	35
2.4.2.4	*Reagents*	36
a)	*Synthesis of bis(4-chloroformylphenyl)isophthalate (vi)*	37
2.4.2.5	*Reagents*	37
a)	*Synthesis of monocarbobenzoxy-hydroquinone (vii)*	37
2.4.2.6	*Reagents*	38
a)	*Attempts to synthesise bis[4-[[4-(benzoxyoxycarbonyl)oxy]-phenoxyl-carbonyl]phenyl-isobenzoxyoxycarbonyl)oxy]phenoxy]-carbonyl]phenyl]isophthalate(viii)*	38
2.4.3	*Preparation of sequentially ordered polymer via route 2*	42
2.4.3.1	*Reagents*	42
a)	*Synthesis of p-carbethoxybenzoic acid (xiii)*	43
2.4.3.2	*Reagents*	43
a)	*Attempts to synthesise 4-hydroxyphenyl-4-carbethoxybenzoate (xv)*	43
2.5	*Conclusions*	47
2.6	*References*	48

Chapter 3 :Thermal Analysis

		Page No.
3.1	*Introduction*	*50*
3.2	*Section I: optical microscopy*	*52*
3.2.1	*Introduction and applications to liquid crystal polymers*	*52*
3.2.2	*Practical considerations*	*56*
3.3	*Experimental*	*57*
3.3.1	*Instrumentation*	*57*
3.3.2	*Sample preparation*	*57*
3.4	*Results and discussion*	*59*
3.4.1	*Thermal behaviour of LCP powder*	*59*
3.4.2	*Effects of reheating LCP powder*	*59*
3.4.3	*Thermal behaviour of LCP films*	*60*
3.4.4	*Thermal behaviour of a thick LCP film*	*60*
3.4.5	*Dependence of the initial form of LCP on mesogenic texture*	*61*
3.4.6	*Thermal behaviour of LCP fibres*	*62*
3.5	*Section II: differential scanning calorimetry*	*63*
3.5.1	*Introduction*	*63*
3.5.2	*Instrumentation*	*64*
3.5.3	*Applications to liquid crystal polymers*	*65*
3.6	*Experimental*	*66*
3.6.1	*Instrumentation*	*66*
3.6.2	*Sample preparation*	*67*
3.7	*Results and discussion*	*68*
3.7.1	*Thermal transitions of LCP powders on heating and cooling*	*68*
3.7.2	*Effects of reheating LCP from the melt*	*68*
3.7.3	*Effects of altering the cooling rate*	*69*
3.7.4	*Effects of annealing in the melt*	*70*
3.7.5	*Effects of annealing at selected temperatures*	*71*

		Page No.
3.7.6	*Effects of remelting after annealing*	*71*
3.7.7	*The glass transtion*	*72*
3.7.8	*Thermal transitions in LCP films*	*72*
3.7.9	*Thermal transitions in LCP fibres*	*73*
3.8	*General conclusions*	*74*
3.9	*References*	*75*

Chapter 4: Structural Analysis

4.1	*Introduction*	*78*
4.2	*Wide angle x-ray scattering*	*79*
4.2.1	*A brief insight into the theory of x-ray diffraction*	*79*
4.2.2	*Determination of crystallinity*	*80*
4.3	*Experimental*	*83*
4.3.1	*Introduction*	*83*
4.3.2	*Sample preparation*	*83*
4.3.3	*Instrumentation*	*84*
a)	*Flat film camera*	*84*
b)	*Diffractometer*	*86*
4.4	*Results and discussion*	*89*
4.4.1	*Introduction*	*89*
4.4.2	*WAXS photographs*	*90*
a)	*Introduction*	*90*
b)	*Qualitative study*	*91*
4.4.3	*WAXS scans*	*92*
a)	*Introduction*	*92*
b)	*Qualitative study*	*93*
i)	*LCP powder versus film*	*93*

		Page No.
ii)	*LCP powder versus melt*	*93*
iii)	*Solvent effects*	*93*
iv)	*Effects of increasing annealing time*	*94*
v)	*Effects of increasing annealing temperature*	*95*
c)	*Determination of % crystallinities*	*96*
4.5	*Conclusions*	*98*
4.6	*References*	*99*

Chapter 5 : Transesterification

5.1	*Introduction*	*101*
5.2	*Small angle neutron scattering (SANS)*	*106*
5.2.1	*Introduction*	*106*
5.2.2	*SANS theory*	*107*
5.3	*Theory of Benoit, Fischer and Zachmann*	*114*
5.4	*Experimental*	*122*
5.4.1	*Introduction*	*122*
5.4.2	*Preparation of deuterated monomers*	*122*
5.4.3	*Preparation of deuterated polymer*	*124*
5.4.4	*Sample preparation*	*125*
5.4.5	*Scattering experiments*	*126*
i)	*Instrumentation*	*127*
ii)	*Data correction and evaluation*	*128*
5.5	*Results and discussion*	*130*
5.5.1	*Scattering curves*	*130*
5.5.2	*Zimm plot analysis: a qualitative study*	*130*
5.5.3	*Molecular weight determination*	132
5.5.4	*Transesterification kinetics*	*133*

		Page No.
5.5.5	*Transesterification initiated by active chain ends: a second model*	*137*
5.6	*References*	*139*

Chapter 6 : Crystallisation Induced Reorganisation

6.1	*Introduction*	*142*
6.2	*Lenz's theory*	*145*
6.3	*Crystallisation-induced reorganisation reactions (CIR)*	*147*
6.4	*Experimental*	*150*
6.4.1	*Sample preparation*	*150*
a)	*Purification*	*150*
b)	*Catalyst reimpregnation*	*150*
c)	*CIR process*	*151*
d)	*Reaction conditions*	*151*
6.4.2	*Experimental techniques used in the structural analysis of treated LCP samples*	*152*
a)	*Differential scanning calorimetry*	*152*
b)	*Polarising optical microscopy*	*153*
c)	*Wide-angle x-ray scattering*	*153*
6.5	*Results and discussion*	*155*
6.5.1	*DSC: phase behaviour and determination of heats and temperatures of transition*	*155*
a)	*Introduction*	*155*
b)	*CIR reaction below the melt*	*155*
c)	*CIR reaction in the melt*	*156*
d)	*CIR reaction in the nematic phase*	*157*
6.5.2	*POM: a qualitative study of the phase behaviour*	*158*

		Page No.
a)	*Introduction*	*158*
b)	*CIR reaction below the melt*	*159*
c)	*CIR reaction in the melt*	*159*
d)	*CIR reaction in the nematic phase*	*160*
6.5.3	*WAXS: qualitative structural analysis and determination of % crystallinity*	*160*
a)	*Introduction*	*160*
b)	*CIR reaction below the melt*	*162*
c)	*CIR reaction in the melt*	*163*
d)	*CIR reaction in the nematic phase*	*164*
6.5.4	*CIR reactions carried out in the absence of the ester-interchange catalyst*	*165*
a)	*Introduction*	*165*
b)	*DSC*	*165*
c)	*POM*	*166*
d)	*WAXS*	*166*
6.5.5	*Identification of structures formed by CIR*	*167*
6.5.6	*Effects of remelting LCP after rearrangement via the CIR reaction*	*170*
6.6	*Conclusions*	*172*
6.7	*References*	*174*

Chapter 7 : General Summary and Suggestions for Further Work

Appendices

Declaration

The work reported in this thesis is original to the author unless acknowledged otherwise, and has not been submitted previously for any qualification.

Abstract

The structural properties and transitions occurring in a random liquid crystalline polymer were studied over a range of thermal conditions using a combination of complementary characterisation techniques, including differential scanning calorimetry, wide angle x-ray scattering and optical microscopy. From the results, ordering in the polymer is observed to increase as a function of temperature and time prior to melting. An anisotropic phase develops at 330°C and degradation occurs at 400°C. The polymer displays a nematic phase on heating and hence is said to be thermotropic. Any order induced by annealing is destroyed on heating well above the polymer's melting point. The material reverts back to its original random structure. This behaviour is attributed to transesterification reactions occurring, over relatively short annealing times (120 seconds) at elevated temperatures. Although order and crystallinity are observed to increase as a function of annealing conditions, very little structural rearrangement is observed to occur for samples annealed over the time range, 0-2 hours. In general, the behaviour of the polymer is very dependent upon its thermal history.

The synthesis of a chemically ordered version of the liquid crystalline polymer of identical composition, was attempted to enable a back to back characterisation with the original random version. Attempts at the synthesis proved, unsuccessful.

Small angle neutron scattering techniques were used to study the mechanism and kinetics of transesterification. The activation energy calculated is identical to the value stated in the literature for PET, suggesting that the reaction mechanism is identical for both the rigid and the flexible polyester. The rate constants calculated for a range of polymers are inversely related to their initial molecular weights thus transesterification appears to proceed via an active chain end mechanism.

A unique route to the formation of highly blocky structures via a process termed crystallisation induced reorganisation (C.I.R.), based upon the transesterification reaction, is discussed in the literature. The present study aims to establish whether a C.I.R. reaction occurs in the random polymer. Samples were annealed at selected temperatures for reaction times ranging from 0-72 hours. An ester-interchange catalyst was impregnated into selected

samples. The polymer was observed to undergo the C.I.R. reaction both above and below the melt, leading to a block structure. The presence of the catalyst did not influence the rate of structure development.

"Nil illegitimum carborundum"

Randal Richards

Chapter 1

Introduction

1.1 *Historical Introduction*

In the late 1970's the plastics industry was involved mainly in the mass production of several main-line polymers and profits were dependent on large output plant efficiency and processing methods. The structural chemistry of such polymers was simple and cheap. However the design and manufacture of a more complex and expensive range of polymers which exhibited unique properties, had recently begun. Research into the design of these materials is now expanding rapidly. The aromatic content of the polymer backbone was increased in an attempt to achieve higher levels of chemical and thermal stability.[1,2] The greatest breakthrough in this field of polymer science, has been in the design of liquid crystal polymers. However, a thorough understanding of the structural properties of these materials is still in its infancy.

A polymer is defined as being liquid crystalline in nature, where the chains are sufficiently rigid to remain mutually aligned in the liquid phase, however the perfect positional periodicity of the crystal is no longer present. In other words, liquid crystals possess long range orientational order without long range positional order. Thus it can be said that the liquid crystal phase is intermediate between a crystal and a liquid leading to the establishment of the term, mesophase.[3] Where a liquid crystal phase forms on melting, the polymer is termed thermotropic and where such a phase forms on solvent addition it is termed lyotropic.

There are three possible ways of forming liquid crystalline polymers.[4-6]

i) by introducing mesogenic groups into a polymer backbone leading to a main-chain liquid crystal polymer

ii) by attaching the mesogenic groups either directly to the polymer backbone or through flexible aliphatic chains, leading to a side-chain liquid crystal polymer

iii) by introducing low molecular weight optically active molecules into the polymer thus inducing the liquid crystalline character.

A schematic presentation of the different types of main-chain and side-chain polymers is given in Figure (1.1)

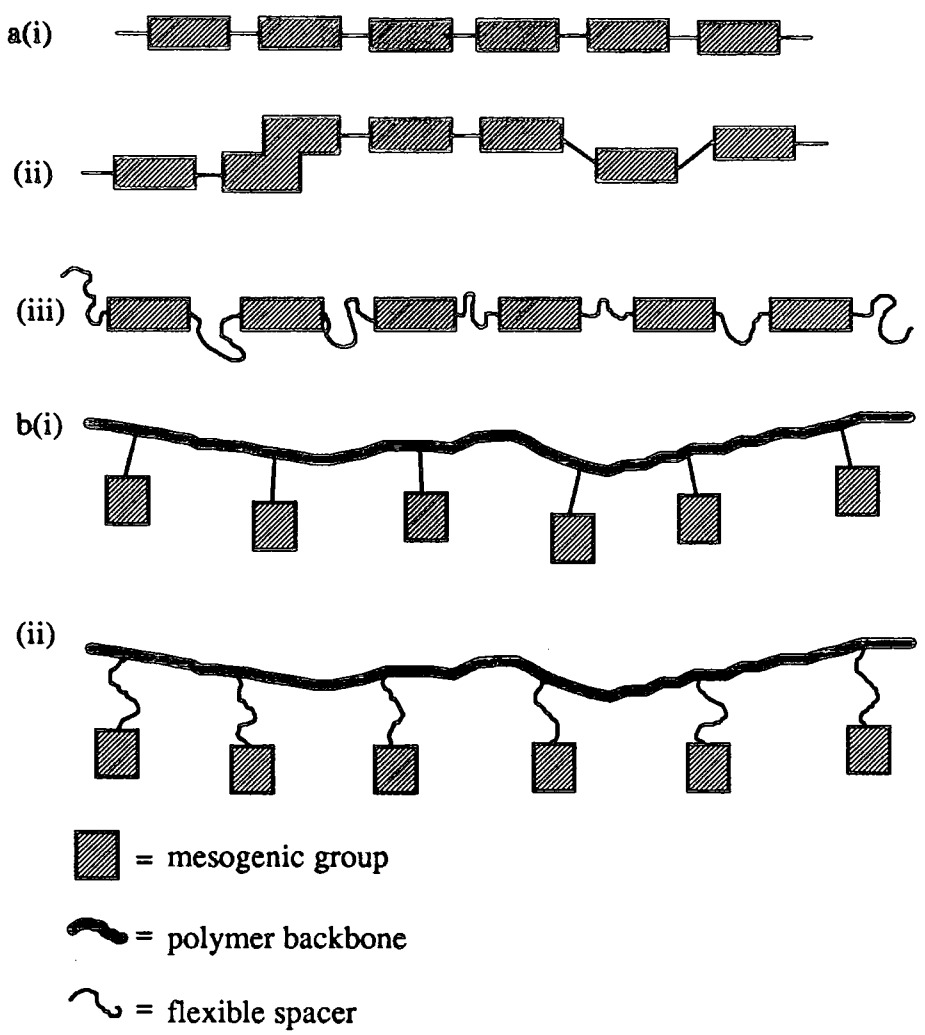

Figure (1.1) a) main-chain polymers (i) linear rigid chain (ii) linear rigid links (iii) linear flexible links

b) side-chain polymers (i) direct linkage of mesogenic groups (ii) attachment of mesogenic groups via flexible spacers.

Three different types of mesophase exist which classify varying types of order. The main types are nematic, smectic and cholesteric. A schematic diagram illustrating the mesogenic arrangements in these mesophases is given in Figure 1.2

Figure (1.2)

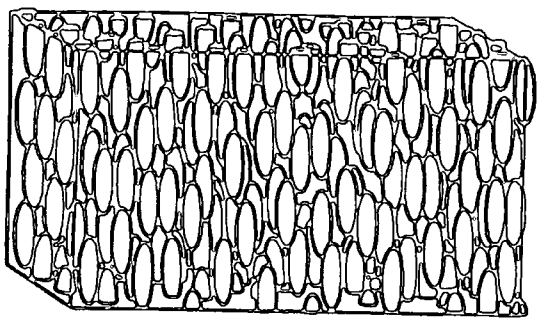

(a) nematic

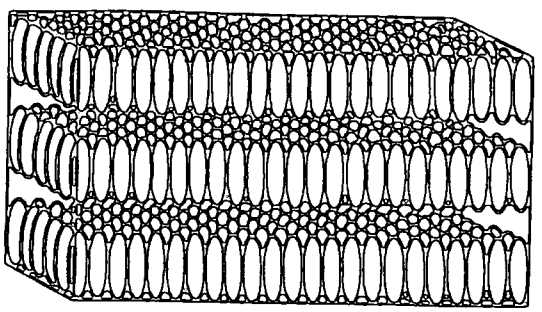

(b) smectic

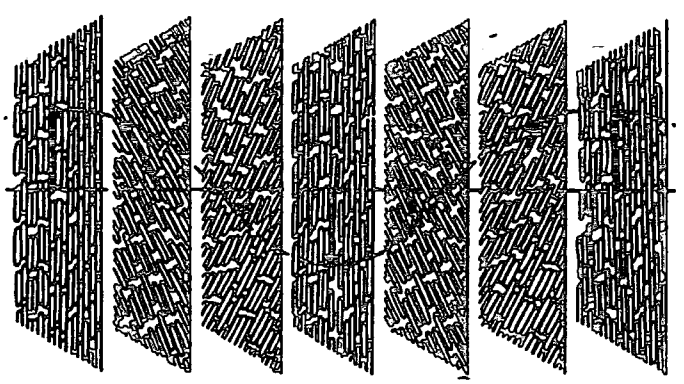

(c) cholesteric

In the nematic phase there is no long range order of the centres of gravity. The only correlation which exists is in the direction of the mesogenic groups. Smectic

phases can be further divided into 7 basic polymorphs.[7] Each one demonstrates a layered structure of the mesogens. These layers can slide over one another. The smectic phase is easily distinguishable by x-ray diffraction and the layer spacing can be measured using this technique. Smectics are more ordered than nematics. The cholesteric phase is equivalent thermodynamically to the nematic phase and results either, if a mesogen is chiral or if a chiral molecule is dissolved in a nematic liquid crystal.

The present work concentrates on the study of a nematic thermotropic main-chain polyester.

For over a century, simple low molecular weight liquid crystal compounds have been recognised and studied.[8] For various natural polymers, the occurrence of liquid crystal phases has been established for several decades, however little characterisation of their properties has been carried out. The history of main-chain liquid crystal polymers is a relatively short one. In 1956, Flory predicted that rigid rod polymers should form a lyotropic solution at a critical concentration.[9] Coincidentally in the same year, lyotropic solutions of a polypeptide, found to form a stable helical conformation in water, were discovered. Around the same period, Conmar Robinson[10] showed that poly(γ-methyl-L-glutamate) (PMLG) and poly(γ-benzyl-L-glutamate) (PBLG) gave liquid crystal solutions in relatively non-protonating solvents. A major advancement was made by DuPont in the mid-1960's in the field of lyotropic systems by the developments of commercial fibres possessing exceptionally high tensile strength and modulus through the use of relatively rigid aromatic polyamides. The fully commercialised product "KEVLAR" based upon poly(p-phenylene terephthalamide) was introduced.

Theoretical studies on the likelihood of obtaining thermotropic polymers were carried out by Papkov and co-workers[11] in 1973 and by Ciferri[24] in 1975. Their findings were in agreement with Flory's rigid-rod studies.[9] The first publications on the existence of thermotropic polymers arising from main-chain conformation did not appear until 1975. Amongst those cited was a patent to DuPont[12] which

describes a range of highly aromatic polyesters and a paper by Jackson and Kuhfuss[13] of the Tennessee Eastman Company describing random copolyesters of poly(ethylene terephthalate) and poly(p-hydroxybenzoic acid). These types of polymers were commercially available at this time under brand names such as X7G and X7H. In the late 1970's Celanese introduced a range of aromatic polyesters based upon poly(hydroxybenzoic acid) and poly(hydroxynaphthoic acid). Progress started to accelerate in this field in the early 1980's. Dartco introduced the wholly aromatic liquid crystal polymer "XYDAR" in 1985. However due to the rigidity of the chain, a processing temperature of 420°C was necessary, requiring significant equipment modifications. As a consequence methods of reducing the processing temperature were developed by altering the structural chemistry. This aspect will be discussed further in section (1.2). ICI introduced a series of liquid crystal polyesters in 1986.[14,15] These materials had significantly lower processing temperatures compared to XYDAR but at the same time were wholly aromatic in nature.

Recent studies have concentrated on understanding the structure/property relationships of liquid crystal polymers. A significant amount of progress has been made recently[16-18] however there is still a long way to go before a thorough understanding of these unique materials can be obtained. The present work attempts to contribute to these efforts.

1.2 *Properties and Applications of Liquid Crystal Polymers*

Extensive research into the study of main-chain liquid crystal polymers was instigated by the discovery of the unique properties and novel processing behaviour exhibited by both nematic, lyotropic and thermotropic systems. The major breakthrough in the field was the discovery of the response of the nematic phase to shearing.[19] Even very low shear rates were sufficient to induce the nematic domains to align parallel to the flow direction resulting in significantly lower apparent viscosities in the anisotropic phase. In addition, where the material under observation forms an anisotropic phase at a higher temperature, the viscosity can appear to be significantly higher in the isotropic phase than in the anisotropic phase at a lower temperature. This type of behaviour, although much more pronounced in polymers, is also observed in simple low molecular weight compounds which exhibit both nematic and isotropic liquid phases.[20]

This section discusses briefly the properties of main-chain liquid crystal polymers in particular. Useful references in the synthesis, characterisation and applications of these polymers are discussed in detail in a book edited by Chapoy in 1985[21] and a bibliography by Hinov published in 1986.[22]

The majority of synthetic liquid crystal polymers are composed of a series of rigid units. These units are characterised individually, by possessing chain-continuing bonds that are either co-linear, such as para-phenylene or parallel and oppositely directed such as 1,5- naphthalene. Such groups are normally based upon cyclic structures. These ring structures need not be aromatic in nature but are normally inherently rigid and form the components of almost all known main-chain synthetic liquid crystal polymers. Some examples of these units are illustrated in Figure (1.3).

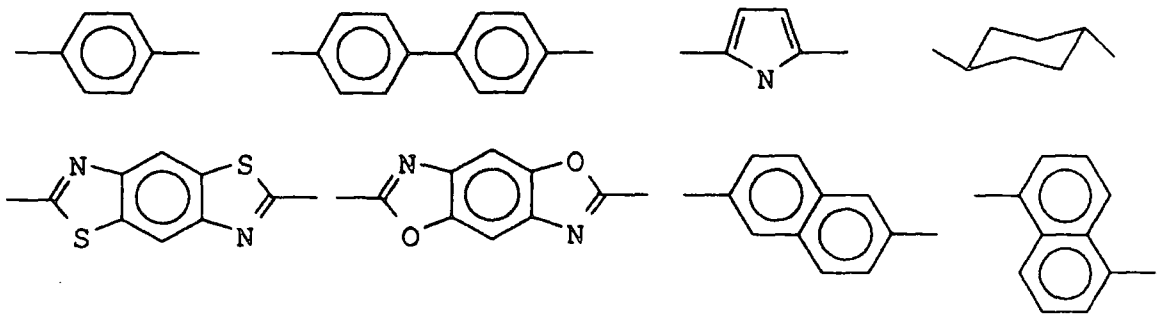

Figure (1.3)

Thermotropic LCP's are based generally on these types of chemical units however, such units in the homopolymer form lead to the formation of crystalline polymers with melting points above the temperatures of decomposition.[23-26]

In order to obtain a liquid crystal phase at a temperature below that of decomposition the polymers must be designed in such a way as to reduce their melting temperature significantly. Lyotropic systems are usually composed of amide linkages where interchain association through the hydrogen bonding of the carbonyl and amide linkage occurs. In this system a liquid crystal phase can only be induced by solvent dissolution. In contrast thermotropic systems are based more usually upon polymers which contain more flexible ester linkages or other linking groups free from hydrogen bonding. Even so, considerable disruption of main-chain order is necessary to depress crystallinity in thermotropic main-chain polymers. There are several routes to reducing the transition temperature of these polymers:

1) the introduction of flexible spacers separating the mesogenic main-chain units

2) substitution of the aromatic rings

3) addition of an element of dissymmetry to the main-chain by copolymerising mesogenic units of different shapes

4) the introduction of rigid kinks into the straight polymer chain.

In general the synthesis of such polymers is very well established.[27-29] Many liquid crystal polymers have been synthesised in a transesterification reactions

which lead to chemically disordered backbones[30,31] hence it is important to understand how chemical disorder along the chain influences phase structure in the fluid state and why chemically random mesogenic chains order to form partially crystalline solids. However to date many of the fundamental physical properties of these materials remain unexplained.

Thermotropic LCP's offer outstanding properties as engineering materials, including resistance to chemical attack and to burning. However, the most impressive property of these materials results from their high molecular orientation producing exceptional stiffness per unit weight in a preferred direction. A further significant mechanical feature, resultant of the molecular orientation, is the low coefficient of thermal expansion since fully extended products cannot flow further. Thus, products manufactured from these materials exhibit excellent dimensional tolerance and as a consequence are especially useful where very accurate and dimensionally stable moulding is required. Both the mechanical properties and the absence of thermal expansion effects are associated closely with all levels of structure within the material. The understanding of these properties is crucial to the commercial development of this type of polymer.

In conclusion thermotropic polymers flow freely, orient efficiently and provide materials with excellent mechanical, chemical and thermal stability. The possibility of using electric and magnetic fields in processing using alternative types of LCP's is being considered and tested. The liquid crystal display industry had discovered that, by attaching such molecules to flexible polymer backbones, refined response characteristics and new routes towards device design are achieved.

1.3 *Experimental Methods Used in the Thermo-Structural Characterisation of LCP*

1.3.1 *Introduction*

In the study of polymers in general, a very wide range of analytical techniques is used to determine their structures.[32,33] The chemical regularity, stereochemical configuration and molecular weight distribution make up the basic molecular structure. In general, chemical techniques are applied in the determination of the level of structure. The physical structure can be affected by processing and involves a wide range of variables e.g. molecular orientation. For example if crystals exist, important variables include: crystal structure; degree of crystallinity and crystal size and arrangement. This type of structure is determined by microscopy, scattering and spectroscopic techniques. The degree of crystallinity can be determined from wide angle x-ray scattering, thermal analysis and from NMR. Optical microscopy, combined with complementary techniques such as light and x-ray scattering, looks at the morphology of the specimen. Thus to conclude, this example stresses the vital importance of using a range of complementary techniques at every point in order to obtain a complete and accurate characterisation of a polymer specimen.

For the majority of liquid crystal polymers, detailed characterisation has proved to be extremely difficult, due to the insolubility of these materials in common, non-degrading solvents. Thus, the use of standard techniques in the structural elucidation of liquid crystal polymers is restricted and often impossible. A large number of liquid crystal polymers are manufactured via transesterification reactions and hence, they possess irregular sequences of structural units. In this instance, the characterisation of their chemical microstructure is of vital importance.[31,34-36]

Many thermotropic main-chain liquid crystal polymers are semi-crystalline in nature and consequently their thermal behaviour is often complicated.[37,38] Random rigid chain polymers frequently display a nematic melt. The type of mesophase can be identified using selected techniques. Structural formation during such a transition is different to that observed in flexible copolymers. The rigidity of the molecules lead to an impossibility of chain folding and an anisotropic molecular motion in the cooled nematic melt.

From these examples, it is crucial that a range of complementary techniques be used, in order to characterise the LCP both fully and unambiguously.

This section presents a brief overview of a few of the techniques appropriate to the study of these materials, concentrating specifically on the techniques used in the structural characterisation of the LCP studied in the present work.

The instrumentation, applications and scope of these techniques are described in more detail in Chapters 3,4 and 5.

1.3.2 *Techniques Applied*

a) *Differential Scanning Calorimetry (DSC)*

The term "thermal analysis" incorporates an extensive range of thermal techniques[39,40] including Dynamic Thermal analysis (DTA), Differential Scanning Calorimetry (DSC), Thermal Mechanical Analysis (TMA) and Thermo-Gravimetric Analysis (TGA). DTA and DSC are very similar techniques in terms of the type of information available. The following parameters can be evaluated from these techniques; glass transition temperature (T_g), melting point, crystallinity, purity, heats of transition, degradation and reaction kinetics. DSC is however a more reproducible technique, and is the method used in the present work. The DSC thermogram is a plot of the differential heat flow versus the temperature or time. The thermal behaviour of a polymer sample has been found

to be very dependent on parameters such as thermal history and annealing conditions. In addition heating and cooling rates exhibit significant effects on the thermal properties of a sample. In some cases, thermal analysis alone can be misleading and ambiguous. The texture of the melt is dependent on the structure of the mesophase and in general cannot be identified by DSC alone. Thermal observations are normally combined with polarising optical microscopy studies. In addition, the identification of multiple transitions commonly observed for LCP's, often requires complementary techniques. These include hot stage microscopy and x-ray diffraction studies. In the present work a detailed study of the thermal transition behaviour is given using DSC in combination with polarising microscopy. These issues are discussed in Chapter 3.

b) *Polarising Optical Microscopy (POM)*

Optical microscopy techniques provide both a rapid overview of and essential information regarding polymer structure. This information is necessary for investigations into the structure/property relations. The morphology of the specimen is described using microscopy whereas the molecular structure must be determined by alternative techniques. In many cases unique optical textures are observed for the various orientations and structures of the three classes of liquid crystals and hence specific phases can be identified. For example thin films of nematic crystals are recognised by the threaded 'schlieren' pattern which appears in the optical microscope in transmission under crossed polars. Liquid crystal polymers exhibit less well defined textures due to their higher viscosities, and hence complementary techniques are required in order to identify the mesophase. Dynamic hot stage microscopy can be used in conjunction with video recorder attachments to provide images of textural and structural changes as a function of temperature and time. Crystal type, size and degree of perfection can also be studied, as well as the study of parameters such as relaxation, purity and

degradation. Sample preparation is relatively simple for this technique. Samples in the form of powders, films and fibres can be studied. Thin films offer the most reproducible and consistent form for analysis and, from experience from the present studies, are seen to exhibit the clearest phase transitions. This technique is used in the identification of morphological transitions as a function of temperature and time. POM complements DSC techniques very effectively. Both techniques are discussed in Chapter 3.

c) *Wide-Angle X-Ray Scattering (WAXS)*

In polymer science, x-ray diffraction is a powerful, analytical technique frequently used to provide information on the order, arrangement and form of packing of molecules. Examples of the type of experimental data obtainable include: phase identification, % crystallinity, crystal size, order, molecular orientation and structure, and identification of amorphous structures. Powder diffraction provides a rapid, technique in the identification of crystalline substances. WAXS is used to characterise the crystalline phase over the range 0.1-1nm. It can be used to determine degree of crystallinity and the size, as well as the orientation and perfection of the crystalline material. Crystalline specimens exhibit sharp rings or peaks. In contrast, amorphous materials exhibit broad diffuse scattering patterns. Annealing of the sample under selected conditions can affect the degree of order significantly, resulting in sharper, more intense peaks. Annealing effects are studied in detail in the present work. X-ray diffraction patterns of unoriented samples can often distinguish between types of mesophase, however this is not always possible. If an oriented sample can be prepared, more detailed structural information can be obtained. Qualitative information, indicative of the degree of order in polymer samples, can be obtained from the appearance of a broad halo or a sharp ring in diffraction patterns. Since polymers are known to be composed of both polycrystalline and amorphous material, in some cases, in particular for

main-chain polymers, x-ray patterns are exhibited which are too diffuse to enable identification of the mesophase. This is not always the case however, since patterns have been reported in the literature[41-44] which are in line with the structure of a nematic liquid crystal polymer. A predominantly qualitative study of both oriented and unoriented samples is presented in Chapter 4.

d) *Small-Angle Neutron Scattering (SANS)*

SANS is a technique used in the structural determination of materials including polymers. The technique is renowned for its unique property ie. the neutron scattering from hydrogen is very different to the scattering from deuterium. Thus the deuterated molecules may be distinguished easily from the hydrogen molecules in a given matrix, and due to the chemical similarity of the molecules, the changes in physical properties due to mixing are negligible. In polymer science, the following information can be obtained from the scattering spectra: the shape of the molecule, the radius of gyration and the molecular weight. Chapter 5 concentrates on the breakdown in molecular weight of a copolyester (LCP) due to bond scission during transesterification. This is achieved by blending chemically similar versions of a hydrogenous and a deuterated copolyester and observing the molecular breakdown as a function of temperature and time. Ultimately, the kinetic parameters and mechanism of the reaction are obtained.

1.4 *Main-Chain Liquid Crystal Polymer Studied*

The main-chain liquid crystal polymer studied in the present work is a high molecular weight, wholly aromatic, rigid-rod terpolyester manufactured by ICI plc. The polyester is composed of isophthalic acid, para-hydroxybenzoic acid and hydroquinone with the composition.

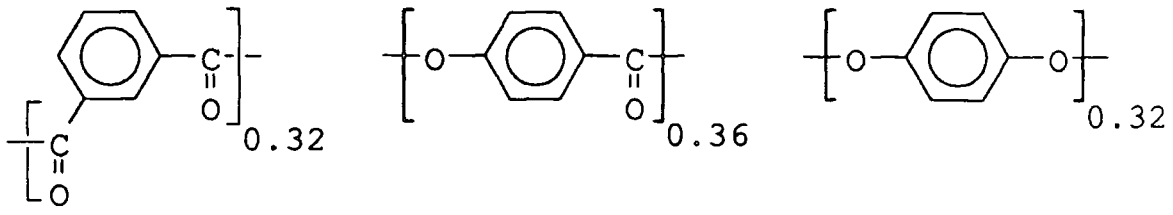

For simplicity, the polyester will be referred to as "LCP" throughout this work. An optimum composition has been selected which exhibits a stable liquid crystalline phase at least 50°C below the decomposition temperature. The incorporation of the isophthalic unit forms a kink in the otherwise linear chain. This unit appears randomly along the chain as a result of the polymerisation process. These factors reduce the melting temperature of the polyester to 270°C, enabling the material to be melt processed successfully.

1.5 *A Synopsis of the Aims of the Present Study*

The main objectives targeted in this work and some of the questions posed are as follows:

1) What effects, if any, result from altering the sequence distribution of the monomeric units along the polymer chain. Does the polymer still exhibit a liquid crystalline phase or is there a significant change in its structural properties?

2) To carry out a thorough thermo-structural characterisation of LCP in order to develop a good understanding of the structural and phase development as a function of temperature and time.

3) To study the mechanism and kinetics of transesterification using SANS techniques. Over what temperature range does the process occur? Does it occur in the solid phase?

4) To observe any structural changes as a result of annealing LCP over an extended time period both in the solid and liquid crystalline phase. Does the addition of an ester-interchange catalyst affect the process? Can the structure be altered significantly and if so, does the polymer still exhibit a liquid crystalline phase and which parameters govern the observed effects?

1.6 *References*

(1) Jin, J-I, Antoun, S., Ober, C., Lenz. R. W., *Brit. Polym. J.* 12 32 (1980)

(2) Cheng, S. Z. D., *Macromolecules* 21 2475 (1988)

(3) Friedel, M. G., *"Les Etats Mesomorphes de la Matiere" Ann. Phys. (Paris)* 18 273 (1922)

(4) Majnusz, J., Catala, J. M., Lenz, R. W., *Eur. Polym. J.*, 184 475 (1983)

(5) Hamb. F. L., *J. Polym. Sci.* A-1 10 3217 (1972)

(6) Higashi, F., Kubota, K., Sekizuka, M., *Makromol. Chem:, Rapid Commun.*, 1 457 (1980)

(7) Sackmann, H., Demus, D., *Mol. Cryst. Liq. Cryst.*, 21 239 (1973)

(8) Dobb, M. G., McIntyre, J. E., *"Advances in Polymer Science*, Springer-Verlag (Berlin) 60, 61 (1984)

(9) Flory, P. J., *Proc. Roy. Soc.* 73, A234 (1956)

(10) Robinson, C., *Trans. Faraday Soc.* 52 571 (1956)

(11) Papkov, S. P., et al, *Vysolcomol. Soed, Ser. B,* 15 357 (1973)

(12) Dupont de Nemours & Co. E. I. (Dupont) (S. L. Kwolek). *B. P. 1,198,081* (priority June 1966, USA)

(13) Jackson, W. J., Kuhfuss, H. F, *J. Polym. Sci., Polym. Chem. Ed.*, 14 2093 (1976)

(14) Imperial Chemical Industries Ltd (ICI) Goodman, I., McIntyre, J. E., Stimpson, J. W., *B.P. 989, 522* (priority Feb. 1962)

(15) ICI Goodman, I., McIntyre, J. E., Aldred, D. H., *B.P 993, 272* (priority May, 1962)

(16) Joseph, E., Wilkes, G. C., Baird, D. G., *Polymer* 26 689 (1985)

(17) Green, D. I., Unwin, A. P., Davies, G. R., Ward, I. M., *Polymer* 31 57 (1990)

(18) George, S., Porter, R., *J. Polym. Sci. (B) Polym. Phys. Ed.*, 26 83 (1988)

(19) Windle, A., *Liquid Crystalline Polymers MRS Bulletin 18* (Nov. 1987)

(20) Porter, R. S., Johnson, J. F., *Rheology* (ed) Eirich, F., New York, Academic Press 4 317 (1967)

(21) Chapoy, L. L., *"Recent Advances in Liquid Crystalline Polymers"* (1985)

(22) Hinov, H. P., *Mol. Cryst. Liq. Cryst.* 136 221 (1986)

(23) Blunstein, A., *"Liquid Crystalline Order in Polymers"*, Academic Press, New York (1981)

(24) Ciferri, A., Krigbaum, W. R., Meyer, R. B., (ed) (1982) *"Polymer Liquid Crystals"* Academic Press, New York 84 (1984)

(25) Liquid Crystal Polymers I, II, III, *"Advances in Polymer Science"* (Springer, Berlin) (59-61) (1984)

(26) Blumstein, A., *"Polymeric Liquid Crystals"*, Plenum Press, New York (1985)

(27) Calundann, G. W. (Celanese) *U. S. Patent 4184996* (1986), *4161470* (1970)

(28) Cao, M. Y., Wunderlich, B., *J. Polym. Sci., Polym. Phys. Ed.*, 23 521 (1985)

(29) Ober, C. K., Jin, J-I., Lenz, R. W., *"Advances in Polymer Science"* 59 103 (1984)

(30) Moore, J. S., Stupp. S. I., *Macromolecules* 21 1217 (1988)

(31) Ober, C., Lenz, R. W., Galli, G., Chiellini, E., *Macromolecules* 16 1034 (1983)

(32) Wunderlich, B., *"Macromolecular Physics"* Academic Press, New York 1 & 2 (1973)

(33) Vadimsky, R. G., *"Methods of Experimental Physics"* R. A. Fava (ed) Academic Press, New York 16B 185 (1980)

(34) Jackson, W. J., Kuhfuss, H. F., *J. Polym. Sci. Polym. Chem. Ed.*, 14 2043 (1976)

(35) Ober, C., Jin, J-I., Lenz, R. W., *Polym. J.* 14 36 (1982)

(36) Moore, J. S., Stupp, S. I., *Macromolecules* 20 273 (1987)

(37) Blumstein, A, Vilasagar, S., Ponrathnam, S., Clough, S. B., Blumstein, R.B.,

J. Polym. Sci. Polym. Phys. Ed., 20 877 (1982)

(38) Noel, C., Laupetre, F., Friedrich, C., Fayolle, B., Bosio, L., *Polymer* 25 808 (1984)

(39) De Vries, A., *Mol. Cryst. Liq. Cryst.*, 10 31 (1970)

(40) Wendtlandt, W. W., *"Thermal Methods of Analysis"* Wiley-Interscience, New York (1974)

(41) Frosini, V., Marchetti, A., de Petris, S., *Makromol. Chem. Rapid. Commun.*, 3 795 (1982)

(42) Antoun, S., Lenz, R. W., Jin, J-I., *J. Polym. Sci., Polym. Chem. Ed.*, 19 1901 (1981)

(43) Lenz, R. W., Jin, J-I., *Macromolecules* 14 1405 (1981)

(44) Nöel, C., Billard, J., Bosio, L., Freidrich, C., Laupêtre, F., Strazielle, C., *Polymer*, 25 263 (1984)

Chapter 2

Synthesis of Ordered LCP

2.1 *Introduction*

An understanding of the structure-property relationships in thermotropic liquid crystal polymers has not been well established. Extensive studies of the structural chemistry associated with these materials have been carried out,[1-5] however the study of their fundamental physical properties and their relationships to molecular variables, remains superficial. Only a few papers exist concerning this topic.[6-9]

The monomer sequence distribution is of significant importance in controlling the properties of copolymers. In the study of liquid crystal polymers the relationship between chemical sequence structure and the physics of these materials remains unclear, hence it is considered relevant to study how the phase behaviour is affected by chemical disorder along the polymer backbone, both in the solid and fluid states and furthermore to establish how the mesomorphic chains order to form partially crystalline solids. These studies are especially applicable to liquid crystal polymers since many of these materials are synthesised via transesterification reactions, which lead to scrambling of the monomeric units and hence the formation of chemically disordered backbones.[10]

In order to elucidate relationships between molecular variables and physical properties, the synthesis and characterisation of a suitable material must first be accomplished. The synthesis of ordered-disordered chemical analogues of main-chain liquid crystal polymers has proven extremely difficult due to either, the problems associated with developing polyesters with a regular sequence distribution along the chain (ie. regioregular polyesters) or the absence of liquid crystallinity in highly regular chains. In the study of aromatic polyesters, difficulties arise in finding suitable polymerisation methods to synthesise ordered materials due to the insoluble nature of the chains. Methods commonly used in the preparation of liquid crystal polymers are discussed in section (2.2). It is due mainly, to these synthetic difficulties that little information is available on the

contrasting physical behaviour between chemically disordered and chemically ordered liquid crystal polyesters.

Main-chain thermotropic polymers generally contain mesogenic units consisting of structures with two or more aromatic or cycloaliphatic units, where these units may or may not be connected by flexible spacers.[11-13] In their study of azoxy mesogenic groups Blumstein and co-workers demonstrated that both molecular structure and assembly have a significant effect on the polymers' properties.[14] Furthermore, altering the type as well as the direction of their connecting bonds had a pronounced effect on the behaviour of these materials. Krigbaum and co-workers[15] synthesised a copolymer composed of diphenol and azelaoyl chloride units under conditions where transesterification did not occur and hence the ester groups were stable. However, the polymerisation method used did not control the direction of the ester bonds and hence the structural units were placed at random along the polymer backbone (ie. the polymer is described as aregic). In a similar study Ober and co-workers[16] showed that the thermal behaviour of the polymers under observation was very sensitive to monomeric sequence distribution. Their studies revealed that systems with alternating head-to-tail, tail-to-head sequences (syndioregic) had less tendency to form a mesophase than aregic materials. The authors studied the syndioregic terpolymer containing terephthalate, oxybenzoate and decamethylene spacers. The polymer melted directly from the crystalline to the isotropic state without exhibiting a mesophase. Thus the randomness of mesogenic group orientations along the polymer backbone can be very important in determining mesophase formation and properties. In addition to the above-mentioned studies, few publications exist reporting on the structure-property relationships of copolyester sequences with identical monomer compositions.

It is in this context, that the aim of the present chapter is to synthesise a chemically regular analogue of LCP. Previous NMR studies have confirmed that LCP is a random terpolymer formed as a result of transesterification reactions

occurring during polymerisation. If the "regular" synthesis is successful, the ordered and disordered polymers can thus be used for studies on the role of chemical sequence in the physics of LCP. This study is however, based upon the assumption that a mesophase will indeed form for the regular polymer. The possibility of the synthesised material being so highly regular that a mesophase may not be observed should not be dismissed. However if such behaviour is observed, it in itself is still considered beneficial to the understanding of the role played by the monomer sequence distribution in LCP. This chapter discusses the attempted synthesis of a chemically ordered analogue of LCP via two different routes. These routes are described in section (2.3) and are both based on low temperature polymerisation reactions (T = 130°C) where transesterification is known not to occur (see Chapter 6) thus the ester linkages remained stable thus allowing control of the monomer sequence along the main-chain. Furthermore each route leads to a polymer composed of a 1:1:1 molar ratio of hydroxybenzoic acid (HBA), hydroquinone (HQ) and isophthalic acid (IPA); practically equivalent to the composition of LCP. The resultant monomeric sequences of the polymers produced by these synthetic routes are discussed below.

Route 1 attempts to synthesise a regioregular version of LCP via the interfacial polycondensation of a symmetric monomer (section (2.3), monomer (X)) with isophthaloyl dichloride. The resultant polymer will possess the following monomeric repeat sequence:

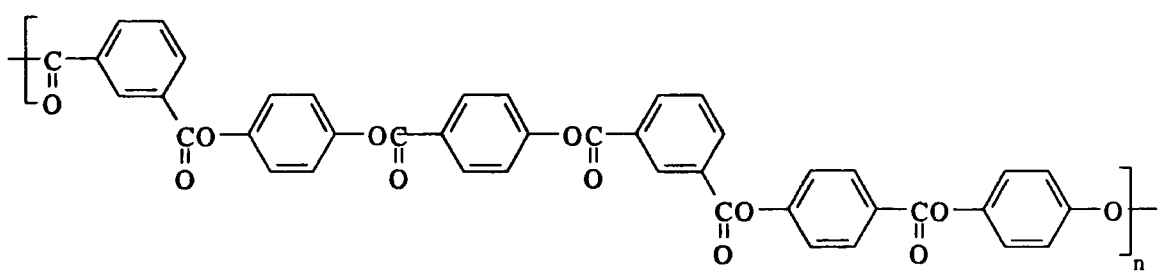

ie (- IPA - HQ - HBA - IPA - HBA - HQ -)$_n$

Figure 2.1 Structure of regioregular polymer via route 1

Route 2 attempts to synthesise a partially ordered version of LCP via a solution polymerisation method based on the reaction of 4-hydroxyphenyl-4-hydroxybenzoate and isophthalic acid (section (2.3.1)). Monomer (IX) is a dimeric diol which is not symmetrical, hence the resulting ordered polymer does not have a strictly ordered monomer sequence: three different triad sequences are feasible simply by reversing the carboxylate group. The resultant polymer is composed of an IPA molecule every 3rd unit. In addition, no two consecutive HBA units occur adjacently along the chain. Thus a polymer of defined order can be synthesised with the following monomer sequence.

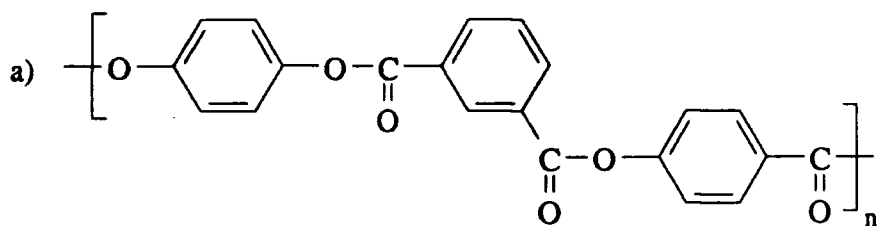

(- HQ - IPA - HBA -)

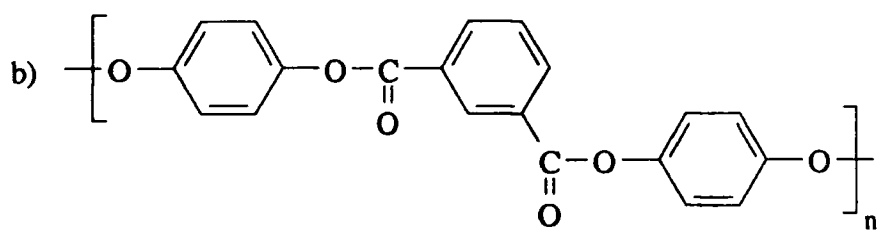

(- HQ - IPA - HQ -)

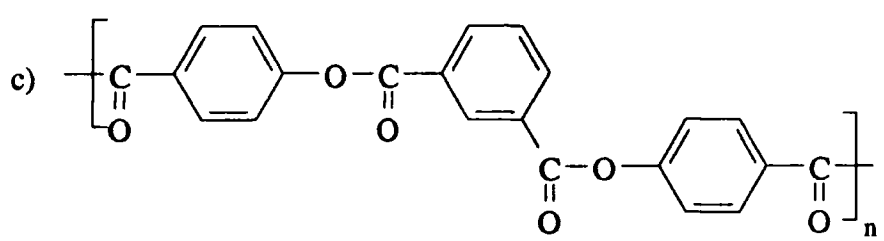

(- HBA - IPA - HBA -)

Figure 2.2 Possible triad structures of partially ordered polymer via route 2

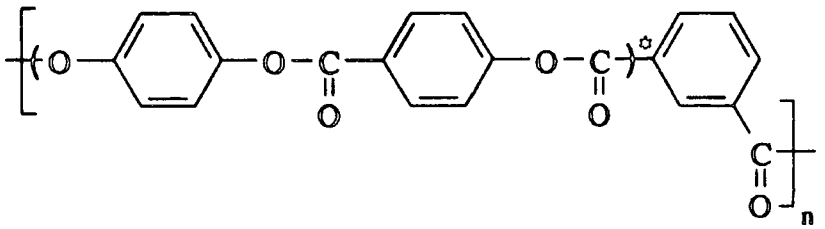

( )* = monomeric diol has equal probability of being reversed

Figure 2.3 Structure of partially ordered polymer via route 2

2.2 *Synthetic Routes to Main-Chain Liquid Crystalline Polyesters and Block Copolymers*

A wide range of structural units are available and in use in the synthetic design of liquid crystal polymers.[17-19] In general these polymers are prepared by step-growth polycondensation reactions. It has been well established that polymers synthesised by such methods are subject to limitations on molecular weight.[20] Considering rigid-rod polyesters, these materials have extremely high melting points and very low solubilities in all available reaction solvents. Due to these characteristics, very high molecular weight materials may only be synthesised using a two-step polymerisation process. The first step could involve either a homogeneous solution polymerisation or a melt polymerisation reaction. The second step involves the reaction of the polymer in the solid state at a temperature slightly below its melt. If carried out under vacuum, the final process is capable of producing materials of extremely high molecular weight.

In general, four basic procedures are used in the synthesis of liquid crystalline polyesters. In theory these procedures can be applied equally to the preparation of aromatic copolyesters from practically any combination of hydroxyacids, dicarboxylic acids and biphenols.[21] These methods are discussed below.

(a) The Schotten-Baumann condensation reaction of an aromatic acid chloride with a phenol can be carried out via any of the following polymerisation methods:

(i) solution polymerisation at elevated temperatures

(ii) interfacial polycondensation at room temperature

(iii) melt polymerisation.

Methods (i) and (ii) are carried out frequently in a chlorocarbon solvent. A base is incorporated into the reaction system to remove the HCl via an inert gas stream or by maintaining the reaction mixture under high vacuum.

(b) Transesterification reactions carried out in the melt at elevated temperatures.

(c) The oxidative esterification reaction of a phenol and an aromatic carboxylic acid in the presence of a phosphorous compound and a chlorocarbon solvent

(d) The polymerisation reaction of mixed anhydrides formed in situ, known to yield polymers of high molecular weight.

In the synthesis of copolyesters the products obtained are generally random in composition however, it has been reported in the literature that if a high melting aromatic copolyester is maintained at temperatures at or near its melting point for long periods of time, the initially random copolymer can reorganise to block structures via ester-interchange.[22] A detailed study of this phenomenon is dealt with in Chapter 6.

The present chapter is concerned with the synthesis of chemically ordered or "regular" copolyesters, hence a brief insight into the problems and methods of block copolymer formation is discussed below. Although many approaches to the synthesis of polymers of a block-like nature have been reported, only a few are capable of generating predictable and well-controlled structures.[10,23] The problems of uncontrolled architecture of these materials can be portrayed by considering interchange reactions which involve the scission and recombination of the polymer fragments, where the polymer contains functional groups in the main-chain which are capable of undergoing exchange. Such materials include polyesters, polysiloxanes and polyamides. The resultant product(s) may contain one, or any combination of the following: the actual homopolymers involved in the reaction; randomised copolymer or block copolymers of unknown length and composition. There are however, a few established techniques which lead to predictable block structures. These techniques are based on either living addition polymerisation or step-growth polycondensation. The success of these reactions is dependent upon various features including: the known concentration and placement of active sites; stoichiometric control to ensure homopolymer contamination is minimal in step-growth systems and the control of the segment

length and placement along the backbone. The interaction of functionally terminated oligomers is often used in the production of block copolymers. Via this method only the intersegment linkages are involved in the polymerisation reaction. In general difunctional species are used leading to $(A\text{-}B)_n$ copolymer structures however monofunctional oligomers can be used to yield A-B or A-B-A structures. Perfectly alternating sequence distributions are obtained only when similar quantities of functional oligomers are used, in order to fulfil stoichiometric requirements and where these oligomers bear equally reactive end groups. In these systems, as in the previous scenario, A-B-A and $(A\text{-}B)_n$ structures can be produced by the interaction of the monomers with monofunctional and difunctional oligomers respectively, under perfect stoichiometric conditions. Problems arise in this method since even under these conditions, imperfections in statistical sequence may result. Furthermore if stoichiometry should deviate from the ideal the resulting products will be even more heterogeneous due to the presence of contaminating block structures or coupled homopolymer.

Another major problem in the production of ordered block copolymers, can result in heteroatom polymers which crystallise during preparation, resulting in insolubilisation. This characteristic leads to limitations in both molecular weight and the control of block sequence distribution. This problem is especially relevant in the formation of aromatic copolyesters, where the rigidity of the units involved in the polymerisation reaction, is sufficiently high that these materials prove to be insoluble in most known reaction solvents. In the worst scenario, the polymerisation of such materials will not be achievable, at least not under conditions mild enough to allow the control of the monomeric sequence along the chain.

2.3 *Synthetic Routes to Ordered LCP*

2.3.1 *Regioregular LCP: route 1*

This method is based on a synthetic route proposed by Moore and Stupp[24] in the preparation of a sequentially ordered and regioregular terpolymer which exhibits liquid crystallinity. The authors previously reported previously on the synthesis of the equivalent random polymer composed of equimolar amounts of the following structural units:

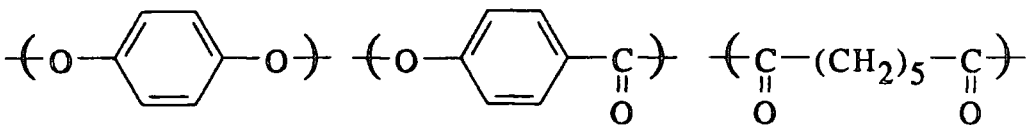

More recently the authors reported on the synthesis of a chemically regular analogue of this random polymer.[25] The resultant polymer had the following monomeric sequence along the main-chain, $(ABCBAC)_n$ which in this context will be referred to as "regio$(ABCBAC)_n$".

By replacing unit C in regio$(ABCBAC)_n$ with an isophthalic acid unit, a regioregular chemical analogue of LCP is generated. The present route attempts to synthesise such an analogue via the procedure used by Moore and Stupp where pimeloyl chloride is replaced directly by equivalent molar quantities of isophthaloyl dichloride throughout the synthesis.

Scheme A

Synthesis of the Symmetrical Monomer

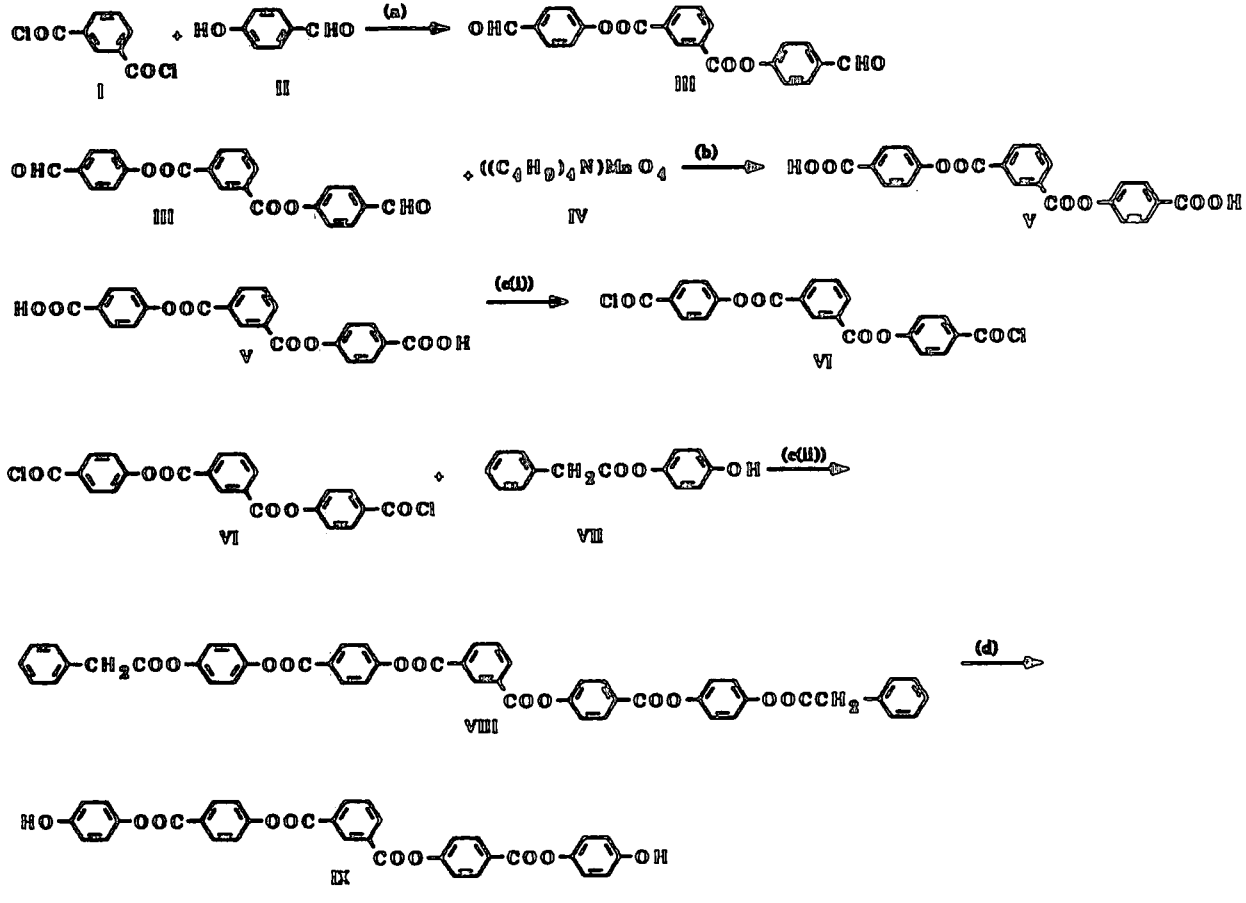

(a) CH_2ClCH_2Cl, DMAP, pyridine, 0°C (b) pyridine, 23°C
(c) (i) $SOCl_2$, DMF (catalyst) (ii) CH_2ClCH_2Cl, DMAP, pyridine, 0°C
(d) 5% Pd-C, cyclohexane, MeOH, THF

The syntheses are attempted under similar reaction conditions using interfacial polycondensation methods. Scheme A illustrates the stepwise route to the symmetric monomer used in the polymerisation reaction. The polymerisation step is shown in Scheme B.

Scheme B

Synthesis of the Regioregular LCP

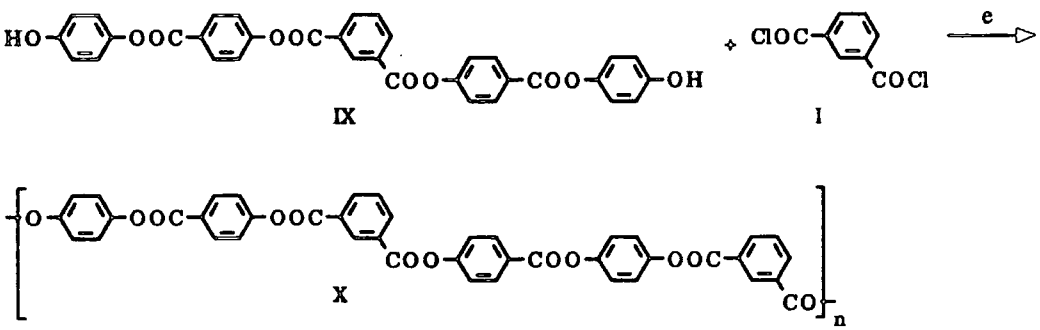

(e) $CHCl_2CHCl_2$, 130°C, 5h

2.3.2 *Sequentially Ordered LCP: route 2*

The second route to the synthesis of a chemically regular analogue of LCP is via a solution polymerisation method adopted from Jin and co-workers[25] in their synthesis of aromatic copolyesters with different monomer sequences. Initially the authors synthesised a random copolyester composed of the same three monomeric units as LCP and of practically equivalent composition. A 1:1:1 molar ratio of HBA, HQ and IPA monomers was used in the synthesis. Recent studies report on the synthesis of a more ordered version of the random copolyester of equivalent composition.[25] IPA is situated at regular intervals along the main-chain, occurring every third consecutive unit. Each of these units is separated by the unsymmetrical dimer of HQ-HBA. The dimer has equal probability of orienting in either direction (ie. HQ-HBA or HBA-HQ). The partially ordered polymer, referred to as "regular LCP", is synthesised by the polymerisation of

4-hydroxyphenyl-4-hydroxybenzoate and isophthalic acid in solution under mild conditions. The stepwise preparation of the unsymmetric monomer is shown in Scheme C and the actual polymerisation step in Scheme D.

Scheme C

Synthesis of the Unsymmetric Monomer: 4-Hydroxyphenyl-4'-carbethoxybenzoate

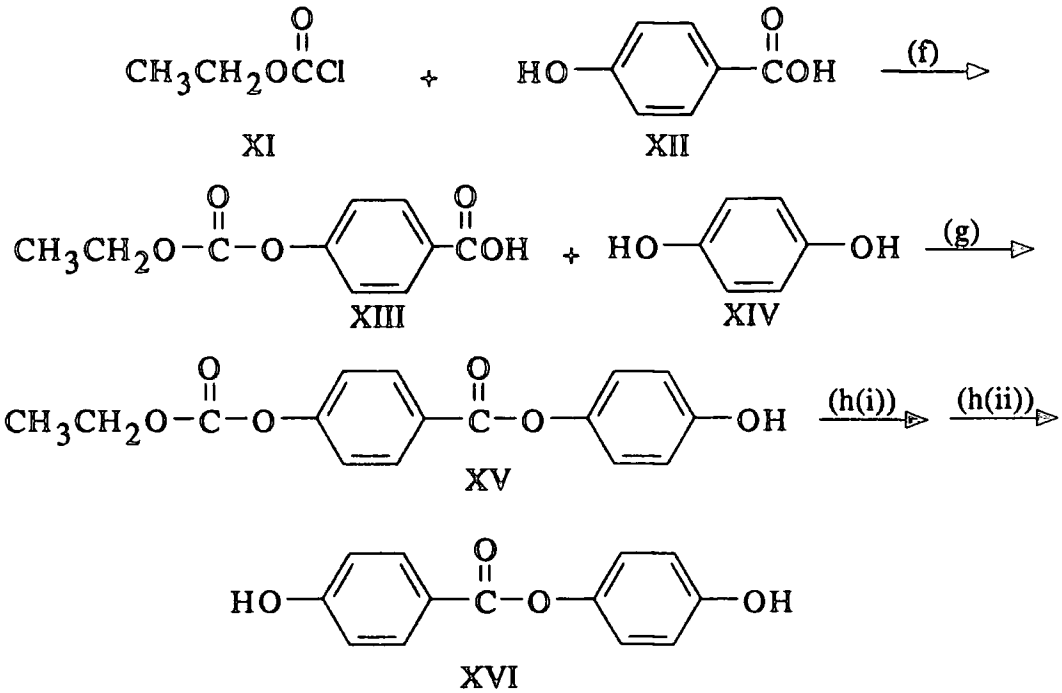

(f) NaOH(aq), 1M HCl, 0°C

(g) N_2, $SOCl_2$, Pyridine, CH_2ClCH_2Cl, 0°C

(h) DMF (i) NaOH (ii)HCl

Scheme D

Synthesis of Regular LCP

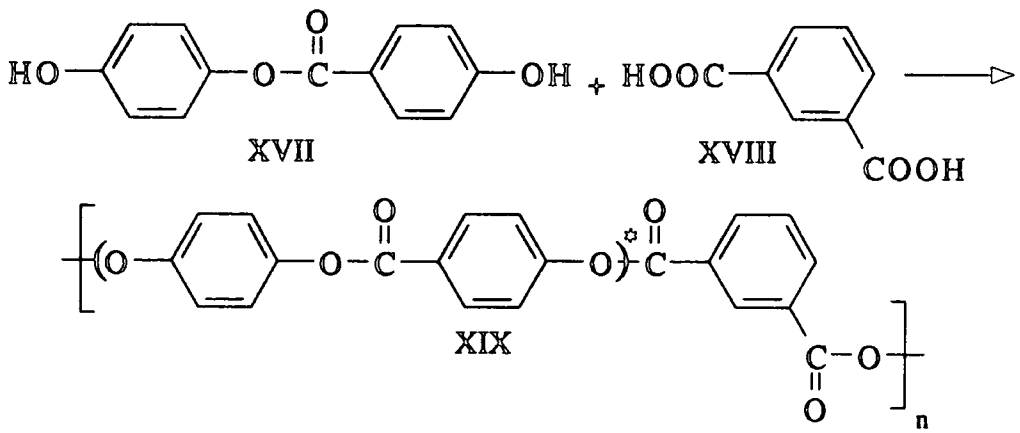

( )* : reversible dimer

2.4 *Experimental*

2.4.1 *Characterisation Techniques*

A Perkin-Elmer 577 grating infrared spectrophotometer was used to record IR spectra. Proton nuclear magnetic resonance spectra were obtained using a Bruker-AC 250 spectrometer. Elemental analysis was carried out using a Carlo Erba Strumentazoine Elemental Analyser - Model 1106. Visible Spectra were recorded using a Perkin-Elmer UV/visible spectrometer.

2.4.2 *Preparation of Regioregular Polymer via Route 1*

This section describes the attempted stepwise synthesis in the preparation of the regioregular polymer. Chemical reaction and molecular structures associated with the synthesis are shown in Schemes (A) and (B) (section (2.3.1)).

2.4.2.1 *Reagents*

Dimethylaminopyridine (DMAP), p-hydroxybenzaldehyde and isophthaloyl dichloride were purchased from Aldrich Chemical Company and were used without further purification. Pyridine, also supplied by Aldrich Chemical Company, was stirred in cerium (IV) sulphate and potassium carbonate for 24h, filtered and distilled. Dichloroethane was purchased from BDH Chemicals and purified by distillation. The organic solvents were stored over molecular sieve prior to use.

(a) *Synthesis and Purification of Bis (4-formylphenyl) isophthalate (iii)*

The synthesis was carried out according to the procedure used by Moore and Stupp[24] where pimeloyl chloride was replaced by equimolar quantities of isophthaloyl dichloride (I). 25g (90%) of crude yellow product were recovered. Purification of the product was achieved by flash chromatography using silica gel eluted with dichloromethane and ethyl acetate (96:4) yielding 23.5g (84.6%) of (II) in the form of a pure white powder. Thin layer chromatography (TLC) confirmed the absence of any impurities.

(Found: C, 18.86; H, 1.00; O; 6.86%. Calculated for ($C_{22}H_{14}O_6$): C, 18.80; H, 1.00; O, 66.89%)

δH($CDCl_3$) (Appendix A, no.1) 7.47 (4H, d), 7.78 (1H, d), 8.02 (4H, d), 8.52 (2H, d), 9.01 (1H, s) 10.05 (1H, s).

IR (cm^{-1}) (Appendix B, no.1) 1680 (aldehyde), 1760 (ester), 825 (p-phenyl), 790, 720 (m-phenyl)

2.4.2.2 *Reagents*

Tetrabutylammonium bromide and potassium permanganate were purchased from Aldrich Chemical Company and used without further purification. Benzene and dichloromethane were supplied by BDH Chemicals, purified by distillation and stored over molecular sieve prior to use.

(a) ***Preparation of Tetrabutylammonium Permanganate (iv)***

The reagent was prepared according to Sala and Sargent.[26] The crude product was purified by recrystallisation from benzene and dichloroethane, yielding 44g (80%) of pure material in the form of purple plates.

Theoretical M.P. = 120°C. Actual M.P. = 120.5°C

(Found: C, 13.81; H, 2.60; N, 1.00%, Calculated for ($C_{16}H_{36}NO_4Mn$): C, 13.67; H, 2.56; N, 1.00 %.)

δH($CDCl_3$) (Appendix A, No. 2) 1.01 (2H, m), 1.45 (2H, m) 1.67 (2H, m), 3.28 (3H, m)

IR(cm^{-1}) (Appendix B, No.2(a)) 900 ($KMnO_4$),

Visible (nm) (Appendix B, No.2(b))

2.4.2.3 *Reagents*

Pyridine and sodium bisulphite were purchased from Aldrich. The solvent was purified using the method described in section (2.4.2.1). Sodium bisulphite was used as supplied. Reagents III and IV were used as prepared.

(a) *Attempts to Synthesise Bis (4-carboxyphenyl)isophthalate) (v)*

(i) *Via Moore and Stupp Method.*[21]

The synthesis was carried out according to the authors' procedure where the dialdehyde used in their reaction was replaced by equimolar quantities of dialdehyde (III). A cream coloured product was recovered in 84% yield. The proton NMR and IR spectra contained a signal at δ=10.05 and an absorption at 1680 cm^{-1} respectively indicating that the product was unreacted starting material.

(ii) *Via method (i) in excess pyridine*

The synthesis was attempted according to method (i). However the quantity of pyridine used in the dissolution of dialdehyde (III) prior to reaction, was increased fourfold since it was suspected that reagent (III) did not dissolve completely in the initial quantity of solvent used, hence inhibiting the oxidation reaction. The quantity of HCl used in the recovery process was increased accordingly to ensure

removal of the pyridine. A cream coloured powder was recovered in a yield of 81%. The presence of a Proton NMR signal at δ=10.05 and the absence of a C=O absorption at 3000 -2500 cm^{-1} by IR indicated that the diacid had not been formed and that the product was unreacted starting material.

(iii) *Via method (ii) for an extended reaction time*

The synthesis was attempted via method (ii) using four times the previous quantity of reaction solvent. The reaction was left stirring for 20 hours, afterwhich the reaction mixture was observed to have undergone a colour change from purple to brown indicating the presence of MnO_2, a product of the oxidation of organic substrates. The resultant product gave a negative test when added to a solution of 2,4-dinitrophenylhydrazine, indicating the absence of an aldehyde. In this attempt, the diacid was prepared successfully .

(Found: C, 18.40; H; 1.00; O, 9.10%, Calculated for ($C_{22}H_{14}O_8$): C, 18.80; H, 1.00; O, 9.20%).

δH($(CD_3)_2SO$) (Appendix A, No. 3) 7.47 (4H, d)), 7.87 (1H, t), 8.05 (4H, d), 8.51 (2H, d), 8.81 (1H, s), 13.0 (1H, s).

IR(cm^{-1}) (Appendix B, No. 3) 3000-2600 (acid), 1720 (ester), 810 (p-phenyl), 800, 730 (m-phenyl).

2.4.2.4 *Reagents*

Thionyl chloride and dimethylformamide (DMF) were purchased from Aldrich Chemical Company and used without further purification. Diacid (IV) required no further purification, however the reagent was dried in vacuo at 80°C for several hours prior to use.

(a) *Synthesis of Bis(4-chloroformylphenyl)isophthalate (vi)*

Diacid (IV) (0.5g, 1.23 mmol) and thionyl chloride (40 cm^3) were placed in a dry 100 cm^3 2-neck round bottomed flask, fitted with a nitrogen inlet and a reflux condenser connected to a drying tube. After the addition of one drop of DMF, the contents were refluxed for several hours. Excess thionyl chloride was removed under vacuum, leaving a buff-coloured solid, which was washed with heptane and dried in vacuo overnight at 40°C. The acid chloride was sufficiently pure to be used in the next step.

(Found: C, 22.30; H, 1.00; O, 7.60; Cl, 5.81%. Calculated for ($C_{22}H_{12}O_6Cl_2$): C, 22.00; H, 1.00; O, 8.00; Cl, 5.83%).

IR (cm^{-1}) (Appendix B , No. 4) 1775 (acyl chloride), 1720 (ester), 820 (p-phenyl), 790, 720 (m-phenyl)

2.4.2.5 *Reagents*

Benzyl chloroformate, hydroquinone and sodium bicarbonate were purchased from Aldrich Chemical Company and used without further purification.

(a) *Synthesis of Monocarbobenzoxyhydroquinone (vii)*

The material was prepared according to the method of Olcott.[27] The crude product was recrystallised 5 times from methanol and distilled water (50:50% vol). The resulting product, in the form of pure white flat prisms, was obtained in 25% yield. Theoretical M.P. = 120-120.5°C. Actual M.P. =120.3°C.

(Found: C, 14.01; H, 1.00; O, 5.30%: Calculated for ($C_{14}H_{12}O_5$) : C, 14.00; H, 1.00; O, 5.33%)

δH($CDCl_3$) (Appendix A, No. 5) 7.42 (5H, m), 7.07 (2H, d), 6.74 (2H, d), 5.65 (1H, s), 5.26 (2H, s).

IR(cm^{-1}) (Appendix B, No. 5) 3300 (phenyl), 1700, 1200 (ester), 1220-1180 (-OH), 820 (p-phenyl), 750, 700 (m-phenyl).

2.4.2.6 *Reagents*

All organic solvents, DMAP and oxalyl chloride were purchased from Aldrich Chemical Company. Pyridine was purified as described in section (2.4.2.1). All other solvents were distilled prior to use. Reagents VI and VII were used directly, without further purification.

(a) *Attempts to Synthesise Bis[4-[[4-(benzoxyoxycarbonyl)oxy]phenoxy-carbonyl]phenyl]isophthalate (viii)*

Intermediate (VIII) could not be synthesised directly according to the method of Moore and Stupp.[24] The acid chloride used in the authors' synthesis contains a flexible pimeloate unit whereas acid chloride (VI) contains a rigid isophthalate unit. Due to the increased rigidity of the molecules in the present system, reagent (VI) proved to be only sparingly soluble in the authors' solvent system and it was anticipated that, if synthesised successfully, intermediate (VIII) would be insoluble in this solvent system as a result of its increasing rigidity. Hence an alternative solvent system was considered.

(i) *In pyridine*

Reagent (VII) (0.84g, 3.44mmol), DMAP (0.024g, 0.2mmol) and pyridine ($8.08cm^3$) were added to a $250cm^3$ 3-neck flask fitted with a nitrogen inlet and an addition funnel. The solution was cooled to 0°C and the addition funnel was charged with the diacid chloride (VI) dissolved in pyridine ($30cm^3$). This mixture was added dropwise to the stirring solution (VII). After the addition was

complete, the contents were stirred for a further 30 minutes whilst maintaining the reaction at 0°C. Excess pyridine was removed by distillation under reduced pressure and a dark brown solid was obtained by vacuum filtration. The crude product was washed with 0.5NHCl ($40cm^3$) and dried in vacuo for 24h at 40°C (76% yield). From the IR spectrum the absorption at $3300cm^{-1}$ indicated that the product was unreacted starting material.
(Found: C, 14.96; H, 1.00; O, 8.72%. Calculated for ($C_{36}H_{22}O_{10}$): C, 19.64; H, 1.00; O, 7.27%)

(ii) ***In pyridine over an extended reaction period***

Analytical tests confirmed reagent (VIII) to be pure however reagent (VI) was found to contain traces of thionyl chloride, by chemical analysis. This impurity, the only one detected, was removed by washing (VI) with liberal quantities of anhydrous ether until all traces of the material had disappeared. The reaction was carried out as in method (i) increasing the reaction time to two hours. IR analysis indicated a CH_2 absorption at $2950cm^{-1}$. The IR absorption at $3300cm^{-1}$ was absent. Chemical analysis indicated that the product (VIII) had not been isolated, if in fact it had been formed at all.
(Found: C, 12.80; H, 1.00; O, 8.74%)

(iii) ***Via direct reaction of (V) with a pre-formed thionylchloride/pyridine complex[28] (Scheme E)***

Thionyl chloride (1.298g 11 mmol) was added to a 250 cm^3 2-neck flask, fitted with an addition funnel. The contents were cooled to 0°C and the addition funnel was charged with pyridine ($10cm^3$). The pyridine was added slowly to the thionyl chloride, over a period of 10 minutes, afterwhich the reaction was stirred for a further 30 minutes. The addition funnel was then re-charged with a mixture of

diacid (V) (1.015g, 2.5mmol) in pyridine (15cm^3). The thionyl chloride/pyridine solution was maintained at 0°C and the solution of (V) was added over a period of 10-20 minutes. The cooling bath was removed and the reaction mixture stirred at room temperature for 20 minutes. Reagent (VIII) (1.22g, 5mmol) was added in one batch to the reaction mixture and the whole solution was heated between 60-80°C for 5 hours. The resulting product was obtained by solvent evaporation in the form of a creamish-white precipitate, which was washed with 0.5N HCl and recovered by vacuum filtration. The synthetic pathway taken is illustrated in Scheme E. From the IR spectrum, an O-H stretch at 3300cm^{-1}, characteristic of a phenol, confirmed that the product was unreacted starting material.

Scheme E

Preparation of VIII via direct reaction of V with a preformed thionyl chloride-pyridine complex

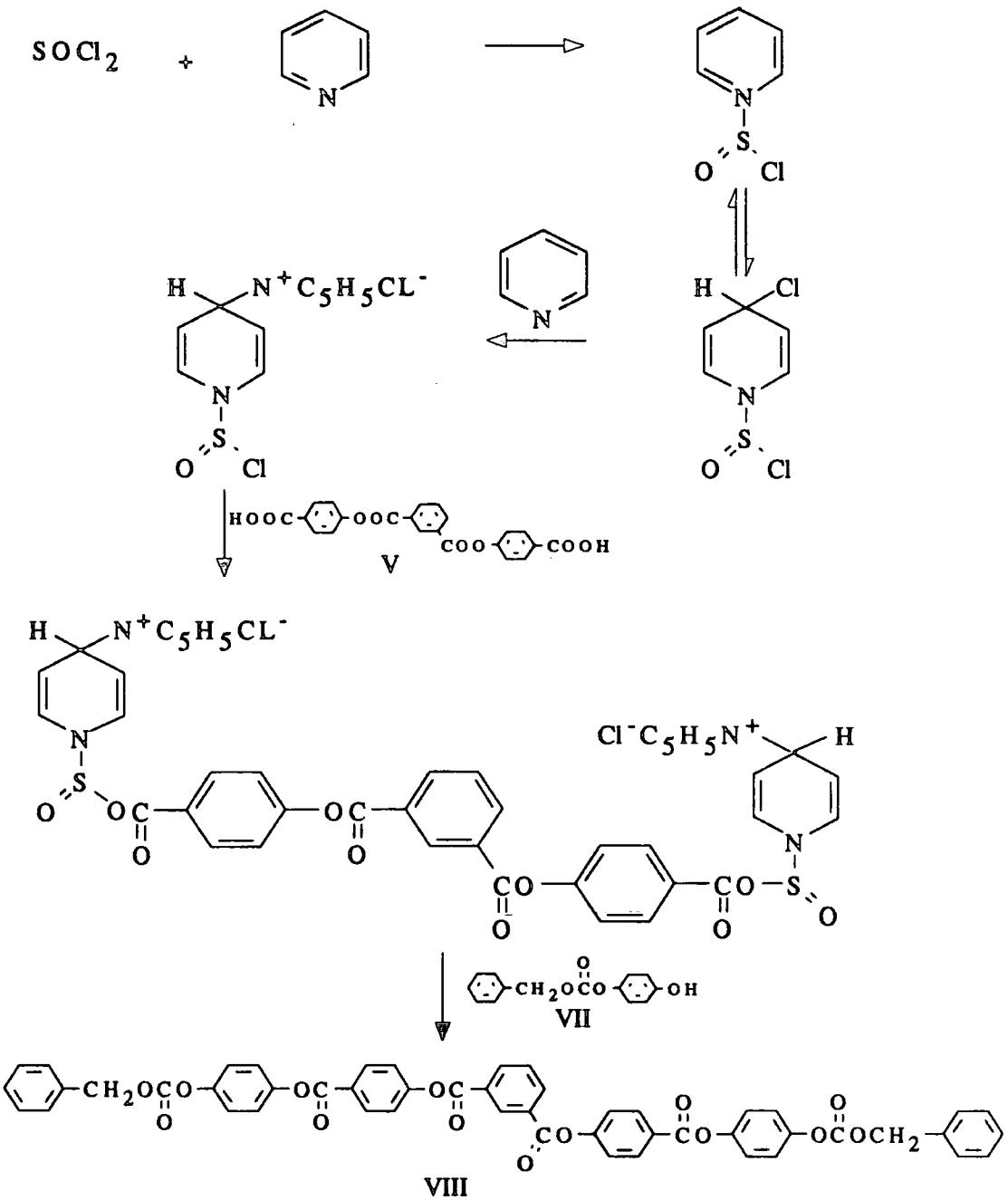

(iv) *Via oxalyl chloride using an alternative catalyst: DMAP*

Diacid chloride was prepared by refluxing (V) in excess oxalyl chloride for several hours in the presence of 0.005g DMAP. Excess oxalyl chloride was removed by distillation at reduced pressure under nitrogen. The reaction was continued according to the procedure in method (ii), however the reaction time was increased to 4 hours and maintained at room temperature after the addition of solution (VI) to solution (VII) was complete. A buff-coloured precipitate was recovered in 72% yield. The presence of a phenolic absorption at 3300cm^{-1} in the IR spectrum, confirmed that the product was unreacted starting material. Again the synthesis of (VIII) proved unsuccessful. The experiment was abandoned at this stage.

2.4.3 *Preparation of Regular Polymer via Route 2*

This section describes the attempted stepwise synthesis of the regular polymer. The routes taken and the molecular structures of the reagents are shown in Schemes C and D in section (2.3.1).

2.4.3.1 *Reagents*

Ethyl chloroformate and p-hydroxybenzoic acid (HBA) were purchased from Aldrich Chemical Company and used without further purification. Sodium hydroxide pellets and acetone were purchased from BDH Chemicals. Acetone was distilled before use.

(a) *Synthesis of p-Carbethoxybenzoic Acid (xiii)*

The material was prepared according to Cowie and co-workers.[29] The crude product was purified by recrystallisation from water and acetone yielding a white powder (82%). Theoretical M.P. =158°C. Actual M.P. =158.2°C

(Found: C, 11.90; H, 1.00; O, 7.80%. Calculated for ($C_{10}H_{10}O_5$): C, 12.00; H, 1.00; O, 8.00%).

δH(acetone-d_6) (Appendix A, No. 6) 10.3 (1H, s), 8.07 (2H, d), 7.601 (2H, d), 4.30 (2H, t), 1.29 (3H, d).

IR (cm^{-1}) (Appendix B no.6) 3000-2500- (-OH), 2980, 1420, 1370 (C_2H_5-), 1680, 1170 (ester), 840 (p-phenyl).

ms (m/e) 211, 138, 121, 93, 81

2.4.3.2 *Reagents*

Thionyl chloride, hydroquinone and sodium bicarbonate were purchased from Aldrich Chemical Company and used directly as supplied. Pyridine, also purchased from Aldrich, was purified using the method described in section (2.3.1). Acetone and 1,2-dichloroethane were supplied by BDH Chemicals. The solvents were distilled before use. Reagent XII was used without further purification.

(a) ***Attempts to Synthesise 4-Hydroxyphenyl -4-carbethoxybenzoate (xv)***

(i) ***In pyridine/thionyl chloride***

Thionyl chloride (1.83cm^3, 25mmol) was added to a 250cm^3 3-neck flask, fitted with a mechanical stirrer, an addition funnel, a nitrogen inlet and a drying tube. The contents of the flask were then cooled to 0°C with constant stirring. The addition funnel was charged with pyridine (8.01cm^3, 100mmol) which was added

dropwise to the stirring mixture maintaining a temperature of 0-5°C for 30 minutes. P-carbethoxybenzoic acid (XII) (5.00g, 24mmol) dissolved in pyridine ($15cm^3$) was added dropwise to the pyridine/thionyl chloride mixture over a period of 60 minutes. To a $100cm^3$ single neck flask, was added hydroquinone (XIV) (7.93g, 72mmol) dissolved in pyridine ($20cm^3$). This solution was added dropwise to the stirring solution of XIII in the pyridine/thionyl chloride mixture. On completion of the addition, the mixture was allowed to stand overnight and the solvent was removed using a rotary evaporator. The crude product was washed with distilled water, followed by a dilute aqueous $NaHCO_3$ solution and again with distilled water several times. A light brown precipitate in a yield of 92% was obtained. The IR spectrum resembled that of the starting material, however the sharp phenolic peak at $3300cm^{-1}$ was absent, as well as the broad band characteristic of carboxylic acids ($3000\text{-}2500cm^{-1}$) hence it was proposed that through the dropwise addition of (XIII) to (XIV), disubstitution of the hydroquinone had occurred.

(Found: C, 16.84; H, 1.00; O, 7.80%. Calculated for ($C_{16}H_{14}O_6$): C, 13.71; H, 1.00; O, 6.86%).

(ii) *Via the method of Jin et al*[25]

The material was prepared according to Jin and co-workers[25] yielding a brown oil which was reprecipitated from acetone and distilled water several times. A fine brown powder was recovered in 40% yield.

IR(cm^{-1}) (Nujol) (Appendix B, No.7) 3300 (-OH) 1760, 1730, 120 (ester), 810 (p-phenyl).

^1H NMR analysis suggests that there are impurities present in the system. Two hydroxyl signals suggest that hydroquinone may be present. IR analysis confirms the presence of a phenolic absorption which is attributed to the desired product (XV). Mass spectrometry also confirms the presence of XV. However it is

apparent that one or more impurities are present. TLC tests in a 50:50 vol.% acetone/hexane mixture indicated 3 spots, 2 of which corresponded to the starting materials (XIII) and (XIV).

(iii) *Via acid chloride*

To a 100cm^3 single neck flask, fitted with a reflux condenser and drying tube, was added (1.019g, 4.85mmol) of (XIII) and thionyl chloride (20cm^3). The mixture was refluxed overnight after which excess thionyl chloride was removed by distillation under reduced pressure. From IR analysis (Appendix B, No.8) the presence of a COCl absorption at 1770cm^{-1} and the absence of the -OH absorption at 3000-2500cm^{-1} confirms that the acid chloride has been formed. Assuming 100% conversion, the acid chloride (1.8g, 4-85mmol) was dissolved without purification, in 1,2-dichloroethane (20cm^3). Hydroquinone (XIV) (2.67g, 24.25mmol) was added to a separate flask, the acid chloride solution was added dropwise to the solution of (XIV). The synthesis was continued using the procedure described in method (i). The crude product was stirred in an aqueous sodium bicarbonate solution for 4 hours, recrystallised from acetone and water and dried in vacuo at 40°C for 24 hours.

(iv) *Via acid chloride for an extended reaction time*

The synthesis was carried out according to method (iii) however the reaction time was increased to 4 hours. All solvents, including thionyl chloride, were dried and freshly distilled before use. The product, a brown oil, was recovered by vacuum filtration and washed repeatedly with aqueous dilute sodium bicarbonate solution and distilled water (Found. C, 15.0; H, 1.0; O, 6.8%. Calculated for ($C_{16}H_{14}O_6$) : C, 13.7; H, 1.0; O, 6.8%). Mass spectrometry indicated the presence of hydroquinone. Column chromatography was used in an attempt to separate the

products. The column was packed with silica gel eluted with a 50:50 vol% acetone/hexane mixture. The product, a white powder, was recovered by solvent evaporation in a yield of 27%. (M.P. = 240°C). Only one spot was present on the TLC plate. These tests were carried out using the method described in section (2.4.3.2(a)(i)). A light brown solid was obtained in a yield of 61%.

δH (acetone-d_6) (Appendix A, No.9) 9.65(s), 8.91(d), 8.74(d), 8.02(d), 7.05(m), 5.00(d), 3.61(s), 2.01(m).

^{1}H NMR analysis suggests that product XV has been synthesised again however several impurities are present.

(v) *In triethylamine*

The synthesis was carried out according to method (ii) using equivalent quantities of triethylamine, as opposed to pyridine as the reaction solvent. The crude product was recrystallised 3 times from acetone and water. A cream-coloured powder was recovered in 34% yield. From IR spectrometry an -OH absorption present at 3420cm^{-1}, characteristic of formate esters, suggested that product XV had been formed. These results were confirmed by the presence of the characteristic peak by mass spectrometry at m/e = 320.

2.5 *Conclusions*

Attempts to synthesise the regioregular analogue of LCP via the interfacial polycondensation of a symmetric monomer with isophthaloyl dichloride proved unsuccessful. With each synthetic step to the symmetric monomer, the molecule increased in length and rigidity. The failed attempts at subsequent syntheses are attributed to the inability of the intermediates to react due to their insolubility in most reaction solvents, hence the experiment was abandoned.

Attempts to synthesise the partially-ordered analogue of LCP, proved difficult. During the stepwise synthesis to the monomeric diol, intended to be used in the final solution polymerisation reaction, impurities present in the system inhibited continued reaction. Due to lack of time and exhaustive attempts at these syntheses, again it was decided that the experiment should be abandoned.

2.6 *References*

(1) Roviello, A., Sirigu, A., *J. Polym. Sci. Polym. Lett. Ed.* 13 456 (1975)

(2) Roviello, A., Sirigu, A., *Eur. Pol. J.* 15 61 (1979)

(3) Strzelecki, L., Van Luyen, D., *Eur. Pol. J.* 16 299 (1980)

(4) Blumstein, A., Siraramakrishnan, K. N., Blumstein, R. B., Clough, *S. B., Polymer* 23 47 (1982)

(5) Asrar, J., Toriumi, H., Watanabe, J., Krigbaum, W. R., Ciferri, A., Preston, J., *J. Polym. Sci., Polym. Phys. Ed.* 21 1119 (1983)

(6) Ober, C., Jin, J-I, Lenz, R. W., *Adv. Polym. Sci.* 59 103 (1984)

(7) Noel, C., Monnerie, L., Achard, M. F., Hardoin, F., Sigaud, G., Gasparoux, H., *Polymer* 22 578 (1981)

(8) Zheng-Min, S., Kleman, M., *Mol. Cryst. Liq. Cryst.* 111 321 (1984)

(9) Hardoin, F., Achard, M.F., Gasparoux, H., Liebert, L., Strzelecki, L., *J. Polym. Sci., Polym. Phys. Ed.* 20 975 (1982)

(10) Kotliar, A. M., *Macromol. Rev.* 16 367 (1981)

(11) Jin, J. I., Lenz. R. W., *Macromolecules* 14 1405 (1981)

(12) Lenz, R. W., *Polym.* 1 105 (1985)

(13) Bhaskar, C., Kops, J., Marcher, B., Spangaard, H., in *"Recent Advances in Liquid Crystalline Polymers"* Chapoy, L., (ed) Elsevier Applied Science Publishers NY (1985)

(14) Blumstein, A., Asrar, J., Blumstein, R. B., in *"Liquid Crystals and Ordered Fluids, Volume 4"* Griffin, A. C., Johnson, J. F., (eds) Plenum Publishing Corp. NY (1984)

(15) Krigbaum, W. R., Lader, J. J., Ciferri, A., *Macromolecules* 13 554 (1980)

(16) Ober, C, Lenz, R. W., Galli, G., Chiellini, E., *Macromolecules* 16 1034 (1983)

(17) Dobb, M. G., McIntyre, J. E., *Adv. Polym. Sci.* 60/61 61 (1984)

(18) Uematsu, I., Uematsu, Y., *Adv. Polym. Sci.* 59 37 (1983)

(19) Jackson, W. J., Kuhfuss, H. F., *J. Polym. Sci. Polym. Chem.* Ed. 14 2043 (1976)

(20) Morgan, P. W., *"Condensation Polymers by Interfacial and Solution Methods"* Interscience Publishers, NY (1965)

(21) Higashi, F., Kokubo, N., Goto, M., *J. Polym. Sci., Polym. Chem. Ed.* 18 2879 (1980)

(22) Lenz, R. W., Schuler, A. N., *J. Polym. Sci., Polym. Symp.* 63 343 (1978)

(23) Smith, J. G., Kiber, C. J. Shulken, R. M. Jr., *Kingsport, T. U.S.Pat.* 3,483,157 (1969)

(24) Moore, J. S., Stupp, S. I., *Macromolecules* 21 (5) 1217 (1988)

(25) Jin, J. I., Lee, S. H., Park, J. J., *Polymer Bulletin* 20 19 (1988)

(26) Sala, T., Sargent, M. V., J. C. S. *Chem. Comm.* 253 (1978)

(27) Olcott, H. S. J. *Org. Chem.* 59 392 (1937)

(28) Higashi, F., Mashimo, T., Takahashi, I., *J. Polym. Sci., Polym. Chem. Ed.*, 24 97 (1986)

(29) Cowie, J. M. G. *Macromolecules* 21 (9) 2865 (1988)

(30) McLenaghan, A. D. W. M., *Ph. D. thesis, University of Strathclyde* (1991)

Chapter 3

Thermal Analysis

3.1 *Introduction*

The thermal characterisation of polymeric materials covers several aspects of materials science and a wide variety of thermal techniques are available which can be applied to the understanding of these materials.[1-3] The present chapter provides an insight into the techniques used and the results obtained in the thermo-structural characterisation of LCP.

It is impossible to discuss the results obtained from thermal analysis, a macroscopic technique, without an initial understanding of the molecular structure of matter, in other words, the microscopic structure. Two techniques which provide such information, relevant to the analysis of polymers, are optical microscopy and differential scanning calorimetry (DSC). In the present study a combination of these techniques is used to develop an understanding of the structure-property relationships in LCP. Optical microscopy provides information regarding the structure of polymers ie. the polymer morphology, whereas DSC, with the aid of supporting analytical techniques, can measure such parameters as glass transition temperature, crystalline melting point and heat of melting as well as identifying thermal degradation and oxidation reactions, rapidly and conveniently. In the study of liquid crystal polymers, multiple thermal transitions are often obtained[4,5] which require complementary hot-stage microscopy techniques in order to identify the phases formed.

The thermal characterisation of LCP involves detailed studies using both techniques however, due to the diverse and individual nature of each, they are dealt with separately. Consequently this chapter has been subdivided into two sections. The first section considers the techniques and practical aspects of optical microscopy, its applications to liquid crystal polymers and the results obtained pertaining to the morphology of LCP powder, solvent-cast films and fibres. A polarising optical microscope equipped with a hot-stage is used in an attempt to gain qualitative information on any morphological changes and phase transitions occurring as a function of temperature and to identify the type of mesophase formed. In addition, annealing and quenching effects are studied.

The second section provides a brief introduction to thermal analysis, concentrating on Differential Scanning Calorimetry and its use in the characterisation of LCP. The thermal transitions occurring in the polymer were identified from analysis of both the heating and cooling curves obtained with the aid of the microscopy results discussed in sections (3.4.1) and (3.4.2). It is well established that the thermal history of a polymeric material can alter its thermal behaviour significantly,[6-9] hence a study of the effects of varying the heating and cooling rates, in addition to the effects of annealing the LCP samples, is carried out.

As in section I, LCP powders, films and fibres are studied. The succeeding chapter deals with the thermo-structural characterisation of LCP using wide angle x-ray scattering techniques (WAXS); another common supporting characterisation technique used in polymer science. WAXS studies discussed in Chapter 4, are both relevant and complementary to the ultimate thermal characterisation of LCP however, due to the scope of this work being slightly different to that of the present chapter, it was felt that the former merited a separate study. Viney and Windle in their study of the mesomorphic polymer X7G, manufactured by Tennessee Eastman Company,[10] observed the formation of thick and thin regions of the materials in the melt when studied between glass slides.[11] The thick region showed little structural detail compared to the thin region, which exhibited a defined nematic texture. It is important to be aware of the significant variation in textures with the thickness of specimen under observation using polarising microscopy studies.

3.2 *Section I: Optical Microscopy*

3.2.1 *Introduction and Applications to Liquid Crystal Polymers*

Microscopy is defined as "the study of the fine structure and morphology of objects with the use of a microscope". The technique of light microscopy has been established for over 200 years and since the earliest days of polymer science, some 50 years ago, the light microscope has played an important role in determining the microstructure and texture of bulk polymers. The theory of light microscopy is well established and many texts deal with the fundamental and practical aspects of this technique.[12-14]

In the optical microscope, an image is produced by the interaction of light with an object or specimen. This image can reveal fine detail either in or on the specimen. Magnifications over the range x2 to x2000 are obtainable. A schematic diagram illustrating the major components of a transmission light microscope together with relative positions of these components and also the path taken by the rays of light passing from the lamp filament up through the microscope to the eyepiece, is shown in Figure 3.1.

Polarising microscopy is the study of the microstructure of objects using their interaction with polarised light.[15] The technique has been used widely in the study of polymers and liquid crystals.[16] In addition to the basic features of the light microscope (Figure 3.1), the polarising microscope has two polarisers: the first, positioned in the substage condenser and the second above the objective lens. The instrument is also equipped with a rotatable stage. The polarisers are made of polaroid film which transmit plane polarised light. In general the arrangement in the microscope is crossed polarisers. When the polarisers are crossed their vibration directions are orthogonal and consequently the analyser cannot transmit any light transmitted from the polarisers. Hence if no specimen is present or an isotropic specimen is being studied, the field of view will appear dark. In contrast optically anisotropic, birefringent materials may

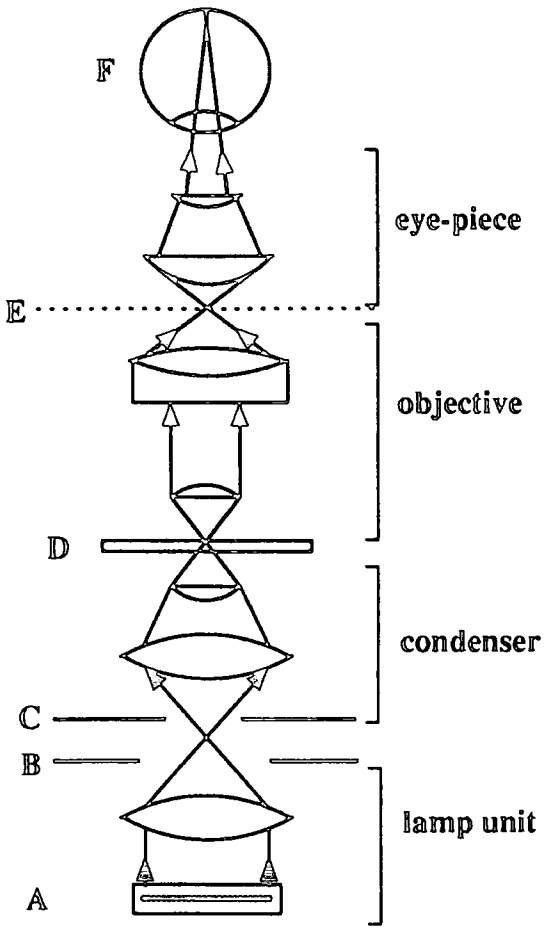

Figure 3.1 Schematic diagram of a standard transmitted light microscope A, lamp; B, Field Iris Diaphragm; C, Aperture Iris Diaphragm; D, Specimen; E, Primary Image Plane; F, Eye

appear bright between crossed polarisers. When light is passed through birefringent materials, it is split into two plane polarised waves which vibrate in planes perpendicular to one another; the refractive index of the material is different in direction. Anisotropic specimens can appear brightly coloured when viewed between crossed polarisers using white light. The colours are referred to as polarisation or interference colours.[17] The polarising microscope can therefore be used to image and characterise ordered regions in polymers provided that the sample is optically anisotropic. The uses of polarised light in polymer science are determined by the type of polymer under examination (eg. semi-crystalline or amorphous). In semi-crystalline polymers the most common structural feature identified is the spherulite, a 3-dimensional assembly of

semi-crystalline material which has grown radially from the central nucleus. The organisation of the molecular chains in these features has not as yet, been clearly established.[18,19] In general amorphous polymers appear dark between crossed polarisers unless other forms of birefringence are present eg. strain birefringence.[20,21] The present work is concerned with the use of this technique in the study of a liquid crystal polymer. A brief overview of the information obtainable is given below.

Molecular order in liquid crystal polymers is studied using polarised light microscopy. The general procedure and possible images obtained have been discussed in detail in the literature.[16,22,23] Windle and co-workers[24] have studied thermotropic copolyesters using this technique. The authors concluded that the data obtained is frequently difficult to interpret due to the wide range of textures observed. The molecular ordering in a thermotropic liquid crystal polymer decreases generally as a function of increasing temperature. The following sequence of phase changes usually occurs however, not all possible phases may be apparent.

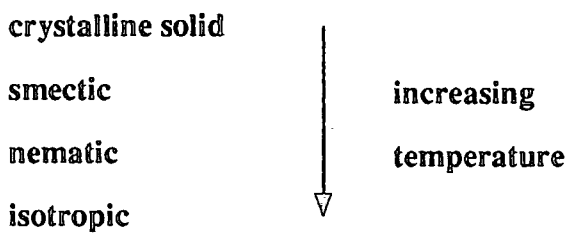

Furthermore the liquid crystalline phase may be observed on cooling, as well as on heating, from the melt. Polarising hot-stage microscopy can be used in the identification of optical textures in the liquid crystals. These unique textures are observed for the various structural orientations of the three classes of liquid crystals, namely: nematic, cholesteric and smectic. Liquid crystal polymers generally exhibit the same textures as their monomeric counterparts. Nematic crystals are identified by a dark schlieren texture (Figure 3.2(a)). Cholesteric phases display a planar Grandjean or fingerprint texture, within which reflection colours are displayed (Figure 3.2.(b)). The textures of polymeric smectic phases are non-planar and consist of smectic layers. These phases resemble the focal conic and fan-shaped patterns observed for low molecular weight smectics (Figure 3.2(c)).

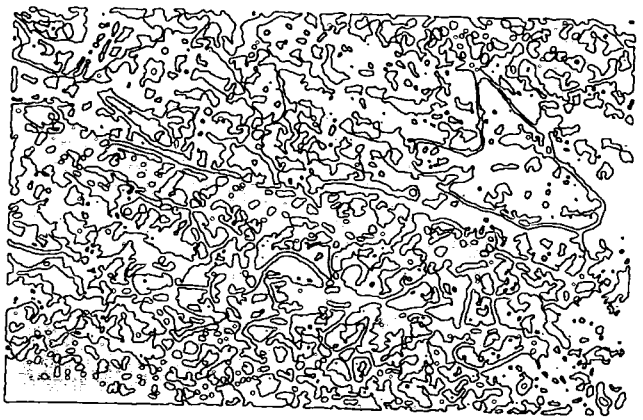

a) Nematic

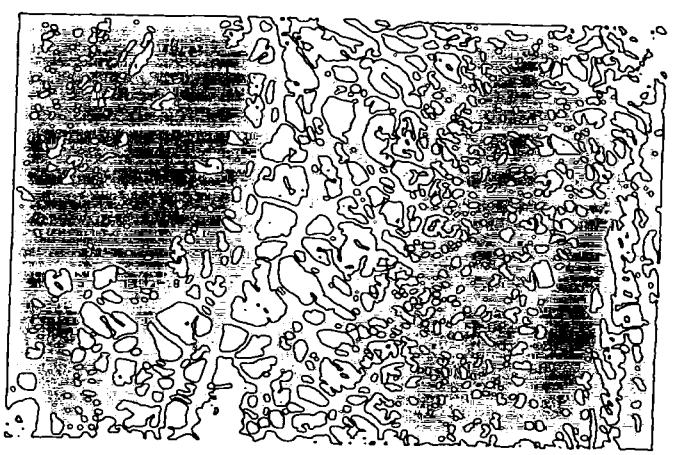

b) Cholesteric

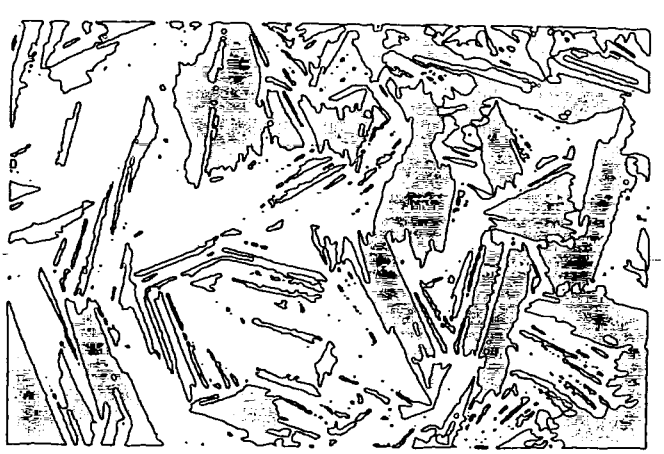

c) Smectic

Figure 3.2: Liquid crystal polymer textures veiwed with plane polarised light

3.2.2 *Practical Considerations*

There are very few special instrumental requirements for the use of practical microscopy in the study of polymers in general. However a couple of problems encountered which are valid to the present study are worth mentioning. Firstly, sample preparation; a very important step in the study of materials by microscopy, must be carried out with care and precision in order to obtain accurate, unambiguous results. The present study examines LCP in the form of powders and fibres. In general, these forms are best studied using Scanning Electron Microscopy,[25] however they are adequate for the present examinations. Secondly, problems arise using the light microscope since, as the resolving power increases the depth of field decreases, and consequently only a very small area of the surface is in focus at any one position of the stage. As a consequence, the specimen particles in focus may not be representative of the whole area of the sample.

3.3 *Experimental*

3.3.1 *Instrumentation*

Hot-stage microscopy experiments were carried out using an Olympus BH-2 polarising microscope equipped with a Linkam THM600 Hot-stage and Linkam TMS1 Temperature Control. Optical micrographs were recorded using a JVC video camera connected to a Sony Colour Video Printer UP-5000P and Sony Colour Monitor KX14CP1.

3.3.2 *Sample Preparation*

(a) *Polymer Purification*

LCP was purified by dissolving the as-received pellets in an 80:20% volume mixture of trifluoroacetic acid (TFA) and dichloromethane (DCM) respectively. The mixture was centrifuged for 40 minutes at 15°C and a speed of 8000rpm using a Beckmann J2-21M/E centrifuge.

The supernatant liquid was decanted into an excess volume of methyl ethyl ketone (MEK), a non-solvent, resulting in precipitation of the polymer. The white ribbon-like product was dried in vacuo at ambient temperatures for a period of 12 hours.

(b) *Powder Specimens*

Purified LCP was ground to a very fine powder in a mortar and pestle with dry ice. Using a small spatula, a few grains of polymer were sprinkled onto a glass coverslip and a second coverslip placed on top. The assemblage was then mounted in the hot-stage, ready for analysis to begin.

(c) *Film Specimens*

Purified LCP (1g) was added to a mixture of 95:5% volume of TFA/DCM. The solvents were distilled and dried prior to use. The polymer mixture was allowed to stand for 48 hours to ensure complete dissolution. A few drops of the resulting solution were placed on a glass coverslip and the solvent was allowed to evaporate, producing thin polymer films. These films were adhered to the coverslips and placed in a vacuum oven at 40°C for several hours to ensure complete evaporation of the solvent. The specimens were then removed from the oven and a second coverslip was placed directly over the film. The samples were then ready to be mounted on the hot-stage.

(d) *Fibre Specimens*

Purified LCP was melted at a temperature of 300°C on an aluminium sheet placed on a hot-stage. The temperature was raised gradually to 330°C until fine, flexible, even fibres could be withdrawn rapidly from the melt using fine tweezers. A thermocouple was used to calibrate the hot-stage and to record the temperature throughout the fibre pulling process. Each fibre was approximately 0.2mm in diameter. A fibre of about 10mm in length was placed between two glass coverslips and placed in the hot-stage sample holder.

3.4 *Results And Discussion*

3.4.1 *Thermal Behaviour of LCP Powder*

Optical Micrographs illustrating the morphological changes and phase transitions occurring in LCP powder as a function of temperature are given in Figure 3.3. The primary heating cycle is run over the range, 25-450°C. At ambient temperatures (25°C) a very small amount of birefringence is observed between crossed polars, indicating a slight degree of crystallinity in the specimen. The birefringence increases slowly as a function of temperature. At 338°C, the field of view is bright and slightly coloured. Strong birefringence is observed at 362°C. At this temperature the specimen becomes molten and begins to flow. Bright colours, typical of mesophases in thermotropic polyesters, are observed however the texture of the mesophase cannot be identified clearly. The field of view remains extremely bright to about 400°C afterwhich it begins to darken. The final micrograph in Figure 3.3(b), was taken without using crossed polars, to emphasise the formation of a clear melt ie. the isotropic phase, at 434°C. At this temperature, the specimen appears completely dark between crossed polars. Degradation occurs at 450°C, indicated by the presence of large voids in the specimen.

3.4.2 *Effects of Reheating LCP Powder*

LCP was heated into the anisotropic melt. Optical micrographs of the primary heating cycle are shown in Figure 3.4(a). The field of view appears completely dark at 126°C however, small regions of birefringence develop in the specimen as a function of temperature and at 337°C, the anisotropic melt was observed. The specimen was held at constant temperature afterwhich it was quenched rapidly (100°C min^{-1}) to ambient temperatures. On quenching, the anisotropic phase is "frozen-in"; a feature common to thermotropic polymers. Optical micrographs of a second heating cycle, carried out after quenching are given in Figure 3.4(b).

FIGURE 3.3(a) LCP POWDER (heating run 1)

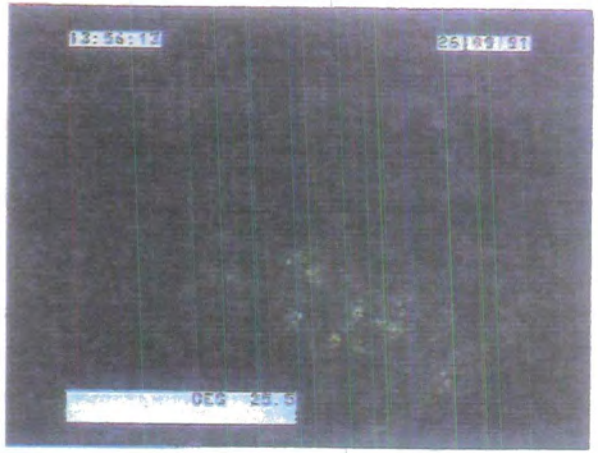

25.5degC

184.2degC

274.6degC

320.6degC

(x 400) crossed polars

FIGURE 3.3(b) LCP POWDER (heating run 1 (cont.))

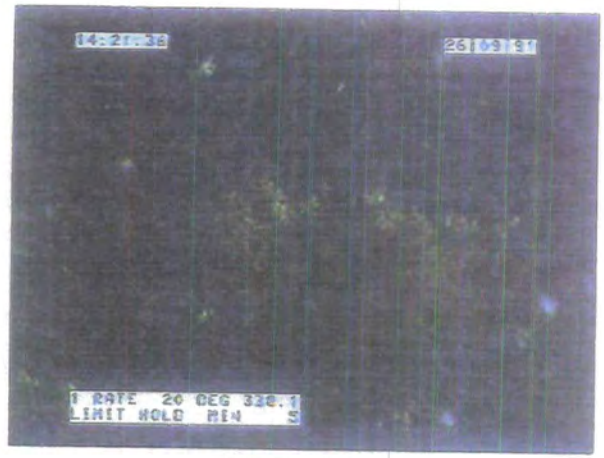

338.1degC

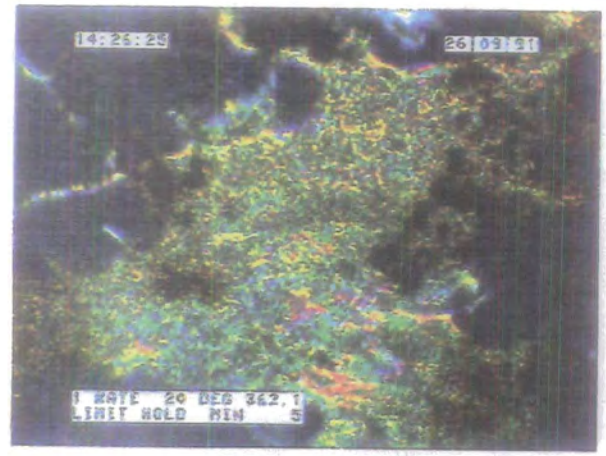

362.1degC

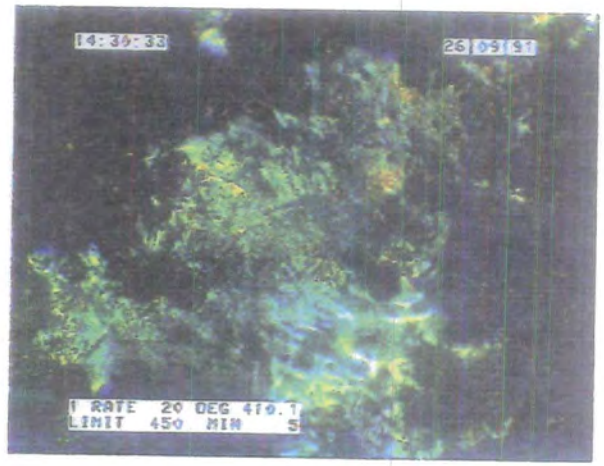

410.1degC

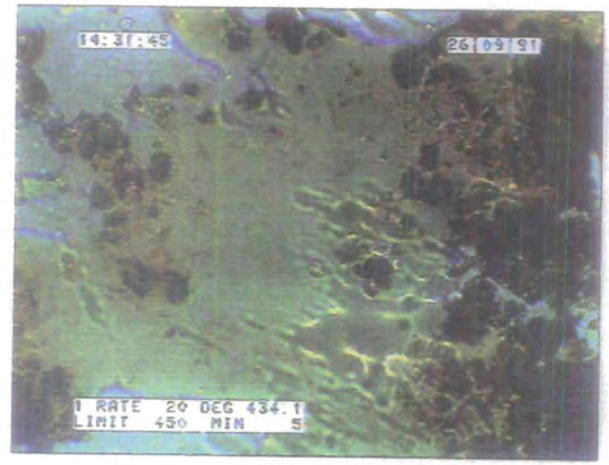

434.1degC

(x 400) crossed polars

FIGURE 3.4 LCP POWDER (effects of reheating)

(a) before quench

126.9degC

337.7degC

(b) after quench

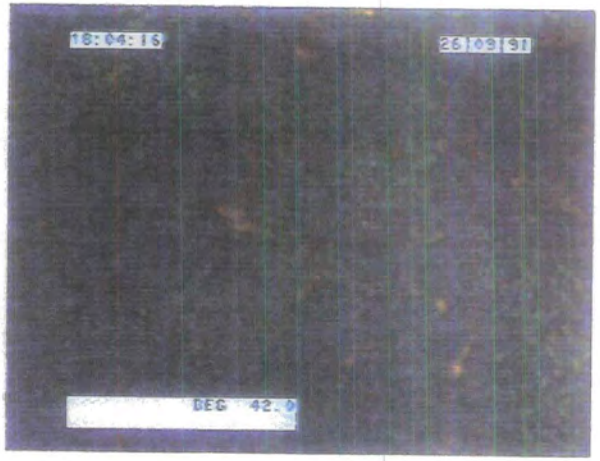

42.0degC

197.1degC

(x 400) crossed polars

FIGURE 3.4 (continued)

(b) after quench

350.5degC

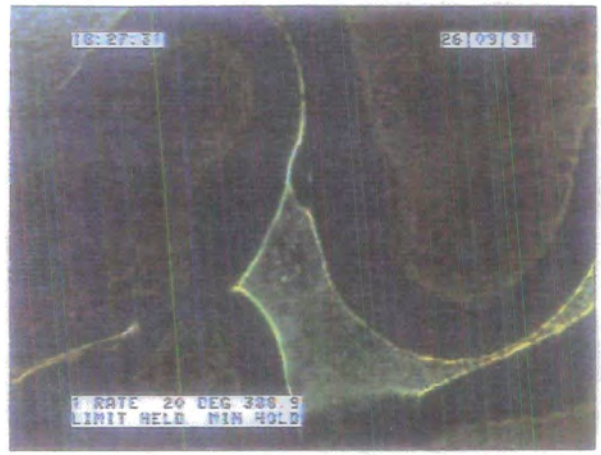

388.9degC

(b) after quench

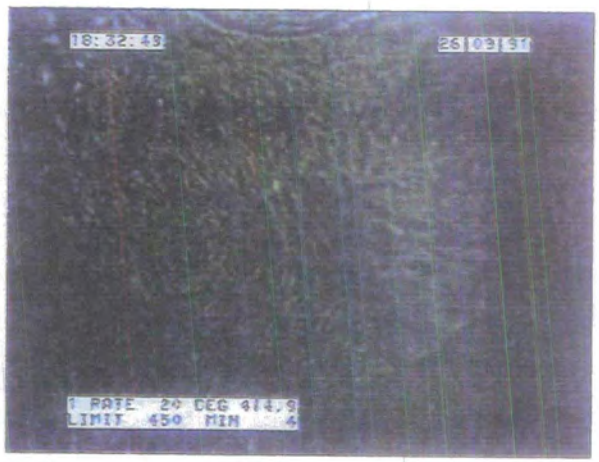

414.9degC

449.6degC

(x 400) crossed polars

The specimen appears strongly birefringent at room temperature. This birefringence is maintained throughout the heating cycle. The specimen begins to flow at 350°C and a fine thread-like pattern, typical of a nematic phase is observed. At 388°C two phases begin to develop indicated by the formation of bright and dark regions. It is proposed that these phases are due to both anisotropic and isotropic regions present in the sample. The possibility of dark regions resulting from homeotropic alignment of LCP between the glass coverslips has been dismissed since, on touching the upper coverslip, the field of view remained dark.[26] The specimen began to degrade rapidly at 410°C. Complete degradation had occurred by 450°C. A transition from the nematic to the isotropic melt is not observed.

3.4.3 *Thermal Behaviour of LCP Thin Films*

Heating runs were carried out on a thin LCP film over the range 25-500°C. Figure 3.5 illustrates the morphological changes and phase transitions occurring in the specimen as a function of temperature. At 28°C, no birefringence is observed in the specimen. Random coloured regions begin to develop as a function of temperature above 180°C and at 295°C, the sample exhibits brightly coloured birefringence. The specimen begins to flow at 330°C and the colours become stronger. The fine threadlike pattern, observed at 330°C becomes increasingly dense as a function of temperature. The field of view remains bright at 399°C. At this temperature a thinner region of the same specimen, viewed between crossed polars, exhibits the characteristic schlieren texture typical of nematic melts. As temperature is increased further, the field of view begins to darken. Complete degradation has occurred by 470°C.

3.4.4 *Thermal Behaviour of a "Thick" LCP Film*

The thickness of the sample was not measured however for simplicity the film, known to be significantly thicker than the specimen studied in section (3.4.3), will be referred to as

FIGURE 3.5(a) THIN FILM (heating run 1)

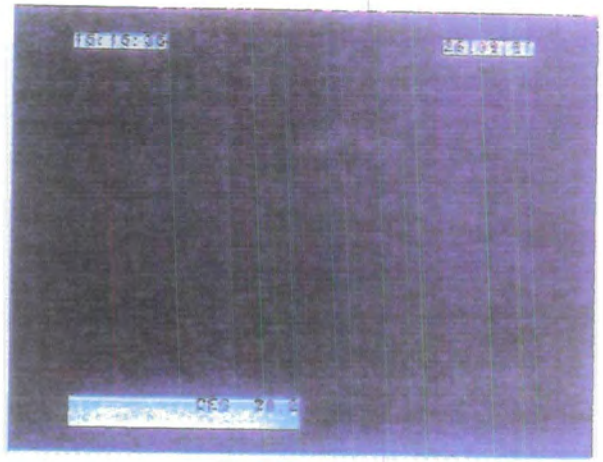

28.2degC

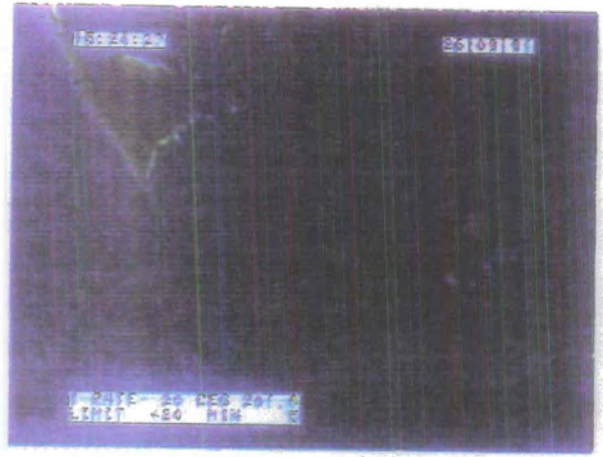

201.0degC

295.4degC

330.7degC

(x 400) crossed polars

FIGURE 3.5(b) LCP FILM (heating run 1 (cont.))

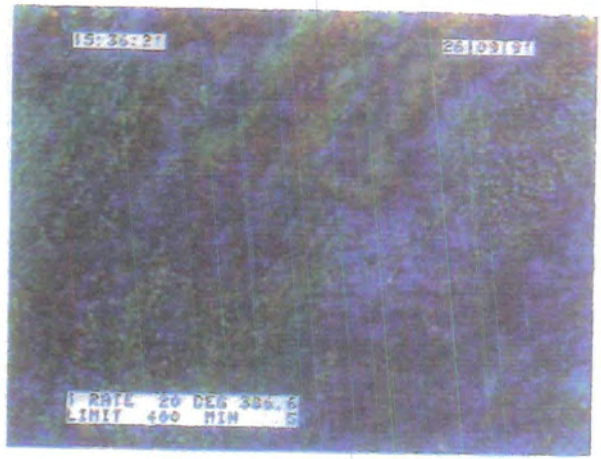

386.6degC

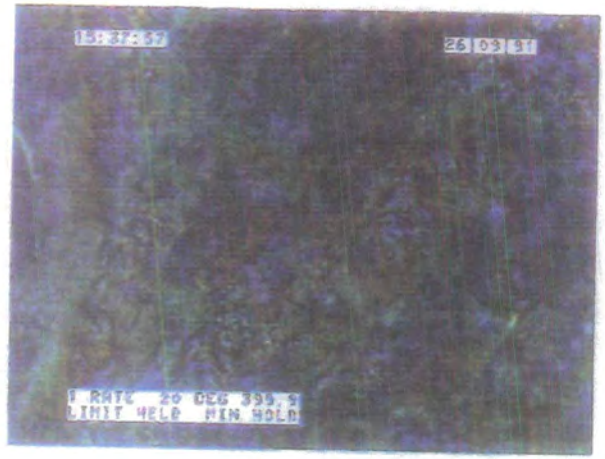

399.9degC

399.9degC

470.8degC

(x 400) crossed polars

the thick film. The specimen appeared completely dark between crossed polars at ambient temperatures. No birefringence was observed in the sample below 200°C. Above this point the birefringence increased as a function of temperature. The anisotropic melt forms at 338°C and the sample appears highly coloured. At this point a vague thread-like pattern begins to develop and becomes increasingly dense as a function of temperature. This pattern is still apparent in the birefringent material at 381°C.

The transition from the anisotropic to the isotropic melt, observed in LCP powder specimens, is not observed prior to degradation. The latter process begins at 410°C which is apparent from the rapid formation of large voids in the specimen.

The results obtained in the present section are compared to those obtained in section (3.4.3) for a thinner film. Although the actual specimen thicknesses were not measured, the results confirm that the optical behaviour varies according to the thickness of the specimen. Optical transitions are more apparent in thinner specimens.

3.4.5 *Dependence of the Initial Form of LCP on Mesogenic Texture*

Figures (3.7)-(3.10) illustrate the differing optical nature of nematic phases according to the initial form of LCP. LCP powders, films and fibres are compared. LCP powder exhibits coloured birefringence and a schlieren texture at 380°C (Figure 3.7). The disclinations are distributed sparsely and at random throughout the specimen. In addition, the size, shape and abundance of these features vary across the area of the specimen. The LCP film (Figure 3.8) exhibits a schlieren pattern at 400°C which remains consistent over the entire area of the specimen. No interference colours are observed however the sample is strongly birefringent. The size, shape and abundance of the disclinations remain unchanged throughout the specimen area. The anisotropic melt of a very thin LCP film (Figure 3.9) exhibits a spherulitic-like structure. The "Maltese Cross" patterns characteristic of spherulites do not alter their position as the specimen is rotated through 360 degrees. The spherulites increased in size as a function of temperature, eventually impinging on one another at 330°C. The perimeters of these

FIGURE 3.6 LCP THICK FILM (heating run 1)

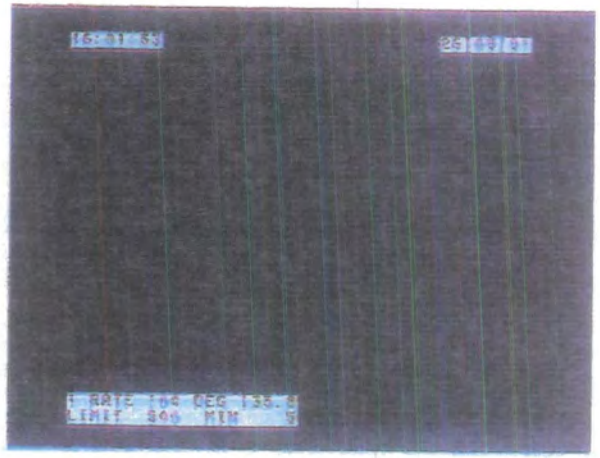

135.8degC

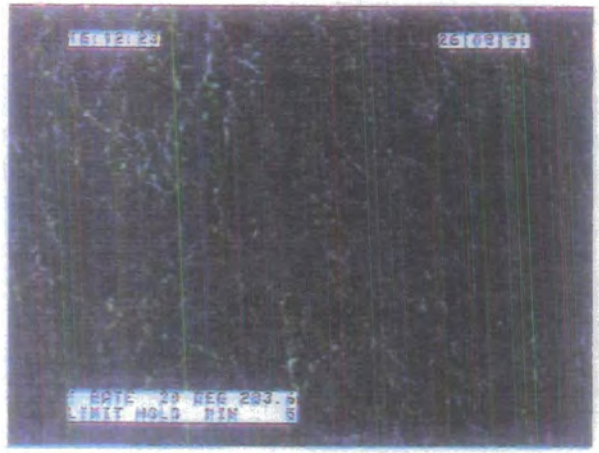

283.6degC

338.8degC

381.3degC

(x 400) crossed polars

FIGURE 3.7 LCP POWDER

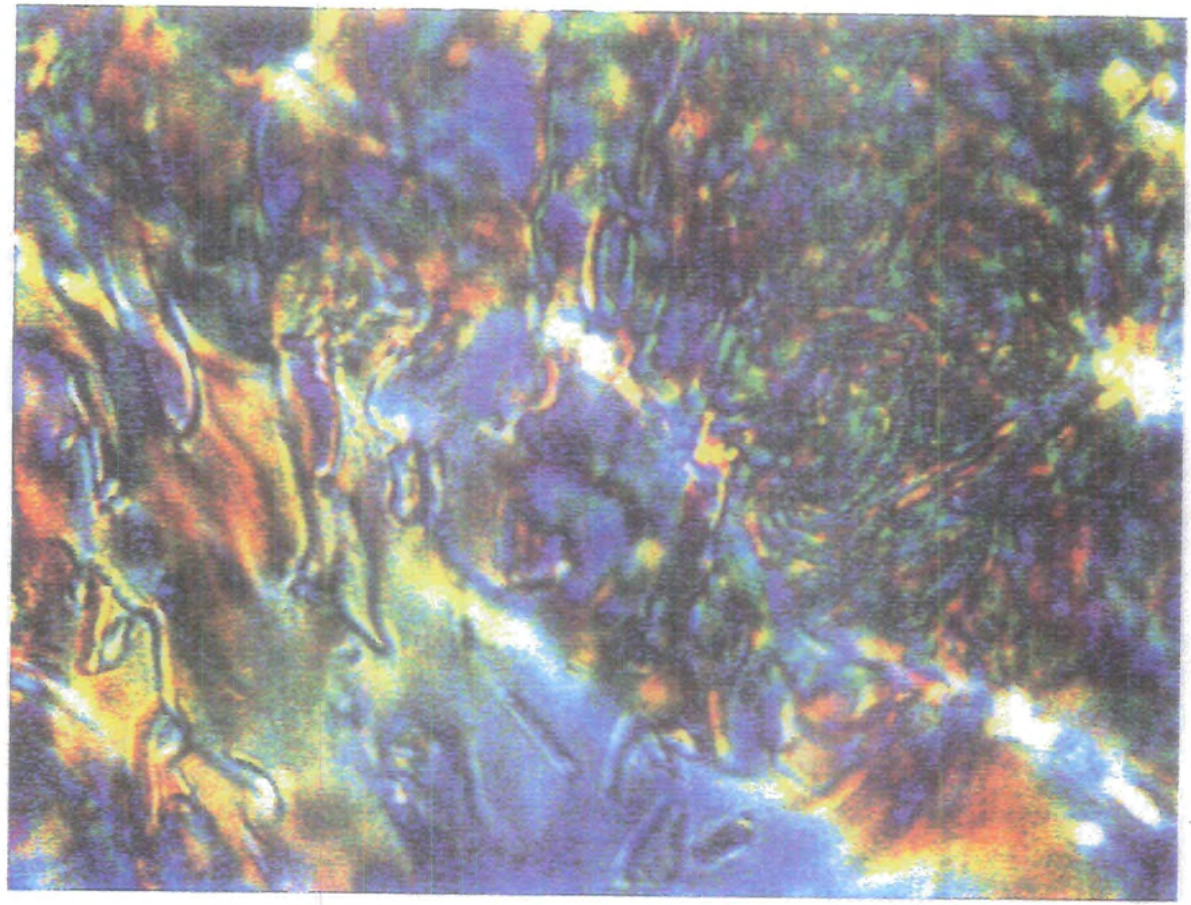

(x 400) crossed polars

NEMATIC PHASE @380degC

FIGURE 3.8 LCP FILM

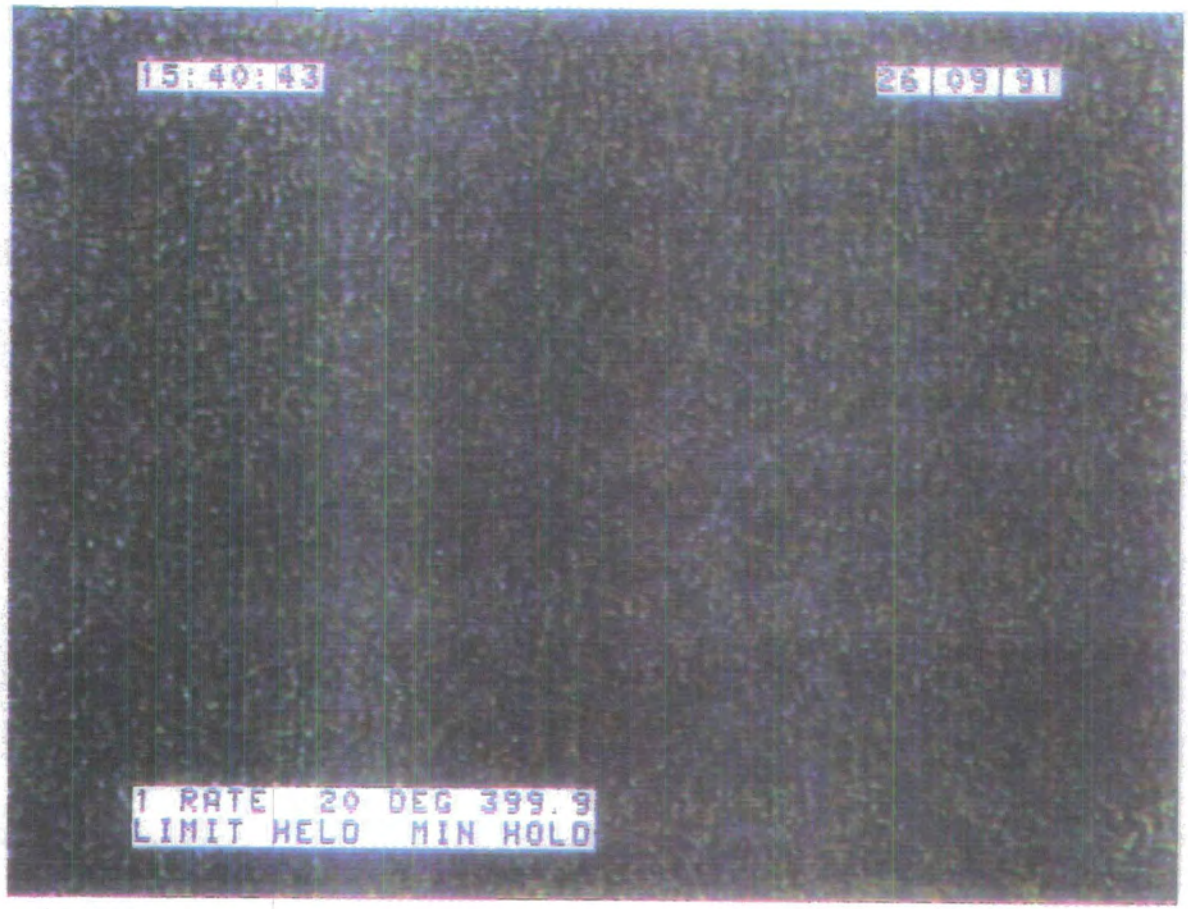

(x 400) crossed polars

NEMATIC PHASE @400degC

FIGURE 3.9 LCP THIN FILM

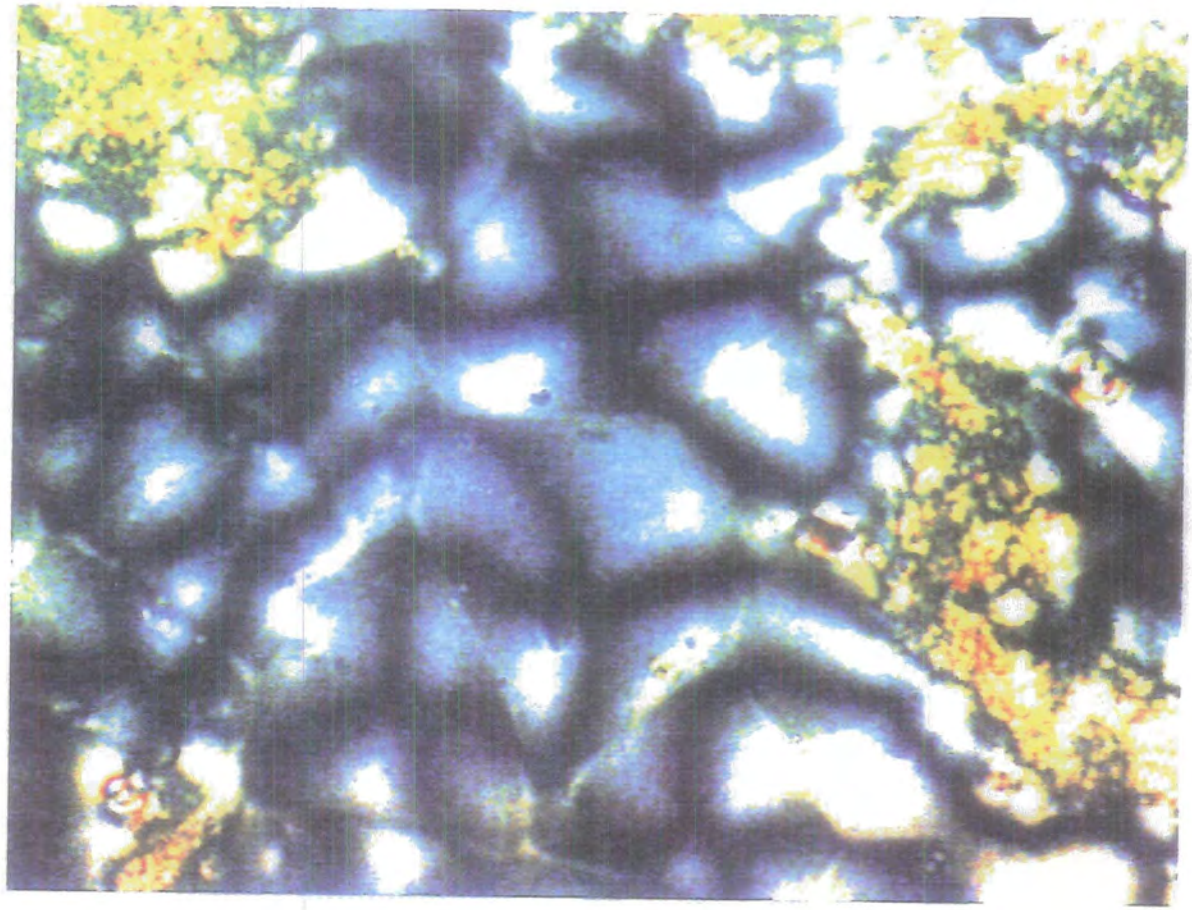

(x 400) crossed polars

NEMATIC PHASE @380degC (spherulitic-like structure)

features are very apparent. Smaller birefringent areas are distributed at random throughout the specimen and small banded spherulites are scattered throughout these regions. It cannot be concluded with certainty whether the texture produced was a type of schlieren pattern or was in fact due to the growth of spherulites, a feature of semi-crystalline polymers. Detailed studies of this behaviour were not possible since these results could not be reproduced. Since the specimen was observed to degrade immediately on heating above 400°C. It is possible that the polymer film did not form an anisotropic melt.

An optical micrograph of an LCP fibre drawn in the anisotropic melt at 330°C, cooled and viewed between crossed polars at ambient temperature, is shown in Figure 3.10. The specimen exhibits brightly coloured birefringence. Fine, dark lines along the length of the sample indicate that the fibre is highly oriented along the draw direction.

3.4.6 *The Thermal Behaviour of LCP Fibres*

As mentioned in section (3.4.5) fibres drawn from the melt on LCP powder specimens exhibit strong birefringence and high orientation along the draw direction at ambient temperatures (Figure 3.10). As the fibre is heated, the strong birefringence is maintained. At 380°C the fibre forms an anisotropic melt similar to that exhibited in Figure (3.7). A transition from the anisotropic to the isotropic melt is not observed. Degradation begins at 420°C, confirmed by the appearance of voids in the specimen.

FIGURE 3.10 LCP FIBRE (drawn @330degC)

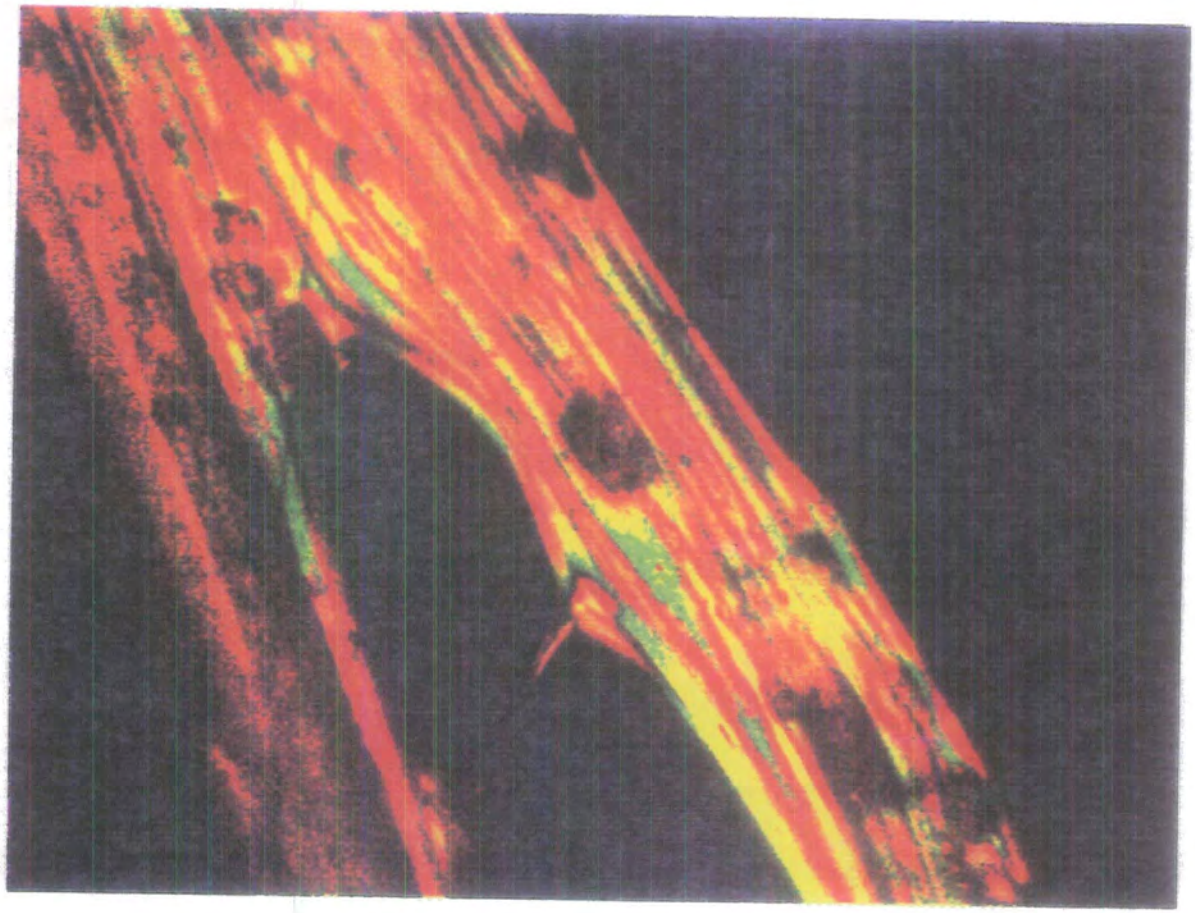

(x 400) crossed polars

NEMATIC PHASE @380degC

3.5 *Section II: Differential Scanning Calorimetry*

3.5.1 *Introduction*

In addition to characterisation of the liquid crystal mesophase by polarising microscopy, the most common technique for studying liquid crystalline polymers is by thermal analysis. Thermal analysis is defined as the expression encompassing a group of techniques in which a physical property of a specimen and/or its reaction products are measured as a function of temperature.[1] An extensive amount of literature covering the theory, instrumentation and applications of the techniques used is available.[13,27,28] This section provides a brief introduction to thermal analysis, concentrating on Differential Scanning Calorimetry. The instrumentation, scope and experimental aspects of this technique will be discussed with a view to its application to polymer science and the characterisation of LCP.

Accurate techniques in temperature measurement have existed for more than a century, however the DSC was not developed until 1964.[29] The history of thermal analysis is well documented[30-32] and is not discussed in the present work.

The DSC thermogram plots differential heat flow versus temperature and/or time, in other words it reflects changes in the energy of the system under investigation. These changes may be chemical or physical in origin. The technique is therefore particularly useful in the study of polymers, since structural changes or the polymerisation reaction are undoubtedly accompanied by energetic effects, hence such parameters as glass transition temperature, crystallisation, melting, curing, oxidation and degradation can be characterised.

In DSC, a small sample and a reference material are heated at a constant rate and either the power consumption or the heat flow is measured as a function of temperature and time. The thermal properties of the sample can be measured directly from the difference between the heat required by the sample and reference materials. A power-compensated DSC is used in the present study. Its operation is discussed briefly below.

A schematic of the DSC cell is given in Figure (3.11). The temperature of the sample and reference materials are maintained at identical values by supplying heat to the two cells. The quantity of heat necessary to maintain these conditions is then recorded as a function of temperature or time. The control of temperature and its role in obtaining a curve of differential power versus temperature is discussed elsewhere.[30] An advantageous feature of this instrument results from the use of separate heaters to supply heat to the sample and reference holders. Due to the purely electrical nature of the measurements, the conversion factors for the calculation of enthalpy or heat capacity are independent of temperature. Turi provides an excellent review of the theory and application of DSC.[3]

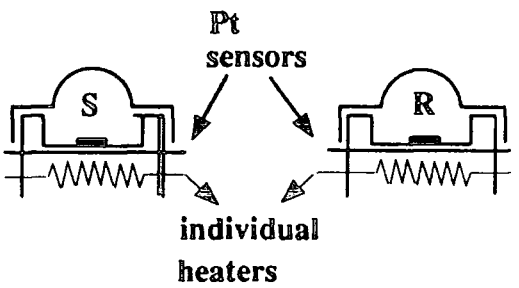

Figure 3.11 Schematic of a Power-Compensated DSC Cell

3.5.2 *Instrumentation*

Two types of instruments are in regular use in Differential Scanning Calorimetry and as a result, this technique is difficult to classify. The two instruments referred to are the heat-flux DSC and the power compensated DSC. The latter was mentioned in section (3.5.1). There are obvious differences in detail between these two instruments, however certain standard features are common to both operating temperatures in the range 175-730°C and heating and cooling rates of 0.1-200°Cmin^{-1} are obtainable. However, in the routine study of polymers in general, scanning rates of 10-20°C min^{-1} are used. Sub-milligram quantities of polymer provide a signal to noise ratio which give adequate results, yet larger quantities (20-40mg) of material can also be studied. However as the

quantity of material studied decreases, the selection of a sample representative of the whole material becomes increasingly difficult.

3.5.3 *Applications to Liquid Crystal Polymers*

The thermal behaviour of side-chain liquid crystal polymers is well established and has been reviewed extensively in the literature.[31-34] Main-chain liquid crystal polymers exhibit more complex thermal behaviour but in general samples show a glass transition, melting transition, mesophase-mesophase and/or mesophase-isotropic transition when examined by DSC.[35,36] In addition to these transitions, further low-temperature first order transitions may be observed. These may result from the following:

i) Recrystallisation of the polymer chains during melting. This suggests that two interchangeable forms of the polymer exist, which differ only in their degrees of crystal size and perfection.

ii) Differences in crystal morphologies, where these differences are presumed to be large enough to prevent any structural changes occurring during a DSC scan. Consequently it is assumed that the melting endotherms are due to the material's structure before the scan.

iii) Polymorphism.

For these reasons, it is difficult to interpret the thermal curves of these materials obtained by DSC. The use of a complementary characterisation technique is thus especially important in the study of main-chain liquid crystal polymers.

3.6 *Experimental*

3.6.1 *Instrumentation*

Analysis was carried out using a Perkin-Elmer DSC7 Differential Scanning Calorimeter. This is a computer-controlled instrument of power compensation design. The DSC7 was linked to a Perkin-Elmer TAC7/PC Instrument Controller and a Dell PC. The Perkin-Elmer Controlled Cooling Accessory was used to achieve subambient conditions and controlled cooling. The instrument allows the direct calorimetric investigation and analysis of the thermal properties of both solids and liquids and is programmed to scan at a linear rate for the study of thermal reactions. The temperature range obtainable with this instrument is -175-730°C. The theory based on the power compensation design is described in section (3.5.2). Platinum resistance heaters supply a quantity of electrical energy to the sample and reference holders, this energy supply is continually adjusting in order to maintain the two holders at identical temperatures with respect to one another throughout the scan. The electrical signal obtained is measured directly in energy units (mW) providing the electrical movement of the exothermic and/or endothermic peak areas. The Perkin-Elmer DSC design measures the energy of a transition directly and thus provides accurate calorimetric information. Dry nitrogen was used as the purge gas creating an inert atmosphere in the sample holder and liquid nitrogen was used as the coolant in controlled cooling experiments. Thermal scans were run at 20°C min^{-1} unless stated otherwise. All thermal runs were normalised to a mass of 1g in order that the magnitude of the transitions could be compared directly for differing sample weights. Calibration was achieved using indium and lead standards. The transition temperatures are recorded as the maximum exothermic or endothermic peak temperature. All initial experiments, unless stated otherwise, examine the thermal behaviour of LCP powder.

3.6.2 *Sample Preparation*

a) *Powder Specimens*

LCP was purified according to the method used in section (3.3.2(a)). Approximately 3-8mg of polymer were weighed accurately to 4 significant figures, into an aluminium sample pan. The pan was then sealed and placed inside the sample holder in the DSC cell. An empty aluminium pan and lid were used as a reference.

b) *Film Specimens*

Solvent-cast films were prepared according to the procedure in section (4.3.2(b)). Small pieces of film were cut from the original samples and were prepared for DSC analysis using the method described in section (3.6.2(a)).

c) *Fibre Specimens*

Fibres were prepared according to the procedure in section (3.3.2(d)). The specimens were cut into strips of an approximate length of 1mm, weighed and sealed inside the aluminium pans as described in section (3.6.2(a)).

3.7 *Results and Discussion*

3.7.1 *Thermal Transitions of LCP on Heating and Cooling*

Figure 3.12 displays the thermograms obtained for a typical heating and subsequent cooling scan of LCP powder. The heating scan shows a biphasic exotherm over the range: 140-180°C. From microscopy results (section (3.4.1)) this transition is due to crystallisation. The two peaks observed in the biphasic exotherm are attributed to different regions of LCP (ΔH_c=6.86Jg^{-1}) crystallising at different temperatures. Multiple endotherms, characteristic of random liquid crystalline copolyesters, are present over the range: 276-335°C. These transitions correspond to the melting of LCP (section (3.4.1)) and are attributed to the crystalline to nematic, and possibly even nematic to isotropic phase transitions observed to occur in LCP. A sharp exotherm is observed on cooling the sample from the melt, indicating a large amount of supercooling (≈50°C). Equivalent magnitude for the heats of fusion (ΔH_f=7.49Jg^{-1}) and recrystallisation ($\Delta H_{recryst}$= 7.57Jg^{-1}) are obtained for the heating and cooling scans respectively. The magnitude for the heat of fusion is low, characteristic of random liquid crystalline polymers. [37-39] The results obtained for the cooling scans are entirely reproducible. Figure 3.13 illustrates the reproducibility of heating runs. Frequently, single exothermic peaks only are observed, corresponding to the second larger peak. Multiple endotherms are always obtained over the range, 275-335°C, however the sharpness of the peaks varies from sample to sample. All heats of transition are reproducible to ±0.2Jg^{-1} and similarly, all temperatures of transition, to ±2°C.

3.7.2 *Effects of Reheating LCP from the Melt*

Figure 3.14 illustrates the effects of reheating LCP from the anisotropic melt. An LCP sample was heated to 340°C and quenched to 25°C. The same sample (reheat 2) reheated under identical conditions did not exhibit a crystalline exotherm, characteristic

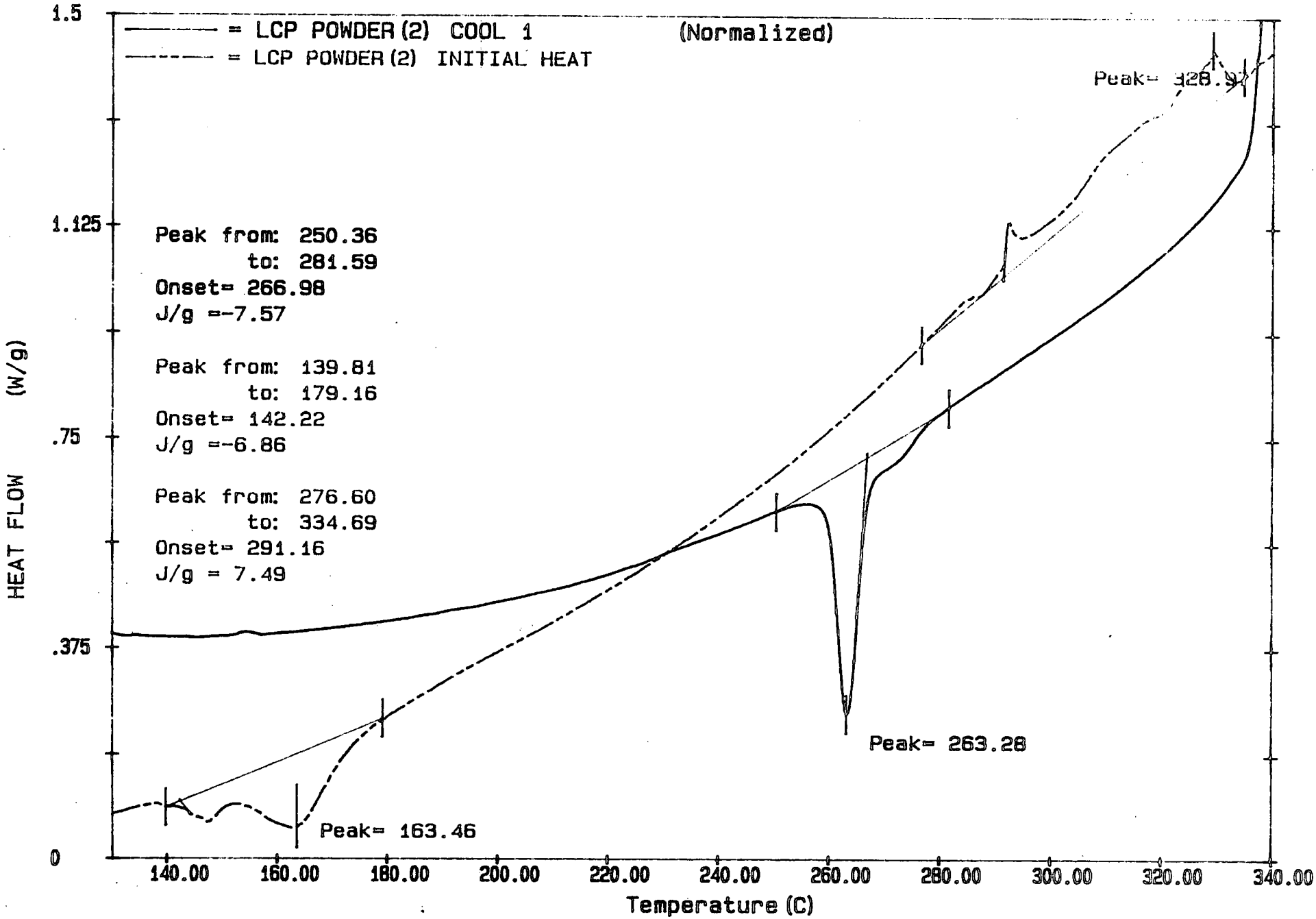
1.5
1.125
.75
.375
0
HEAT FLOW (W/g)
——— = LCP POWDER(2) COOL 1 (Normalized)
------ = LCP POWDER(2) INITIAL HEAT
Peak= 328.97
Peak from: 250.36
to: 281.59
Onset= 266.98
J/g =-7.57
Peak from: 139.81
to: 179.16
Onset= 142.22
J/g =-6.86
Peak from: 276.60
to: 334.69
Onset= 291.16
J/g = 7.49
Peak= 263.28
Peak= 163.46
140.00
160.00
180.00
200.00
220.00
240.00
260.00
280.00
300.00
320.00
340.00
Temperature (C)

Figure 3.12

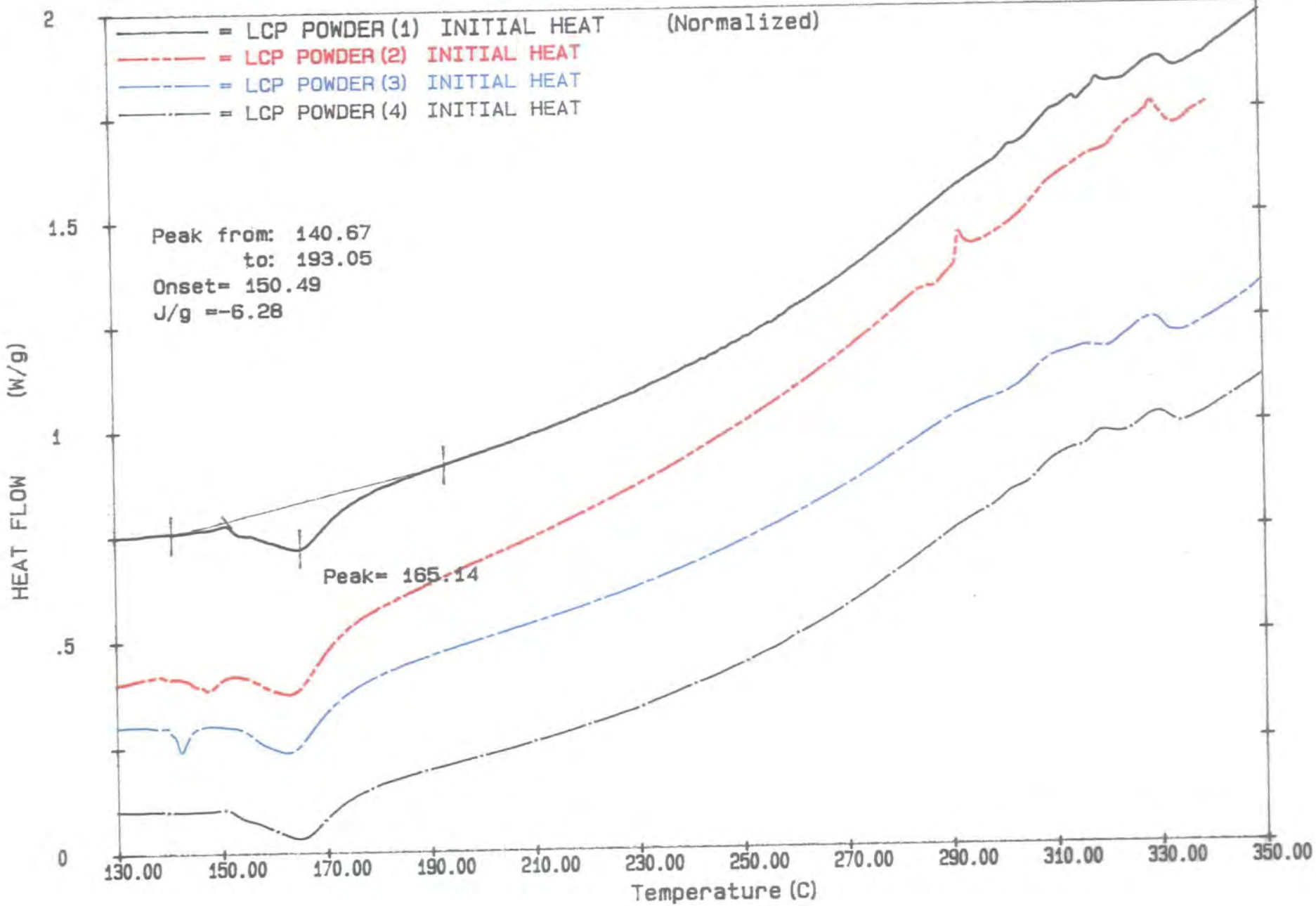
= LCP POWDER (1) INITIAL HEAT (Normalized)
= LCP POWDER (2) INITIAL HEAT
= LCP POWDER (3) INITIAL HEAT
= LCP POWDER (4) INITIAL HEAT
Peak from: 140.67
to: 193.05
Onset= 150.49
J/g =-6.28
Peak= 165.14
HEAT FLOW (W/g)
Temperature (C)
2
1.5
1
.5
0
130.00
150.00
170.00
190.00
210.00
230.00
250.00
270.00
290.00
310.00
330.00
350.00

Figure 3.13

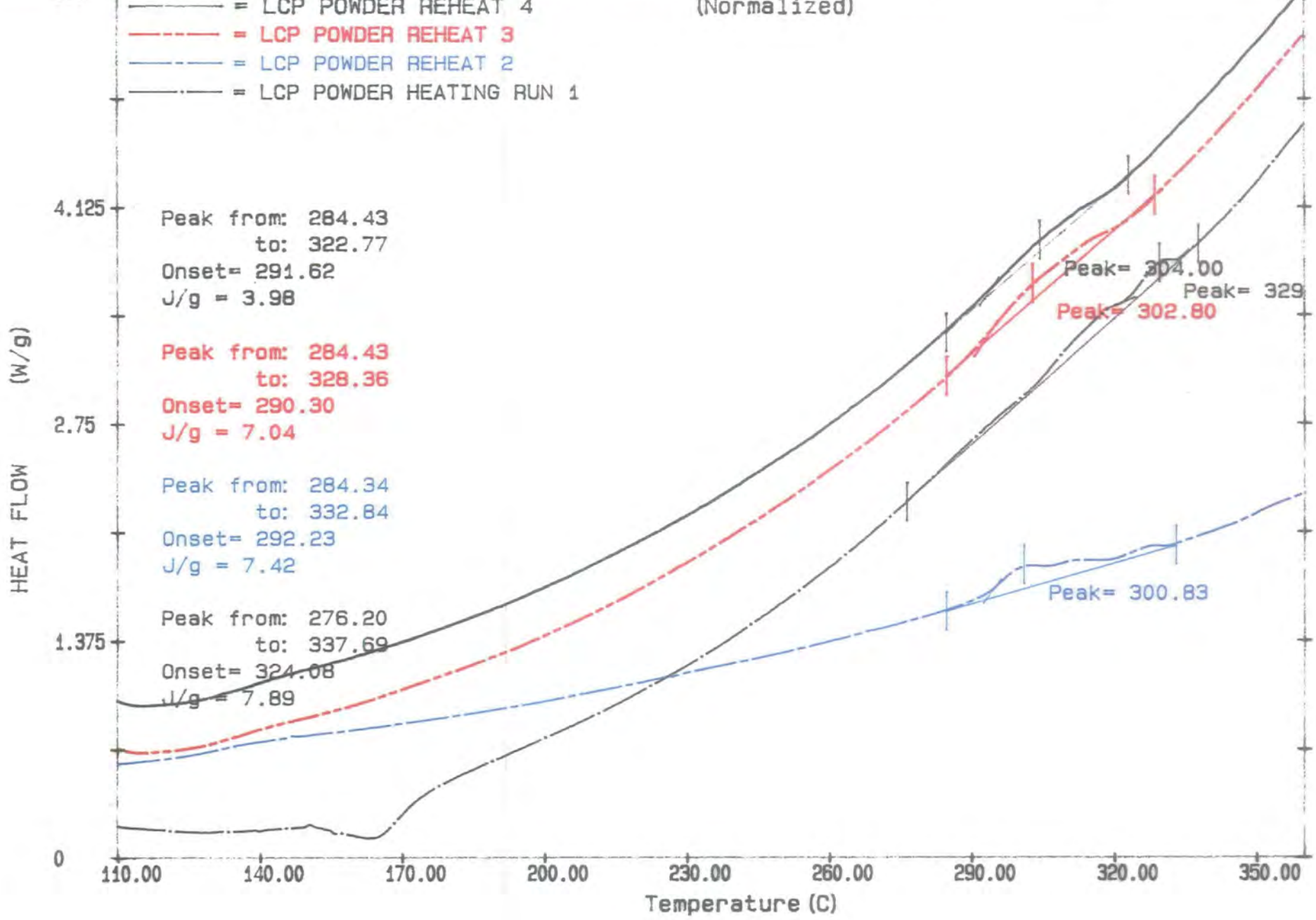
= LCP POWDER REHEAT 4
= LCP POWDER REHEAT 3
= LCP POWDER REHEAT 2
= LCP POWDER HEATING RUN 1
(Normalized)
Peak from: 284.43
to: 322.77
Onset= 291.62
J/g = 3.98
Peak from: 284.43
to: 328.36
Onset= 290.30
J/g = 7.04
Peak from: 284.34
to: 332.84
Onset= 292.23
J/g = 7.42
Peak from: 276.20
to: 337.69
Onset= 324.08
J/g = 7.89
Peak= 304.00
Peak= 329
Peak= 302.80
Peak= 300.83
HEAT FLOW (W/g)
4.125
2.75
1.375
0
110.00
140.00
170.00
200.00
230.00
260.00
290.00
320.00
350.00
Temperature (C)

Figure 3.14

of the primary heating scan. Multiple endotherms were still observed over a smaller temperature range.

In each successive reheat, the crystallisation exotherm is absent and a decrease in both the heat of fusion and temperature range over which the phase exists, result. The initial peak in the multiple endotherm becomes increasingly dominant and shifts to higher temperatures with each subsequent heat. Eventually, on the 4th heat (reheat 4) one peak only is observed. Table 3.1 gives the values of the heats and temperatures of transition obtained for each scan.

Heat No.	ΔH_c Jg^{-1}	ΔH_m Jg^{-1}	T_m °C	T_{range} °C
1	6	8	324	276 - 338
2	-	7	301	284 - 333
3	-	7	303	284 - 328
4	-	4	304	284 - 323

Table 3.1

Effects of Reheating LCP

3.7.3 *Effects of Altering the Cooling Rate*

The effects of altering the rates of controlled heating and cooling in LCP were examined. The results obtained for cooling scans proved to be very reproducible, whereas those obtained for the heating scans were not, hence the former are discussed in the present study. LCP samples were heated to 340°C and held isothermally for 15 minutes, in order to achieve equivalent thermal histories prior to cooling. Cooling rates over the range 5-100°C min^{-1} were studied. The resultant cooling scans are shown in Figures 3.15(a) and (b). The magnitudes of the heats of recrystallisation increase and the temperatures of recrystallisation decrease significantly as a function of increasing cooling rate. These results are expected since the extent of supercooling increases as the sample is cooled at a faster rate. The temperature range over which the transition occurs increases with

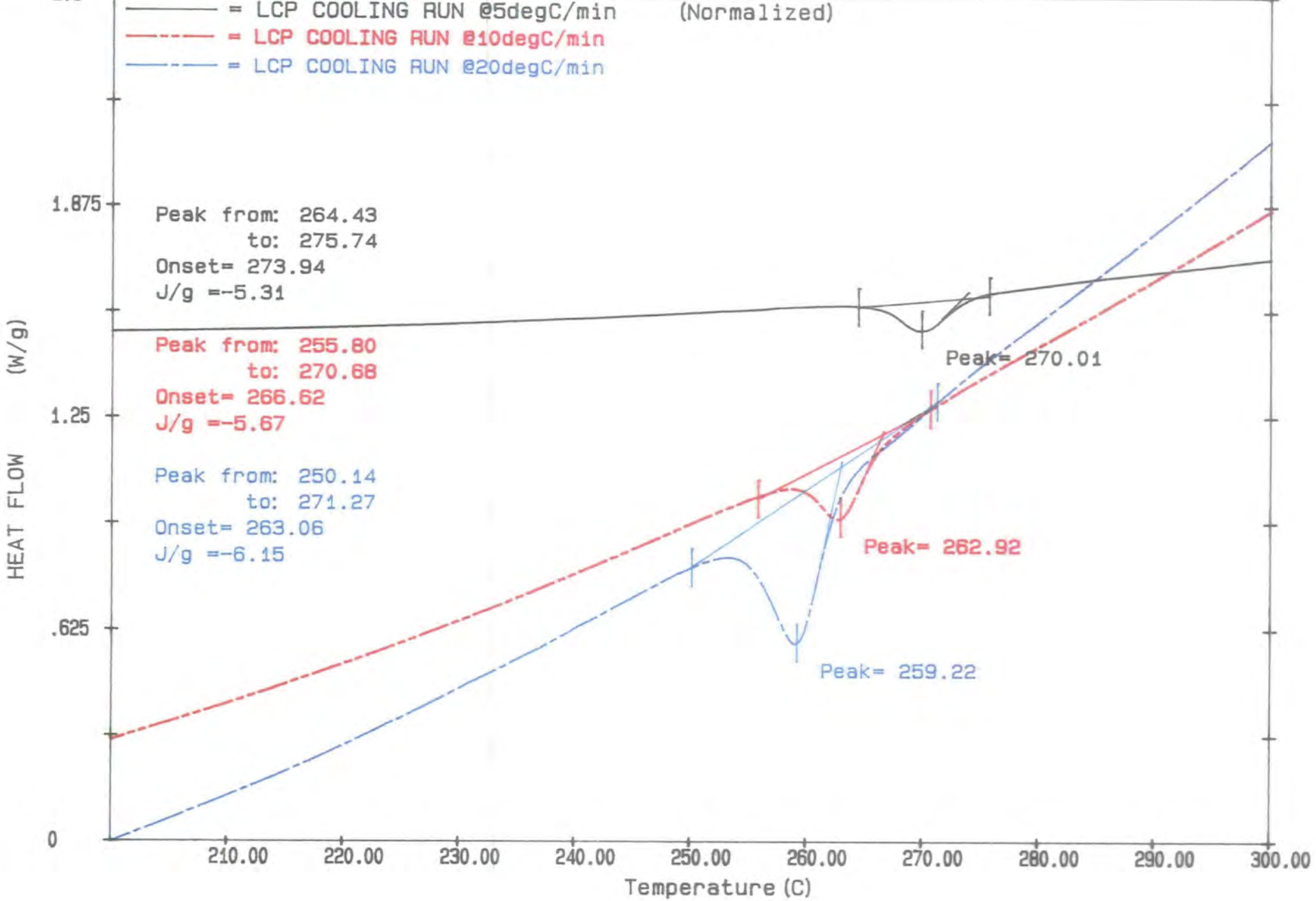
= LCP COOLING RUN @5degC/min (Normalized)
= LCP COOLING RUN @10degC/min
= LCP COOLING RUN @20degC/min
Peak from: 264.43
to: 275.74
Onset= 273.94
J/g =-5.31
Peak from: 255.80
to: 270.68
Onset= 266.62
J/g =-5.67
Peak from: 250.14
to: 271.27
Onset= 263.06
J/g =-6.15
Peak= 270.01
Peak= 262.92
Peak= 259.22
HEAT FLOW (W/g)
1.875
1.25
.625
0
210.00
220.00
230.00
240.00
250.00
260.00
270.00
280.00
290.00
300.00
Temperature (C)

Figure 3.15(a)

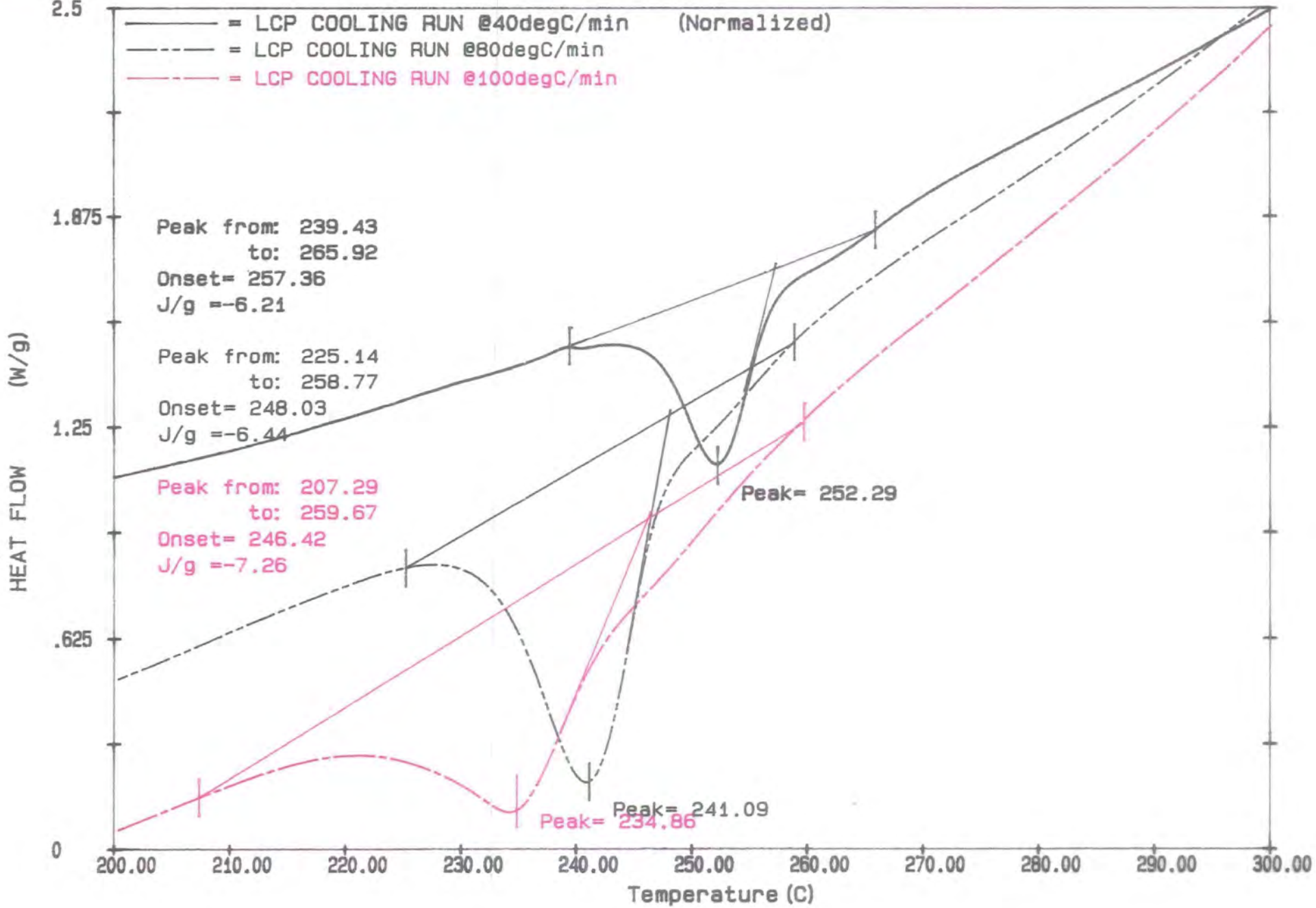
= LCP COOLING RUN @40degC/min (Normalized)
= LCP COOLING RUN @80degC/min
= LCP COOLING RUN @100degC/min
Peak from: 239.43
to: 265.92
Onset= 257.36
J/g =-6.21
Peak from: 225.14
to: 258.77
Onset= 248.03
J/g =-6.44
Peak from: 207.29
to: 259.67
Onset= 246.42
J/g =-7.26
Peak= 252.29
Peak= 241.09
Peak= 234.86
HEAT FLOW (W/g)
2.5
1.875
1.25
.625
0
200.00
210.00
220.00
230.00
240.00
250.00
260.00
270.00
280.00
290.00
300.00
Temperature (C)

Figure 3.15(b)

increasing cooling rate also as expected. The effects of heat and temperature of recrystallisation as a function of cooling rate are plotted in Figure 3.16. Table 3.2 lists the values of the thermal parameters.

Cooling Rate $^{o}Cmin^{-1}$	$\Delta H_{recryst}$ Jg^{-1}	$T_{recryst}$ ^{o}C	T_{range} ^{o}C
5	-5.3	270	264 - 276
10	-5.7	263	256 - 271
20	-6.2	259	250 - 271
40	-6.2	252	239 - 266
80	-6.4	241	225 - 259
100	-7.3	235	207 - 260

Table 3.2

Effects of Altering Cooling Rate

3.7.4 *Effects of Annealing in the Melt*

The effects of annealing LCP samples in the melt for varying time intervals were investigated. As in section (3.7.4) the cooling scans were examined. The LCP samples were annealed at 340°C for time periods ranging from 0-60 minutes.

On annealing, the LCP samples were cooled at a constant rate to 25°C. The resultant cooling scans are shown in Figures 3.17(a) and (b). The values obtained for the heats and temperatures of recrystallisation decrease with increasing annealing time. It is proposed that the LCP samples become increasingly ordered in the melt and consequently, the energy released in transforming the liquid to the solid will decrease. Effects on temperatures and heats of recrystallisation are plotted as a function of annealing time in Figure 3.18. The thermal parameters are listed in Table 3.3.

EFFECTS OF COOLING RATE ON THERMAL PARAMETERS

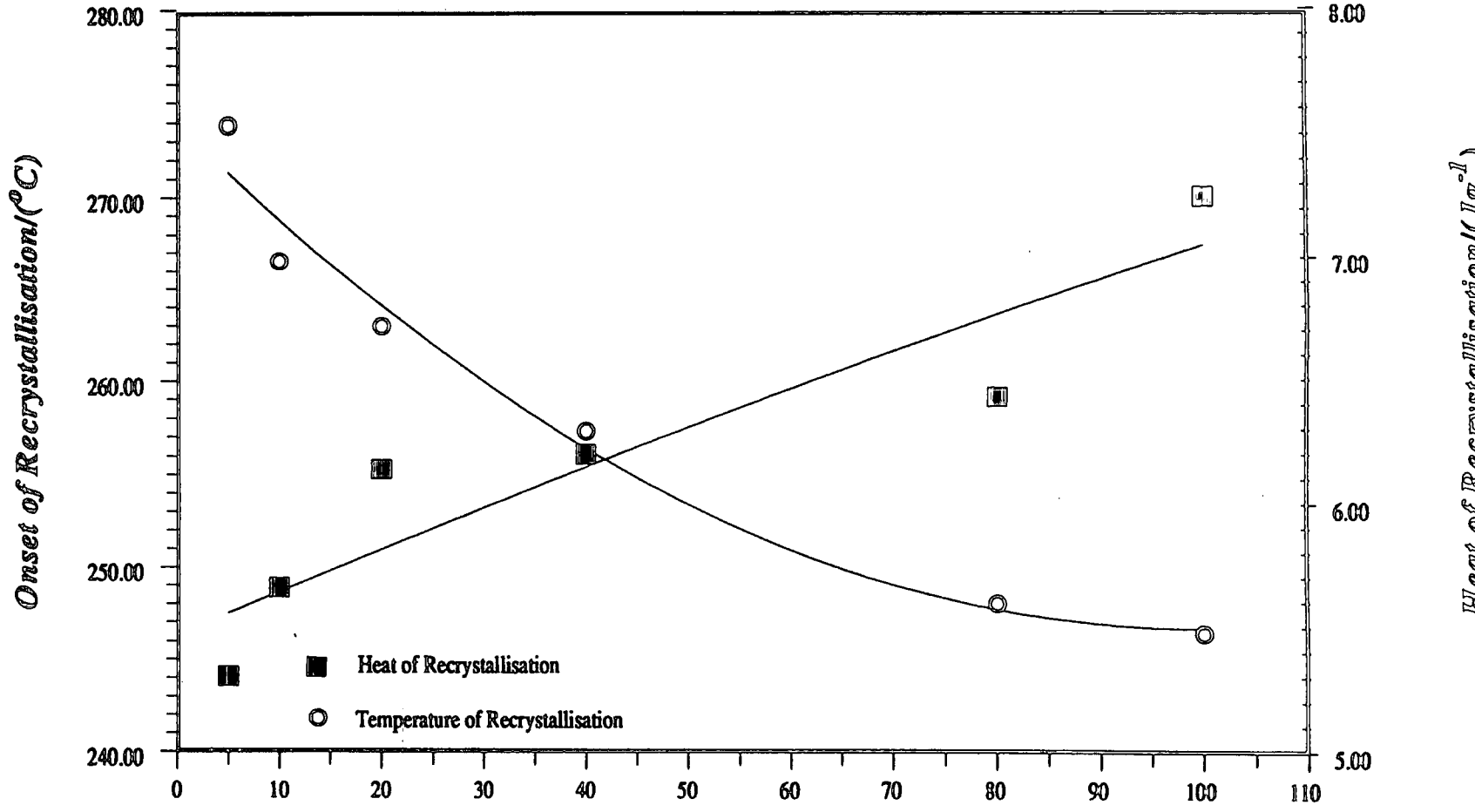

Figure 3.16

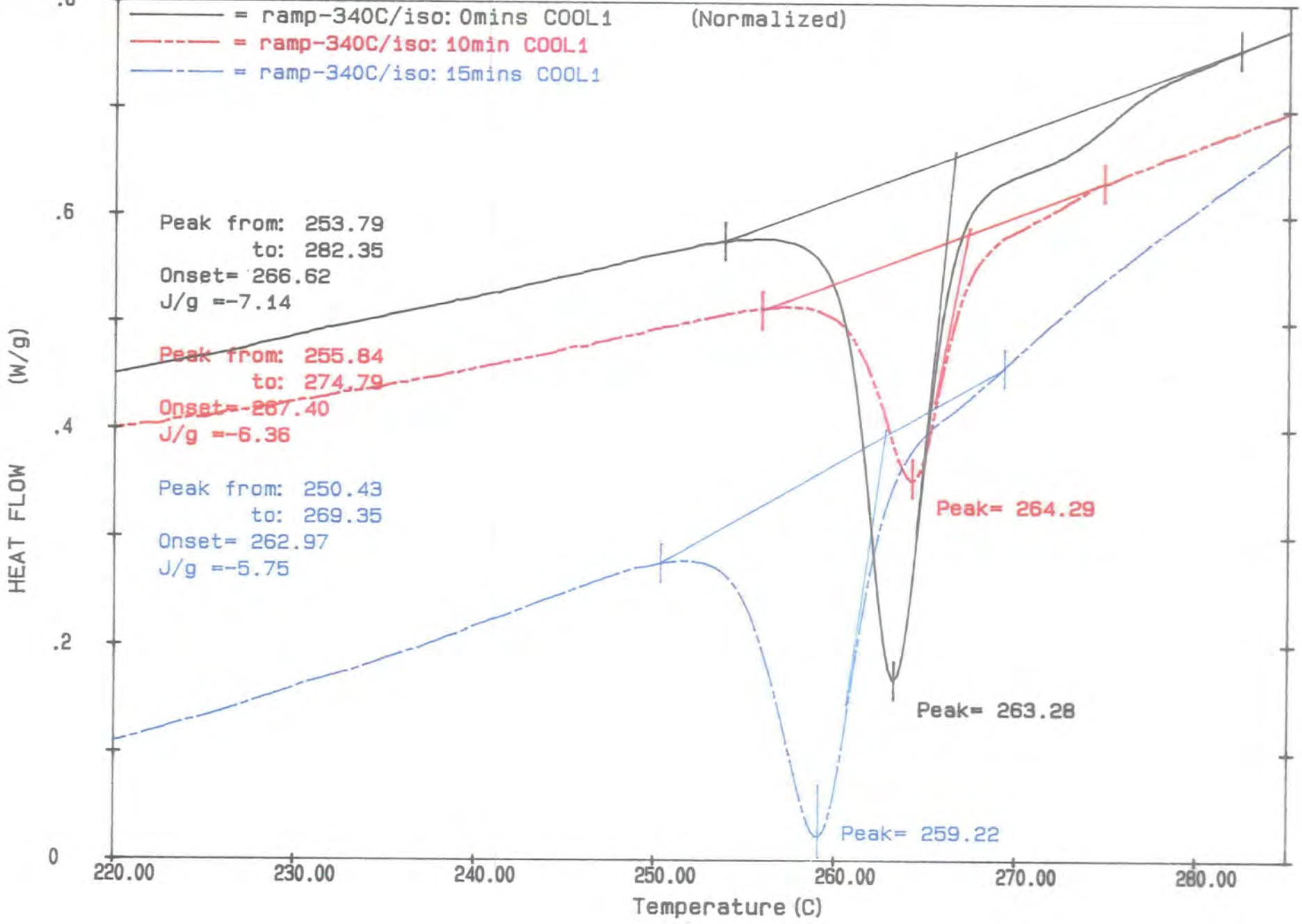
= ramp-340C/iso: 0mins COOL1 (Normalized)
= ramp-340C/iso: 10min COOL1
= ramp-340C/iso: 15mins COOL1
Peak from: 253.79
to: 282.35
Onset= 266.62
J/g =-7.14
Peak from: 255.84
to: 274.79
Onset=-267.40
J/g =-6.36
Peak from: 250.43
to: 269.35
Onset= 262.97
J/g =-5.75
Peak= 264.29
Peak= 263.28
Peak= 259.22
HEAT FLOW (W/g)
.6
.4
.2
0
220.00
230.00
240.00
250.00
260.00
270.00
280.00
Temperature (C)

Figure 3.17(a)

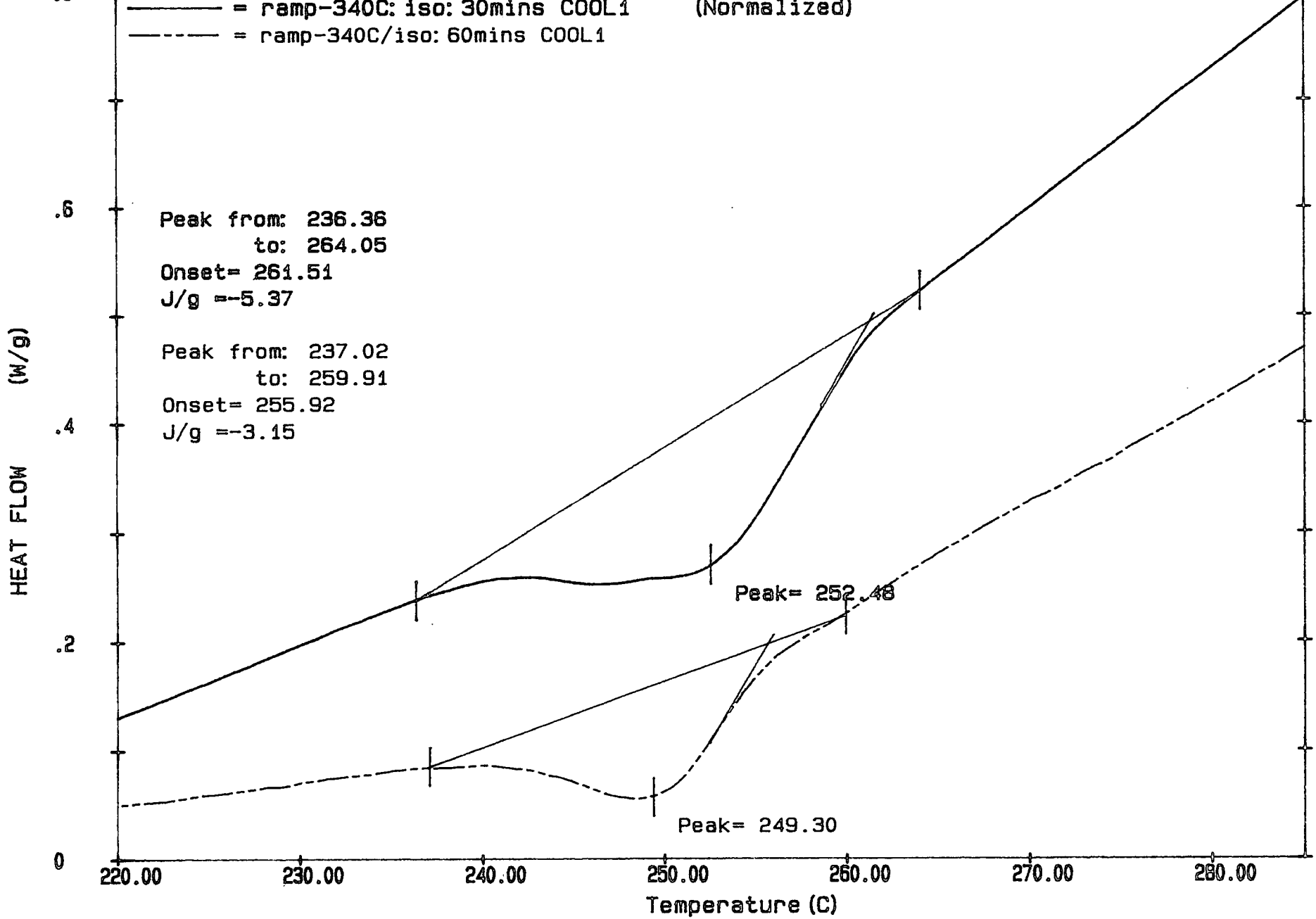
——— = ramp-340C: iso: 30mins COOL1 (Normalized)
——---- = ramp-340C/iso: 60mins COOL1
Peak from: 236.36
to: 264.05
Onset= 261.51
J/g =-5.37
Peak from: 237.02
to: 259.91
Onset= 255.92
J/g =-3.15
Peak= 252.48
Peak= 249.30
HEAT FLOW (W/g)
0
.2
.4
.6
220.00
230.00
240.00
250.00
260.00
270.00
280.00
Temperature (C)

Figure 3.17(b)

EFFECTS OF INCREASING ANNEALING TIME IN ANISOTROPIC MELT

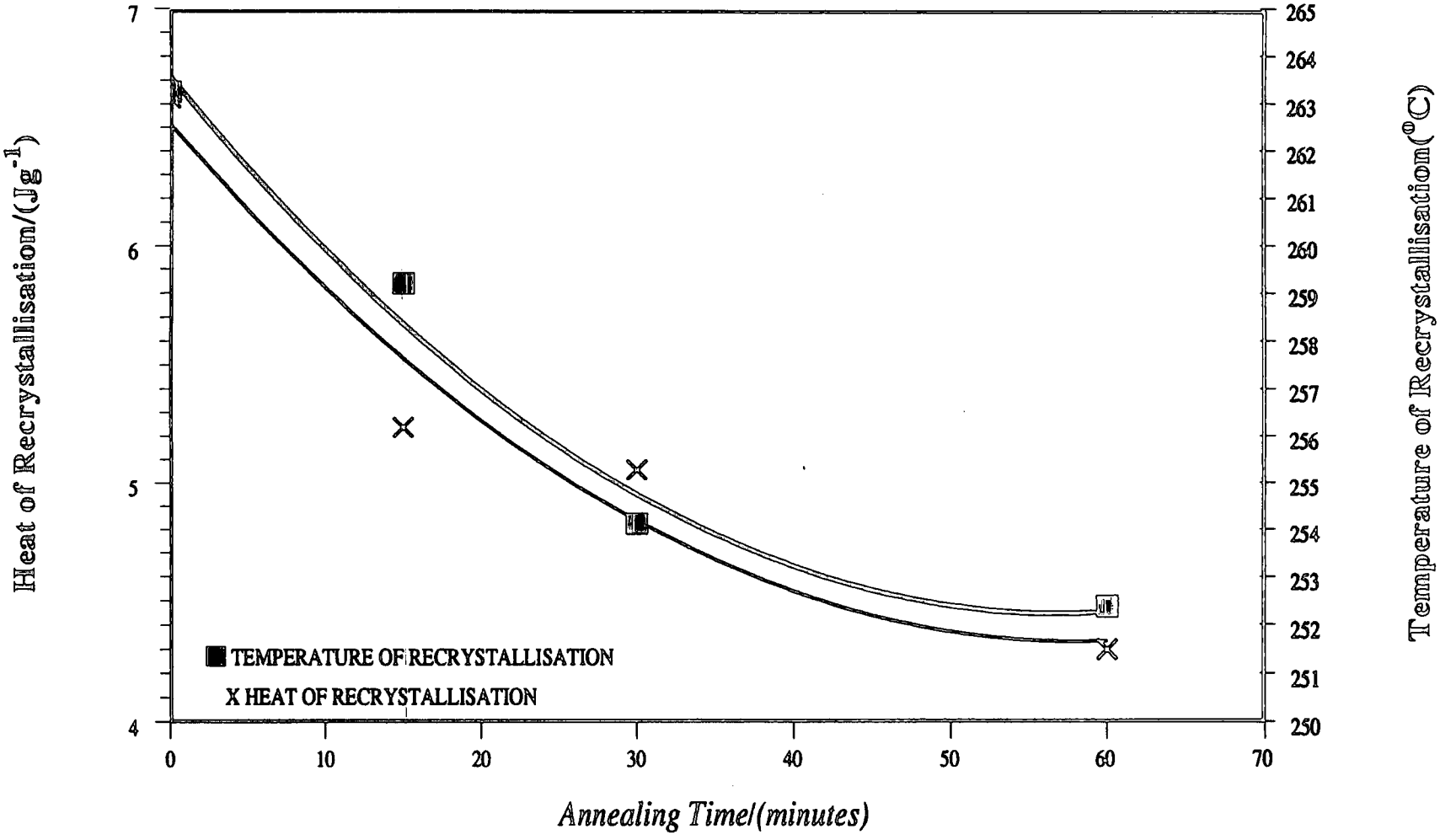

Figure 3.18

Annealing Time Minutes	$\Delta H_{recryst}$ Jg^{-1}	$T_{recryst}$ °C	T_{range} °C
0	-7.1	263	254 - 282
10	-6.4	264	255 - 278
15	-5.8	259	250 - 269
30	-5.4	252	236 - 264
60	-3.2	249	237 - 260

Table 3.3

Effects of Annealing in the Melt

3.7.5 *Effects of Annealing at Selected Temperatures*

LCP samples were annealed at 130°C, 160°C and 270°C for 30 minutes. After annealing, heating was continued to 340°C. The selected annealing temperatures correspond to the onset of the following thermal transitions: the glass transition, crystallisation and melting. The glass transition is discussed in section (3.7.7). The heating scans of the polymer samples obtained after annealing are given in Figure 3.19. No trends are apparent in the thermal transitions of samples annealed at 130°C and 160°C. The multiple endotherms observed are almost equivalent to those obtained for the unannealed LCP sample. However, LCP annealed at 270°C exhibits a sharp single endotherm and a heat of fusion of $15.43Jg^{-1}$ ie. twice the value of the heat of fusion corresponding to the unannealed sample. This dramatic increase is attributed to the sample having sufficient mobility and energy to order at the onset of melting and hence more energy is required to induce melting.

3.7.6 *Effects of Remelting after Annealing*

The previous section discussed the effects of annealing at various temperatures below the melt. LCP, annealed at 270°C for 30 minutes, exhibits a large sharp melting

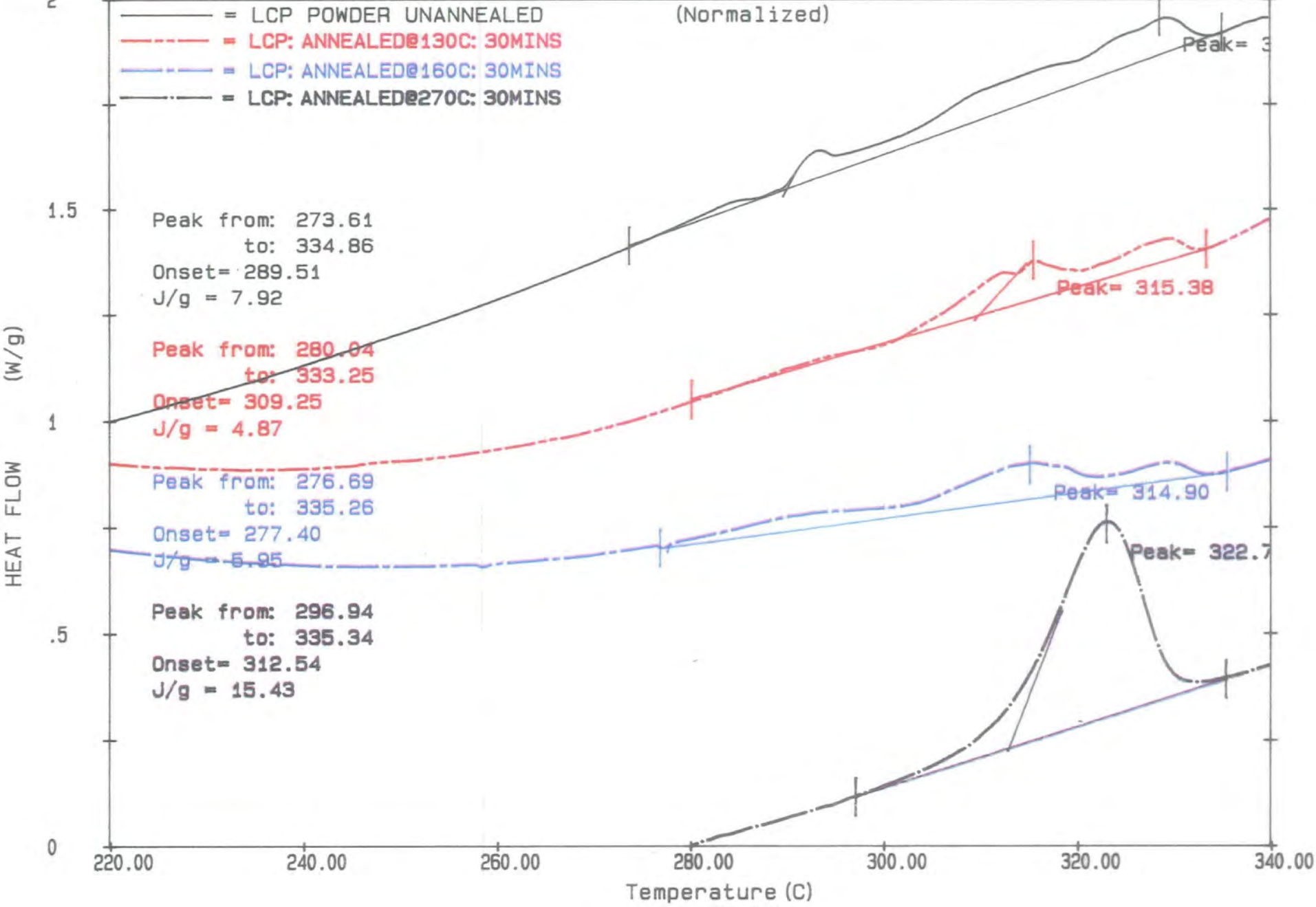
= LCP POWDER UNANNEALED
= LCP: ANNEALED@130C: 30MINS
= LCP: ANNEALED@160C: 30MINS
= LCP: ANNEALED@270C: 30MINS
(Normalized)
Peak= 3
Peak from: 273.61
to: 334.86
Onset= 289.51
J/g = 7.92
Peak from: 280.04
to: 333.25
Onset= 309.25
J/g = 4.87
Peak= 315.38
Peak from: 276.69
to: 335.26
Onset= 277.40
J/g = 5.95
Peak= 314.90
Peak from: 296.94
to: 335.34
Onset= 312.54
J/g = 15.43
Peak= 322.7
HEAT FLOW (W/g)
2
1.5
1
.5
0
220.00
240.00
260.00
280.00
300.00
320.00
340.00
Temperature (C)

Figure 3.19

endotherm. This transition is compared to the endotherm obtained on remelting of the sample (Figure 3.20). The annealed sample was heated above its melting transition to 340°C and cooled. The second heating scan displays a multiple endotherm. The values obtained for the heat and temperatures of transition are identical to those obtained for unannealed LCP. These results suggest that the ordering resulting from annealing at 270°C, is completely destroyed on remelting and the sample reverts back to its original random structure.

3.7.7 *The Glass Transition*

The appearance of the glass transition is observed only at low heating rates. In some cases it cannot be detected in the primary heating scan for an LCP sample since it is blocked out by the crystallisation exotherm, however the transition becomes apparent in the subsequent heating cycles. The position and size of the transition remain constant with each successive heat. It is reversible and also detectable in DSC cooling runs, run at slow scan rates. Figure 3.21 illustrates a typical glass transition observed for an LCP sample using a heating rate of $5°Cmin^{-1}$. The calculated value for the glass transition temperature is 127.57°C from scan to scan.

3.7.8 Thermal Transitions in LCP Films

The majority of characterisation techniques employed in this text examine LCP films as opposed to LCP powders (ie. WAXS, SANS and POM) and hence it was intended to carry out a thorough examination of the thermal properties of the films using DSC techniques. A comparison between the results obtained for LCP powder and films could not be made however since the results obtained for standard DSC heating runs for the latter proved to be very irreproducible. Figure 3.22 illustrates several of the thermograms obtained for unannealed LCP films. The samples were all prepared using an identical procedure. In all cases the crystallisation exotherm observed in the LCP

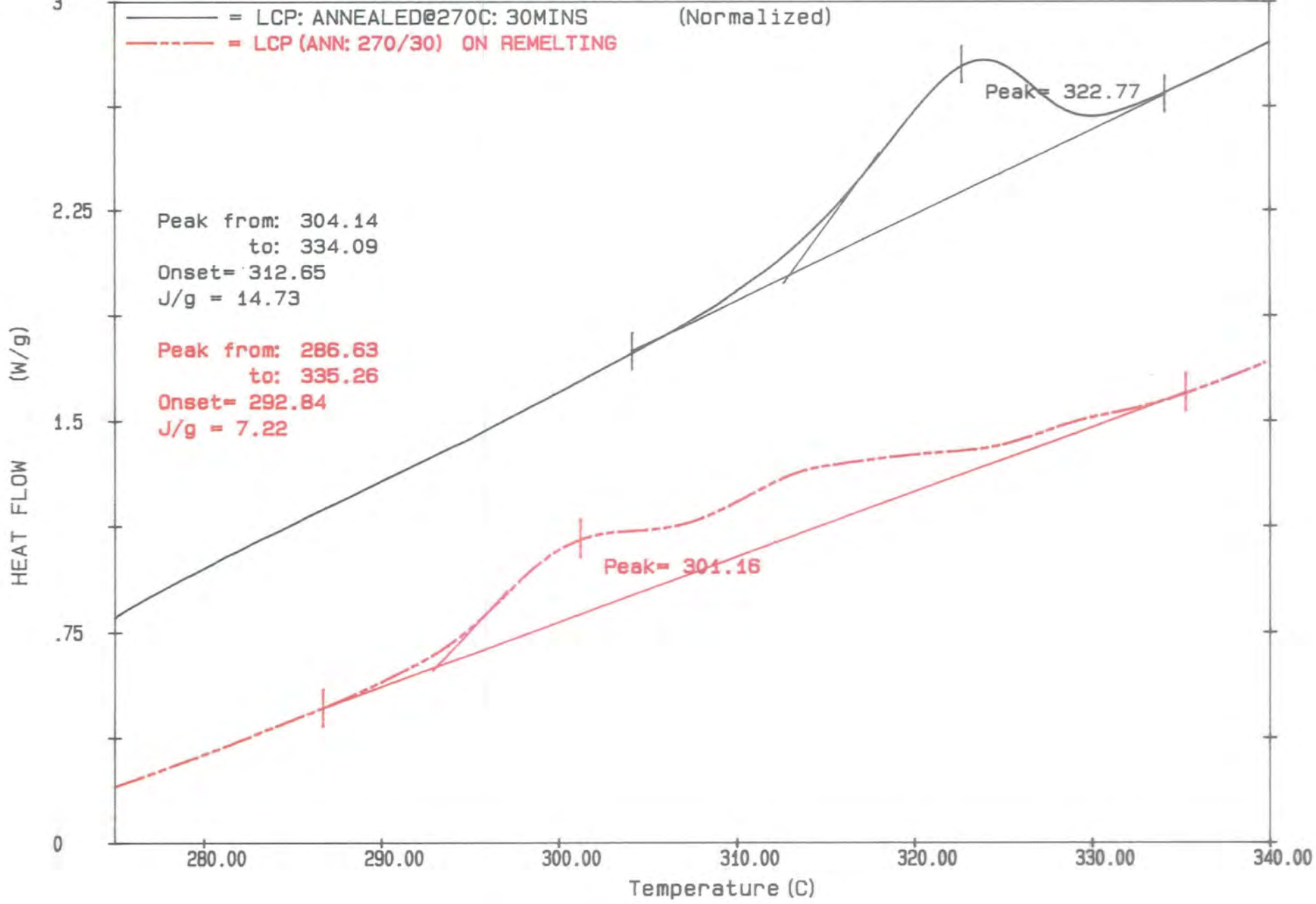
= LCP: ANNEALED@270C: 30MINS (Normalized)
= LCP (ANN: 270/30) ON REMELTING
Peak= 322.77
Peak from: 304.14
to: 334.09
Onset= 312.65
J/g = 14.73
Peak from: 286.63
to: 335.26
Onset= 292.84
J/g = 7.22
Peak= 301.16
HEAT FLOW (W/g)
3
2.25
1.5
.75
0
280.00
290.00
300.00
310.00
320.00
330.00
340.00
Temperature (C)

Figure 3.20

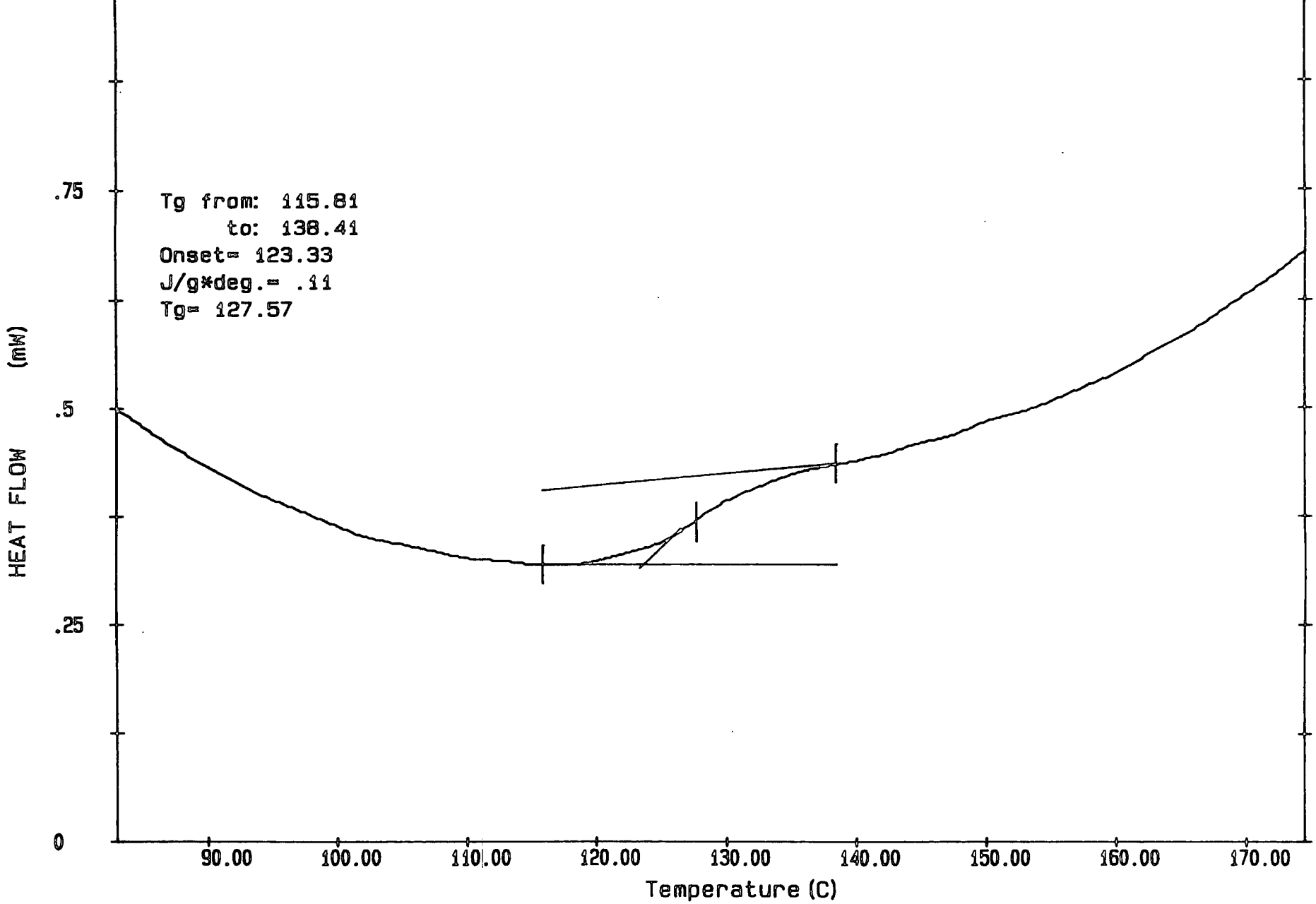
Tg from: 115.81
to: 138.41
Onset= 123.33
J/g*deg.= .11
Tg= 127.57
HEAT FLOW (mW)
.75
.5
.25
0
90.00
100.00
110.00
120.00
130.00
140.00
150.00
160.00
170.00
Temperature (C)

Figure 3.21

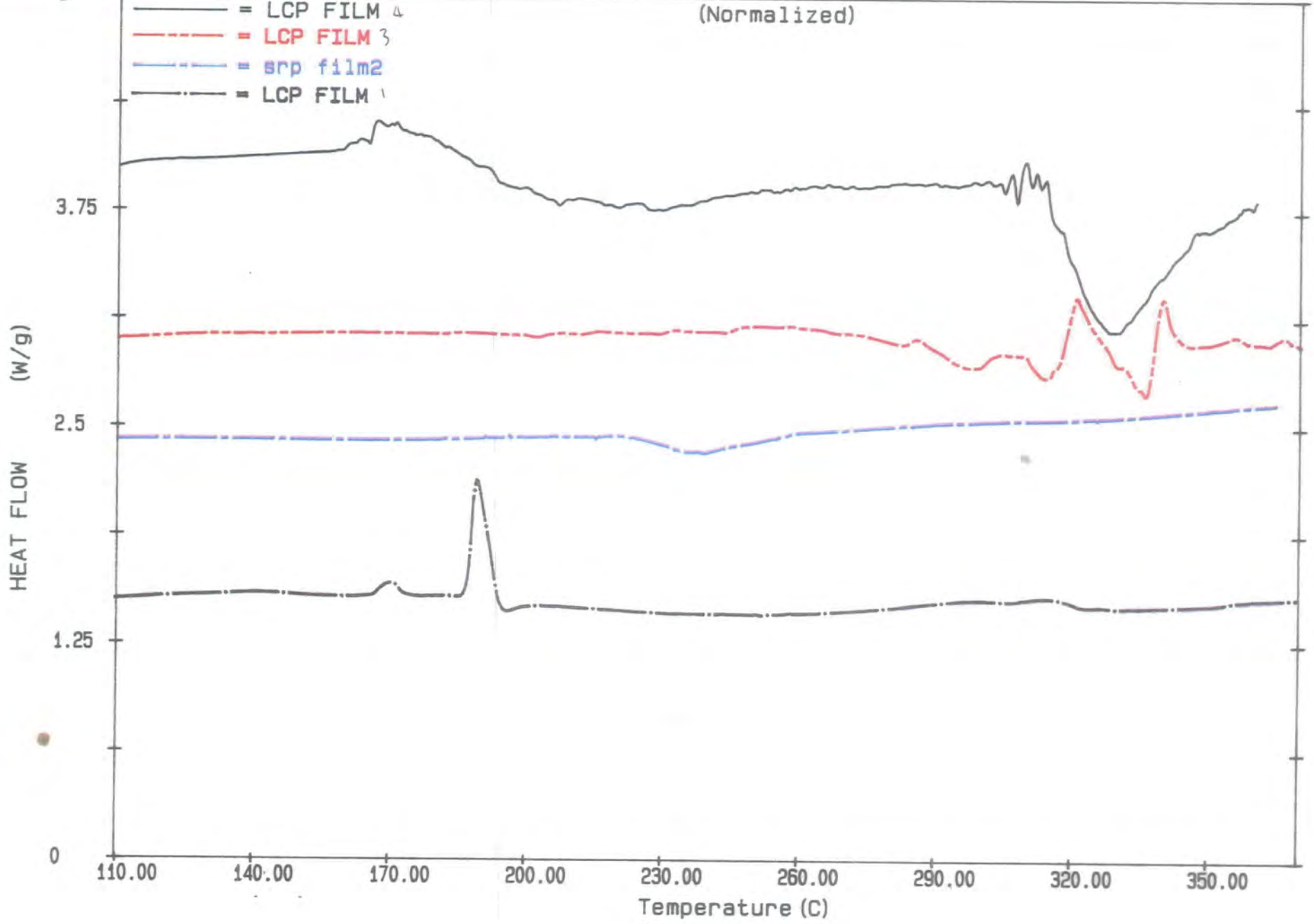
= LCP FILM 4
= LCP FILM 3
= srp film2
= LCP FILM 1
(Normalized)
HEAT FLOW (W/g)
3.75
2.5
1.25
0
110.00
140.00
170.00
200.00
230.00
260.00
290.00
320.00
350.00
Temperature (C)

Figure 3.22

powder scan is absent. Speculation suggests that some form of crystallisation occurs during preparation of the films, possibly as a result of dissolution or solvent evaporation. However the reasoning remains inconclusive. Film 1 exhibits two small, sharp endotherms over the range 160-200°C. These transitions occur at temperatures too low to be attributed to melting and cannot be attributed to crystallisation; an exothermic process. Film 2 exhibits a small broad endotherm over the range 210-260°C which, although this temperature range is higher than expected for crystallisation, this transition could be attributed to this process. Film 3 exhibits a multiple transition over the range 280-350°C, corresponding to the melting range for LCP (section 3.4.1)) However, due to the inconsistent nature of the baseline no thermal parameters could be calculated from this scan. The baseline in Film 4 is also very inconsistent and again no conclusions can be drawn on the thermal behaviour of the film from this scan. Polarising microscopy results did not aid in the identification of the transition observed in these samples. Due to the unreliable and unexplainable nature of the heating scans, the experiments on LCP films were abandoned at this stage.

3.7.9 *Thermal Transitions in LCP Fibres*

LCP fibres were scanned over the temperature range, 25-400°C. Figure 3.23 compares the heating scans of LCP powder and LCP fibres. The crystallisation exotherm observed for LCP powder is absent for the fibre sample. From microscopy (section (3.4.6)), ordering occurs during the fibre-drawing process and this ordering is maintained on cooling to ambient temperatures. LCP powder is initially amorphous and undergoes a crystallisation transition. Due to the initial crystalline order in the fibres, no equivalent transition occurs. On the basis of these results, it is not surprising due to the highly ordered nature of the fibres, that the heat of fusion is significantly larger than that obtained for the powder. The calculated values are given in Figure 3.23. A sharp single melting endotherm, typical of more ordered polymers is observed for the LCP fibres.

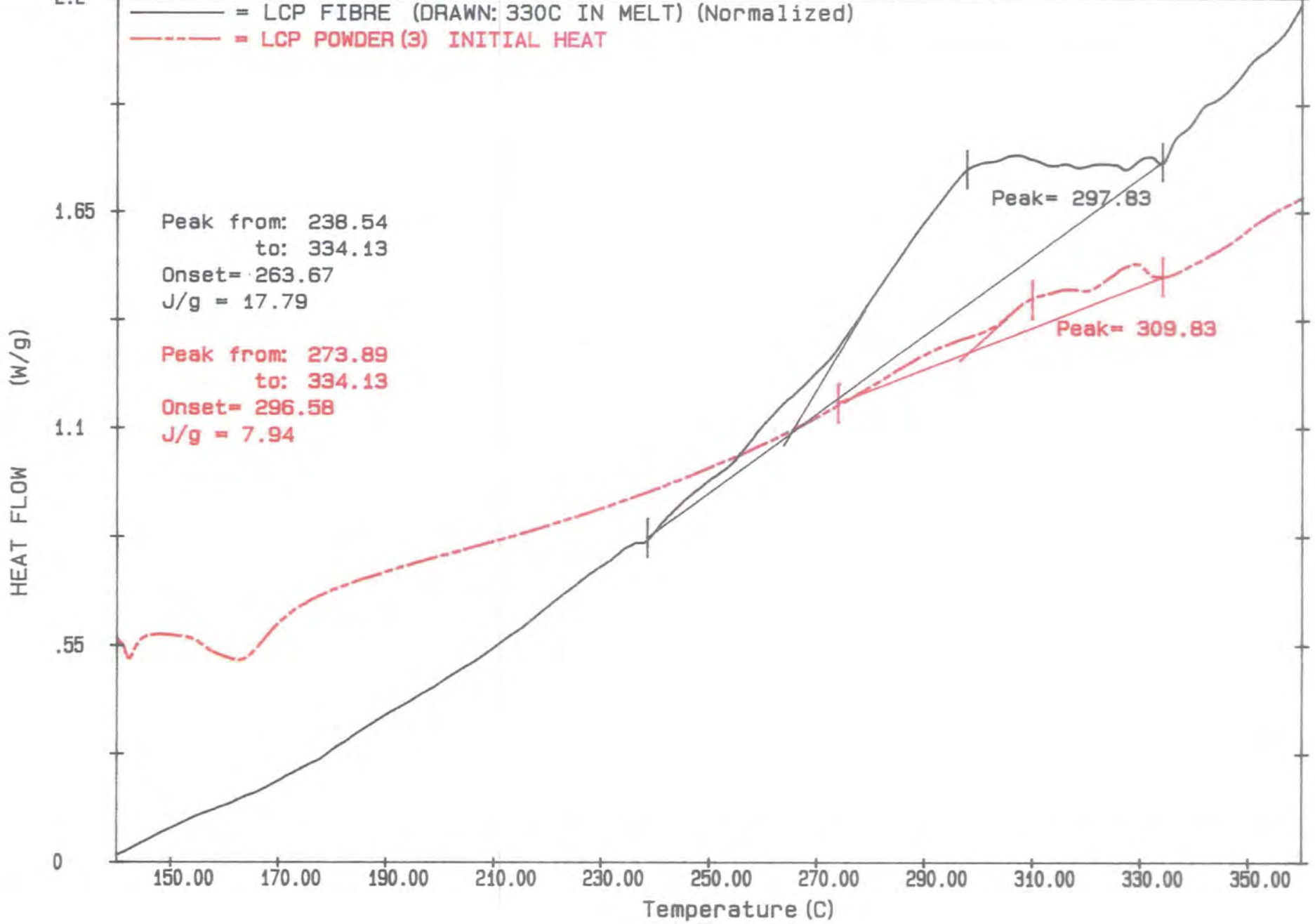
= LCP FIBRE (DRAWN: 330C IN MELT) (Normalized)
= LCP POWDER (3) INITIAL HEAT
Peak from: 238.54
to: 334.13
Onset= 263.67
J/g = 17.79
Peak from: 273.89
to: 334.13
Onset= 296.58
J/g = 7.94
Peak= 297.83
Peak= 309.83
HEAT FLOW (W/g)
1.65
1.1
.55
0
150.00
170.00
190.00
210.00
230.00
250.00
270.00
290.00
310.00
330.00
350.00
Temperature (C)

Figure 3.23

3.8 *General Conclusions*

LCP powder is almost completely amorphous at ambient temperatures. The polymer undergoes its glass transition at 130°C. Above this temperature, the material begins to crystallise. The crystallisation process continues on heating and melting begins at 270°C. A nematic melt develops and remains stable to 380°C. The nematic phase undergoes a transition to the isotropic phase prior to degradation at 420-430°C. From these results, LCP is classified as a thermotropic, nematic terpolyester.

The liquid-crystalline structure which develops in the LCP melt, is retained on quenching to room temperature. This observation coincides with the absence of a crystallisation transition in the subsequent heating run since the quenched sample is now partially ordered.

Annealing at temperatures well below the melt does not appear to have any noticeable influence on the thermal behaviour of LCP. In contrast, annealing at the onset of melting increases the ordering and hence the degree of crystallinity in LCP due to the greater mobility of the polymer chains. LCP powder which has become ordered by annealing, reverts back to its original random structure on remelting. This process is attributed to rapid ester-interchange reactions occurring above the melting point. Microscopy results reveal that LCP films are slightly more crystalline than LCP powder at ambient temperatures suggesting that ordering occurs, to a small extent, during preparation of the films. The films exhibit nematic melts at equivalent temperatures to the powder however the transition to the isotropic melt is not observed. Fibres drawn from the melt are highly oriented along the draw direction. These structures are retained on cooling. The degree of crystallinity for the fibres is significantly higher than that obtained for LCP powder, even after annealing.

(1) Wendtlandt, W. W. *"Thermal Methods of Analysis"* 2nd ed., Vol. 19 Wiley, New York (1974)

(2) Lenz, R. W. *Pure and Applied Chem.* 57(7) 977 (1985)

(3) E. Turi, Ed., *"Thermal Characterisation of Polymeric Materials"* Academic Press, New York (1981)

(4) Moore, J. S., Stupp, S. I., *Macromolecules* 20 273 (1987)

(5) Laus, M., Caretti, D., Angeloni, A. S., Galli, G., Chiellini, E., *Macromolecules* 24 1459 (1991)

(6) Cheng, S. Z. D., *Macromolecules* 21 2475 (1986)

(7) Butzbach, G. D., Wendorf, J.H., Zimmerman, J. H., *Polymer* 27 1337 (1986)

(8) DeMeuse, M. T., Jaffe, M., *Polym. Adv. Technol.* 1 8 (1990)

(9) Lin, Y. G., Winter, H. H., *Macromolecules* 21 (1988)

(10) Jackson, W. J., Kuhfuss, H. F., *J. Polym. Sci. Polym. Chem. Ed.* 14 2043 (1976)

(11) Viney, C., Donald, A. M., Windle, A. H., *J. Mater. Sci.* 18 1136 (1983)

(12) Clark, G. L.,(ed) *"The Encyclopaedia of Microscopy"*, Reinhold, New York (1961)

(13) Spencer, M., in *"Fundamentals in Light Microscopy"*, Cambridge University Press, Cambridge (1982)

(14) McLaughlin, R. B., in *"Special Methods in Light Microscopy"*, in The Microscope Series, Volume 17, Microscope Publications, London (1977)

(15) Richardson in *"Optical Microscopy for Materials Sciences"* Marcel Dekker, New York (1971)

(16) Sawyer, L. C., Grubb, D. T., in *"Polymer Microscopy"*, Chapman and Hall (eds) Cambridge University Press, Cambridge (1987)

(17) Mason, C. W., in *"Handbook of Chemical Microscopy"*, 4th Ed., Wiley, New York (1983)

(18) Basset, D. C., in *"Principles of Polymer Morphology"*, Cambridge University

Press, Cambridge (1985)

(19) Ward, I. M., (Ed.), in *"Structure and Properties of Oriented Polymers"* Applied Sciences, London (1975)

(20) Kahar, N., Ducket, R. A., Ward, I. M., *Polymer* 19 136 (1978)

(21) Trznadel, M., Kryszewski, M., *Polymer* 29 418 (1988)

(22) Demus, D., Richter, L., *Textures of Liquid Crystals, Verlag Chemie, Weinheim* (1978)

(23) Krigbaum, W. R., *J. Appl. Polym. Sci., Appl. Polym. Symp.* 41 105 (1985)

(24) Windle, A. H., Viney, C., Mitchell, G. R., *Polymer Communications* 24 145 (1983)

(25) Hearle, J. W. S., Sparrow, J. T., Cross, P. M., in *"The Use of Scanning Electron Microscopy"*, McGraw Hill, New York (1974)

(26) Noel, C., Friedrich, C., Laupêtre, F., Billard, J., Bosoi, L., Strazielle, C., *Polymer* 25 (2) 263 (1984)

(27) Wendtlandt, W. W., in *"Handbook of Commercial Scientific Instruments"*, Volume 2, Dekker, New York

(28) Yamamoto, A., Yamada, K., Maruta, M., Akiyama, J., in *"Thermal Analysis"*, Schwenker, R. F., Garn, P. D., Volume 1, Academic Press, New York (1969)

(29) Watson, E. S., O'Neill, M. J., Justin, J., Brenner, N., *Anal. Chem.* 36 1233 (1964)

(30) Wendtlandt, W. W. and Gallagher, P. K., in *"Thermal Characterisation of Polymeric Materials"*, Academic Press, New York (1981)

(31) Wiedemann, H. G., *Chem-Ing-Tech.*, 36 1105 (1964)

(32) Wunderlich, B., in *"Macromolecular Physics, Volume 2, Crystal Nucleation, Growth, Annealing"*, Academic Press, New York (1976)

(33) Finkelmann, H., in *"Polymeric Liquid Crystals"*, Ciferri, A., Krigbaum, W. R., Meyer, R. B., (eds) Academic Press, New York (1982)

(34) Hahn, B., Wendorff, J. H., Portugall, M., Ringsdorf, H., *Coll. and Polym. Sci.* 259

(9) 876 (1981)

(35) Noel, C., in *"Recent Advances in Liquid Crystal Polymers"*, Chapoy, L. L., (ed), Elsevier, New York (1985)

(36) Meesi, W., Menczel, J., Gaur, J., Wunderlich, B., *J. Polym. Sci., Polym. Phys. Ed.*, 20 719 (1982)

(37) Sauer, T. H., Zimmermann, J. J., Wendorff, J. H., *Coll. and Polym. Sci.* 265 210 (1987)

(38) Butzbach, G. D., Wendorff, J. H., Zimmermann, J. H., *Makromol. Chem. Rapid Commun.* 6 821 (1985)

(39) Meurisse, P., Noel, C., Monnerie, L., Fayolle, B., *Brit. Polym. J* 13 55 (1981)

Chapter 4

Structural Analysis

4.1 *Introduction*

X-rays were discovered by Roentgen in 1895.[1,2] Their use in radiography was established almost immediately despite the fact that the phenomenon of x-rays was not understood. It was not until 1912 that the exact nature of x-rays was established and soon after, x-ray crystal diffraction studies began.[3,4] X-rays are electromagnetic waves of the same nature as light however they possess much shorter wavelengths. The wavelength of x-rays used in diffraction studies, lies within the range: 0.5-2.5Å, whereas the x-ray region of the electromagnetic spectrum lies within the range: 0.1-1000Å. The theory, instrumentation and practical considerations in x-ray diffraction are well documented[5-8] and will not be dealt with to any great extent in this text.

The present chapter compares data for as-prepared and annealed LCP films in order to investigate possible changes in structure as a result of heat treatment using wide-angle x-ray scattering (WAXS) techniques. The samples were annealed at selected temperatures ranging from the glass transition to above the melt. The results obtained are studied mainly on a qualitative basis, where the changes in the intensity and sharpness of the Bragg peaks, obtained from equatorial 2Θ scans, are related to changes in structure and crystallinity. LCP samples, in the forms of both powders and films are examined and their structural behaviour, compared. X-ray photographs illustrate the orientation patterns in LCP films and fibres treated under selected annealing conditions. The percentage crystallinities were calculated for the majority of the samples studied. The variations in this parameter, as a function of annealing temperature and time are discussed. Essentially the analysis of the polymer samples using WAXS techniques complements the results obtained by thermal analysis as described in Chapter 3 and as a consequence, leads to a thorough understanding of the thermo-structural behaviour of LCP.

4.2 *Wide Angle X-Ray Scattering (WAXS)*

4.2.1 *A Brief Insight into the Theory of X-Ray Diffraction*

The theory of x-ray diffraction is not unlike the theory of electron and neutron diffraction. The latter is discussed in Chapter 5 and hence a detailed theoretical study is not included in the present chapter. Although these theories are very similar with respect to one another, the sample geometries (eg. thin films or bulky samples) required by these particle beams are significantly different thus imposing limitations or, in some cases, advantages on their use. The interactions between x-rays and matter lead to both absorption and scattering of the x-rays. The present study is concerned with obtaining structural information. Such information is obtained solely from scattering and hence absorption is not considered here. Scattering occurs partly without and partly with, a slight change in wavelength. Only the former is of interest since it gives rise to systematic interference effects between rays scattered by different volume elements of the structure. This type of scattering, known as coherent scattering, results from collisions of photons with electrons which are so tightly bound to the atomic nuclei that no energy exchange can occur. Scattering involving change in wavelength, referred to as incoherent scattering, leads to a loss of energy of the photon to the electron which in turn is promoted to a higher energy level or is ejected from the atom. Incoherent scattering gives rise to a continuous background in diffraction experiments.[9] This background scattering must be subtracted in order that accurate structural information can be obtained. A general relationship between structure and scattered intensity has been derived and is discussed in detail in the literature.[10-13] Structural details are determined from plots of intensity versus scattering angle.

4.2.2 *Determination of Crystallinity*

The evaluation of the crystallinity of a polymer is of significant importance in the investigation of its morphology. The concept of the crystallinity in a polymer is based on the two phase approximation of the polymer structure which assumes that uniform crystalline and amorphous regions can be distinguished. The model is generally accepted as the basis for the description of polymer morphology. The crystallinity may be represented in a number of ways: either by weight (ψ) or volume (ϕ), or simply by describing it as the degree of order in a polymer. Where ρ, ρ_C and ρ_D represent the densities of a polymer specimen, the 100% crystalline polymer and the 100% amorphous polymer respectively, the following relationships exist:

$$\psi = \phi\rho_c / \rho \qquad \text{and} \qquad (1-\psi) = (1-\phi)\,\rho_a / \rho \qquad (4.1)$$

Various methods for determining the degree of crystallinity in polymers using x-rays have been devised and are described in detail in the literature.[14-16] Such methods are referred to as being based on either external, or internal comparison. The former method involves the comparison of the intensity of the components in a sample with the intensity of that component in 100% concentration whereas the latter is based on the comparison and use of the intensities of both components. Ruland's method[17] based on external comparison is the most universal and is justified theoretically, however a number of alternative methods have been proposed and applied.[18-20] In his version, a standard procedure for separating the crystalline peaks from the amorphous halo, plus incoherent scattering was applied. This procedure requires knowledge of the shape of the amorphous background in order to determine the intensity due to the crystalline peaks alone. Vonk's method[21] assumes that this information is available. This method of analysis is shown diagrammatically in Figure (4.1).

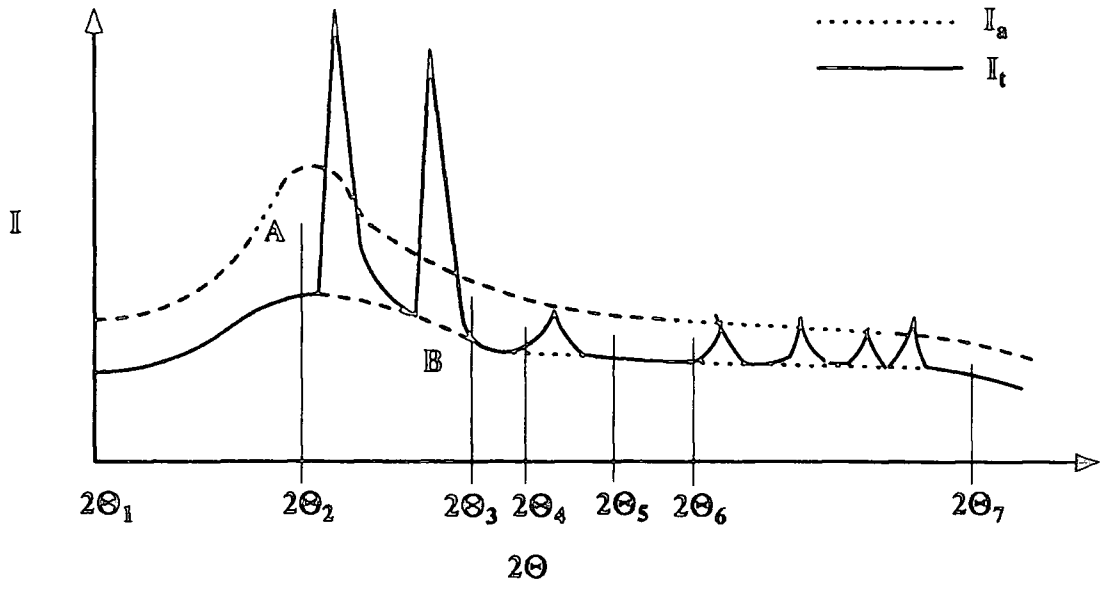

Figure (4.1) Procedure for separating the crystalline peaks from the continuous background in the X-ray diagram

The diffraction curves are obtained for a polymer (I_t) and the 100% amorphous sample (I_a) where the latter curve is represented by curve A. The number of 2Θ values, numbered $2\Theta i$ are presented.

It is assumed that no crystalline peaks occur in the intervals ($2\Theta_1$-$2\Theta_2$) and ($2\Theta_3$-$2\Theta_4$) etc. However in the intervals $2\Theta_2$-$2\Theta_3$, $I_B = I_A C$ represents the relation used to construct the background curve where C is a factor which varies linearly between the values C_2 at $2\Theta_2$ to C_3 at $2\Theta_3$ etc., and I_B represents the resultant intensity of the fitted amorphous curve. In Vonk's analysis the intensity at $2\Theta_i$ is evaluated by fitting I_t to a quadratic equation. General correction factors and practical aspects taken into account are discussed in detail in the literature.[11,21] As mentioned, methods of evaluating crystallinity require that the intensity due to amorphous scattering, be separated from the overall scattering before this parameter can be determined. This method presents a serious problem in the analysis of several polymers, due to the amorphous template being unobtainable. Furthermore the scattering from the molten polymer does not provide an acceptable template since the interchain distances may increase due to thermal expansion and consequently the shape of the amorphous halo in the melt and in

the solid could be significantly different.

Recently, Murthy and Minor[22] devised a procedure obtaining a reliable description of the amorphous scattering by polymer x-ray diffraction analysis and from these results, the crystallinities of a variety of polymers were evaluated. The authors studied a highly crystalline sample where they regarded the intensity not attributable to the crystalline peaks as being due to amorphous scattering. This amorphous halo was used as a template in the analysis of the diffraction patterns of less crystalline samples. This method is very valuable in the evaluation of crystallinity for polymers where a reliable amorphous specimen cannot be obtained.

In the present study an amorphous halo is obtained for the LCP melt (Figure (4.7)) thus a reliable amorphous halo is available. The method used for obtaining the degree of crystallinity in the LCP samples is based on Ruland's method, where the amorphous curve is fitted to the crystalline curve after subtraction of the scattering due to background. The areas under the corrected curves are calculated for the diffractometer scans over the range, 2Θ = 10-35° yielding the intensity due solely to the crystalline Bragg peaks (I_c) and the amorphous sample (I_a). The fractional crystallinity is calculated from the relation:

$$x_c = \frac{I_c}{I_c + I_a} \qquad (4.2)$$

4.3 *Experimental*

4.3.1 *Introduction*

WAXS techniques can be used in the structural determination of synthetic polymers. In this work, LCP films and fibres are studied. X-ray studies involved the use of both flat film camera and scanning diffractometer techniques. All quantitative results are obtained from the diffractometer scans. Before WAXS experiments could be carried out, it was necessary to fulfil the following experimental requirements:

a) the preparation of LCP films and fibres

b) the accurately controlled annealing of LCP films.

The present chapter provides an account of the sample preparation, instrumentation and experimentation involved. Analysis of the results obtained, both on a qualitative and a quantitative basis, illustrates the effects of thermal annealing as a function of temperature and time. WAXS results were used to complement the results evaluated from thermal analysis of LCP, as discussed in Chapter 3, using DSC and POM. From analysis and comparison of the results obtained using these 3 techniques, a thorough understanding of the thermo-structural behaviour of LCP is established.

4.3.2 *Sample Preparation*

a) Polymer Purification

LCP was purified, as described in section (3.3.2(a))

b) Film Specimens

The purified polymer was dissolved in a TFA/DCM mixed solvent system in the ratio 95/5% volume. Both solvents were dried and distilled over $MgSO_4$ and distilled prior to use. The resulting mixture contained 4% wt/vol of LCP. The mixture was allowed to stand for 48 hours to ensure complete dissolution. Approximately $10cm^3$ of the LCP solution was poured into a teflon casting dish (100 x 100mm) of thickness, 2.5mm. A watch glass was placed over the dish and the solvent, allowed to evaporate slowly to virtual dryness. An additional $10cm^3$ of LCP solution were then poured over the initial layer and the evaporation procedure was repeated. This process was carried out 5-6 times, leading to the formation of a flexible "rubbery" film. The film was then removed carefully, from the dish and cut into strips of 50 x 15 mm. These strips were sandwiched between glass slides and dried in vacuo for one week. The temperature of the oven was increased gradually from 25°C to 100°C over this period, to ensure complete solvent removal. The resulting films of approximately 1mm in thickness (adequate for x-ray analysis) were supported in aluminium sample holders which were mounted in the x-ray beam.

c) Fibre Specimens

LCP fibres were obtained using the method described in section (3.3.2(d))

4.3.3 *Instrumentation*

(a) Flat Film Camera

The flat film camera is a simple and convenient tool for recording the characteristic features of unoriented and oriented materials and hence, is frequently used in the x-ray study of synthetic polymers. A quick inspection of a flat film pattern will help assess

whether the polymer is crystalline or amorphous, oriented or unoriented, and will decide semi-qualitatively on the degree of perfection of the crystalline regions. A schematic diagram of a flat film camera is given in Figure (4.2).

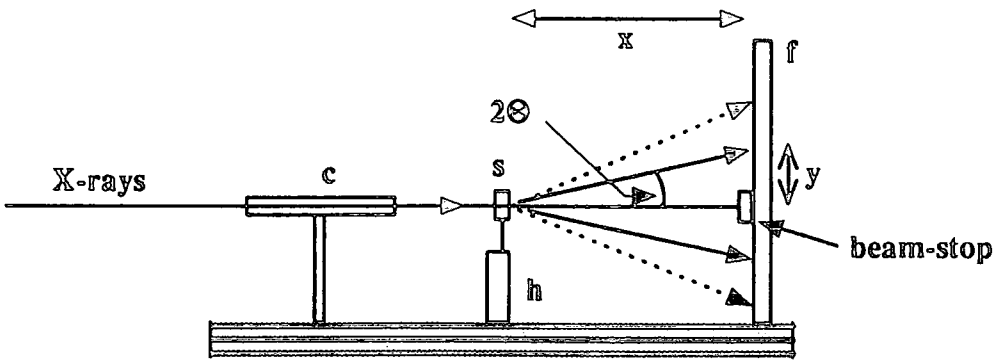

Figure (4.2) Scheme of a flat film camera

The incident beam travels through a collimator (c), which produces a fine beam of parallel x-rays. Specimen (s) is situated on the specimen holder (h) and the x-rays are scattered onto a film cassette (f), where the diffraction pattern is recorded. The film is sandwiched between the metal back and the front opaque paper. A beam stop, usually a lead disk of ~0.5mm thickness, is placed directly in front of the film holder to prevent the transmitted beam from striking the film. The Bragg angle corresponding to any diffraction spot or ring can be derived from

$$\tan 2\Theta = y/x \qquad (4.3)$$

where y is the distance from the spot (or ring) to the centre of the film and x is the specimen to film distance. The experimental set-up in the present work involves a flat plate camera on a Hiltonbrooks DG-2 X-ray Generator. X-rays were generated from a copper tube run at 40kV and 30mA. No filtering methods were used. The sample to film distance was 5cm for all LCP films and fibres studied.

(b) Diffractometer

The x-ray detector used in a diffractometer is in the form of a movable counter, as opposed to the photographic film used in the camera. Three different types of counters are described elsewhere in the literature.[5,23,24] The counter is located on the circumference of a circle centred on the specimen surface. Figure (4.3) shows the focusing arrangement used in this type of diffraction instrument.

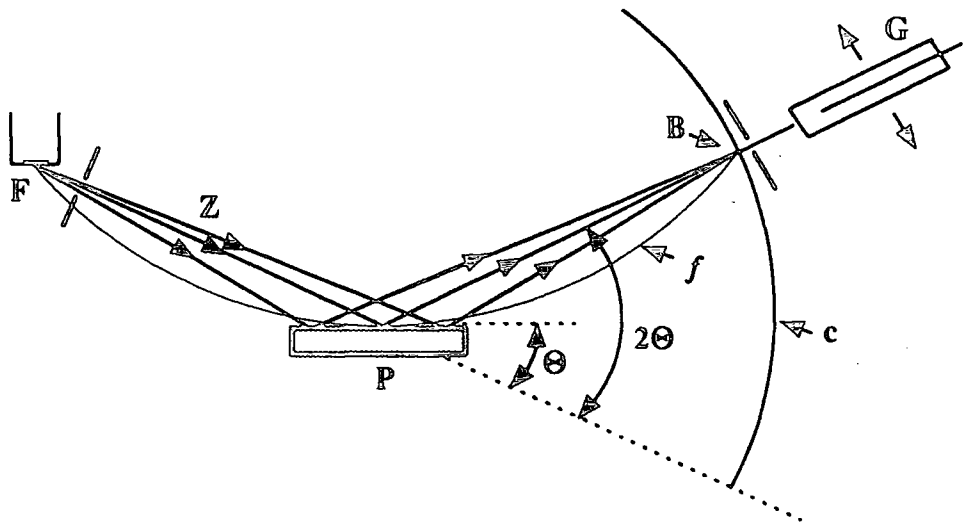

Figure (4.3) X-ray Diffractometer Focusing Arrangement

The x-ray beam diverging from the focus, f, irradiates the surfaces of a flat specimen situated at P. In general the rays, diffracted at a Bragg angle Θ by appropriately oriented crystallites on the specimen surface, converge to a single line at B. The receiver slit of a counter tube is placed at point B and the tube is moved along the goniometer circle, C about the axis, P in order to scan angles 2Θ. The flat specimen is rotated about P, also at half angular speed and therefore always remaining tangential to the focusing circle if moved through F, P and B. This set-up is known as the Bragg-Brentano focusing geometry.[25] The main reason for using a flat specimen, is to take advantage of the focusing action in order to increase the intensity of weak diffracted beams, so that they

can be measured with accuracy. Strictly, the specimen should be curved in order to fit the focusing circle and to achieve perfect focusing at B. The focusing circle is not of constant size; its radius increases as the 2Θ angle decreases. Due to the lack of perfect focusing for flat specimens, some broadening of the diffracted beam results at B. However the consequences are not too serious as long as the amount of divergence of the incident beam is not too large. The amount of 2Θ divergence and lateral divergence in the Bragg-Brentano geometry is illustrated in Figure (4.4).

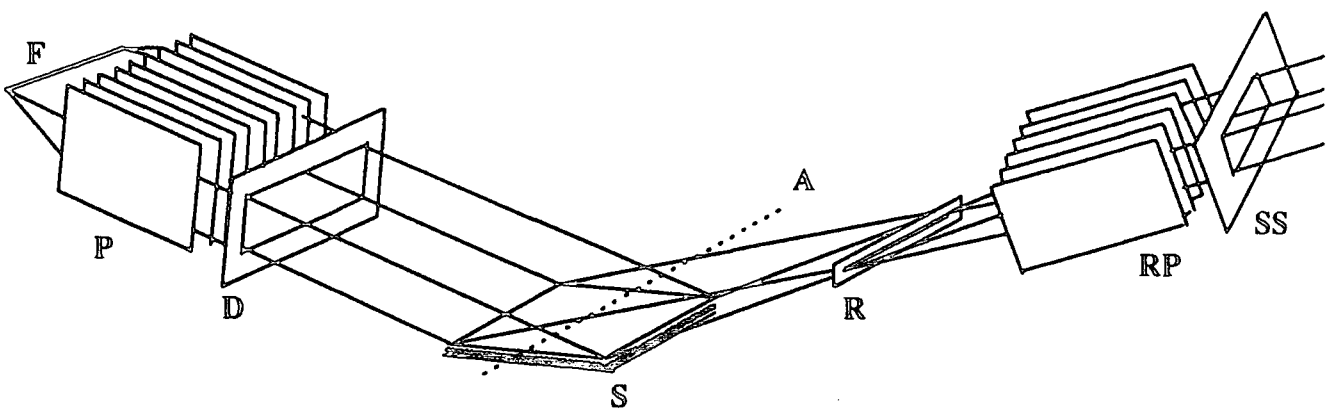

Figure (4.4) Vertical and Lateral Divergence in a Diffractometer

The divergence in 2Θ is governed mainly by the effective focal size, the apertures of the divergence and receiver slits, D and R, and by the depth of penetration of the x-rays into the sample. A scatter slit, SS, situated between R and the detector, reduces the background scattering. Two sets of vertical parallel plate collimators, P and RP, placed between the focus and specimen, and the specimen and scatter slit respectively, are used to control lateral divergence. The choice of both the divergence slit, D and scatter slit, SS are dictated by the angular range to be scanned.[5,25] Generally the thinner the sample the lower the diffracted intensity since deeper layers no longer contribute. However this contribution decreases with distance from the surface. The instrumental line breadth of a diffracted line profile will be determined mainly by the angular aperture of the receiving slit R, but the intensity of this line will depend on the slit aperture and on the focal spot dimensions of the x-ray tube. A conventional automatic powder diffractometer in addition to the counter tube, includes amplifiers, a pulse height analyser, scaling circuit

with printer and a rate-meter with chart recorder. The functions of each of these devices are described elsewhere.[5]

In the present work, two different diffractometers were used in the study of the structural behaviour of LCP as a function of temperature:

(I) A Philips Scanning Diffractometer, a PW/1730 Generator and a PW1050/30 Goniometer with proportional detector producing CuKα radiation were run in transmission and a single nickel filter was used. The slit sizes selected were 1/6", 4° and 4° where the former is the divergence slit and the latter two are the receiver slits for the x-ray source.

(II) A Siemens Diffractometer (Type F) connected to a Siemens Kristalloflex 4 X-Ray Generator with internal stabilisation. The x-rays were generated from a copper tube and a Ni filter was used to give CuKα radiation. The detector used was a scintillation counter.[26]

4.4 *Results and Discussion*

4.4.1 *Introduction*

This section looks at preliminary work carried out on the structural characterisation of LCP. It must be stressed that the majority of results are purely qualitative and that this study is by no means considered to be complete. The polymer samples studied were not aligned (with the exception of a brief study on LCP fibres) and consequently, a reliable quantitative characterisation of molecular arrays using x-ray techniques could not be carried out.

The main aim of the work was to observe any structural changes in LCP as a result of thermal annealing over a selected range of temperatures and times. WAXS experiments were carried out mainly on LCP films since these were considered to be the most consistent, handleable form for these studies. However, comparative data for untreated LCP powders and fibres were included in the analysis for completeness.

Annealing conditions were selected from preliminary DSC studies (section 3.4). Temperatures such as glass transition, crystallisation, melting and mesophase transitions were amongst those studied. Annealing times were selected over the range: 0-120 minutes.

Preliminary WAXS studies were carried out on scanning diffractometer (I) at ICI, Wilton. From the results obtained, it became evident that a wider range of annealing times would aid in the understanding of the initial observations. Studies were continued thereafter at the University of Leeds, where WAXS photographs were obtained for selected LCP samples. Further work was carried out using their scanning diffractometer (II) on a wider range of samples. Final WAXS experimentation was carried out again at ICI, Wilton, where selected samples were rerun in order to calculate the relative percentage crystallinities (x_{cr}). Thus, all data presented in this work was run on diffractometer (I) in order to eliminate calibration errors/discrepancies etc. between the instruments used.

Qualitative information on the degree of order and mesophase type was obtained from the WAXS photographs. From spectra obtained from the WAXS diffractometers, any changes in intensity and peak position as a result of annealing, can be associated with changes in crystallinity and structure of the polymer. A qualitative analysis of such changes was carried out as a function of temperature and time and a quantitative analysis of the spectra provided an estimate of the crystallinity for each sample.

Ultimately it was intended that thermal analyses and quantitative WAXS studies on identical LCP samples, be carried out in order to conclude on any direct relationships between x_{cr} and/or heats of fusion thus enabling the study of the effects of thermal annealing on the entropy of the system. Unfortunately this proved to be impossible due to the irreproducibility of the DSC scans obtained for these LCP films. However, some annealing studies were carried out on LCP powders treated over a range of times (section (3.7.8)). It would be considered inaccurate as well as unscientific to draw direct conclusions from the DSC results for LCP powders and WAXS results for films due to the possible errors in preparation and slight behavioural differences between the sample forms. In this case however, the natures of the forms are considered sufficiently similar to make speculations. It would be advantageous to carry out simultaneous DSC/WAXS studies at the Daresbury facilities in Cheshire, in order to draw firm conclusions on the results presented in this work.

4.4.2 *WAXS Photographs*

a) Introduction

WAXS photographs were obtained for both LCP films, annealed under specific conditions and LCP fibres drawn directly from the melt. Each sample was placed at a distance of 5cm from the x-ray source and the fibres were stacked vertically in bundles in the beam. Annealing temperatures and times were selected from thermal analysis

results presented in Chapter 3. The photographs obtained are presented in Figure 4.5. Calculation of scattering intensity angles was not carried out since these values can be obtained directly, and with greater accuracy, from 2Θ diffractometer scans. These scans will be discussed later on in this work, and hence calculation of the 2Θ angles from the photographs was considered unnecessary.

b) Qualitative Study

From a quick inspection of the scattering patterns obtained for samples (a)-(e), it is obvious that a random orientation exists within the annealed polymer films, identified from the circular nature of the scattering intensities. Figure 4.5(a) represents the pattern obtained for LCP annealed at 180°C for 30 minutes (ie. the region of the crystallisation exotherm, discussed in section (3.4). These rings appear sharp, representative of a small degree of ordering.

It will be demonstrated later in these studies, that the 3 rings of identical radii, occurring in photographs (a), (b) and (d), represent the 3 major Bragg peaks, characteristic of the LCP structure.

Figure 4.5(b) represents an LCP film annealed at the onset of melting (270°C) for 30 minutes. Again, the presence of the rings, although not as sharp as those given in (a) indicate that a certain degree of ordering is present. Figure 4.5(c) illustrates the scattering pattern for LCP annealed at 330°C for 2 minutes. From DSC and microscopy studies, LCP is observed to melt under these conditions. The observations correlate well with the scattering pattern, where a diffuse halo, characteristic of an amorphous melt and an absence of ordering is observed. An identical sample was annealed in the melt for 60 minutes. From thermal analysis, LCP was observed to re-order in the melt. Figure 4.5(d) illustrates the scattering pattern obtained under these conditions. The presence of sharp rings confirms the proposed structural development which occurs with annealing. The pattern is similar to that obtained for samples annealed below the melt (ie. Figures 4.5 (a) and (b)) suggesting that a similar structure re-develops upon melting. Figure 4.5(e) represents the scattering pattern obtained for LCP annealed above the melt

Figure 4.5

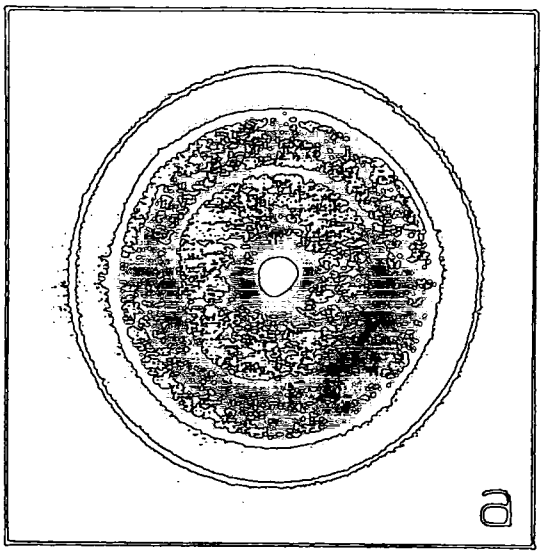

180degC/ 30 mins

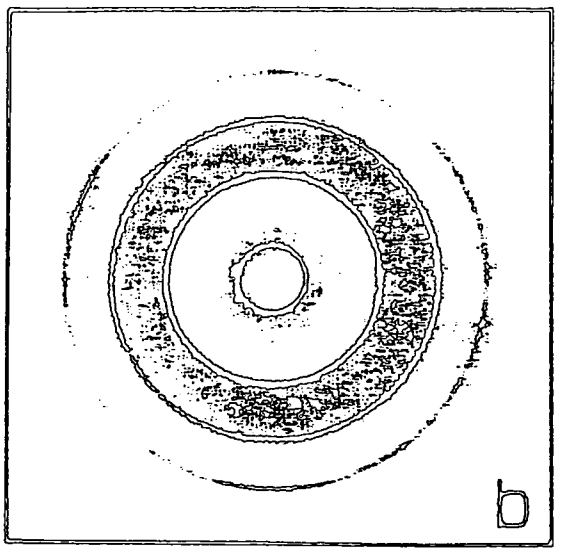

270degC/ 30 mins

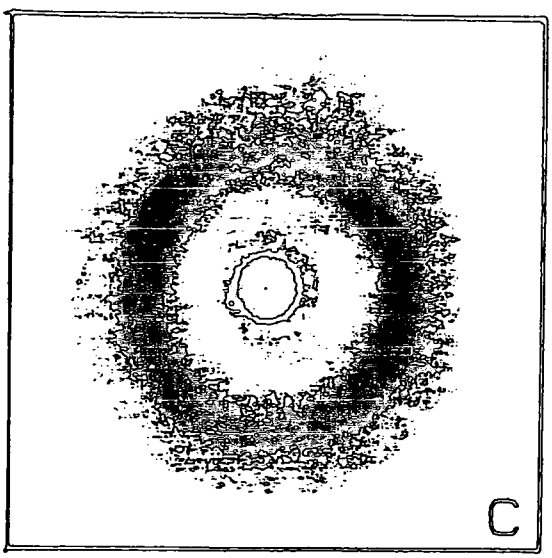

330degC/ 2 mins

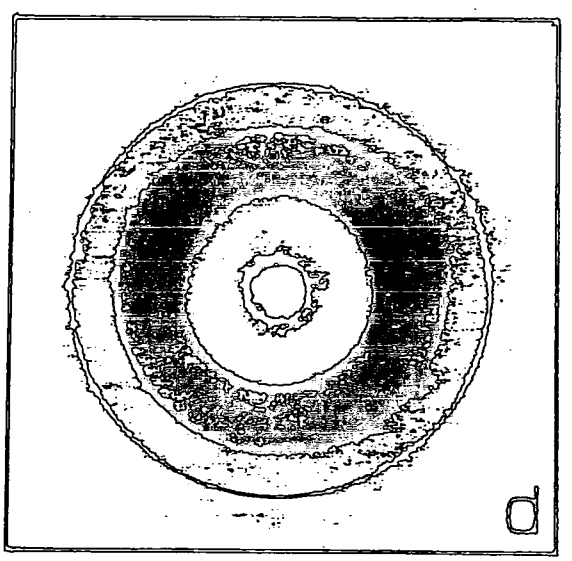

330degC/ 80 mins

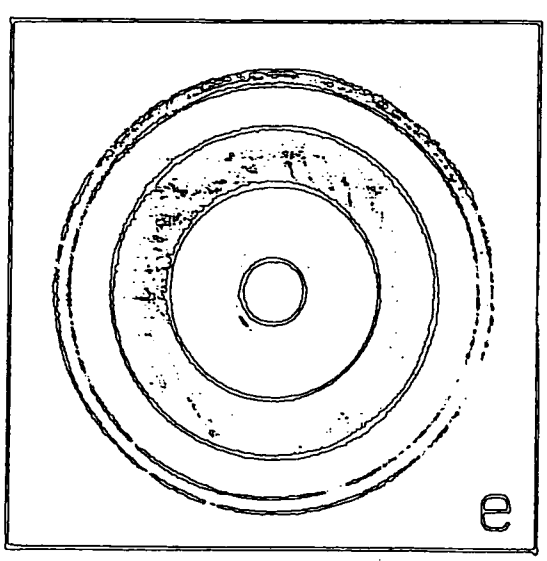

340degC/ 10 mins

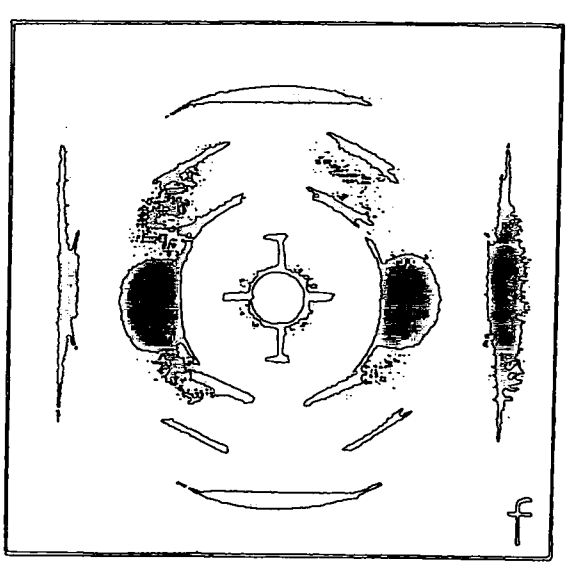

340degC (fibre).

WAXS photographs: LCP annealed at different temperatures

(ie. T = 340°C, t = 10 minutes). A fourth outer ring has developed, characteristic of a further structural development above the melt. In addition, the rings appear sharp and distinct, suggesting that the polymer can exist in an ordered form in the region of the anisotropic melt. The scattering pattern obtained for LCP fibres drawn from the anisotropic melt, is illustrated in Figure 4.5(f). The presence of a number of distinctive arcs and lines along the meridian, confirms that the polymer fibre has oriented along its draw direction.

4.4.3 *WAXS Scans*

a) Introduction

A qualitative study of the structural developments of LCP films as a function of temperature and time is discussed. Analysis of the data obtained from the 2Θ diffractograms was considered to be unnecessary, since a brief study by Blundell and co-workers has been covered in the literature.

From DSC and microscopy studies, discussed in Chapter 3, crystallinity and structural rearrangement are influenced by annealing. The aim of this work is to confirm these observations and to note any consequential changes in structure. From the literature an increase in sharpness and intensity of the Bragg peaks is associated with an increase in degree of ordering. It must be stressed that the data has been corrected for background scattering however no corrections been made for sample thickness. The latter parameter was not measured accurately, however each sample was approximately 1mm in thickness. The thickness influences the scattering intensity and hence any alterations in intensity could not be compared between samples. The intensities are thus recorded using an arbitrary scale however any apparent trends are recorded and discussed.

b) Qualitative Study

i) LCP Powder Versus Film

Figure 4.6 compares the 2Θ scans obtained for the as-prepared LCP powder and film. The powder sample is almost completely amorphous, identified by the absence of Bragg peaks, however a smooth halo, characteristic of amorphous material, exists. In contrast, the 2Θ scan recorded for the film exhibits small, broad Bragg peaks, confirming that a small amount of ordering is present. These results correlate well with DSC and microscopy observations (section 3.8) where LCP films appear slightly crystalline on preparation. Since no thermal treatment is involved in the preparation of these films, it is proposed that the slight degree of ordering present is due to the alignment of the molecules in the solvent.

ii) LCP Powder Versus Melt

A comparison of the diffractograms obtained for the powder versus the melt are given in Figure 4.7. The unannealed powder exhibits a very slight amount of order in comparison to the 100% amorphous melt. The halo obtained for the melt was used as a template in the calculation of the crystallinities dealt with in section (4.4.3(c)).

iii) Solvent Effects

The insolubility of LCP has proved to be a major drawback in its characterisation. The standard solvent mixture used throughout this work in the preparation of LCP films (ie. TFA/DCM) was replaced by hexafluoropropanol (HFP), since solvent was observed to influence the polymer's behaviour (section 3.8). Hence, a quick experiment was carried out to examine the effects (if any) of altering the solvent system. Diffractograms of LCP films cast from TFA/DCM (i) and HFP (ii) are given in Figure 4.8. It is obvious from

Figure 4.6

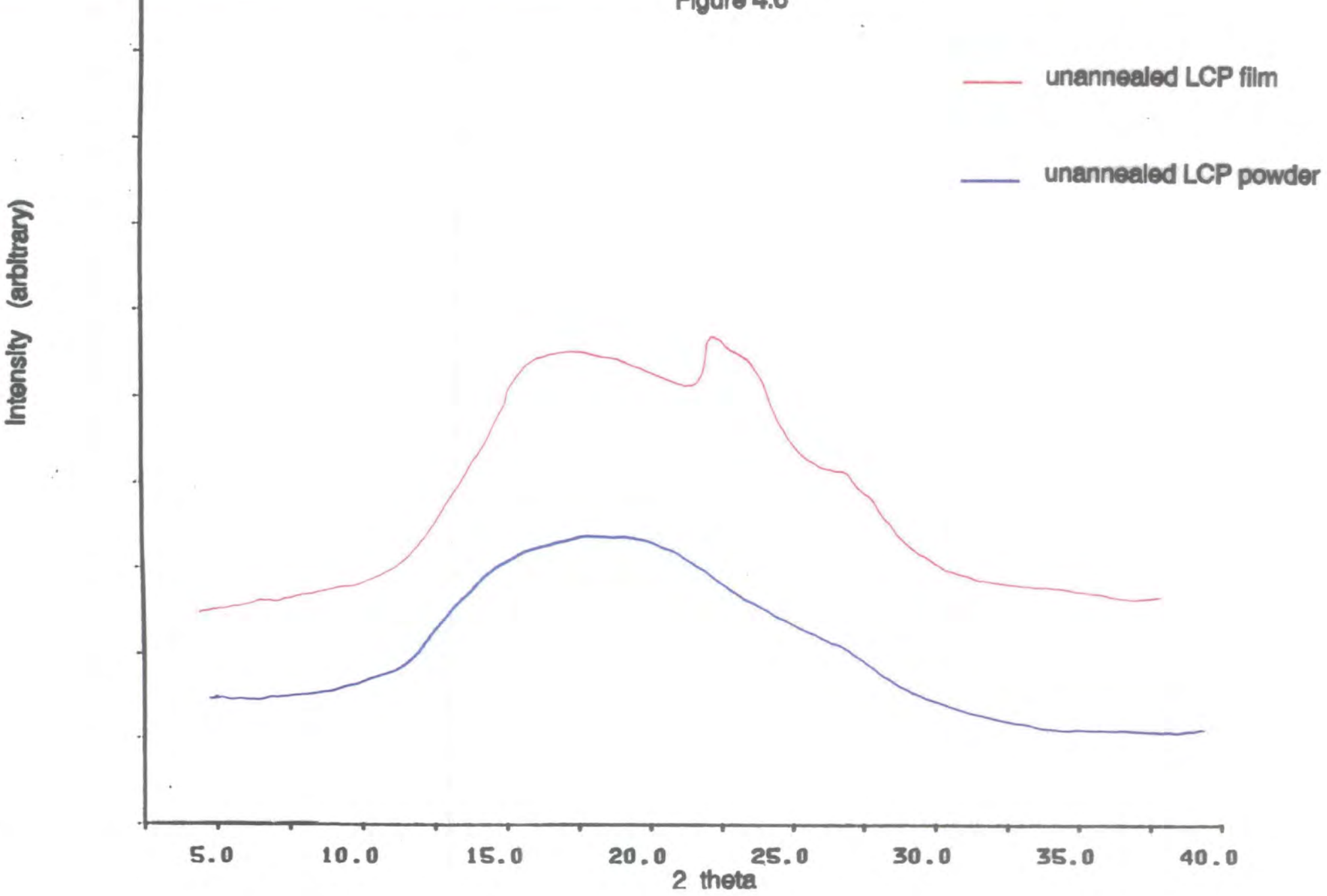
unannealed LCP film
unannealed LCP powder
Intensity (arbitrary)
5.0
10.0
15.0
20.0
25.0
30.0
35.0
40.0
2 theta

Figure 4.7

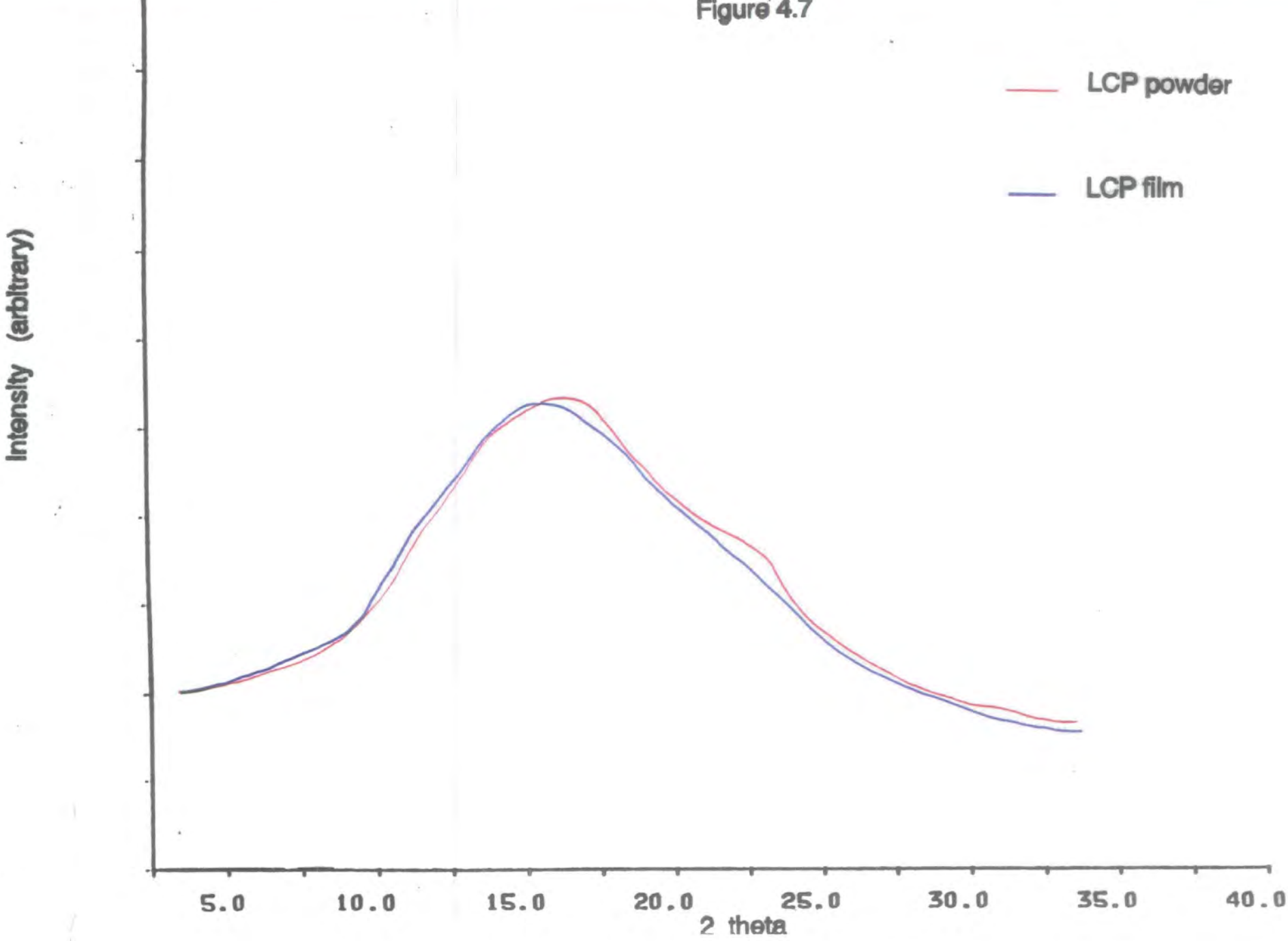
LCP powder
LCP film
Intensity (arbitrary)
5.0
10.0
15.0
20.0
25.0
30.0
35.0
40.0
2 theta

Figure 4.8

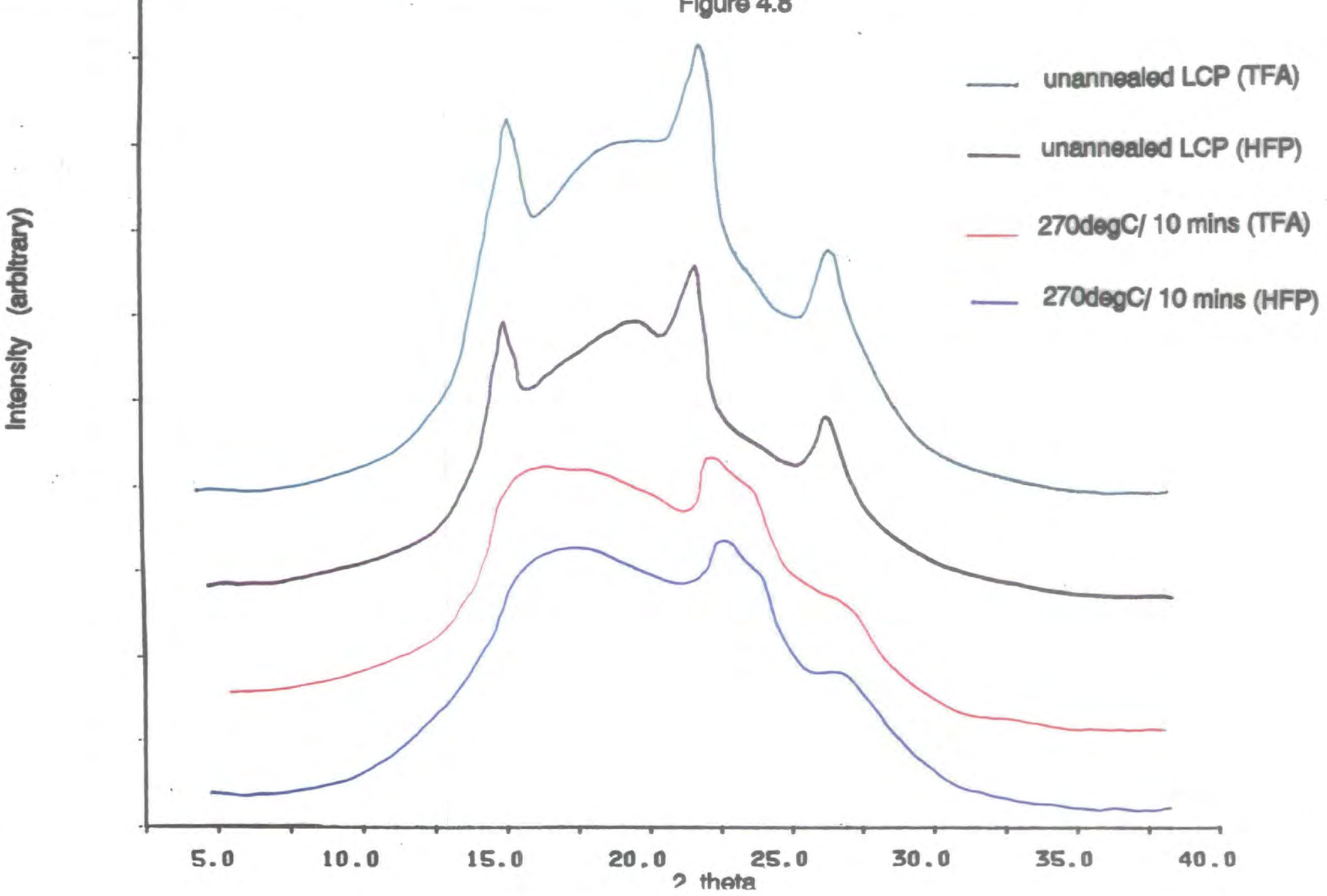
unannealed LCP (TFA)
unannealed LCP (HFP)
270degC/ 10 mins (TFA)
270degC/ 10 mins (HFP)
Intensity (arbitrary)
5.0
10.0
15.0
20.0
25.0
30.0
35.0
40.0
2 theta

the scans obtained that for the samples studied, solvent type does not affect structural development in LCP.

iv) Effects of Increasing Annealing Time

The influence of increasing annealing time was studied over a range of selected temperatures. Temperatures corresponded to specific thermal transitions, including Tg, crystallisation and melting. Times ranged from 0-120 minutes.

Figure 4.9 illustrates the effect of increasing annealing time for sample treated just above the Tg of the polymer for t = 5 minutes, a very slight development in peak intensity and sharpness is observed at $2\Theta = 22.5°$ however for LCP annealed for 10 minutes, a significant, rapid development of this peak and a further two peaks at $2\Theta = 16.5°$ and 17.5°, occurs. This scattering pattern is identical to that obtained by Blundell and co-workers[27] for annealed LCP samples, and appears frequently throughout these studies. As annealing time increases, the structure continues to develop, apparent from the increasing sharpness and intensity of the Bragg peaks. Thus, it may be concluded that there is sufficient mobility in LCP just above its Tg, for structural development to occur. Similar behaviour is observed for LCP annealed at 180°C and 270°C (Figures 4.10 and 4.11). Again the Bragg peaks increase in sharpness and intensity as a function of time, however the peak observed at $2\Theta = 22.5°$ increases gradually as a function of time, whereas at $2\Theta = 16.5°$, the initial small, broad peak increases dramatically with time. For T = 270°C, the characteristic peak at $2\Theta = 16.5°$, is already well established, and together with the remaining peaks, increases gradually in sharpness and intensity with increasing annealing time. Figure 4.12 illustrates the diffractograms for LCP annealed at 300°C, just after the onset of melting. The degree of ordering has reduced significantly in comparison to lower temperatures studied, however the peak present at $2\Theta = 16.5°$ continues to increase in intensity as a function of annealing time. Figure 4.12 illustrates the diffractograms for LCP annealed at 300°C, just after the onset of melting. The degree of ordering has reduced significantly in comparison to lower temperatures

Figure 4.9 (T anneal = 130 degC)

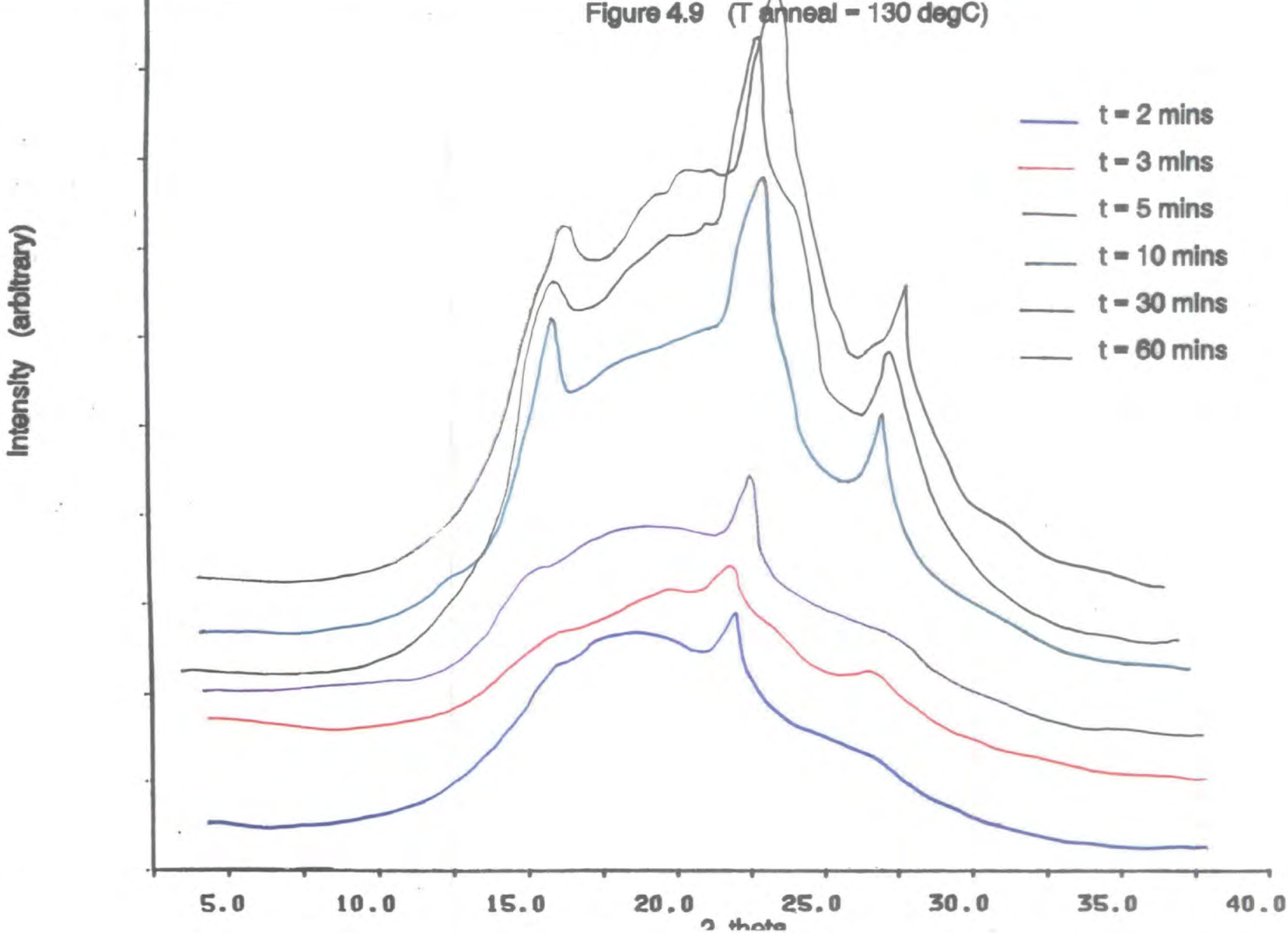

Figure 4.10 (T anneal = 100 degC)

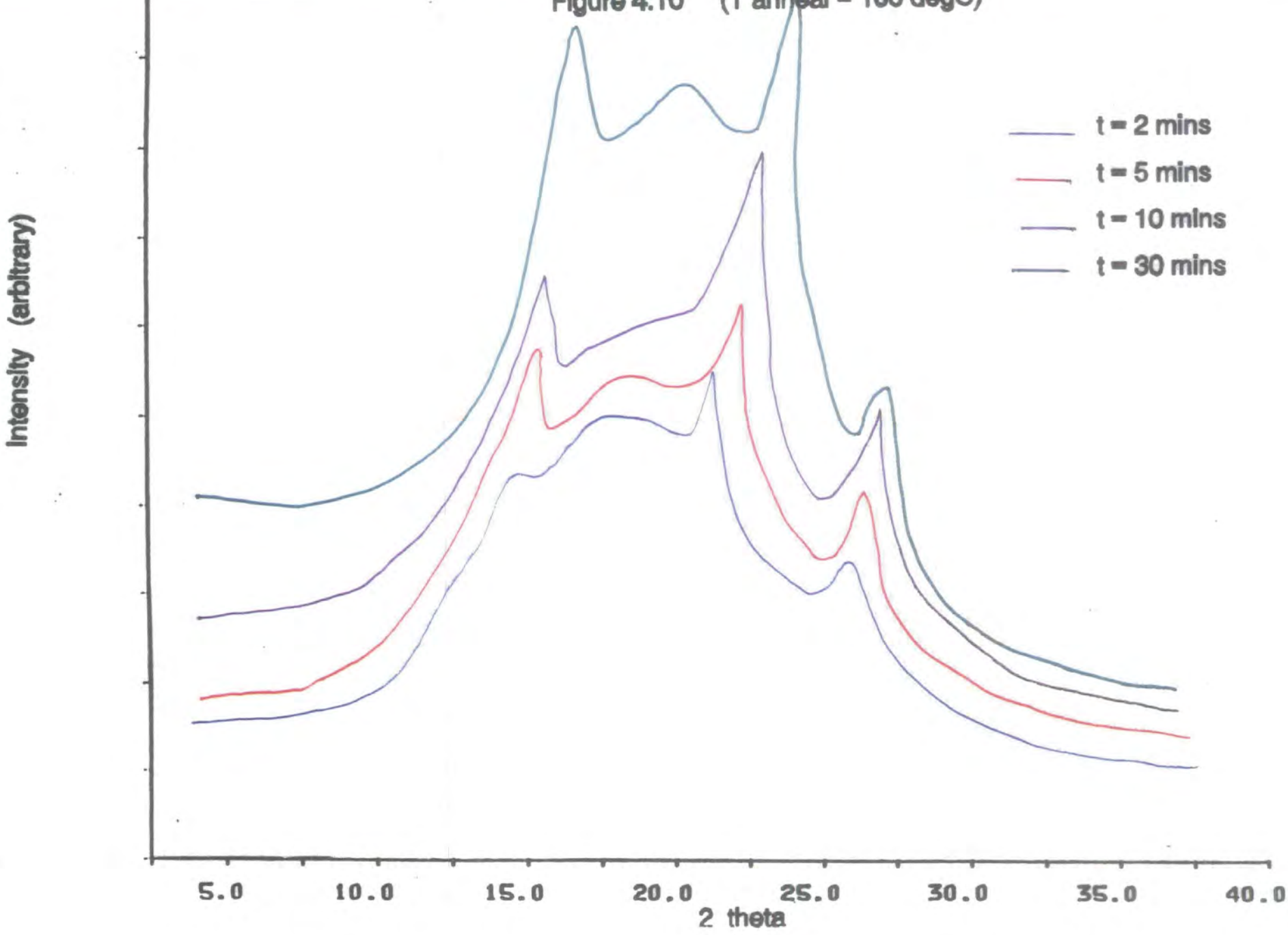

Figure 4.11 (T anneal = 270 degC)

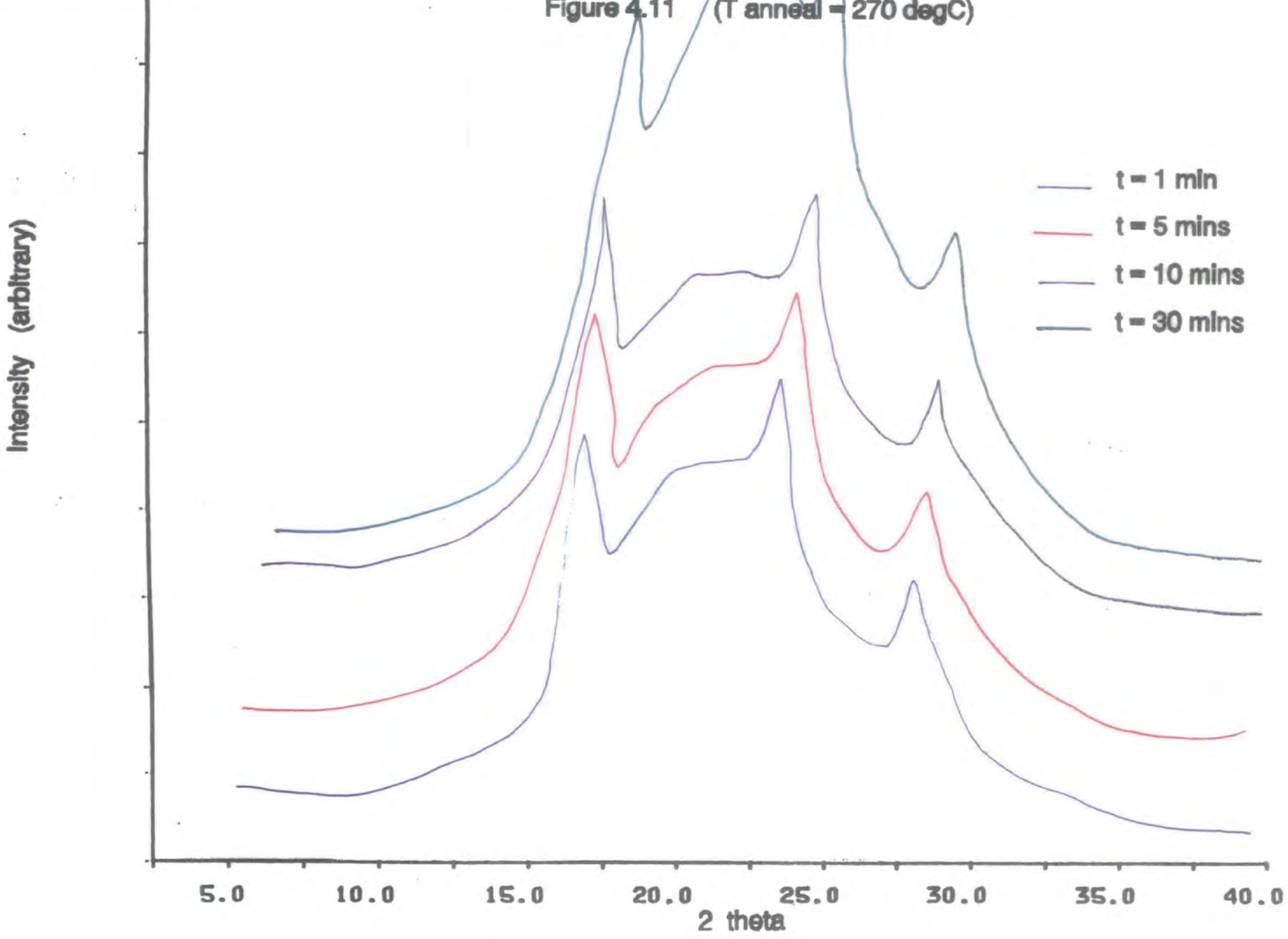

Figure 4 12 (T anneal = 300degC)

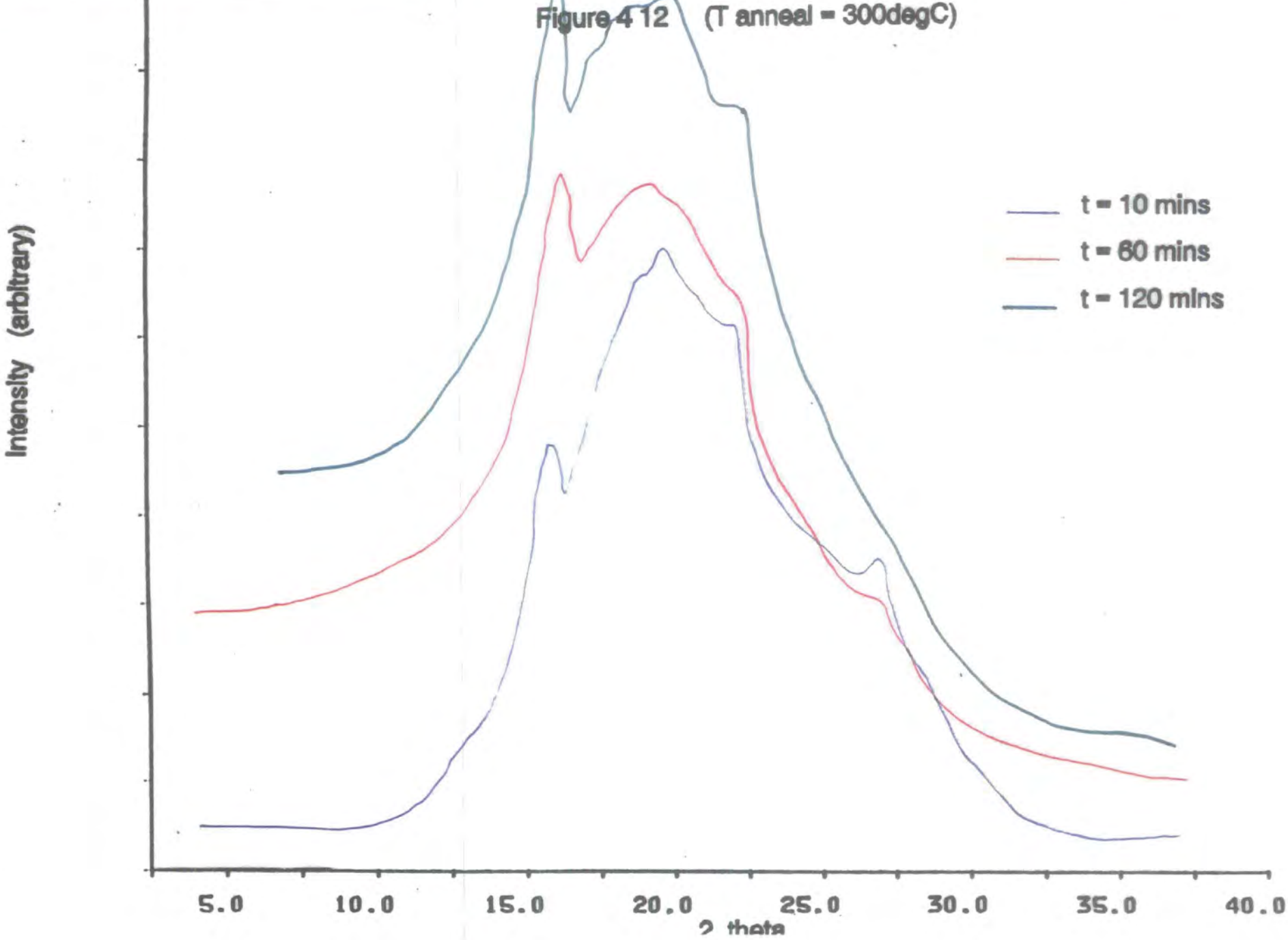

studied, however the peak present at $2\Theta = 16.5^{\circ}$ continues to increase in intensity as a function of annealing time. In addition, a fourth peak has begun to develop at $2\Theta = 21^{\circ}$ suggesting that the polymer undergoes a small amount of structural rearrangement when heated just above the onset of melting.

Diffractograms for samples annealed in the amorphous melt are given in Figure 4.13. For LCP annealed for t = 2 minutes, the sample appears completely amorphous however Bragg peaks are observed to develop as a function of annealing time, suggesting that reordering occurs in the melt.

v) Effects of Increasing Annealing Temperature

The diffractograms illustrated in Figures 4.14-4.16 illustrate the structural behaviour/developments occurring in LCP with increasing annealing time over the temperature range, T = 130 - 340°C.

2Θ scans obtained for samples annealed for t = 10 minutes are given in Figure 4.14. No significant structural rearrangement is observed, however the quantity of peaks increases for samples annealed above the melt. For samples annealed below the melt, ordering is observed to increase as a function of temperature.

For LCP samples annealed for 30 minutes (Figure 4.15) again, ordering appears to increase as a function of temperature; below the melt however structural rearrangement occurs for LCP annealed in the anisotropic melt.

Figure 4.16 illustrates diffractograms obtained for LCP samples annealed for 60 minutes. The scans demonstrate significant structural rearrangement occurring in LCP. The characteristic diffraction pattern alters gradually and at T = 180°C, the peak at $2\Theta = 16.5^{\circ}$ dominates. Above the melt, the intensities of the peak diminishes and for $2\Theta = 22.5^{\circ}$ and 27.5°C, they disappear completely. The peak, persistent at $2\Theta = 16.5^{\circ}$, diminishes slightly for samples annealed above 180°C, and for the sample annealed in the anisotropic melt, further small peaks have just begun to develop at $2\Theta = 14^{\circ}$, 26.5°, 27.5° and 29°.

Figure 4.13 (T anneal = 330 degC)

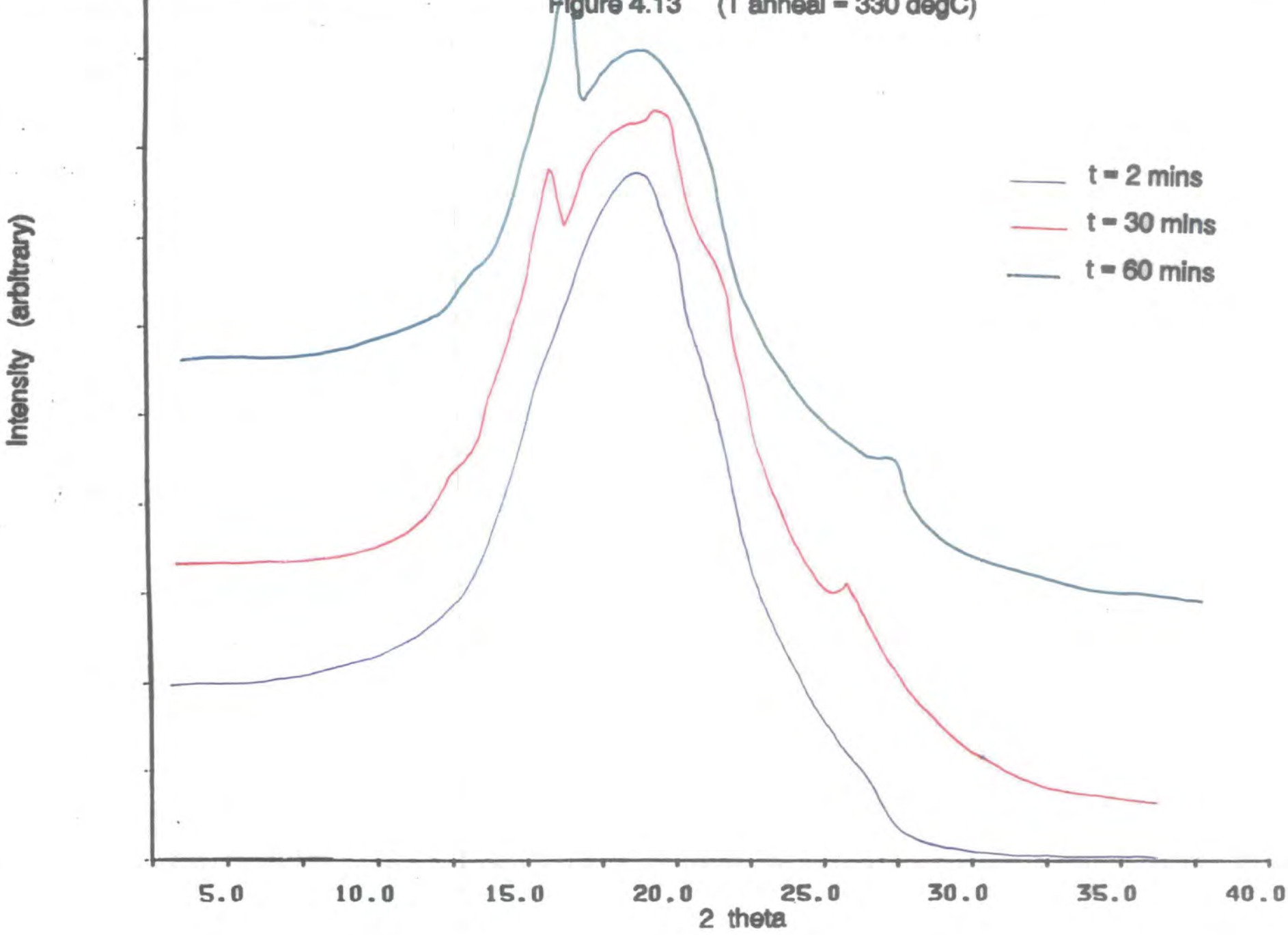

Figure 4.14 (t anneal = 10 minutes)

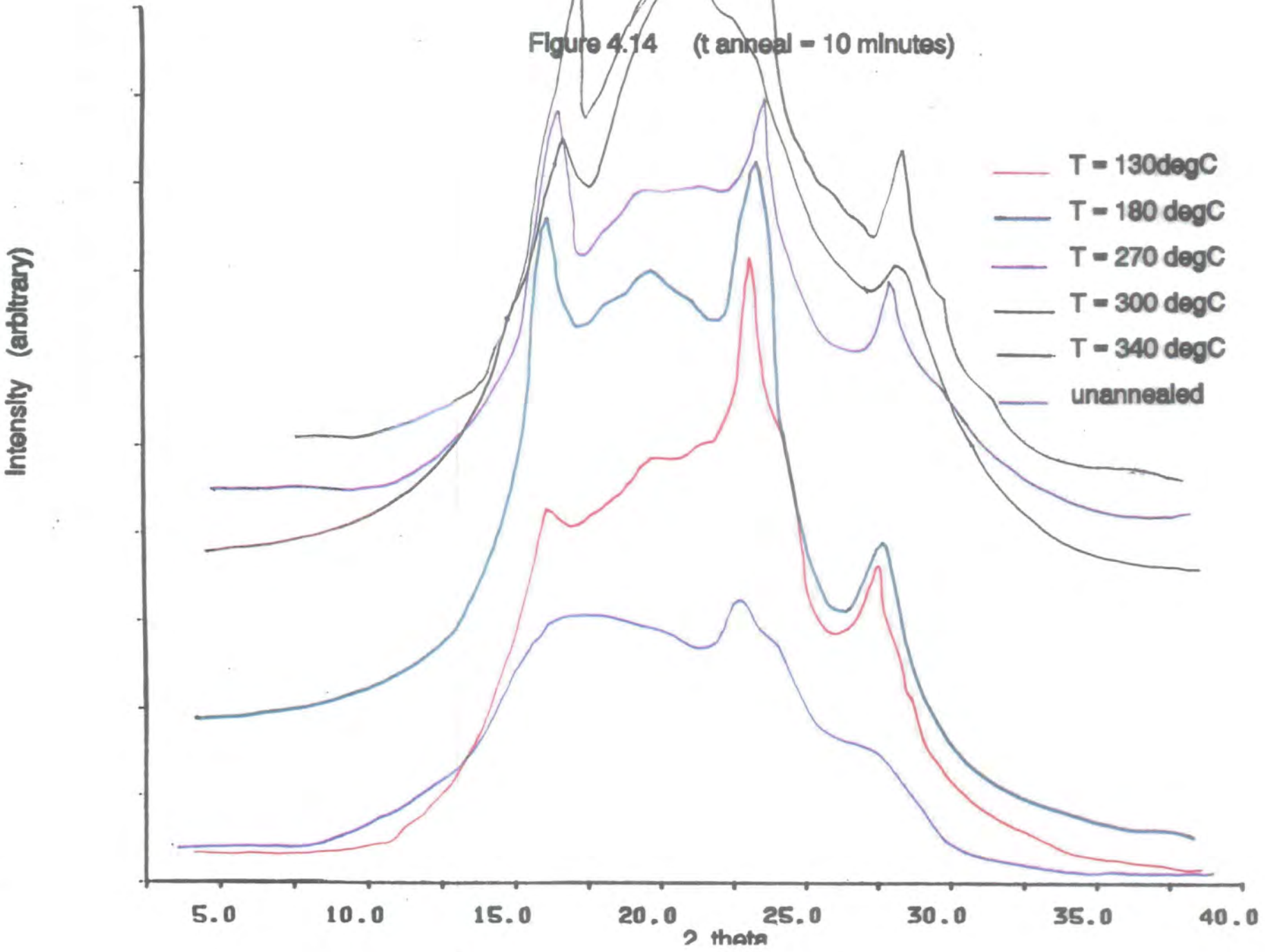

Figure 4.15 (t anneal = 30 mins)

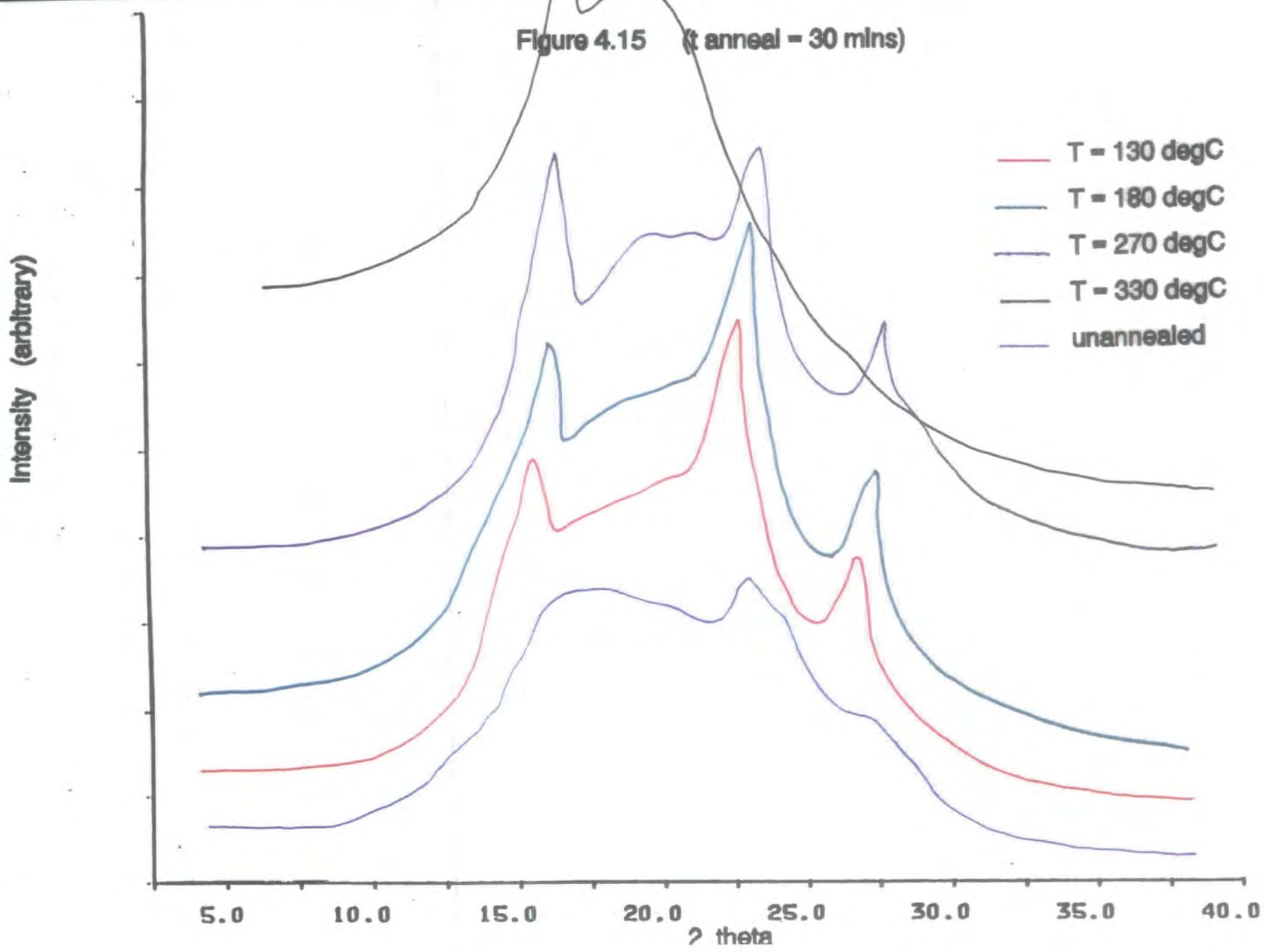

Figure 4.16 (t anneal = 60 minutes)

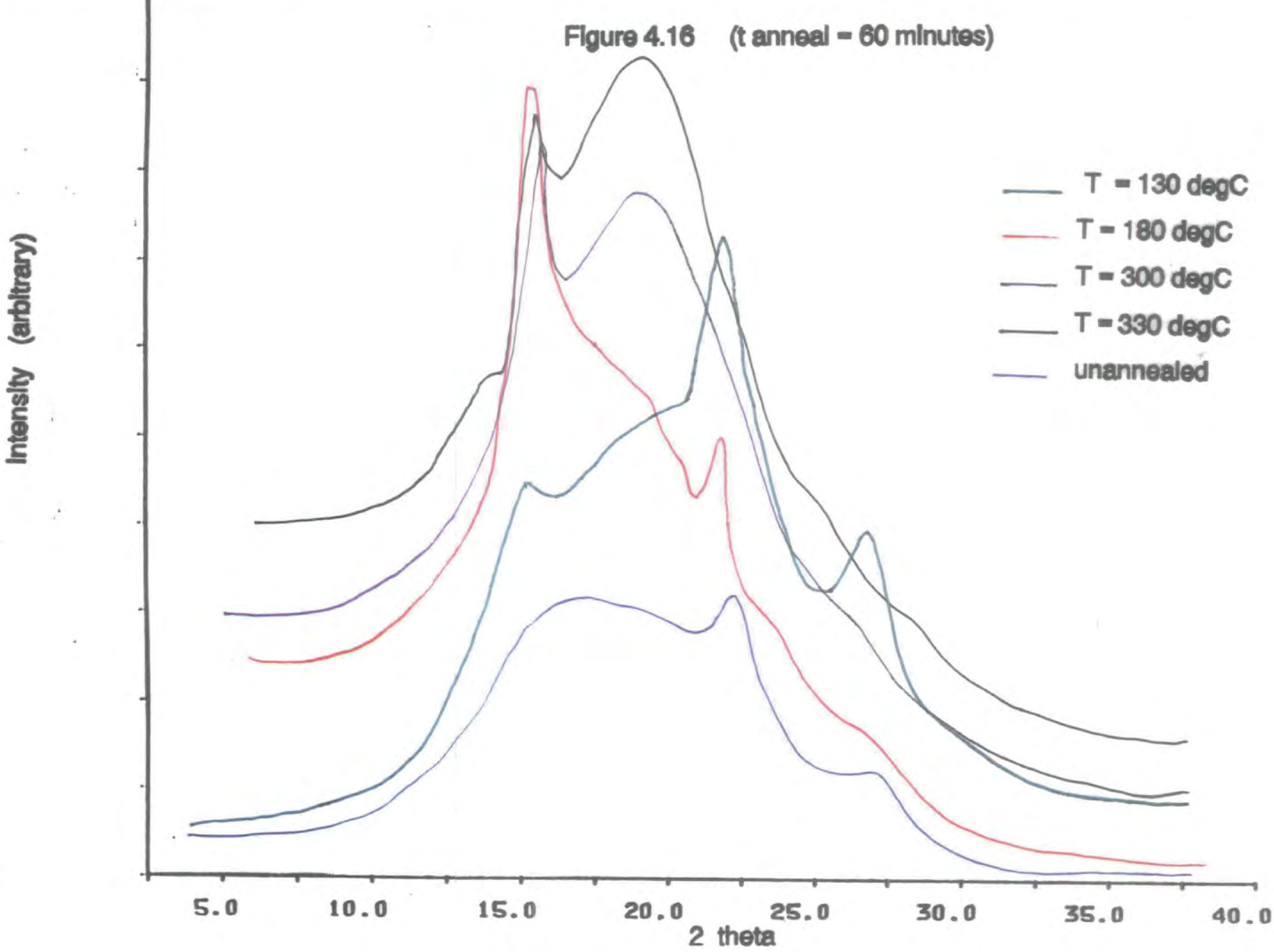

c) Determination of % Crystallinities

The calculated values of % crystallinity for the annealed polymer samples are given in Table (4.1). Due to the large number of errors involved in data evaluation, which in the worst scenario have been observed to vary up to 30%, the calculated values are used solely as a guide to demonstrate any changes in crystallinity as a function of annealing temperature and time. A limited number of samples were run due to shortage of time on the instrument. Selected diffractograms illustrating the scattering due to the "semi-crystalline" polymer, the amorphous polymer and the crystalline regions only are given in Figures 4.17-4.20.

t / minutes	x_{cr} /%					
	T/°C Ambient	130	160	270	300	330
0	11	-	-	-	-	-
2	-	14	12	14	-	0
5	-	12	14	16	-	-
10	-	17	18	18	11	-
30	-	18	22	9	-	6
60	-	18	24	24	5	9
120	-	-	-	-	8	-

Table 4.1

LCP powder was found to exhibit almost negligible crystallinity (0.5%) whereas an approximate value of 11% was calculated for the LCP film. In general, the values of % crystallinity increase as a function of both temperature and time for samples annealed below the melt. For samples heated in the anisotropic melt, x_{cr} increases with increasing

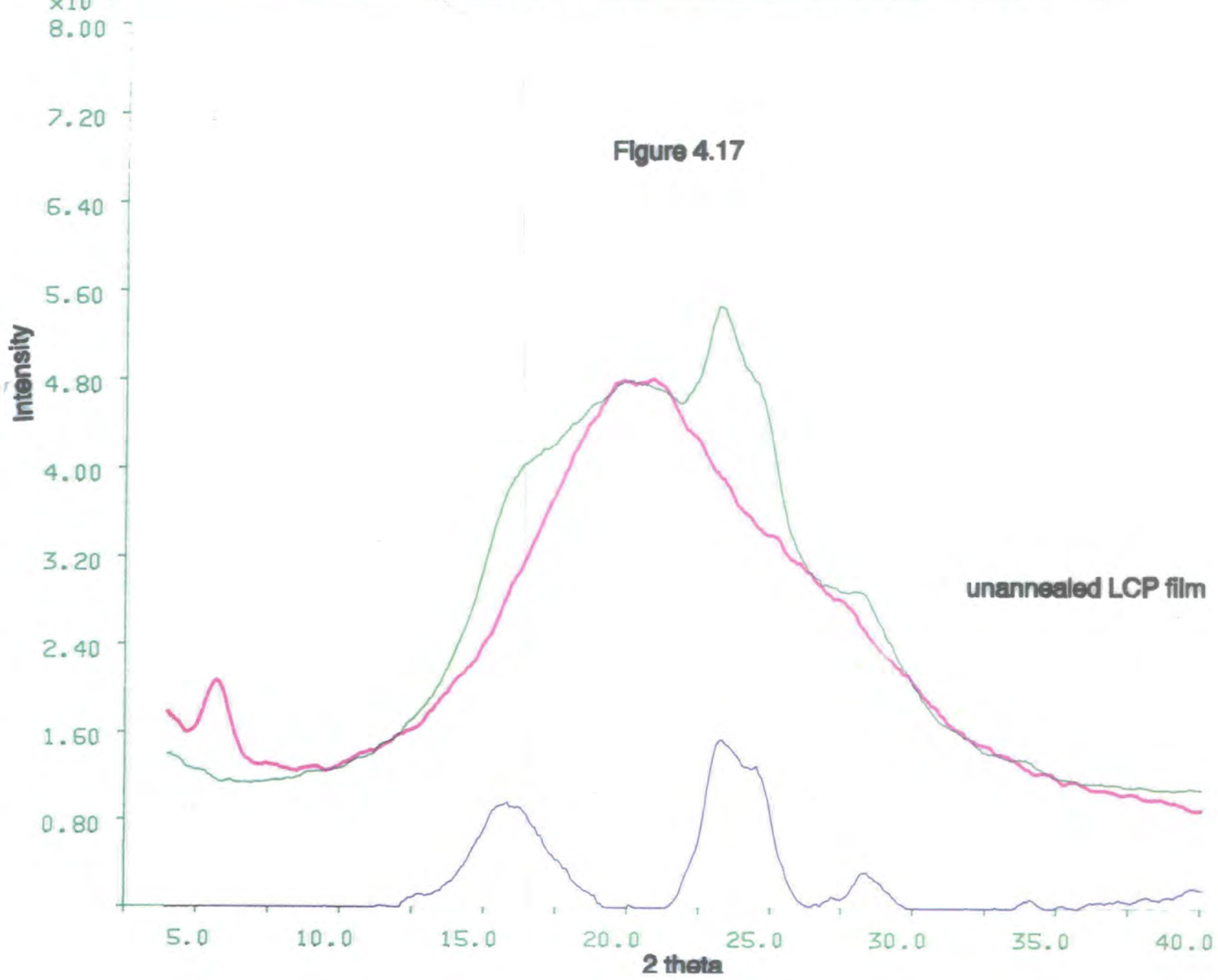
x10
8.00
7.20
6.40
5.60
4.80
4.00
3.20
2.40
1.60
0.80
Intensity
unannealed LCP film
5.0
10.0
15.0
20.0
25.0
30.0
35.0
40.0
2 theta

Figure 4.17

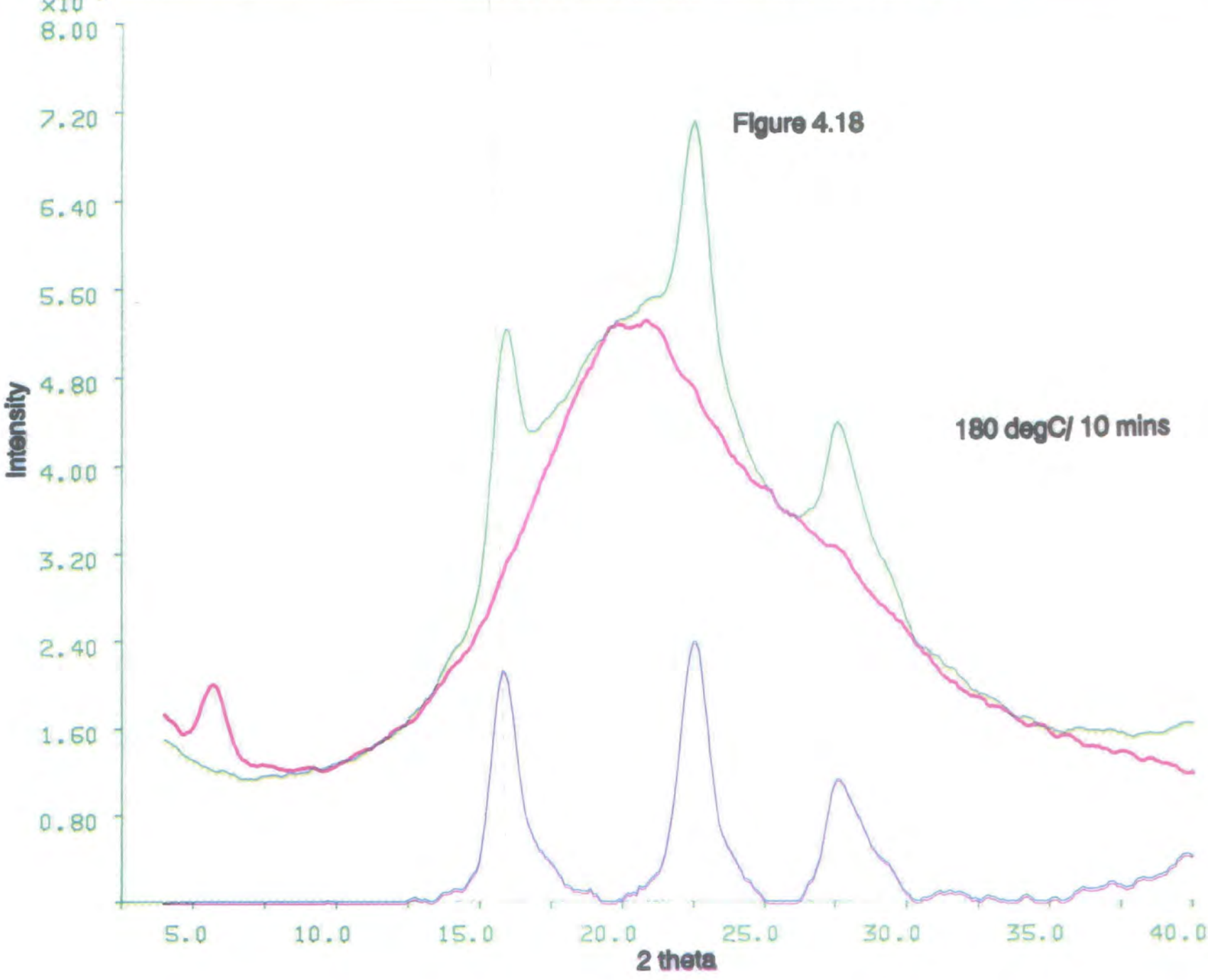
x10
8.00
7.20
6.40
5.60
4.80
4.00
3.20
2.40
1.60
0.80
Intensity
5.0
10.0
15.0
20.0
25.0
30.0
35.0
40.0
2 theta
180 degC/ 10 mins

Figure 4.18

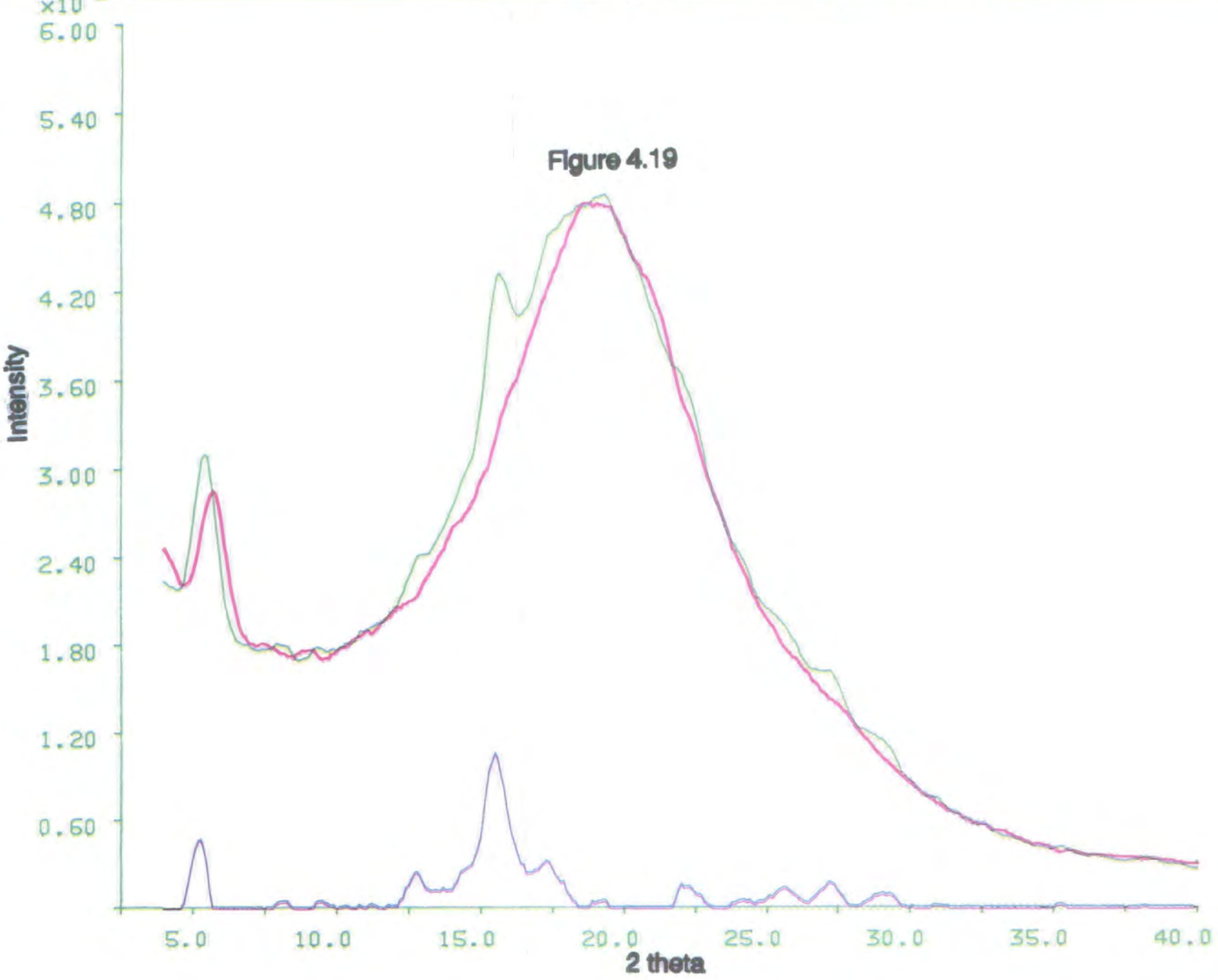
x10
6.00
5.40
4.80
4.20
3.60
3.00
2.40
1.80
1.20
0.60
Intensity
5.0
10.0
15.0
20.0
25.0
30.0
35.0
40.0
2 theta

Figure 4.19

Figure 4.20

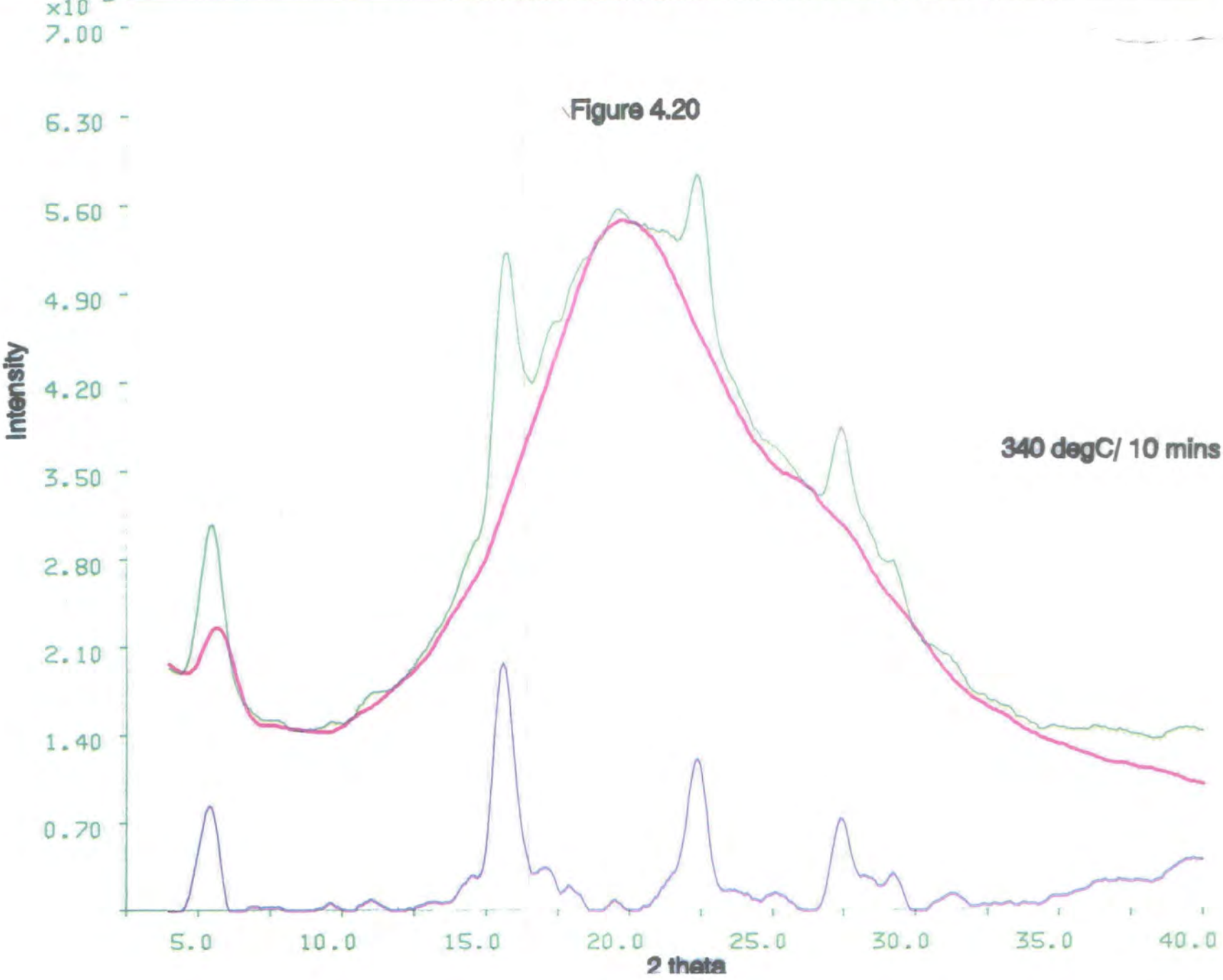
x10
7.00
6.30
5.60
4.90
4.20
3.50
2.80
2.10
1.40
0.70
Intensity
340 degC/ 10 mins
5.0
10.0
15.0
20.0
25.0
30.0
35.0
40.0
2 theta

the errors involved, no definite trends could be confirmed and hence any conclusions remain speculative. The main observation from the calculations of x_{cr}, is that even over relatively long annealing periods (ie. t = 60 minutes) the maximum crystallinity achieved was approximately 24%, demonstrating that a small degree of ordering only can be achieved under the specified conditions.

4.5 *Conclusions*

The structural behaviour of unannealed LCP powders and films was examined by WAXS. The results demonstrate that the powder exhibits almost negligible crystallinity and hence is categorised as being almost completely amorphous. In contrast, LCP films exhibit a significant amount of crystallinity. These results correlate well with those obtained from thermal analysis. Since film preparation involves the addition of solvent, the effect of altering the solvent system used was studied. Identical results were obtained and hence it is proposed that the ordering present in the films can only result from molecular alignment in the solvent during film preparation. Highly oriented LCP samples were obtained by drawing fibres from the anisotropic melt phase. From WAXS studies, LCP was found to exhibit random orientation, typical of this type of material. An amorphous melt was obtained at a temperature of 330°C. Structural development is observed to occur above the melt, in the anisotropic state, where a slight amount of structural rearrangement is observed to occur. In general, the polymer structure does not alter for samples annealed below the melt, however crystallinity and ordering can be induced under selected conditions. Again, for samples annealed in the region of the anisotropic melt, an increase in ordering is observed as a function of time.

Further investigations involving detailed data correction and evaluation, would clarify the speculative work, dealt with in this chapter. A quantitative analysis of the results was never intended, however it would be advantageous to this study. The main aim of the work was to confirm the observations made from thermal analysis. This was achieved and the results obtained in the present chapter, and those in Chapter 3, were found to support and complement each other very effectively.

Thus it may be concluded that ordering in LCP can be increased by annealing both below the melt and in the anisotropic phase. A maximum crystallinity of 24% was obtained for LCP annealed under relatively severe conditions. LCP was found to exhibit random orientation, however oriented samples were obtained for LCP fibres drawn from the melt.

(1) Azaroff, L. V., *Elements of X-ray Crystallography*, McGraw-Hill Book Company Inc., New York (1968)

(2) Kakudo, M., Kasai, N., *X-Ray Diffraction by Polymers*, Elsevier Publishing Co. Ltd., Amsterdam (1982)

(3) Azaroff, L. V., Schummann, C. A., *Mol. Cryst. Liq. Cryst.*, 122 309 (1988)

(4) Alexander, L. E., *X-Ray Diffraction Methods in Polymer Science* Wiley-Interscience, New York (1969)

(5) Laue, M. V., *Ann. Phys.*, 41 971 (1913)

(6) Darwin, C. G., *Phil. Mag.*, 27 315 (1914)

(7) James, R. W., *The Optical Principles of the Diffraction of X-rays*, G. Bell and Sons Ltd., London (1948)

(8) Hosemann, R., Bagchi, S. W., *Direct Analysis of Diffraction by Matter*, North Holland Publishing Company, Amsterdam (1982)

(9) Balta-Calleja, F. J., Vonk, C. G., *X-ray Scattering of Synthetic Polymers Vol. 8*, A. D. Jenkins (ed), Elsevier Science Publishers B.V.(1989)

(10) Klug, H. P., Alexander, L. E., *X-ray Diffraction Procedures for Polycrystalline and Amorphous Materials*, John Wiley and Sons, New York (1974)

(11) Blackwell, J., Cheng, H. M., Biswas, A., *Macromolecules* 21 39 (1988)

(12) Erdemir, A. B., Johnson, D. J., Karacan, I. Tomka, J. G., *Polymer* 29 597 (1988)

(13) Murthy, N. S., Correale, S. T., Minor, H., *Macromolecules* 24 1185 (1991)

(14) Noel, C., in *Polymeric Liquid Crystals*, A. Blumstein (Ed) Plenum Press, New York (1963)

(15) Statton, W. W., *J. Appl. Polym. Sci.*, 7 803 (1963)

(16) Blundell, D. J., MacDonald, W. A., Chivers, R. A., in *High Performance Polymers Vol. 1 No. 2* (1989)

(17) Ruland, W., *Acta Cryst.*, 14 1180 (1961)

(18) Goppel, J. M., Arlman, J. J., *Appl. Sci. Res.*, A1 462 (1949)

(19) Wakelin, J. H., Virgin, H. S., Crystal, E., *J. Appl. Phys.*, 30 1654 (1959)

(20) Hermans, P. H., Weidinger, A., *J. Polym. Sci.*, 5 565 (1950)

(21) Vonk, C. G., *J. Appl. Cryst.*, 6 148 (1973)

(22) Murthy, N. S., Minor, H., *Polymer* 31 996 (1990)

(23) Dowling, Hendee, Kohler, Parish, *Philips Tech. Rev.* 18 262 (1956)

(24) Drever, J. I., Fitzgerald, R. W., *Mater. Res. Bull.*, 5 101 (1970)

(25) Parrish, W., Hamacher, E. A., Lowitzch, K., *Philips Tech. Rev.* 16 123 (1954)

(26) Giessen, B. C., Gordon, G. E., *Norelco Rep.*, 17 (2) 17 (1970)

(27) Blundell, D. J., Willcocks, H., *ICI Internal Report* (1988)

Chapter 5

Transesterification

5.1 *Introduction*

Interchange reactions occurring in condensation polymers are of significant industrial importance, since through minimising molecular weight fluctuations during processing and polymerisation, they can lead to more uniform polymers and ultimately, can be used to achieve block copolymers via a melt blending process.

Flory assumed in his classical work on molecular size distribution in linear condensation polymers,[1,2] that after condensation, a given pair of functional groups will not react further with its neighbours. Later, Flory demonstrated that the final molecular weight distribution would be determined by the equilibria between the polymer molecules of different molecular weight and not by their initial rates of formation.[3] Further studies showed that, on heating a mixture of two polyesters, the viscosity decreased.[4] By relating the melt viscosity to the weight average molecular weight, he demonstrated that as the blend of polymers approached the most probable equilibrium distribution, similar rates of ester-interchange and esterification were also observed.

Extensive studies based on Flory's analysis were carried out by Kotliar.[5] He assumed the random nature of the interchange reaction to be a two step process. The first step involves the random cleavage of s bonds per number average molecule afterwhich, in the second step, c chain ends are recombined under the assumption that all free ends have an equal probability of being coupled. Providing this theory is correct, during the interchange process the number of chain ends cleaved is equal to the number of chain ends recombined, hence there is no overall change in the number of molecules.

The interchange route involves reactions between polymers which contain in their backbones, functional linkages capable of undergoing exchange. Such materials include polyesters, polyamides and polysiloxanes.[6-8]

This study concerns interchange involving condensation type polymers, hence polyesters only are discussed.

Three types of interchange processes can occur in polyesters and are shown in the following reactions, where the chains are terminated either by hydroxyl or carboxyl groups:[9]

i) *Intermolecular alcoholysis*

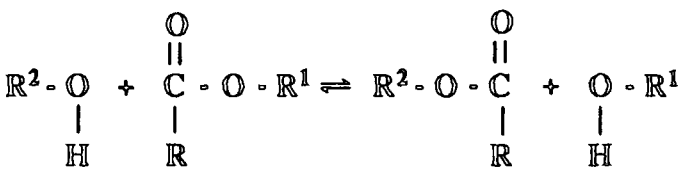

During alcoholysis, cleavage of the acyl oxygen occurs leaving the alkoxy group intact.

ii) *Intermolecular Acidolysis*

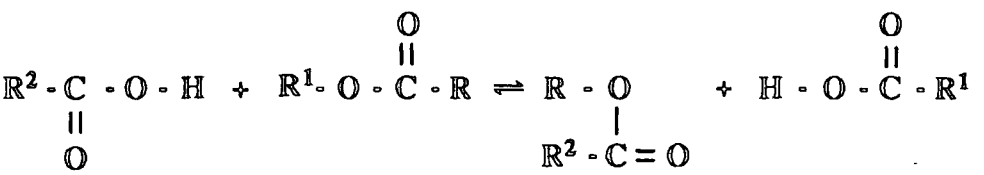

Acidolysis is known to be much slower than alcoholysis, however the reaction is very similar but it involves the acid group cleavage of either the acyl or alkyl oxygen. If cleavage of the acyl oxygen occurs, an anhydride intermediate is formed, followed by reaction of an alcohol to give either a new ester with the acyl group exchanged, or the original ester.

iii) *Ester-Ester Interchange*

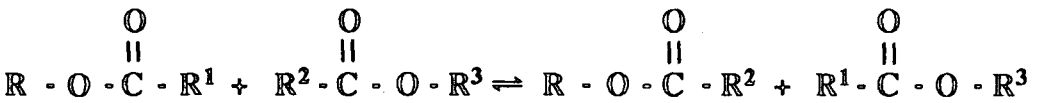

Ester-ester interchange, also known as transesterification, occurs where the esters react

to exchange their acyl groups. An excellent review of the various interchange reactions by Kotliar can be found in the literature,[10] however since the present study is concerned with transesterification, a few examples where this reaction was observed to occur are discussed below.

In 1953 Kursanov and co-workers[11] used the exchange between carboxyl ended poly (hexamethylene sebacate) and diethyl 2,3-di-deuterosuccinate to demonstrate ester-ester interchange. However, failure to use end-capped polymers may have invalidated their interpretation. Charch and Shivers[12] reported (1959) on the ester-interchange by blending poly(ethylene terephthalate) and poly(ethylene succinate) in a 40/60 mole ratio. The resultant block copolymer had an initial melting point of 250°C decreasing to 150°C in 100 minutes. The reported melting point of the random copolymer was 120°C. Further studies in the 1960's on mixtures of homopolyesters heated as a melt blend also showed a reduction in melting temperature as a function of time.[13,14] More recently (1976) Ramjet and Sedgwick[15] studied the kinetics of the ester-ester interchange reactions between poly(ethylene adipate) and poly(trimethyl adipate) by mass spectrometric techniques. They found that the enthalpy change was essentially zero, which is consistent with an associative type mechanism where the breaking and making of bonds occurs simultaneously.

Several authors report on the preparation of block copolyesters by means of the limited transesterification of a blend of two homopolyesters at very high temperatures.[16] Initially ester-interchange leads to the formation of large segments but as the reaction proceeds, interchange continues and the segments become increasingly shorter until finally, at equilibrium, a random copolymer is obtained. The structure of the block copolymers produced appears very difficult to control and the products are usually blends of homopolymers and copolymers of very high polydispersity. In the 1970's, Lenz and co-workers investigated the important factors such as composition, catalyst type, reaction temperature and reaction time in the reorganisation of random to block

copolyester acetals.[17-20] In their studies the authors were able to show significant increases in the block structure of random copolymers heated below the melt as a consequence of interchange reactions. The succeeding chapter discusses this concept in greater depth.

Although a significant amount of progress has been made in the understanding of interchange reactions in recent years, there remains a lack of information of a quantitative nature on matters such as the kinetics and the mechanism involved in these reactions. The problem of immiscibility of polymer blends further complicates the quantitative analysis of the rates of interchange. Very recently however, the situation has improved somewhat.

Kugler and co-workers[21] studied the kinetics of transesterification in PET, using small angle neutron scattering (SANS) techniques on blending a hydrogenous polymer with its deuterated equivalent. During transesterification, as mentioned earlier, simultaneous scission and recombination of the bonds occurs leading to the formation of a random homogeneous copolymer. As transesterification progresses the apparent molecular weight of the deuterated polymer will therefore decrease since SANS is sensitive to isotopic labelling (section 5.2.1). However the average molecular weight determined by other techniques, such as light scattering or GPC analysis will remain constant during the reaction since these techniques are insensitive to deuterium labelling. Kugler and co-workers' analysis relied upon the knowledge of the molecular weights (obtained by light scattering) of the PET blends as the reaction progressed and established that in PET the process follows Arrhenius behaviour. From their analytical treatments they were able to calculate the kinetic parameters of transesterification. Benoit and co-workers[22] have proposed a theoretical analysis of the problem where a complete quantitative interpretation of the results, obtained solely from the SANS spectra during transesterification of a blend of hydrogenous and deuterated polymers, is made. This method is used to determine the kinetics of the reaction and it is using this treatment that

the kinetic parameters and mechanism of transesterification in LCP are obtained (section 5.5.4).

5.2 *Small Angle Neutron Scattering (SANS)*

5.2.1 *Introduction*

Neutron scattering has proved to be an extremely effective technique in the structural elucidation of condensed matter.[23-25] The key property which makes this technique unique is based on the variation of the neutron nuclear scattering from one isotope to another. This is an invaluable feature since nuclear contrast factors can be varied by isotopic substitution. An important example in structural analysis is the contrast between hydrogen and deuterium, since the total scattering from hydrogen exceeds that of deuterium by an order of magnitude. Another advantage of this particular substitution is that any consequential chemical shifts are almost negligible. Other fundamental properties of the neutron which make it a useful tool in the investigation of condensed matter include:

i) the wavelength of a neutron lies between 1 and 20Å, an appropriate range for the investigation of intra- and inter-molecular dimensions

ii) neutron absorption is very small for most atoms and hence bulk samples can be studied

iii) the magnitude of the energy of a neutron is similar to the excitation energies of condensed matter and hence an investigation of molecular rotations, vibrations and translations may be undertaken

iv) the neutron's magnetic moment interacts with unpaired electrons and magnetic excitations enabling the study of the magnetic structure and dynamics of matter.

In the present work, since energy analysis is not required and only structural details are necessary, elastic scattering only is discussed ie. scattering which does not involve the transfer of energy between neutron and molecule. The theory of elastic scattering and its use in structural evaluation is discussed in section (5.2.2).

5.2.2 *SANS Theory*[26-29]

Neutron scattering measurements are normally based on the analysis of the scattered intensity with respect to its scattering vector and energy. From this analysis, an interpretation of the structural properties of the scattering system can be made. A basic scattering experiment is illustrated in Figure 5.1. An incident beam of intensity I_0 and wave vector k, is scattered by the target producing a wave vector k' of intensity, I. From the vector diagram, (Figure 5.2) the change in the wave vector on scattering is represented by Q, the scattering vector

$$\mathbb{Q} = \mathbb{k} - \mathbb{k}' \qquad (5.1)$$

And from Figure (5.1)

$$\mathbb{Q} = \mathbb{k}^2 + (\mathbb{k}')^2 - 2\mathbb{k}\cos 2\Theta \qquad (5.2)$$

For elastic scattering $|k| = |k'| = 2\pi/\lambda$, where λ is the neutron wavelength, Thus

$$\mathbb{Q} = \left(\frac{4\pi}{\lambda}\right)\sin\Theta \qquad (5.3)$$

The quantity measured is the partial differential scattering cross section denoted by $d^2\sigma/d\Omega\, dE'$ which represents the fraction of neutrons with an energy between E' and (E' + dE') being scattered into a solid angle between Ω and $d\Omega$. The amplitude of a wave scattered from a single atom of the target sample becomes small even in the region of adjacent atoms. This condition holds when the cross-sections for each atom are small in comparison to the square of the average separation of these atoms. If this condition is satisfied, the total scattering amplitude for the sample is equal to the sum of those for individual atoms.[30] Referring again to Figure (5.1), since only elastic collisions are considered and if the neutron flux is I_0 (number area^{-1} time^{-1}), the number of neutrons scattered per unit time into the solid angle $d\Omega$ is $I_0(d\sigma/d\Omega)d\Omega$ (=I)

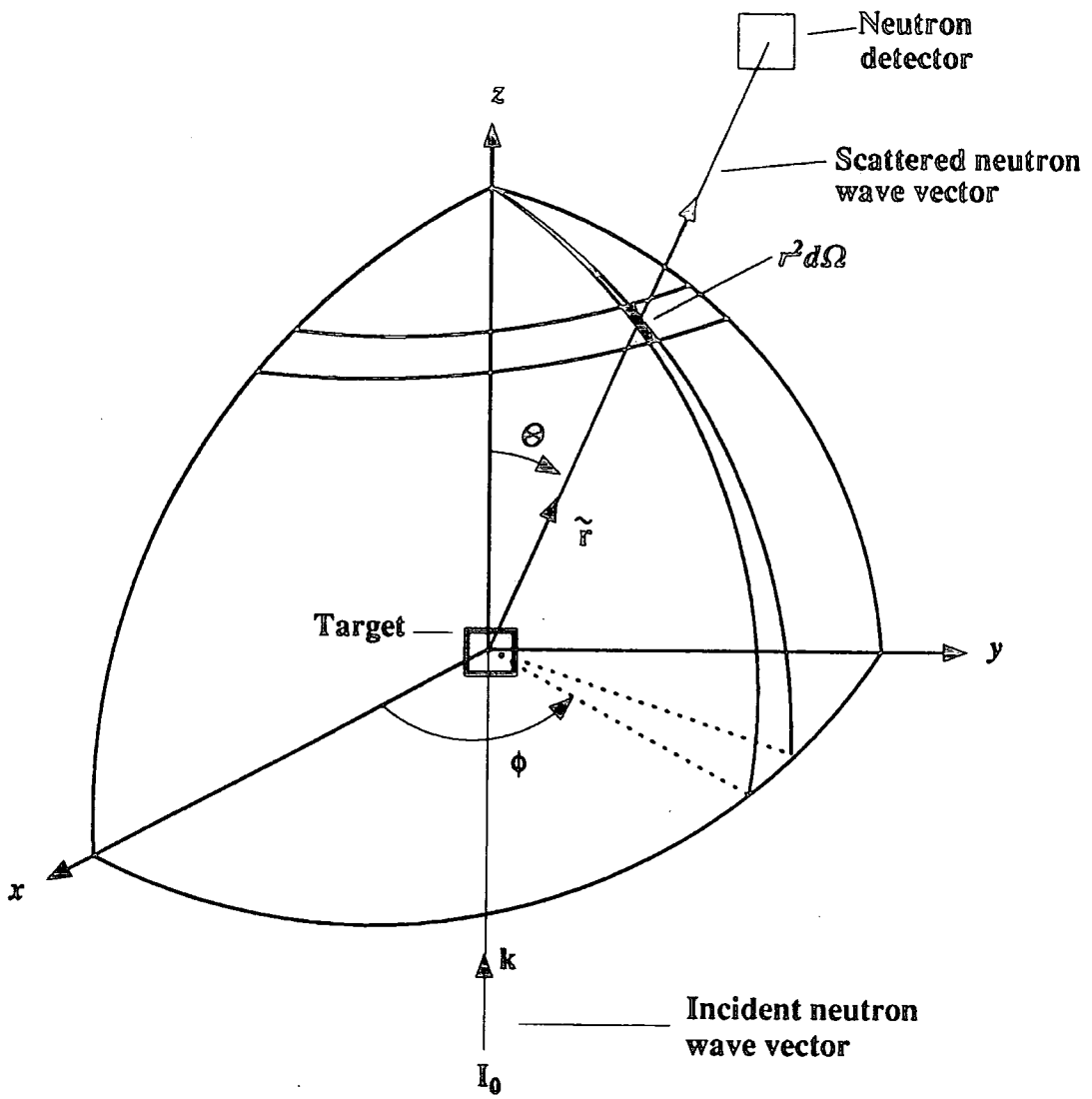

Figure (5.1) **Schematic Diagram of a Scattering Experiment**

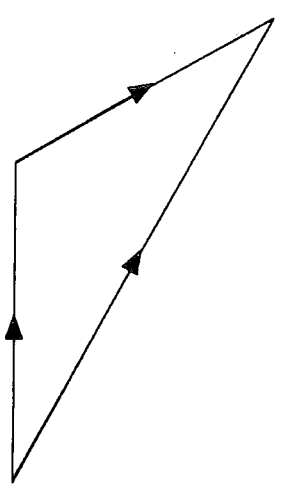

Figure (5.2) **Scattering Vector Diagram**

Consider the case of scattering from a bound nuclei. This type of scattering is dependent on the neutron-nucleus interaction which from experimentation, is known to be much less than the wavelength of low energy neutrons and the nuclear radius is only about an order of magnitude greater. Thus, only s-wave scattering is obtained ie. it is isotropic and hence it can be characterised by a single parameter b, the scattering length. Values of b are both atom dependent and isotope dependent. The neutron-nucleus interaction potential is based on the Fermi pseudo-potential defined as[31]

$$V(r) = \frac{2\pi\hbar^2}{m} b\gamma (r-R) \qquad (5.4)$$

Where m is the mass of a neutron, h is Planck's constant and the only form of V(r) which gives isotropic scattering is the delta function $\gamma(r - R)$ where R is the position of the nucleus .

From basic scattering theory, it can be derived[26]

$$\frac{d\sigma}{d\Omega} = |k'|\tilde{V}|k|^2 \qquad (5.5)$$

where $(d\sigma/d\Omega)$ is the cross-section and $\tilde{V}$ is the interaction potential between the incident neutron and the target sample. Assuming k is at the origin (ie R = 0) then by substituting equation (5.4) into equation (5.5)

$$\frac{d\sigma}{d\Omega} = | b \int dr \exp(-k'r) \gamma r \exp(-kr) |^2 = b^2 \qquad (5.6)$$

thus

$$\frac{d\sigma}{d\Omega} = b^2 \qquad (5.7)$$

and hence the total cross section

$$\sigma = 4\pi |b^2| \qquad (5.8)$$

So far neutron and nuclear spin have been neglected and the target, assumed to be a single spinless isotope. The value of b is dependent on the relative orientation of the neutron and nuclear spin. If the scattering from an array of nuclei is considered and spin

is accounted for, where the scattering length of the i^{th} and j^{th} nuclei are denoted b_i and b_j and the position of these nuclei, described as $\mathbb{R}_i$ and $\mathbb{R}_j$ respectively then:

$$\frac{d\sigma}{d\Omega} = \sum_{ij} \exp[\,iQ.(\mathbb{R}_i-\mathbb{R}_j)\,](b_i b_j) \qquad (5.9)$$

Generally, b is dependent on which isotope is positioned at R_i and what nuclear spin is associated with that particular isotope

$$\text{if } i \neq j \quad \overline{b_i b_j} = \bar{b}_i\,\bar{b}_j = |\bar{b}|^2$$

$$\text{however if } i = j \quad \overline{b_i b_j} = \overline{|b_i|^2} = \overline{|b|^2}$$

thus

$$b_i b_j = |\bar{b}^2| + (\overline{|b|^2} - |\bar{b}|^2) \qquad (5.10)$$

and substituting equation (5.10) into equation (5.9), the cross-section can be written as

$$\frac{d\sigma}{d\Omega} = \left(\frac{d\sigma}{d\Omega}\right)_{incoh} + \left(\frac{d\sigma}{d\Omega}\right)_{coh} \qquad (5.11)$$

where the incoherent cross section

$$\left(\frac{d\sigma}{d\Omega}\right)_{incoh} = N(\overline{|b|^2} - |\bar{b}|^2) = N(b - \bar{b})^2 \qquad (5.12)$$

and the coherent cross section

$$\left(\frac{d\sigma}{d\Omega}\right)_{coh} = |\bar{b}|^2 \left|\sum_i \exp(iQ.R_i)\right|^2 \qquad (5.13)$$

It is apparent from equations (5.12) and (5.13) that the coherent and incoherent scattering components are significantly different. In incoherent scattering there is no interference between the waves scattered by the nuclei, the cross-section is completely different and has no dependence on Q. It has a value of zero only for nuclei with zero spin and its magnitude is calculated from tabulated values of incoherent scattering cross-sections,

σ_{inc}. However for coherent scattering there is strong interference. This parameter represents the Fourier transform of the scattering length correlations in the target sample and hence contains all the required structural information.

Consider now, the situation where the target sample is not a pure material but a mixture of N_1 molecules of deuterated polymer and N_2 molecules of hydrogenous polymer. The differential cross-section can be expressed as[28-32]

$$\frac{d\sigma}{d\Omega} = \left(b_{1\,coh} - b_{2\,coh} \frac{\bar{V}_1}{\bar{V}_2} \right)^2 S_{1\,coh}(Q) + N_1 b^2_{1\,incoh} + N_2 b^2_{2\,incoh} \qquad (5.14)$$

and S_{1coh} is the Fourier transform of the density fluctuation correlation function of the scattering centres given by

$$S_{1\,coh}(Q) = \sum_{ij} < \exp\left[iQ\,(r_i - r_j) \right]^2 > \qquad (5.15)$$

For a polymer molecule, the chain segments are considered to be point scatterers and for a Gaussian coil, the coherent scattering law can be expressed as

$$S_{1\,coh}(Q) = \frac{2N_1^2}{(Q^2 \langle s^2 \rangle)} \left[\exp(-Q^2 \langle s^2 \rangle) - 1 + Q^2 \langle s^2 \rangle \right] \qquad (5.16)$$

where s is the response function.

By subtracting the incoherent background scattering, the remaining scattering contains all the information about the structure of the scattering material, hence

$$\left(\frac{d\sigma}{d\Omega} \right)_{coh} = \left(b_{1\,coh} - b_{2\,coh} \frac{V_1}{V_2} \right) S_{1\,coh}(Q) \qquad (5.17)$$

and substituting equation (5.16) into (5.17) gives

$$\left(\frac{d\sigma}{d\Omega} \right) = (b_{1\,coh} - b_{2\,coh}) \left(\frac{\bar{V}_1}{\bar{V}_2} \right) \frac{2N_1^2}{(Q^2 \langle s^2 \rangle^2)} \left[\exp(-Q^2 \langle s^2 \rangle - 1 + Q^2 \langle s^2 \rangle \right] \qquad (5.18)$$

where $\left[b_{1\,coh} - b_{2\,coh}\left(\frac{\dot{V}_1}{\dot{V}_2}\right)\right]^2$ is the contrast factor $K^{(33)}$

The larger the value of K, the more intense the scattering signal, since the scattering intensity is given by

$$I(Q) = \left(\frac{d\sigma}{d\Omega}\right)_{coh} \frac{c}{M} N_A \qquad (5.19)$$

where M is the molecular weight of the polymer, c is the concentration of deuterated species and N_A is Avogadro's number.

By substituting equation (5.18) into equation (5.19)

$$I(Q) = \frac{Kc N_A N_1^2}{M} \frac{2}{(Q^2\langle s^2\rangle^2)} [\exp(-Q^2\langle s^2\rangle - 1 + Q^2\langle s^2\rangle)] \qquad (5.20)$$

Since $N_1 = M/M_0$ where M_0 is the segment molecular weight, then

$$\frac{Kc N_A N_1^2}{M} = \frac{Kc N_A}{M}\frac{M^2}{M_0^2} = K^* c M \qquad (5.21)$$

where $K^* = KN_A/M_0^2$. Hence, y

$$\frac{K^* c}{I(Q)} = \frac{1}{M}\left[\frac{2}{(Q^2\langle s^2\rangle^2)}\right] [\exp(-Q^2\langle s^2\rangle - 1 + Q^2\langle s^2\rangle] \qquad (5.22)$$

The absolute molecular weights can be obtained once the scattering data has been normalised and fully corrected to absolute intensity (section (5.45)), from the Guinier scattering region. This region is defined where $Q < (\langle s^2\rangle^{-\frac{1}{2}})$ and equation (5.22) reduces to

$$\frac{K^* c}{I(Q)} = \frac{1}{M}\left[1 + \frac{Q^2\langle s^2\rangle}{3}\right] \qquad (5.23)$$

The molecular weights are calculated from the data obtained from a plot of I(Q) versus Q^2, at $Q = 0$.

5.3 *Theory of Benoit, Fischer and Zachmann*

Benoit and co-workers have carried out a theoretical analysis of transesterification in which they propose a quantitative interpretation of experimental data obtained using SANS techniques. This data is used to determine accurately the kinetic parameters of the reaction. The theory is based on the study of two polymers of identical molecular weight differing only in their coherent scattering lengths; a hydrogenous and a deuterated polyester are considered. Before the theoretical treatment can be applied, it is assumed that the SANS data has been corrected to absolute intensity, normalised, and the incoherent scattering subtracted. Since monodisperse polyesters are difficult to obtain, polydispersity is accounted for and the isotopic monomers (denoted H and D respectively) are presumed to occupy the same volume and to possess the same value of the statistical step length, b.

If N_T denotes the total number of monomeric units equal to the sum of the number of monomeric units, D and H, denoted N_D and N_H, then the number fraction of D units, x is given below

$$x = \frac{N_D}{N_H + N_D} = \frac{N_D}{N_T} \qquad (5.24)$$

$$1-x = \frac{N_H}{N_T} \qquad (5.25)$$

Where ν_D and ν_H represent the total number of D and H chains respectively , the number average degrees of polymerisation for D and H may be expressed as

$$\eta_D = \frac{N_D^{\,o}}{\nu_D} \qquad \eta_H = \frac{N_H^{\,o}}{\nu_H} \qquad (5.26)$$

Hence if $\eta_T^{\,o}$ represents the number average degree of polymerisation for the total sample, it follows

$$\frac{1}{\eta_T^o} = \frac{x}{\eta_D^o} + \frac{1-x}{\eta_H^o} \qquad (5.27)$$

The scattered intensity is defined by i(Q)

$$i(Q) = \frac{I(Q)}{N_T} \frac{1}{(\rho_H - \rho_D)^2} \qquad (5.28)$$

where Q is the modulus of the scattering vector = $4\pi/\lambda.\sin(\theta/2)$, I(Q) is the scattering intensity obtained directly from a corrected experimental curve, and ρ_H and ρ_D are the coherent scattering lengths of the D and H monomers.

Considering the situation before the start of the reaction where two homopolyesters are present, de Gennes defines an expression generalising for a polydisperse system:[34]

$$i^{-1}(Q) = \frac{1}{x\,\eta_{DW}\langle P_D(Q)\rangle} + \frac{1}{x\,\eta_{HW}\langle P_H(Q)\rangle} - 2\chi \qquad (5.29)$$

where χ is the interaction parameter between the D and H monomeric units and <P(Q)>, the Debye structure factor[35] defined below

$$\langle P(Q)\rangle = \frac{1}{\Sigma\, v_i n_i^2} \sum_i v_i n_i^2\, P_i(Q) \qquad (5.30)$$

According to Benoit,[36] by replacing <P(Q)> by its asymptotic expression and incorporating the expressions proposed by Debye[35] and de Gennes,[34] it follows

$$\frac{1}{i(Q)} = \frac{Q^2 b^2}{12x(1-x)} + \frac{1}{2}\left(\frac{1}{x\,\eta_D} + \frac{1}{(1-x)\eta_H}\right)^2 - 2\chi \qquad (5.31)$$

Equation (5.31) can then be altered, to incorporate the total number average molecular weight of the sample,

$$\frac{1}{i(Q)} = \frac{Q^2 b^2}{12x(1-x)} + \frac{1}{2(1-x)}\left(\frac{1}{\eta_D} + \frac{1}{\eta_H} - \frac{1}{\eta_T}\right) - 2\chi \qquad (5.32)$$

The expression for I(Q) can be used in this range, represented by $R_g^{-1} < Q < b^{-1}$ where R_g is the radius of gyration of the smallest molecule.

After the reaction has started, the system becomes more complex since it contains D and H homopolyesters as well as copolyesters of various compositions.

De Gennes generalised for copolymers[37-39]

$$\frac{1}{i(Q)} = \frac{n_{TW}}{x(1-x)} \frac{<P_T(Q)>}{(n_{HW}<P_H>n_{DW}<P_D> - n_{HW}^2<P_{DHW}^2>)} - 2\chi \qquad (5.33)$$

where n_{TW}, n_{DW} and n_{HW} represent the weight average degrees of polymerisation for the whole polymer, its deuterated and its hydrogenous segment respectively. P_{DHW} is a cross term characterising the interference between the D and H segments of the same molecule, which is defined for a monodisperse system by the relation

$$<P_{DH}(Q)> = \frac{1}{\Sigma v_i n_{Hi} n_{Di}} \Sigma v_i n_{iH} n_{iD} P_{iDH} \qquad (5.34)$$

Where v_i = number of molecules having n_{iH} monomers H, v_{iD} monomers D and a cross structure factor $P_{iDH}(Q)$.

To evaluate this expression in the intermediate range, it is necessary to know the asymptotic expansion of each term in equation (5.29). Benoit and Hadziioannou[40] showed that the cross term does not contribute to the expansion since it decreases faster than the other terms, as Q increases. Hence for block copolymers in the intermediate Q range,

$$\frac{1}{i(Q)} = \frac{Q^2b^2}{12x(1-x)} + \frac{1}{2x(1-x)}\left[\frac{1}{n_D(t)} + \frac{1}{n_H(t)} - \frac{1}{n_T^o}\right] - 2\chi \qquad (5.35)$$

Whereas equation (5.32) describes a mixture of homopolyester, equation (5.35) now

represents a copolymer system, where $n_D(t)$ and $n_H(t)$ are the time dependent number average degrees of polymerisation of D and H respectively and n_T^o is the number average degree of polymerisation of the block copolymer molecules, which is assumed to remain constant according to experimental results. From equation (5.35) a plot of 1/i(Q) versus Q^2 will yield the value of b, from the slope of the scattering curve over the defined Q range. The plot obtained will resemble a figure similar to that in Figure (5.3) where the straight lines represent the experimental scattering data.

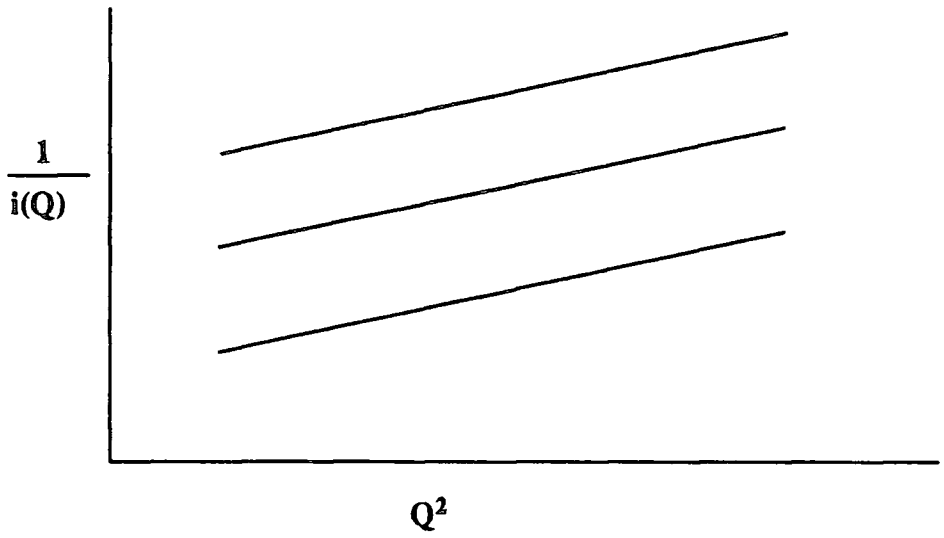

Figure (5.3) Typical Scattering Intensity Plot

On the assumption that the chains are Gaussian, and that this behaviour is unaffected by the reaction, even at the final state, the slope of the lines should not alter. It is noted that the only parameter dependent on time is the intercept, z, the ordinate of the intersection of the experimental lines with the y-axis. This parameter is defined

$$z = \frac{1}{2x(1-x)}\left[\frac{1}{n_D(t)} + \frac{1}{n_H(t)} - \frac{1}{n_T^o}\right] - 2\chi \qquad (5.36)$$

If the total molecular weight remains constant during the reaction, z will increase and i(Q) will decrease as a function of time. The parameter z appears to be the most accessible experimental parameter. Moreover it has greater precision than the values of zero angle scattering and R_g. Previous experiments[32] show that the number average

molecular weight remains unchanged during transesterification therefore throughout the reaction, the number of chain scissions must equal the number of chain recombinations. This hypothesis is illustrated in Model (1a) where the two homopolyesters, H and D, break and reform into two HD copolyester chains. The reaction leads to a decrease in the intermediate scattering intensity as the apparent molecular weight of D decreases. Such a process will be categorised as being efficient.

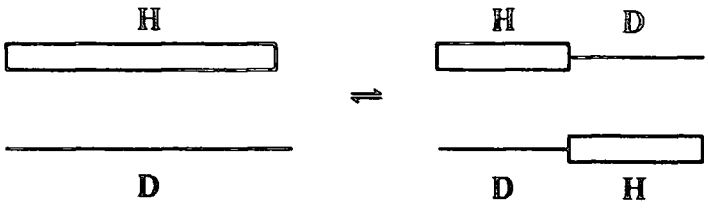

Model (1a)

Model 1 does not however, represent the only reactions taking place in the system. Other reactions which do not introduce any alteration in sequence are also possible. Model (1b) represents the reaction between H monomers only. An identical reaction involving D monomers is equally as probable.

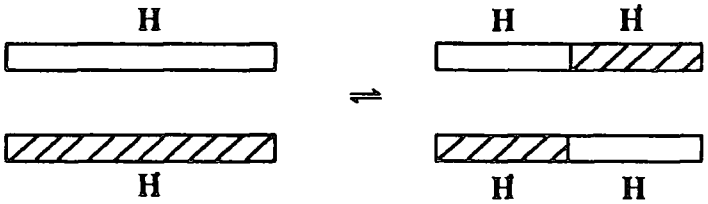

Model (1b)

It is noted that, since no alteration in the number of D and H sequences occurs during this reaction, the intermediate scattering will remain unaffected hence the process may be categorised as being inefficient and will not be considered in this study. Referring again to Model 1, it is evident that every efficient scission and recombination increases both the number of D and H blocks by one unit, hence the original values of ν_D and ν_H on commencement of the reaction become $\nu_D + s$ and $\nu_H + s$ respectively. Their number average degrees of polymerisation are,

$$n_D(t) = \frac{N_D}{\nu_D + s} \qquad n_H(t) = \frac{N_H}{\nu_H + s} \qquad (5.37)$$

By inserting these values into equation (5.36), the quantity z is evaluated obtaining

$$z = \frac{1}{2x(1-x)}\left(\frac{1}{n_H^o} + \frac{s}{N_H} + \frac{1}{n_D^o} + \frac{s}{N_D} - \frac{1}{n_T^o}\right) - 2\chi \qquad (5.38)$$

Referring to z_o as the value of z at reaction time t = 0 it follows;

$$z(t) = z_o + \frac{1}{2x^2(1-x)^2}\frac{s(t)}{N_T} \qquad (5.39)$$

This equation is very simple. The experimental quantity $z(t)-z_o$ is dependent only on the quantities x and N_T, which are known from sample preparation, and not on the interaction parameter nor the initial polyester molecular weights. This is advantageous, since the two latter parameters are difficult to measure. The only limitation in this treatment is that the blocks are assumed Gaussian, both prior to and during the transesterification reaction. This hypothesis could be incorrect at the end of the reaction when the number of monomeric units in each segment becomes very small.

If s(t) represents the number of efficient scissions, as illustrated in equation (5.40)

$$H\text{-}H + D\text{-}D \rightleftharpoons 2\ H\text{-}D \qquad (5.40)$$

and $s_D(t)$, $s_H(t)$ and $s_{HD}(t)$, are referred to as the number of D-D, H-H and H-D bonds at time, t, the rate of the forward reaction is then

$$\frac{ds_{HD}(t)}{dt} = k s_H(t)\, s_D(t) \qquad (5.41)$$

However in the case of the reverse reaction (equation 5.40), the probability of the process leading to a change in the number of sequences is only 1 in 2, hence this reaction is denoted by

$$\frac{ds_{HD}(t)}{dt} = k\left[{}^1/_2\, s_{HD}(t)\right]^2 \qquad (5.42)$$

Noting that the only differences in the two reactions in equation (5.40) are due to isotopic effects, then the rate constants, k, for the processes should be equal. Hence the

overall rate of change of s_{HD} is given

$$\frac{ds_{HD}(t)}{dt} = k \{ [s_H(t)\, s_D(t)] - 1/4 [s_{HD}(t)]^2 \} \qquad (5.43)$$

and at equilibrium

$$[s_{HD}(t)]^2 = 4 s_H(t) s_D(t) \qquad (5.44)$$

If the molecular weights of the initial polyesters are sufficiently large then neglecting end effects, and where the number of D-D and H-H bonds in the initial mixture are equal to the number of D and H monomers N_D and N_H, the equilibrium distribution in equation (5.44) is based on the condition

$$s_D + s_H + s_{HD} = N_T \qquad (5.45)$$

The probability of an efficient scission occurring is equal to $2w_o x(1-x)$, where w_o denotes the probability of the occurrence of an interchange reaction, and the probabilities for a D-D or an H-H reaction occurring are $w_o x^2$ and $w_o(1-x)^2$ respectively. Hence it follows

$$\begin{aligned} s_H &= N_T x^2 \\ s_D &= N_T (1-x)^2 \\ s_{HD} &= N_T 2x(1-x) \end{aligned} \qquad (5.46)$$

Considering the equilibrium distribution for $t = \infty$ equation (5.38) becomes

$$\frac{1}{i(Q)} = \frac{Q^2 b^2}{12x(1-x)} + \frac{1}{2x(1-x)} \left(\frac{1}{n_D^o} + \frac{1}{n_H^o} - \frac{1}{n_T^o} + 1 \right) - 2\chi \qquad (5.47)$$

The values of $1/n_D^o$, $1/n_H^o$ and $1/n_T^o$ can be neglected, since they are very small compared to unity;

$$\frac{1}{i(Q)} = \frac{Q^2 b^2}{12x(1-x)} + \frac{1}{2} \left(\frac{1}{x} + \frac{1}{1-x} \right) - 2\chi \qquad (5.48)$$

The differential equation (5.43) can be solved by eliminating $s_D(t)$ and $s_H(t)$[22] and from

it is obtained

$$s(t) = N_T x(1-x) \left[1-\exp(-\tfrac{1}{2} k N_T t) \right] \qquad (5.49)$$

Inserting this value of s(t) into the expression for $z(t) - z_o$, it follows

$$z(t) - z_o = \frac{1}{2x(1-x)} \left[1-\exp(-t/\tau) \right] \qquad (5.50)$$

where the relaxation time

$$\tau = 2/kN_T \qquad (5.51)$$

From this equation the values of τ can be determined easily from the scattering data and from these values the kinetic parameters for transesterification can be calculated.

5.4 *Experimental*

5.4.1 *Introduction*

SANS techniques as discussed in section (5.2.1) are sensitive to isotopic labelling. The present study relies upon the contrast in scattering intensities between identical versions of a deuterated and a hydrogenous polymer. In order that SANS studies may be undertaken, the following experimental procedures had to be accomplished successfully.

(a) the preparation of a deuterated polymer

(b) the preparation of blends of the deuterated polymer and its hydrogenous equivalent at sufficiently low temperatures where transesterification is known not to occur[32]

(c) the accurately controlled annealing of the blended samples at temperatures where transesterification is known to occur.[32]

The present chapter provides a detailed account of the experimental procedures involved and the results obtained, from which the kinetic parameters of transesterification in LCP are calculated.

5.4.2 *Preparation of deuterated monomers*

a) Hydroquinone-d_4[41]

The monomer was prepared by refluxing hydroquinone (60g) in D_2O (100g) and D_2SO_4 (2%w/v) (used as a catalyst) for a period of 1 hour. All reagents were used directly as supplied by Aldrich. After this time, the solution was allowed to cool slowly leading to the formation of large crystals of partially deuterated hydroquinone which were then recovered by vacuum filtration. To achieve complete deuteration, the reflux and recovery procedure was repeated a further six times using fresh quantities of D_2O and D_2SO_4 each time, yielding a dark pink crystalline solid. Purification by sublimation at a reduced pressure of 0.1mm Hg and a temperature of 353K, resulted in the formation of

large pure, white crystals.

From analysis, mass spectrometry indicated a deuteration level of 91% around the aromatic ring (Figure 5.4(a)). DSC analysis shows a sharp melting peak (onset = 173.48°C (Figure 5.4(b)). From IR Spectroscopy using a KBr disc λ = 3270, 2234 and 1234 cm^{-1} (Figure 5.4(c)). Proton NMR (in D_2O) shows an almost complete absence of protons in the aromatic region (δ:8.65 - 9.5) confirming that the product is highly deuterated around the aromatic ring (Figure 5.4(d)).

b) Hydroxy-benzoic acid-d_4[42]

The monomer was synthesised using the following procedure. A mixture of phenol-d_6 (1.5g), β-cyclodextrin (1.5g) used as an inclusion catalyst, and finely powdered copper (1g) were added to 200 cm^3 of 20 wt% aqueous sodium hydroxide solution. The reaction was initiated by the addition of carbon tetrachloride (30cm^3) and continued at 353K for 15 hours with vigorous stirring under nitrogen afterwhich time the resulting solution was cooled and acidified using hydrochloric acid, followed by extraction with diethyl ether several times . The ether layers were washed with distilled water twice, dried over $MgSO_4$ and evaporated, yielding a dark brown powder. The product was purified by recrystallisation from distilled water over decolourising charcoal. Recrystallisation was repeated 5 times, producing a pure white powder in a low yield of 25%.

From analysis mass spectrometry indicates a deuteration level of > 99% around the aromatic ring (Figure (5.5a)). IR spectroscopy (KBr disc) gives relevant peaks at 3270, 2410, 1460, 1130 and 720 cm^{-1} (Figure 5.5(b)).

c) *Isophthalic acid-d_4*

Previous attempts to prepare deuterated isophthalic acid have proved unsuccessful,[32] hence due to the great expense of deuterated materials and the time limits on the experiment, hydrogenous isophthalic acid, as supplied by Aldrich, was used. The reagent

Mass spectrum: deuterated hydroquinone

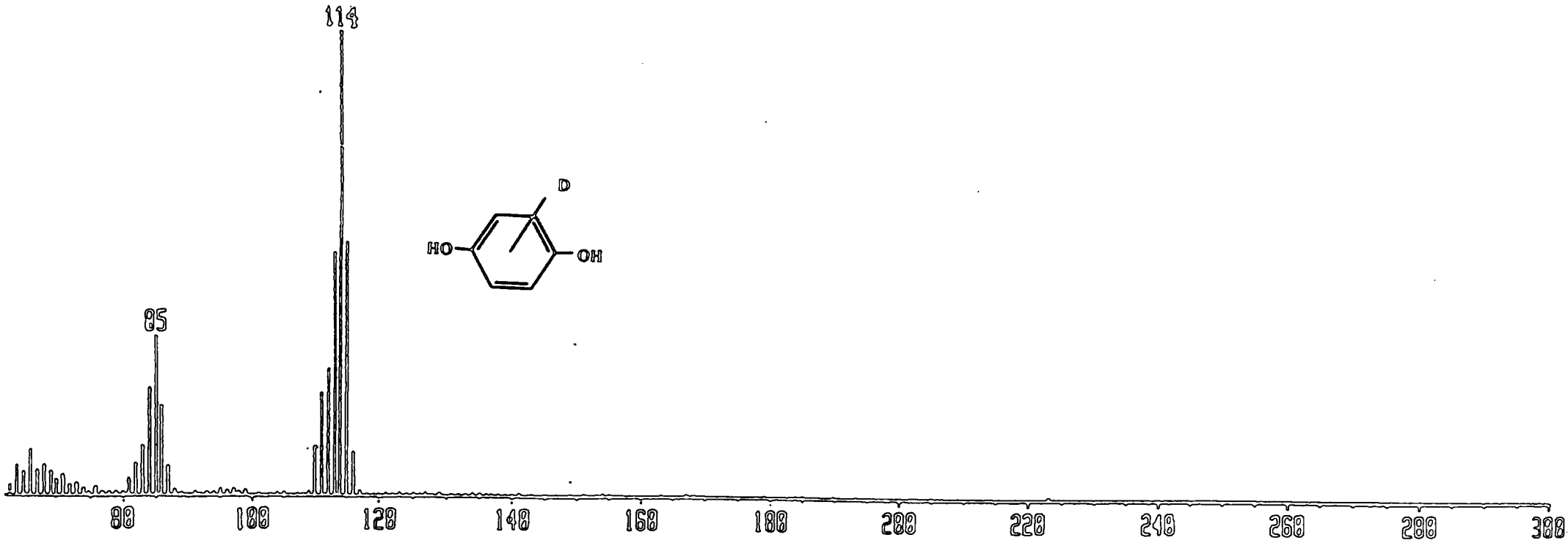

Figure 5.4(a)

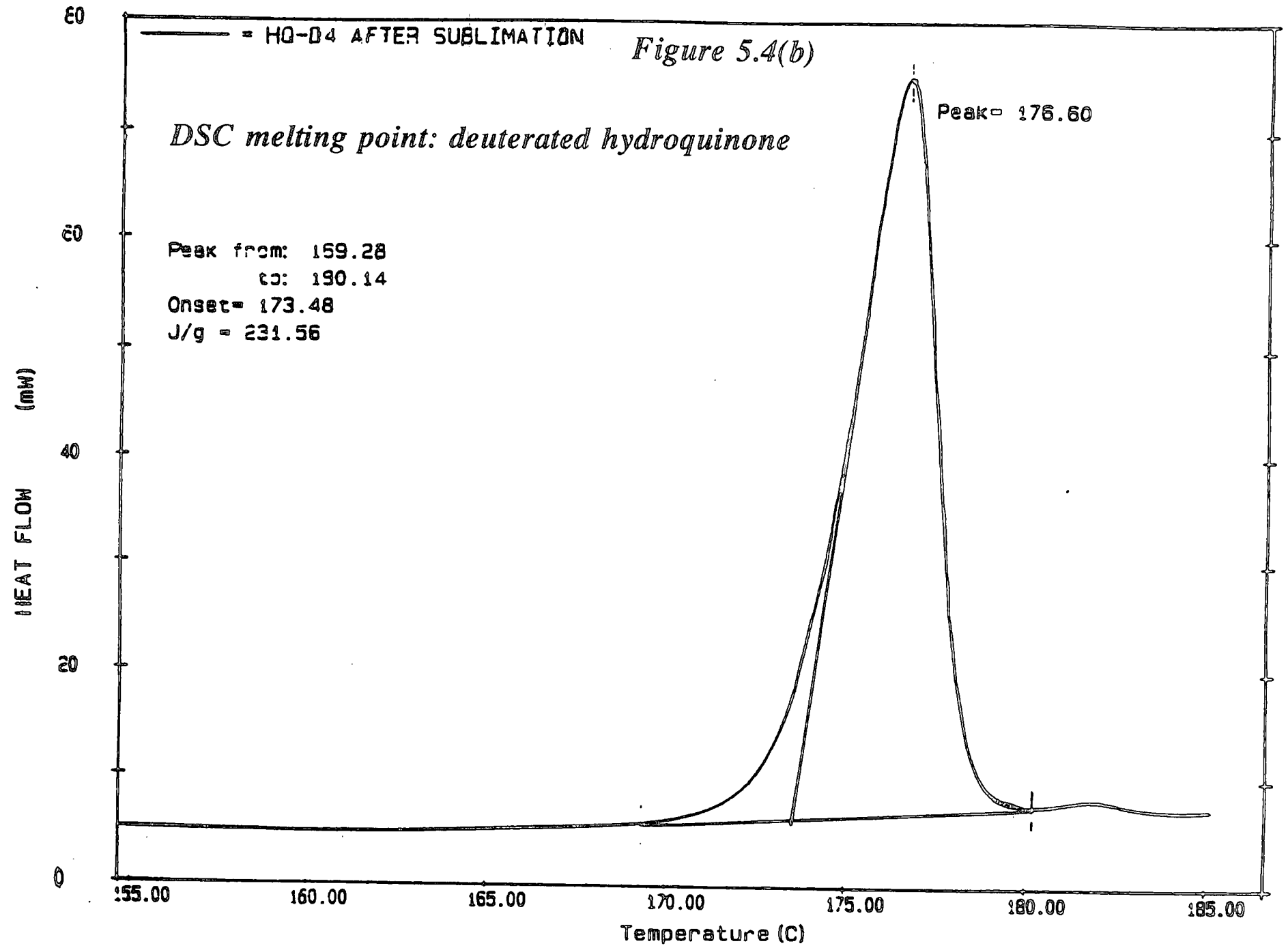

Figure 5.4(b)

DSC melting point: deuterated hydroquinone

IR spectrum: deuterated hydroquinone

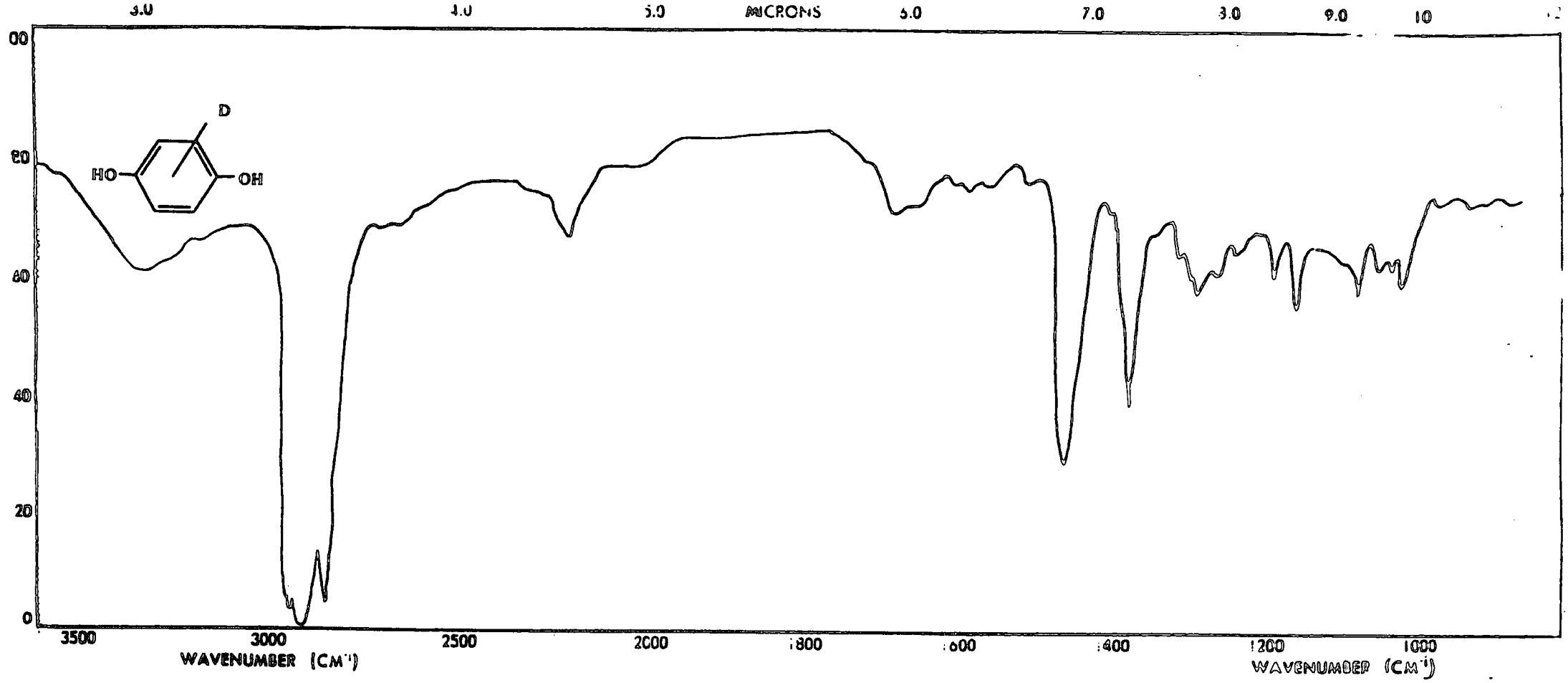

Figure 5.4(c)

RUN ON Dec 17 00
SOLVENT D2O

OBSERVE H1
Frequency 300.052 MHz
Spectral width 6000.0 Hz
Acquisition time 0.744 sec
Relaxation delay 0.000 sec
Pulse width 2.0 usec
Ambient temperature
No. repetitions 120
Double precision acquisition
DATA PROCESSING
FT size 65536
Total acquisition time 7 minutes

Proton NMR spectrum: deuterated hydroquinone

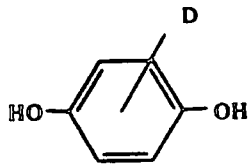

Figure 5.4(d)

Mass spectrum: deuterated HBA

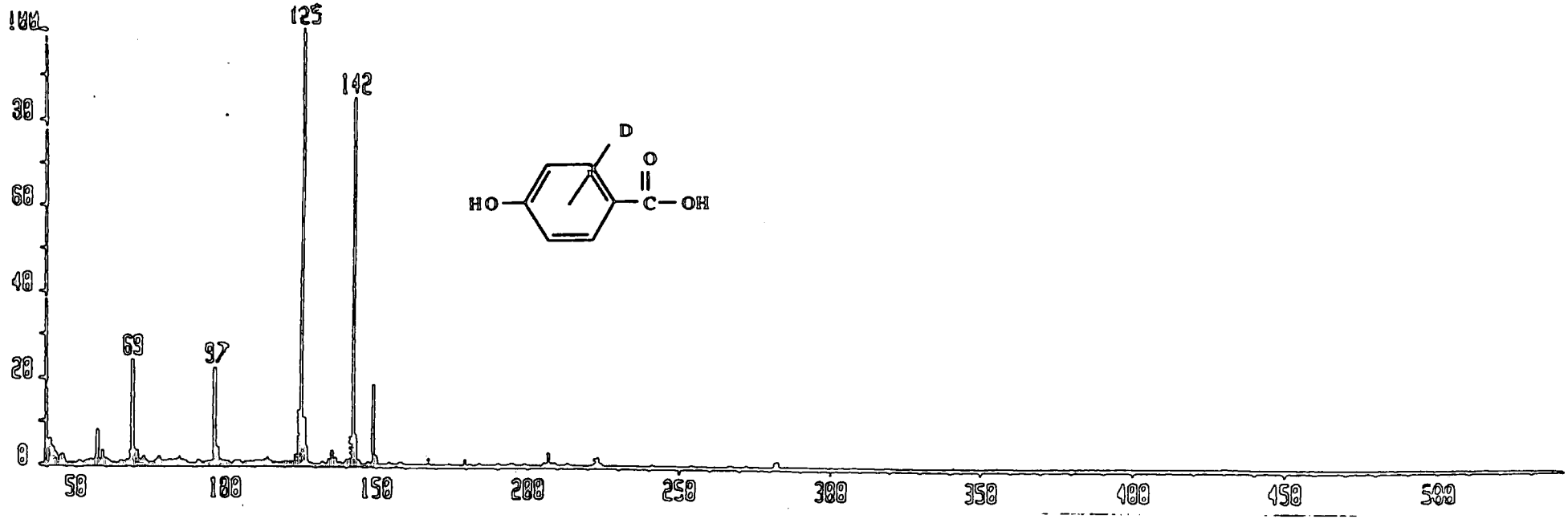

Figure 5.5(a)

IR spectrum: deuterated HBA

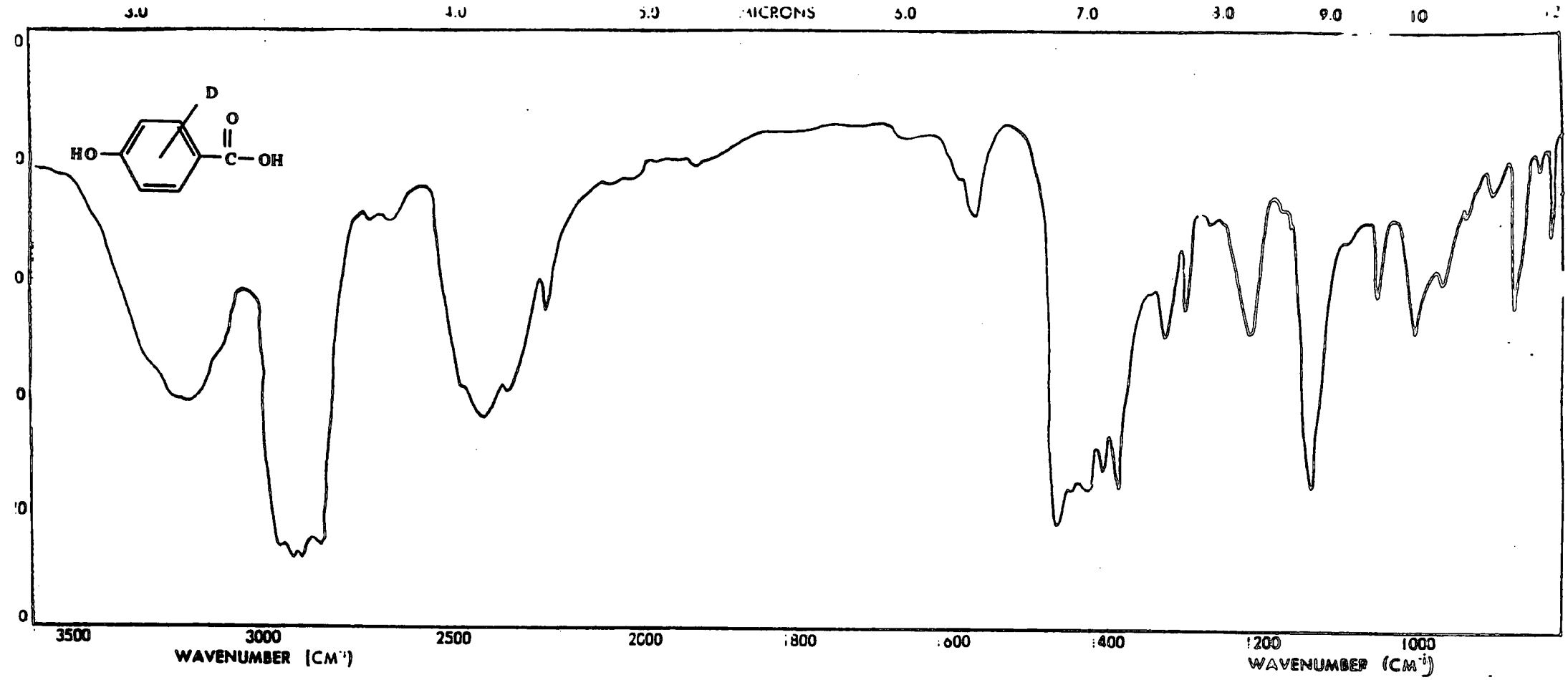

Figure 5.5(b)

was recrystallised in acetone prior to use.

5.4.3 *Preparation of the deuterated polymer*

Initially, the monomers which were synthesised and purified as described in section (5.4.2) were used in the preparation of the deuterated polymer. An identical synthetic route to that used in the preparation of the hydrogenous polymer, a dispersion polymerisation patented by ICI plc [43] was carried out. The reaction was unsuccessful due to the dispersion mixture flocculating during the initial stages of the polymerisation which produced an oligomeric material, useless for the present experimental requirements. The product was confirmed to be an oligomer by analysis using Melt Flow Index techniques. From the results an approximate molecular weight of 8,000 - 10,000g mol^{-1} was calculated. The monomers used in the reaction were analysed using X-ray Fluorescence (XRF) techniques, which revealed the presence of trace amounts of potassium, magnesium and calcium in the deuterated HBA (Table (5.1)).

Monomer	Major	Minor	Trace (≪1000ppm)
HBA-d_4	——	——	K,Ca,Mg
HQ-d_4	——	——	——

Table (5.1) XRF results

The metals were the only impurities identified in the reaction mixture. The source of these impurities is not completely understood, however it is assumed that they could only have originated from the distilled water used in the purification of the deuterated HBA. The trace metals were present in sufficient quantities to cause flocculation of the dispersion mixture.

A second polymerisation was carried out using conditions and materials identical to those used in the initial polymerisation, with the exception of the impure d-HBA being

replaced by its hydrogenous equivalent as supplied by Aldrich and used without further purification. The reaction was successful yielding a high molecular weight polymer with a calculated deuteration level of 30%, adequate for experimental analysis by SANS techniques. For simplicity, throughout this chapter the partially deuterated material will be referred to as the deuterated polymer.

5.4.4 *Sample Preparation*

a) Polymer Purification

Both polymers, the hydrogenous and deuterated, were purified using the procedure described in section (3.3.2(a)).

b) Molecular Weight Determination

Melt Flow Index (MFI) techniques were used to determine the molecular weight of the deuterated material. The value was calculated to be in the range 70,000 - 90,000 $gmol^{-1}$ (MFI =1.8). A batch of hydrogenous polymer of identical MFI to that of the deuterated material, was used in the preparation of the polymer blends.

c) Blend Preparation

The deuterated and hydrogenous polymers, in the ratio 50:50 wt% were blended by co-dissolving them in a mixed solvent system of TFA/DCM in the ratio 95:5% volume. Both solvents were distilled and dried over $MgSO_4$ prior to use. The resulting mixture contained 4% wt/vol of polymer. This mixture was allowed to stand for 48 hours to ensure complete dissolution.

d) Polymer Film Preparation

A small aliquot of the polymer blend solution was poured into a teflon casting dish, and the solvent allowed to evaporate slowly. This procedure was repeated several times leading to the formation of a film. The majority of the solvent was allowed to evaporate

slowly over a period of 72 hours. The resultant pliable film was then cut into disks of 15mm diameter. These disks were then dried in vacuo between glass slides for one week over which time the temperature of the oven was gradually increased from ambient to 100°C. This procedure ensured complete solvent removal. The resulting disks were approximately 0.2mm in thickness. These samples were stacked together in the neutron beam until an optimum thickness of 1mm was obtained. Previous studies on LCP using SLALLS techniques, have confirmed that no molecular degradation nor transesterification occurs under these conditions.[32]

e) Annealing Conditions

Differential Scanning Calorimetry (DSC) was used to determine the various transitions occurring in the polymer as a function of temperature. A typical DSC thermogram is illustrated in Figure (5.6). Previous studies showed that transesterification in LCP did not occur below 523K however the process occurred in a matter of seconds at 603K.[32] From the literature[18-20,40] transesterification is known to occur, in some cases, below the melting point. It was on these bases that the annealing conditions were selected. The blended disks were sandwiched between polyimide film and annealed in an accurately controlled heating press at 533K, 553K, 563K, 588K and 603K over the range 0-180 seconds. After treatment, the samples were removed immediately from the heating press and quenched into an ice/water mixture in order to "freeze-in" the structures developed.

5.4.5 *Scattering Experiments*

The annealing processes lead to the formation of H-D copolyesters as a result of transesterification. During this process, the molecular weight of the isotopically labelled polymer appears to decrease as a function of increasing temperature and time. Values of this parameter are calculated from Zimm plot analysis of the corrected data obtained from the scattering experiments. These experiments were carried out using the LOQ diffractometer at the ISIS facility, Rutherford Appleton Laboratories, Oxfordshire.

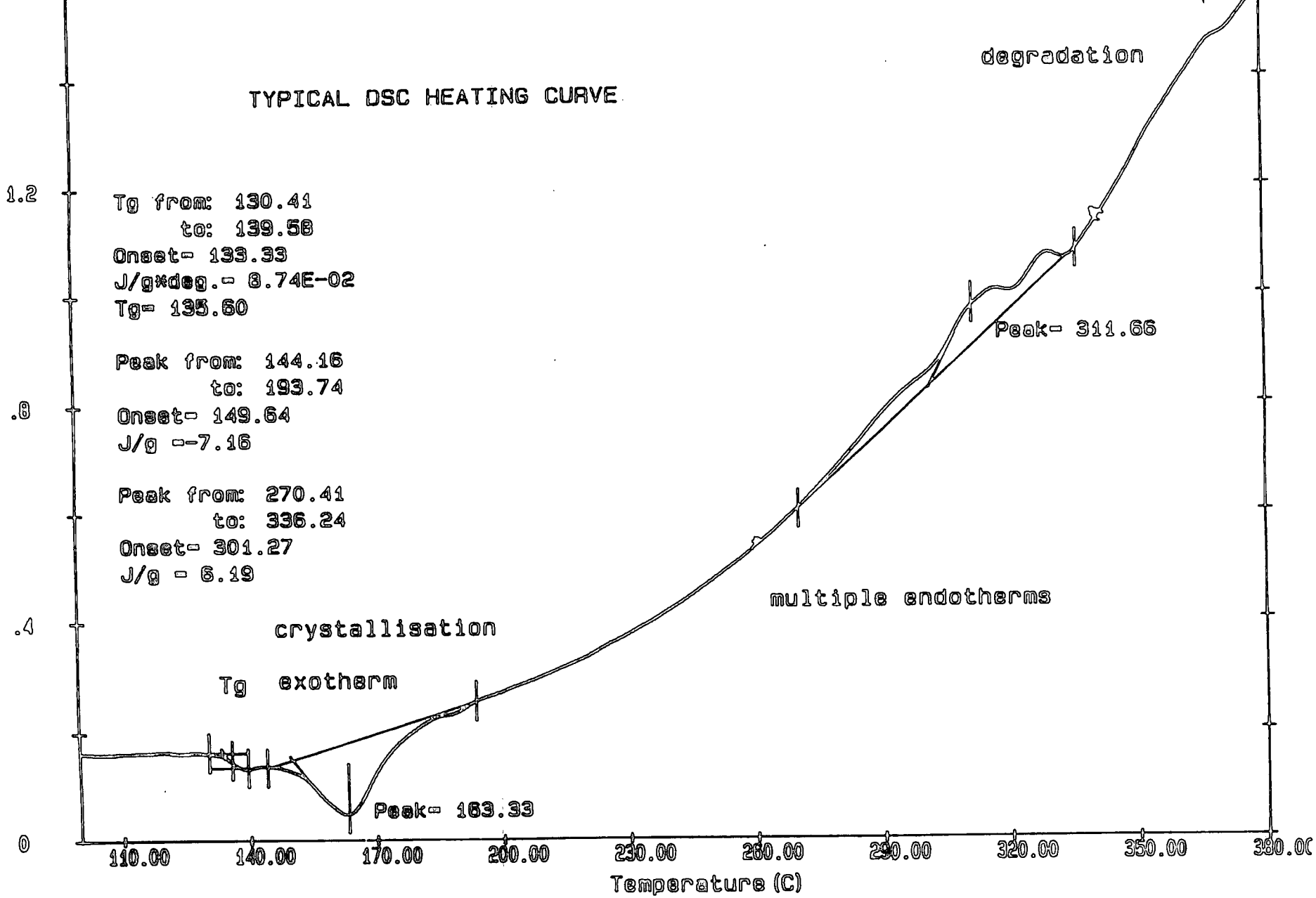
degradation
TYPICAL DSC HEATING CURVE
1.2
Tg from: 130.41
to: 139.58
Onset= 133.33
J/g*deg.= 8.74E-02
Tg= 135.60
Peak from: 144.16
to: 193.74
.8
Onset= 149.64
J/g =-7.16
Peak from: 270.41
to: 336.24
Onset= 301.27
J/g = 6.19
Peak= 311.66
multiple endotherms
.4
crystallisation
Tg exotherm
Peak= 163.33
0
110.00
140.00
170.00
200.00
230.00
260.00
290.00
320.00
350.00
380.00
Temperature (C)

Figure 5.6

The following section discusses:

i) SANS instrumentation

ii) Data correction and evaluation

i) *Instrumentation: the LOQ Diffractometer*

The pulsed neutron source, ISIS, produces fast neutrons by directing an 800MeV proton beam from an accelerator onto a Uranium target; part of the proton's energy is deposited as heat, part to create low energy neutrons and part to create high energy particles including neutrons. The high energy secondaries undergo further interaction, depositing heat and creating more particles hence building up a particle cascade in the target. The average energy of the neutrons which escape from the surface of the target is approximately 1 MeV. In order for these neutrons to be used in scattering experiments, they must be slowed down. This is accomplished by scattering the fast neutrons in moderators situated above and below the target. Various neutron scattering experiments require different energy neutrons which are produced by 3 different types of moderator. The moderated neutrons are then directed to the various instruments through neutron guides. The LOQ diffractometer uses a liquid hydrogen moderator; no attempt is made to monochromate the neutron beam in this instrument. The wavelength distribution of the neutrons is over the range 2-10Å. On exiting the moderator, the incident neutron beam travels into the LOQ diffractometer through a series of benders, apertures and collimators in order to discard any neutrons outwith the stated wavelength range. The beam then proceeds along a flight tube leading to the sample position, situated 10m from the moderator. Scattered neutrons are recorded on a multiwire BF_3 filled detector, separated at a distance of 4.43m from the sample position by a flight tube: the latter being evacuated previously to reduce air scattering. Time of flight analysis is used to record the scattered intensity and data acquisition is performed on a microvax. A schematic diagram of the diffractometer is illustrated in Figure (5.7).

LOQ Diffractometer

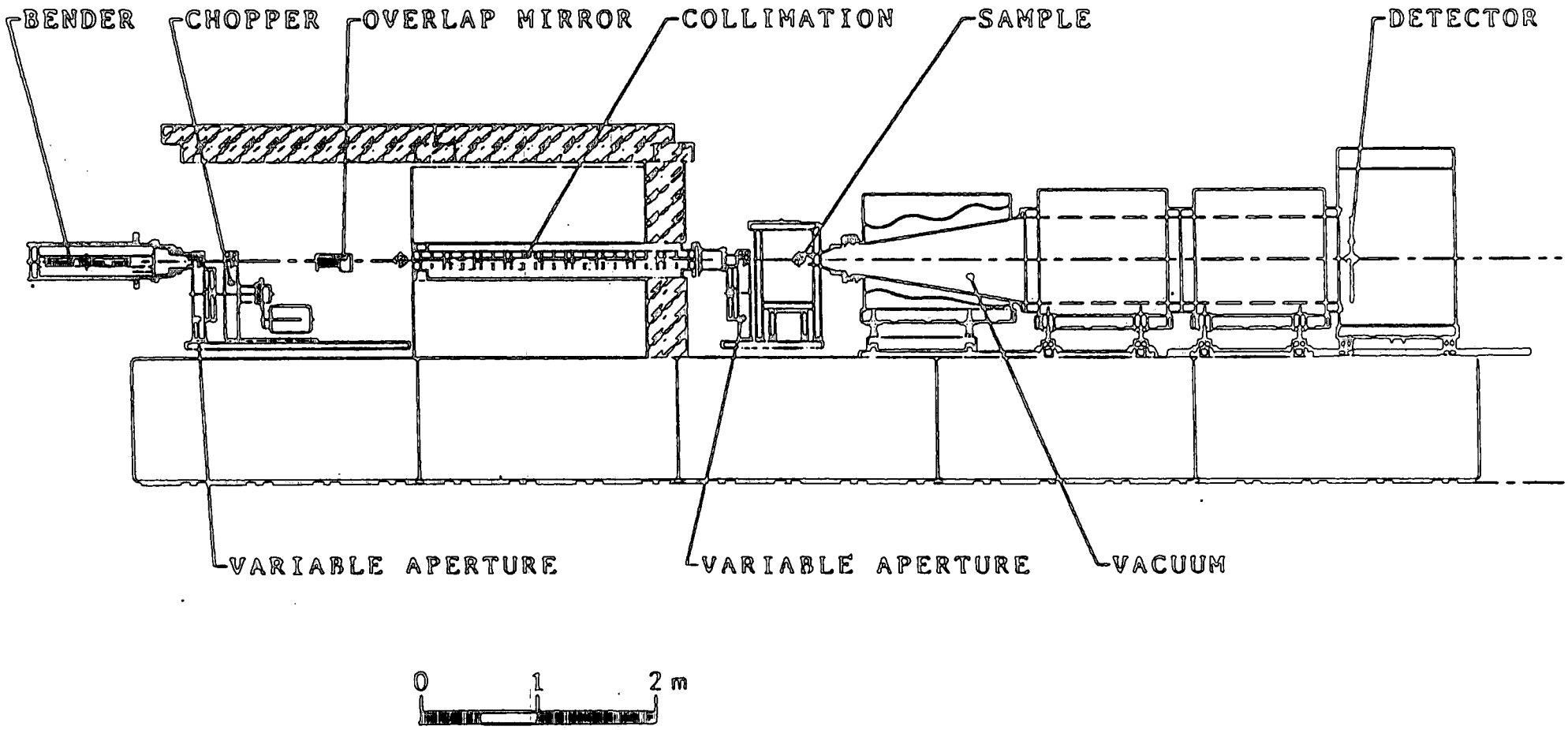

Figure 5.7

Two dimensional scattering diagram

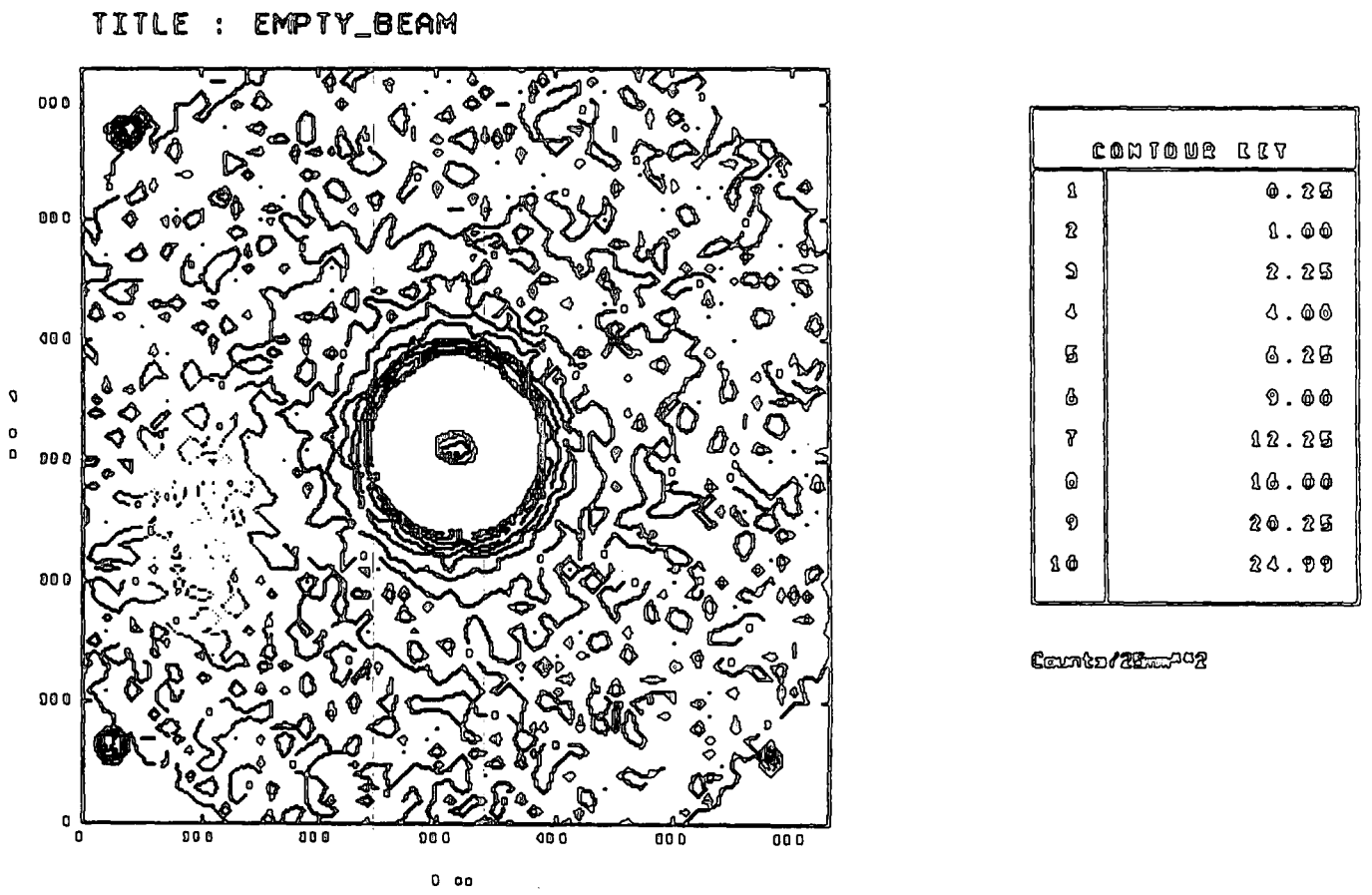

Figure 5.8

Typical scattering curve

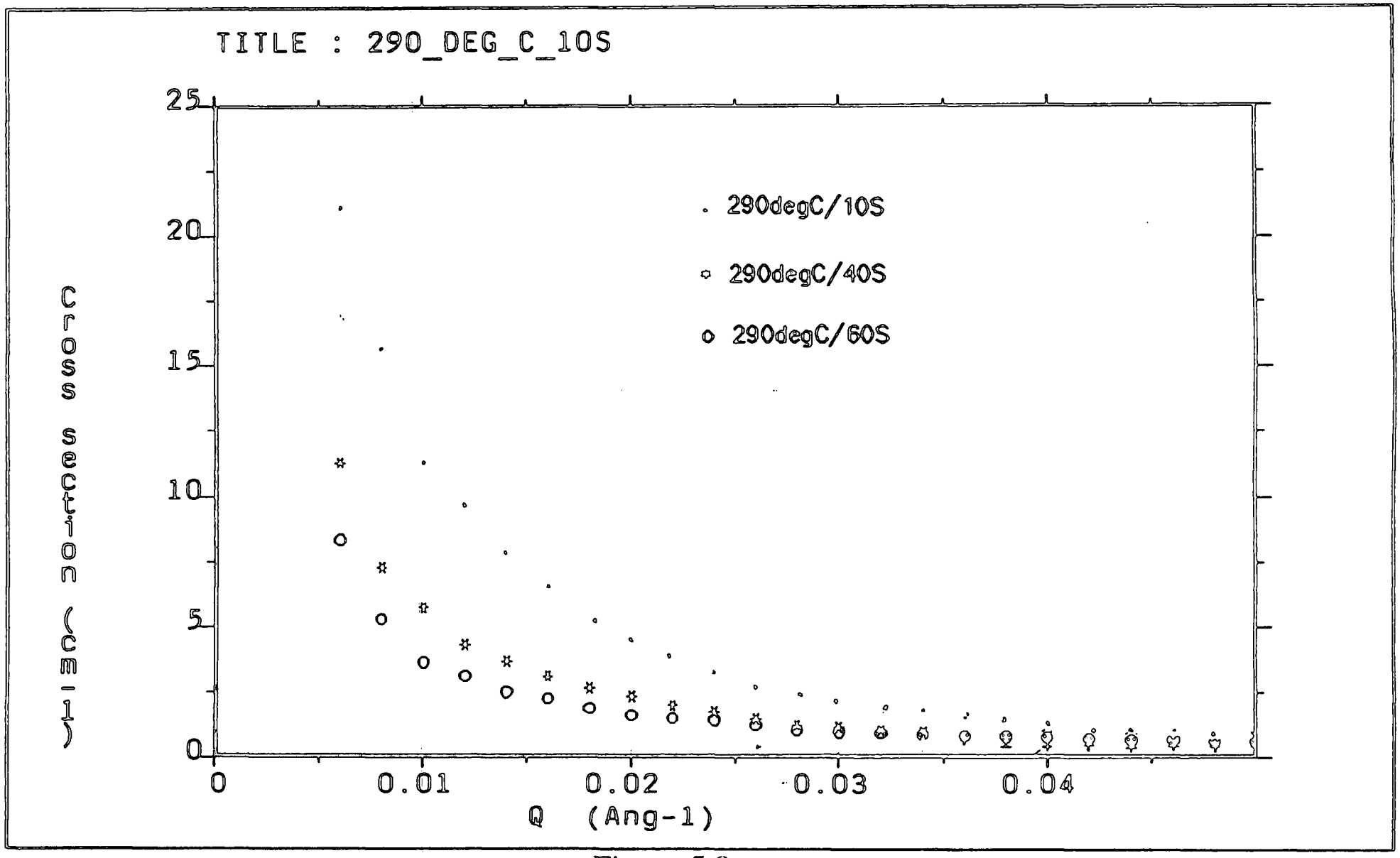

Figure 5.9

ii) *Data Correction and Evaluation*

LOQ data reduction is performed by the COLETTE Program described in detail in the LOQ Users Manual.[45] This program converts the raw time of flight data into a total neutron scattering cross-section ($d\Sigma/d\Omega$) in absolute units. Most of the corrections which may be applied (for example, transmission, monitor counts and detector efficiency) are all dependent on wavelength. Hence, on completion of the experiment, COLETTE may be used to provide a final I(Q) versus Q plot including the subtraction of a sample background run and normalisation to an isotropically scattered standard.

In the present work, the background run was the average sum of the scattering obtained from the hydrogenous and the deuterated LCP sample. Normalisation was carried out using a partially deuterated polystyrene standard of known molecular weight, thickness, contrast factor and level of deuteration. Using COLETTE,[45] the fully normalised cross-section can be obtained by subtracting the sample background (CA) from the sample (SA) and dividing by the normalising cross-section (NO) minus its background (BA). Thus,

$$\frac{d\Sigma}{d\Omega}(\lambda) = \frac{T_{NO}(\lambda)}{T_{SA}(\lambda)} \left[\frac{I_{SA}(\lambda)}{M_{SA}(\lambda)} - \frac{T_{SA}(\lambda)}{T_{CA}(\lambda)} \frac{I_{CA}(\lambda)}{M_{CA}(\lambda)} \right] \Big/ \left[\frac{I_{NO}(\lambda)}{M_{NO}(\lambda)} - \frac{T_{NO}(\lambda)}{T_{BA}(\lambda)} \frac{I_{BA}(\lambda)}{M_{BA}(\lambda)} \right] \frac{d\Sigma}{d\Omega}(\lambda) \qquad (5.52)$$

where $T(\lambda)$ is the transmission of the sample, I indicates the counts on the detector and M, the number of monitor counts.

The data obtained from the diffractometer is initially in the form of two-dimensional scattering (Figure (5.8)). This data is then circularly averaged in order to obtain a one-dimensional scattering curve (Figure (5.9)), which plots I(Q) as a function of Q.

A scattering intensity plot, corrected for transmission factor, scattering due to the empty quartz cell and for thickness, where the latter is normalised to 1mm, is illustrated in Figure (5.9) for a LCP sample transesterified over an increasing time range. Figure (5.10) represents a fully corrected version of the scattering data, accounting for the subtraction of incoherent scattering. The reduced data is in the form required for evaluation of the kinetic parameters of transesterification for LCP.

SCATTERING PLOT

SCATTERED INTENSITY versus SCATTERING VECTOR

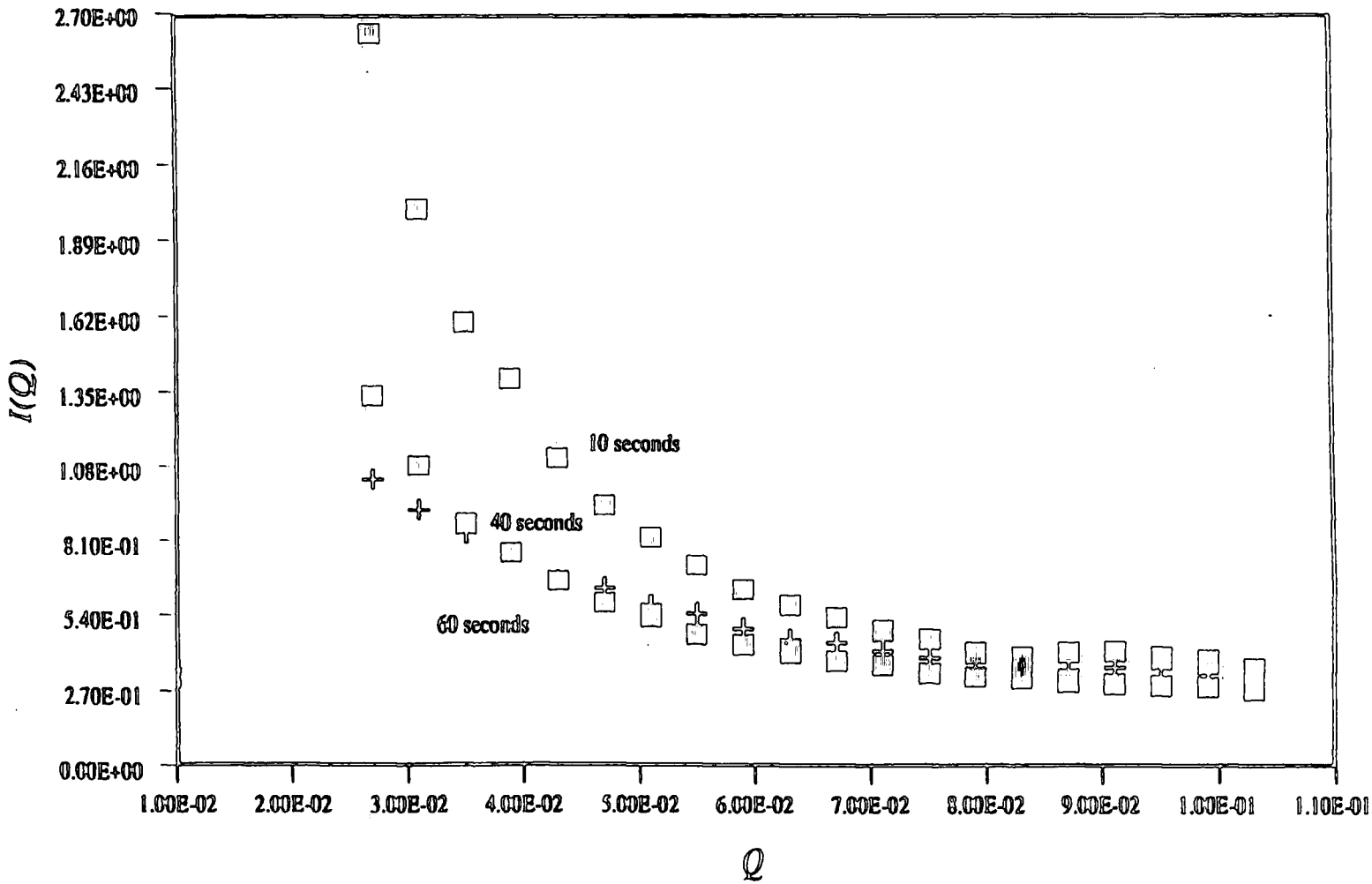

Figure 5.10

5.5 *Results and Discussion*

5.5.1 Scattering Curves

In the previous section, a typical corrected I versus Q plot (Figure 5.10) illustrates the scattering behaviour of a blend which had been transesterified over a range of times (Figure (5.10)). Zimm plots of this data ($I(Q)^{-1}$ vs Q^2) appear to follow a linear behaviour, however it should be noted that at values of $Q < 0.005$Å an additional scattering is observed (Figure (5.11)). Previous studies noted a similar phenomenon[32] and have discussed the reasoning behind this behaviour in detail. It can be attributed to the scattering from voids. The occurrence of voids in solvent cast films can be reduced dramatically by annealing the samples for long periods of time, just above the polymer glass transition temperature. Such a treatment is impractical in the present study since transesterification may occur under these conditions, leading to inaccurate results in the final analysis. However since void scattering was observed only to occur at very low values of Q, correction for this factor is unnecessary since from the theory of Benoit et al,[22] evaluation of the results over an intermediate scattering range only, is required in order to determine the kinetic parameters of transesterification. For simplicity, in this study Zimm plots of the scattering data are presented omitting the effects of void scattering at very low values of Q.

5.5.2 *Zimm Plot Analysis: a Qualitative Study*

Figure (5.12) illustrates the dependence of the reciprocal intensity at different transesterification times (t). The former values appear to increase as a function of t. On extrapolation of each asymptote to the y-axis (at $Q = 0$) from the intermediate Q range, the intercept values can be used to evaluate the molecular weights. The latter will be discussed in detail in section (5.5.3) and from these values, the number average degrees of polymerisation can be calculated. The latter values are then used directly in the

Zimm Plot prior to correction for void scattering at low angles

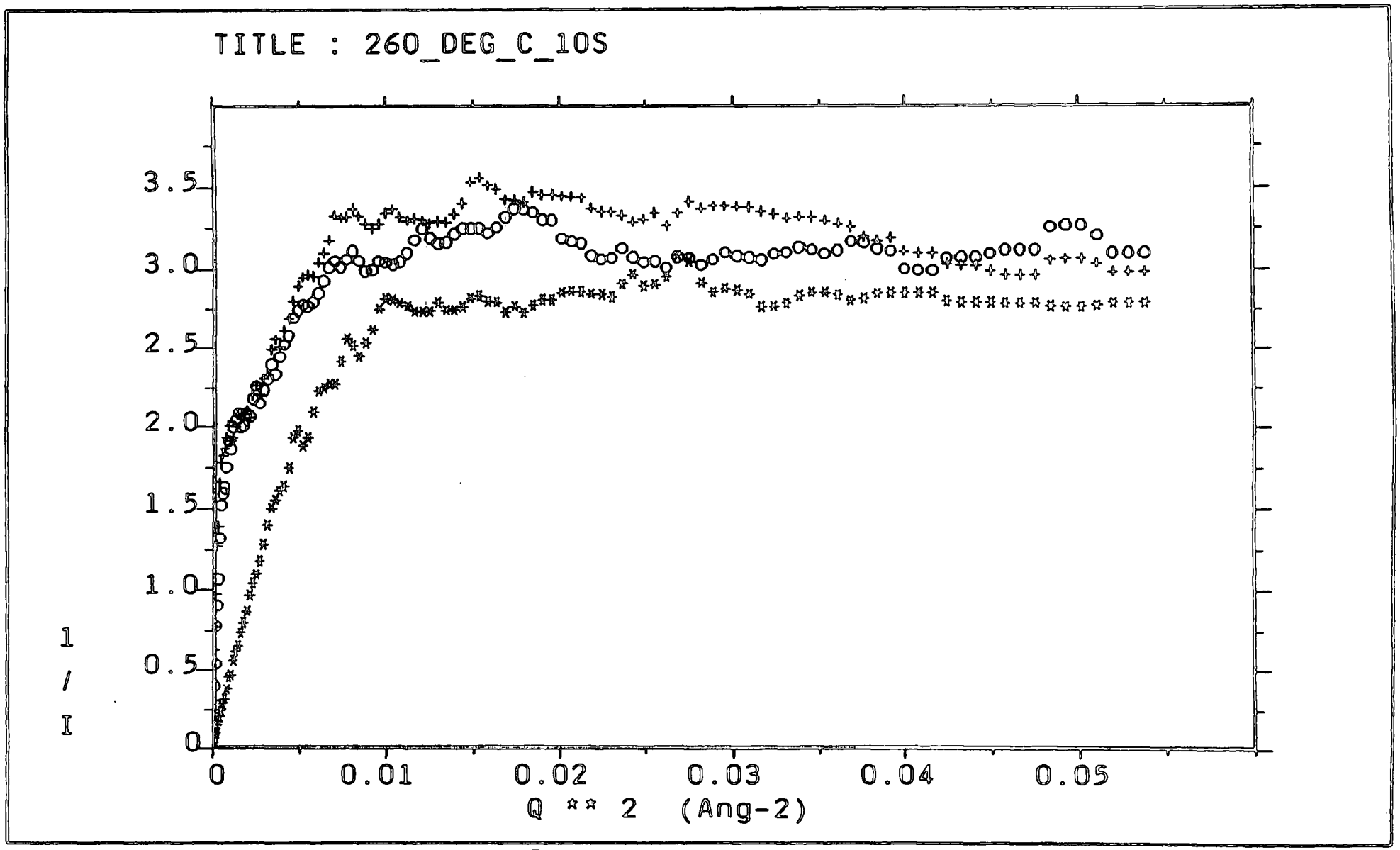

Figure 5.11

ZIMM PLOT

Transesterification Temperature:563K

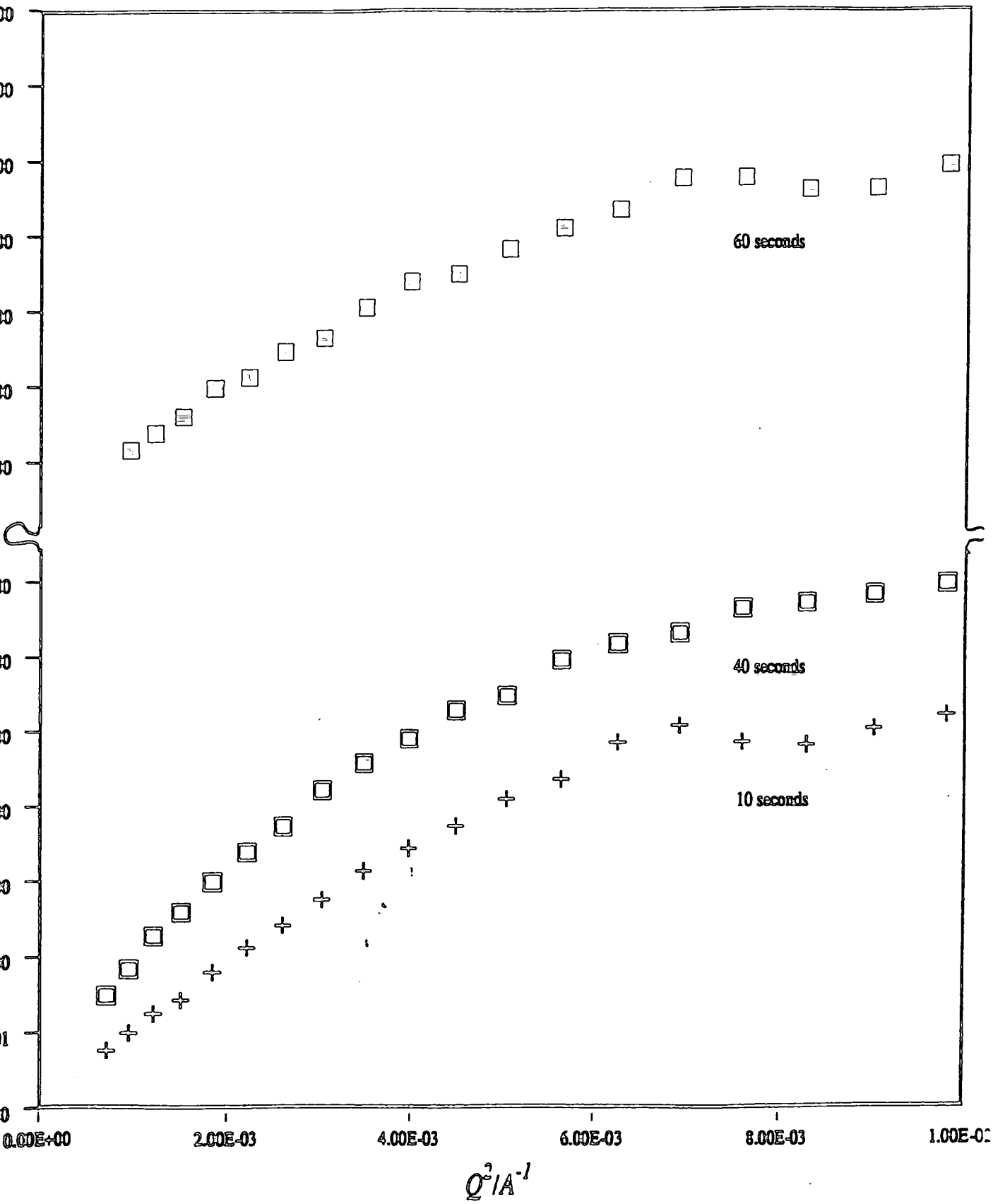

Figure 5.12

evaluation of the kinetics parameters of transesterification. Zimm plots in the intermediate Q range show the behaviour proposed by Benoit et al. The data points form linear plots. These lines, obtained for different reaction conditions, are all parallel to one another. A range of intercepts are obtained on extrapolation of each line to $I(Q)^{-1} = 0$. Extraction of the values of z(t) from these intercepts is not as straight forward as the theoretical method set out by Benoit et al suggests. The true intercepts were obtained by extrapolation of the scattering data plotted in the region $R_g^{-1} < Q < b^{-1}$, where R_g is the radius of gyration of the polymer and b, the statistical step length. In practical terms, this range proved very difficult to define for LCP. From previous SANS studies,[46] using data obtained at a very much lower Q range than that in the present study, the configuration of the molecules of LCP apparently becomes increasingly rod-like with annealing in the temperature range, $T_g \leq Q \leq T_m$. The values of R_g and b increase as a function of annealing time. The present study shows transesterification to occur very rapidly above T_m. There is no direct evidence that this process continues into the melt, however it is presumed that it does, from the results obtained. From the data in the configurational study,[46] the R_g for LCP had an initial value of 57Å (448K) and therefore increased to 69Å (523K). The change in the value of b over this range is small also, increasing from 10Å to 45Å on prolonged annealing. Hence, accounting for these values, the Q range over which the intercepts were extracted was in the region $0.03Å \leq Q \leq 0.1Å$. The lower limit is slightly higher than that proposed by Benoit et al, based upon the values of radius of gyration mentioned above. However these values are calculated from the weight average molecular weights and hence do not pertain to the lowest molecular weight sample obtained during transesterification. Furthermore, the amount of lower molecular weight material will increase as the reaction proceeds; bearing this in mind, the lower Q limit can be relaxed. The reasons for using the proposed Q range can be reinforced by calculating the value of b from the slope of the linear least squares line (Benoit's equation (5.35)) drawn through the data points over the limiting Q values. The calculated values of b were in the range 7Å $\rightarrow$ 14Å; in reasonable agreement with the value of 10Å, calculated from a Murakami plot in earlier studies,[46] for samples of

differing molecular weights annealed at 448K for 60 minutes. From this value, it is concluded that for the relatively short transesterification times studied, the configuration of the LCP molecule does not alter significantly, considering transesterification is so advanced at the most severe conditions studied. However, since b is presented as a squared term in equation (5.35), the slope over the Q range can alter significantly yet the change in b obtained, appears to be a relatively insensitive test for suitability of the proposed Q range used to obtain the intercept for subsequent kinetic analysis.

On comparison of each Zimm plot over the temperature range studied, it would appear that the y-axis intercept for each scattering curve increases as a function of transesterification temperature (T) and time (t), suggesting that the scattered intensity of the labelled species diminishes as the reaction conditions become increasingly severe. Overall at 533K (Figure (5.13)), a small decrease in intensity is apparent over the maximum time interval studied. However, at 603K (Figure (5.14)) a significant decrease in intensity is apparent over a very short period. These observations suggest that transesterification occurs, if somewhat slowly, at 533K however the process is extremely rapid at 603K.

5.5.3 *Molecular Weight Determination*

The apparent molecular weights of the labelled polymer can be obtained from the fully corrected and normalised scattering data, from the equation[27].

$$M = \frac{N_A I_{(0)} \quad K_M}{(\rho_D - \rho_H)^2 \quad C_D(1-C_D)} \qquad (5.53)$$

where M = molecular weight of labelled polymer

N_A = Avogadro Number

$I_{(0)}$= observed intensity at Q = O

C_D = concentration of labelled polymer in gcm^{-3}

K_M = machine calibration constant, converting $I_{(0)}$ to absolute scattering intensity

ZIMM PLOT

Transesterification Temperature:533K

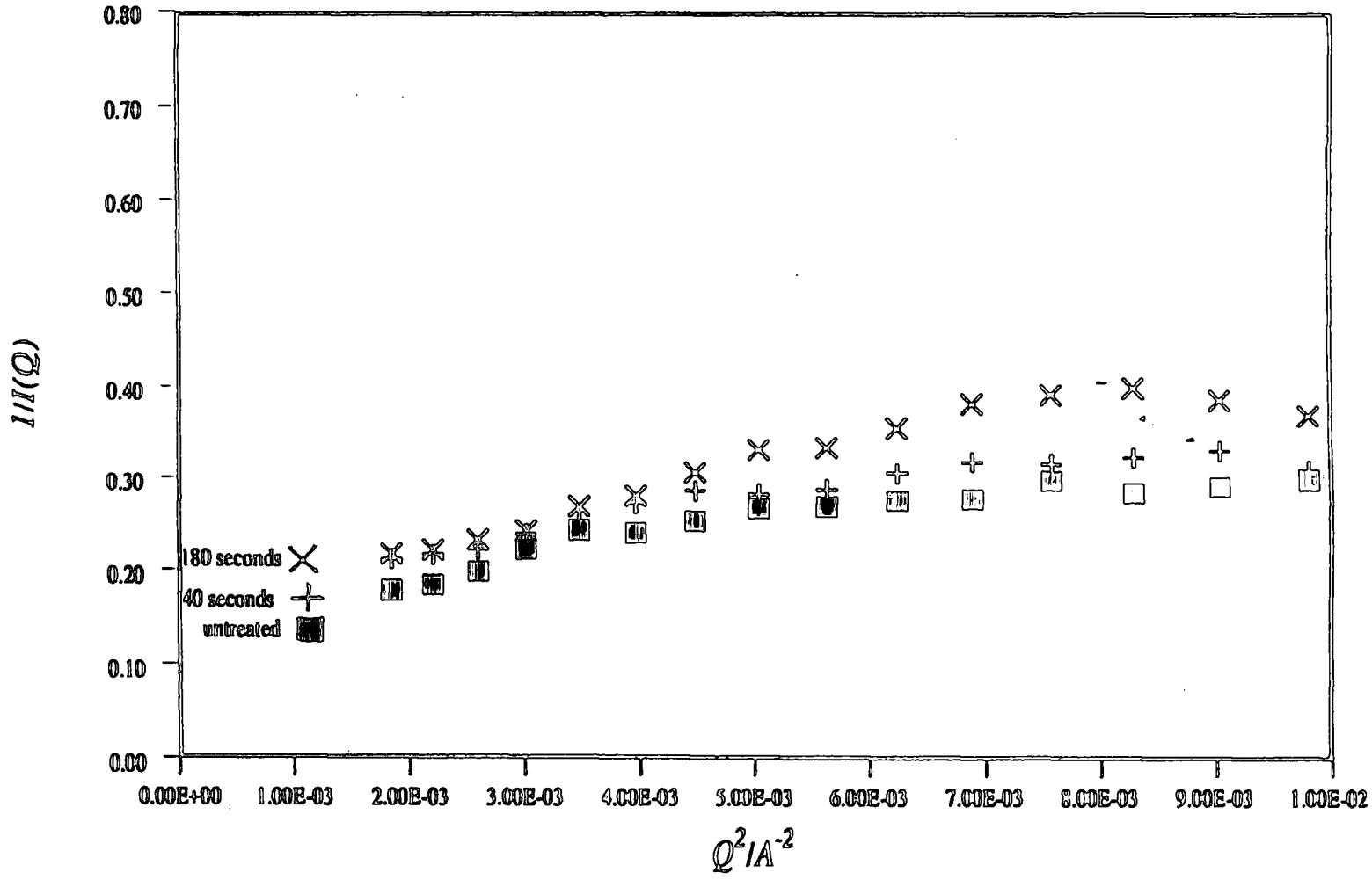

Figure 5.13

ZIMM PLOT

Transesterification Temperature:603K

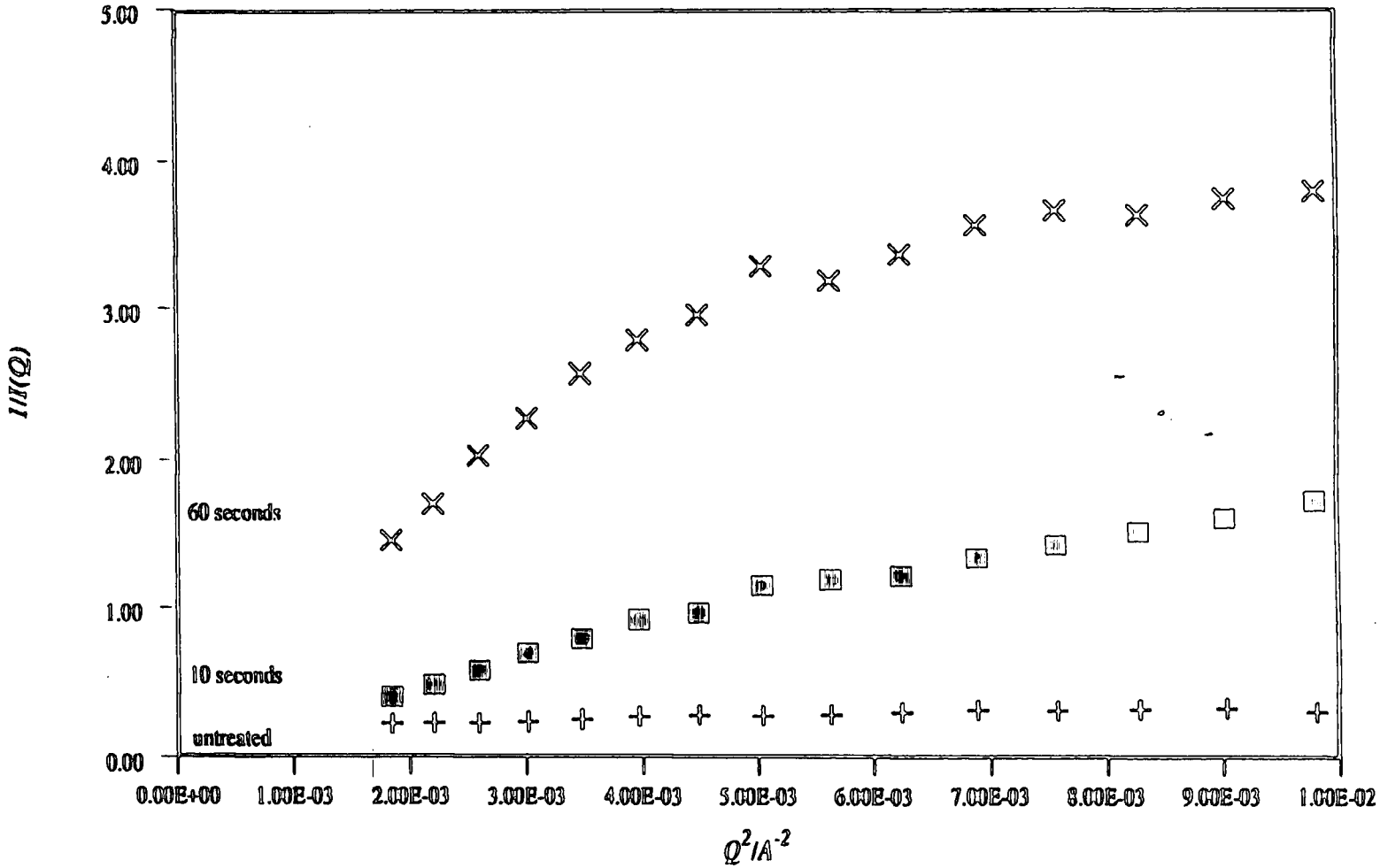

FIGURE 5.14

MOLECULAR WEIGHT versus TRANSESTERIFICATION TIME

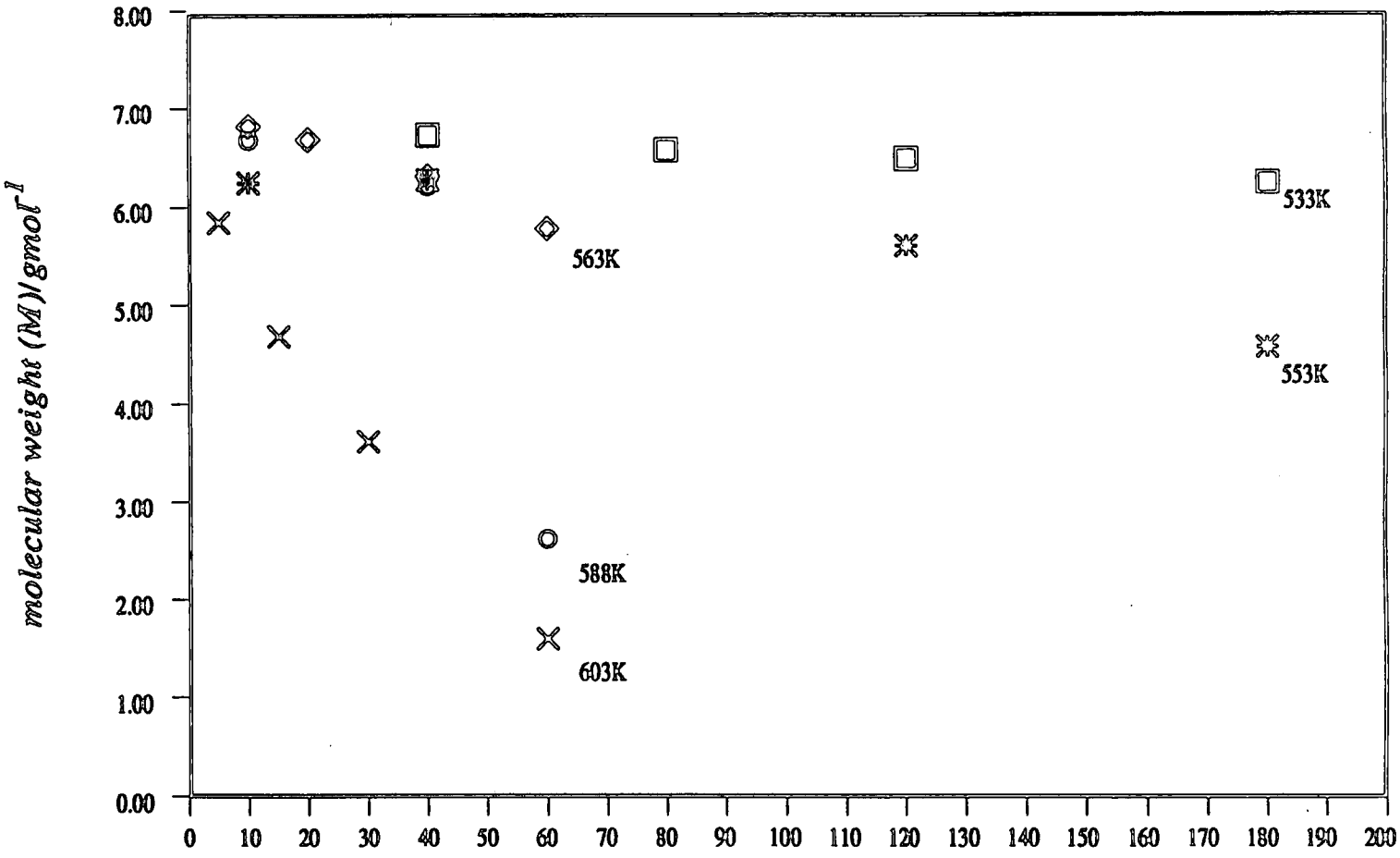

Figure 5.15

ρ_D and ρ_H = scattering length densities of the labelled and unlabelled polymers' respectively

Since the labelled polymer was only partially deuterated, ρ_D was calculated on the average extent of deuteration over the three monomeric units. The calculated values of the molecular weights of the deuterated polymer are plotted as a function of transesterification time for each temperature studied (Figure (5.15)). At the lowest temperature (533K) a slight decrease in molecular weight is observed over a period of several minutes (71,000 - 63,000 $gmol^{-1}$ in 180 seconds). However at 603K, the molecular weight decreases significantly over a very short time period (71,000 - 16,000 $gmol^{-1}$ in 60 seconds). The molecular weight values are listed in Table (5.2). From these results, the extent of transesterification increases as a function of both annealing temperature (T) and time (t).

It is noted that, the initial molecular weight of the polymer obtained in the scattering experiments, falls within the range calculated from the results of the MFI analysis (section (5.4.4)).

5.5.4 *Transesterification Kinetics*

Referring to equation (5.50) in Benoit's theory (section (5.3)),

$$z(t) - z_o = \frac{1}{2x(1-x)}[\,1-\exp(-t/\tau)\,] \qquad (5.50)$$

By rearranging this equation in a more convenient form for analysis, the following equation is obtained:

$$\ln [1-2x(1-x)(z_t-z_o)] = -t/\tau \qquad (5.54)$$

T/K	t/s	$M/10^4 gmol^{-1}$	$(z_t.z_o)/10^{-6}$
533	40	6.76	0.35
	80	6.61	0.52
	120	6.52	0.63
	180	6.28	0.92
553	10	6.28	0.92
	40	6.31	0.88
	120	5.63	1.84
	180	4.60	3.83
563	10	6.85	0.26
	20	6.72	0.40
	40	6.35	0.83
	60	5.81	1.56
588	10	6.71	0.41
	40	6.25	0.96
	60	2.63	1.20
603	5	5.87	1.48
	15	4.71	3.57
	30	3.64	6.70
	60	1.61	24.01

Table (5.2)

LCP Molecular Weights

From a plot of $[1-2x(1-x)(z_t-z_o)]$ versus t, the relaxation time τ, is evaluated from the gradient of the linear plots. The data plotted according to equation (5.54), over the range of temperatures studied, is presented in Figure (5.16). From the values of τ, calculated from the slopes of each line in Figure (5.16), the rate constants per monomeric unit (k) are then evaluated from equation (5.51), (ie. $\tau = 2/kN_T$), recalling that N_T the total number of monomeric units, (section (5.3)) is known from sample preparation. Table (5.3) lists the calculated values of τ and k for each reaction temperature studied. Assuming Arrhenius behaviour, the activation energy of transesterification is calculated from the slope of a plot of ln k versus 1/T.

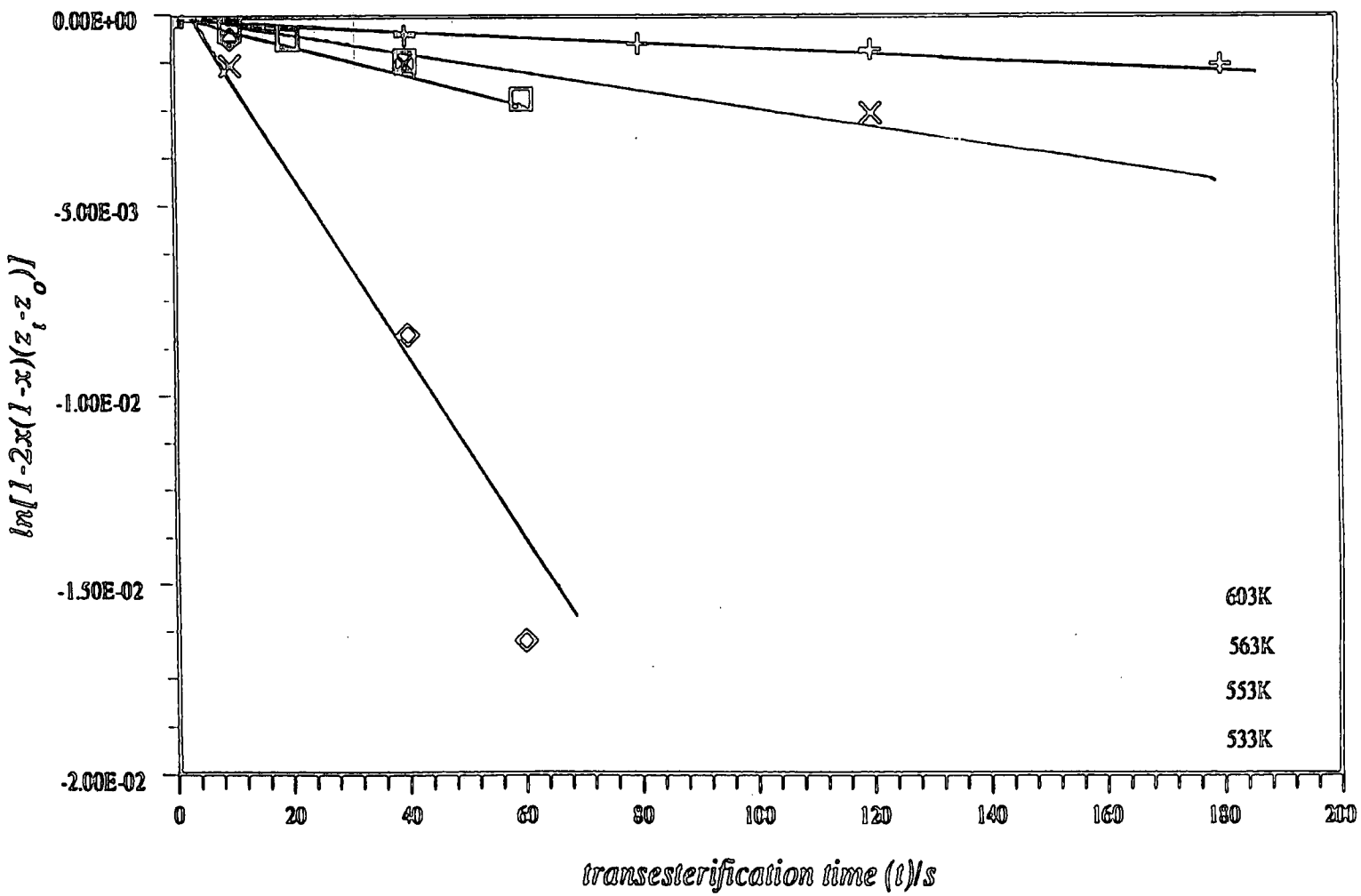
BENOIT PLOT
ln[1-2x(1-x)(z_t-z_o)] versus time
0.00E+00
-5.00E-03
-1.00E-02
-1.50E-02
-2.00E-02
ln[1-2x(1-x)(z_t-z_o)]
0
20
40
60
80
100
120
140
160
180
200
transesterification time (t)/s
603K
563K
553K
533K

Figure 5.16

T/k	slope/10^{-5}	$\tau/10^4$ s	$k/10^{-3}s^{-1}$
533	-0.67	14.90	1.62
553	-2.47	4.05	5.93
563	-34.60	2.89	8.36
588	-27.77	0.36	66.80
603	-55.55	0.18	132.76

Table (5.3)

Values of relaxation times and rate constants

Figure (5.17) shows a linear dependence of lnk versus 1/T, and from the slope, an activation energy (E_a) = 173 (±12)KJ mol^{-1} is obtained. The values of lnk and reciprocal temperature are given in Table (5.4).

In 1987, Kugler and co-workers[21] carried out a quantitative study of the kinetics of transesterification in poly(ethylene terephthalate) (PET). Their methods relied upon prior knowledge of the molecular weights of the transesterified samples before a full analysis could be carried out. In their studies the activation energy for transesterification in PET was calculated.

Albeit that Kugler's method of analysis differs from the method of Benoit employed in the present study in which all the kinetic data is obtained solely from the SANS spectrum, both methods are feasible.

At this point it seems relevant to discuss the structural differences between LCP and PET.

ARRHENIUS PLOT

lnk versus 1/T

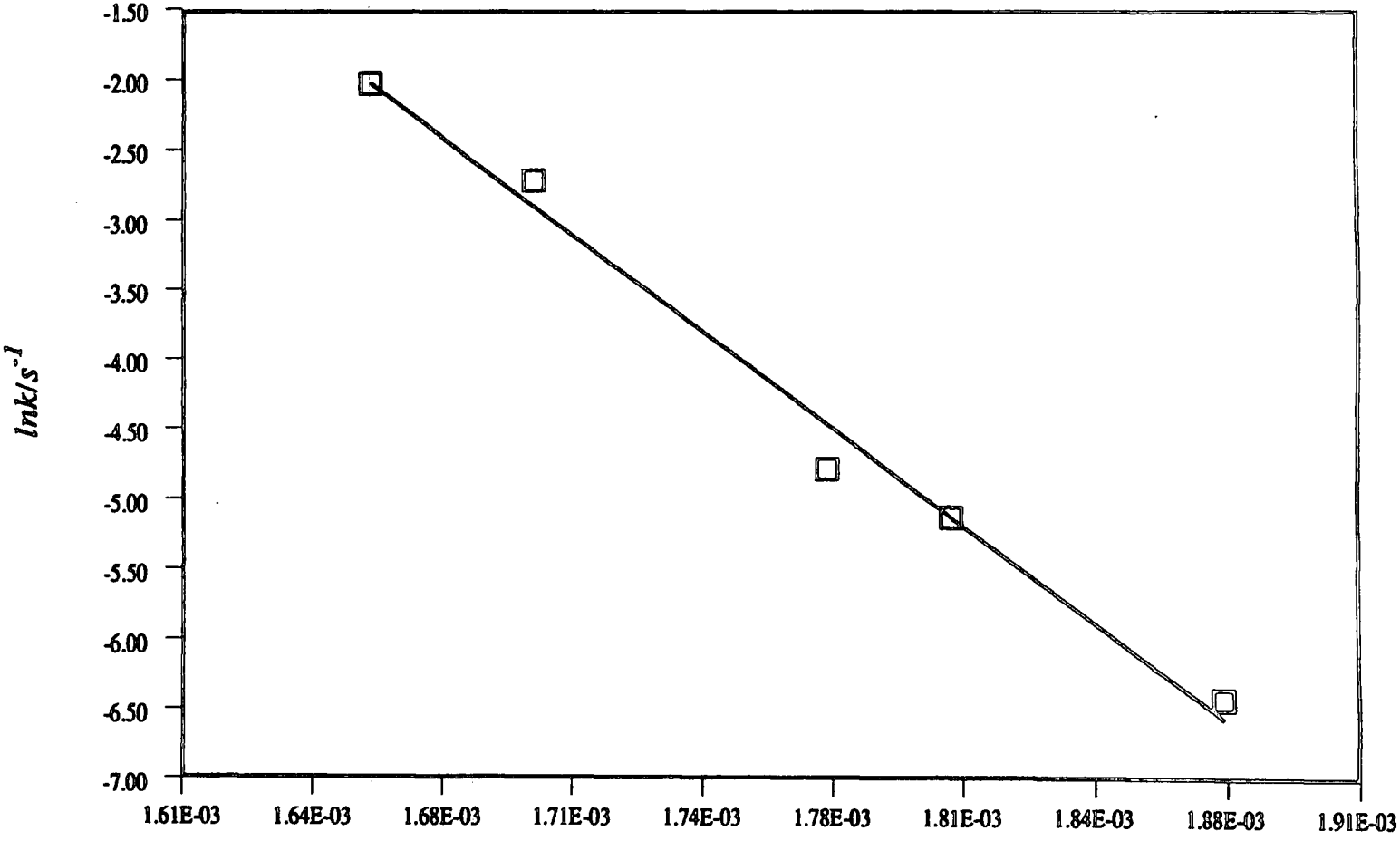

Figure 5.17

$1/T(k) \times 10^3$	-ln k
1.88	-6.43
1.81	-5.13
1.78	-4.78
1.70	-2.71
1.66	-2.02

Table (5.4)

Values of ln(rate constant) and reciprocal temperatures

LCP is a wholly aromatic main chain polyester and hence has a rigid backbone. In contrast, PET units also contain flexible ethylene glycol units along the main chain and hence possess a semi-flexible backbone. Bearing this in mind, a comparison of the activation energies obtained for LCP and PET would thus establish whether or not the nature of the polymer backbone affects the reaction mechanism. Table (5.5) lists the values of the activation energies for both polymers.

POLYMER	E_a/KJ mol^{-1}
LCP	173 ± 12
PET	152 ± 11

Table (5.5)

Activation energies of LCP and PET

On comparison, the values obtained are in acceptable agreement (ie E_a(PET) = 173 $KJmol^{-1}$ and E_a(LCP) = 152 $KJmol^{-1}$) hence it is assumed that the mechanism for the transesterification process is identical for both PET and LCP.

5.5.5 *Transesterification Initiated by Active Chain Ends: a Second Model*

Reaction Model 1 (discussed in section (5.3)), representing the efficient scission and recombination reactions occurring between a hydrogenous and a deuterated polyester, could be criticised as being idealised. Benoit and co-workers propose an alternative model[22] where transesterification is initiated by active chain ends (as illustrated in Model (2)): the active chain end is transferred to the second sequence which again reacts further:

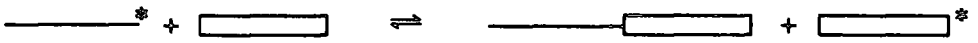

* ≡ active chain end
——— ≡ deuterated polyester
▭ ≡ hydrogenous polyester

Model (2)

Transesterification initiated by active chain ends

In this mechanism, the rate constant is dependent upon the concentration of chain ends in the system, hence as the overall molecular weight of the initial polymer increases, the concentration of chain ends will decrease and hence the rate constant, at a specified temperature, will decrease. However Models (1) and (2) lead to the same kinetic equations therefore the activation energy of the process should remain constant, irrespective of the molecular weight.

To determine the mechanism of transesterification, the kinetic parameters calculated from SANS studies on LCP of a higher molecular weight (104,000 $gmol^{-1}$) were compared with the values used here. For simplicity, the higher and lower molecular weight samples will be referred to as LCP2 and LCP1 respectively. The calculated activation energy for LCP2 was 141.9 (±15) $KJmol^{-1}$, a value in acceptable agreement with that obtained for LCP1, however the rate constants for the transesterification

reaction are considerably smaller for LCP2. The dependence of the rate constants on the reaction temperature are shown in Figure (5.18). The rate constants of transesterification, calculated from data obtained at a temperature of 533K, were compared for the aromatic polyesters (LCP2 and LCP1) and PET. The rate constant for PET was obtained from Kugler and co-workers' analysis.[21] The polyester had an initial molecular weight of 23,000 $gmol^{-1}$, considerably lower than those of the LCP samples.

It must be stressed that this comparison is based solely on the presumption that the same mechanism for transesterification is evident in both LCP and PET. However the presence of the flexible ethylene glycol units in PET, opposed to the wholly rigid nature of LCP as discussed in section (5.5.2), may bear some influence on the value of k. Table (5.6) lists the values of the initial overall molecular weights and rate constants per monomeric unit (at 533K) for the polymers considered.

POLYMER	$M_{INITIAL}$/ $gmol^{-1}$	k / $10^{-3}s^{-1}$
LCP2	104,000	0.59
LCP1	71,000	1.62
PET	23,000	1.87

Table (5.6)

Variation of rate constant with initial molecular weight

The results show the rate constant to be a decreasing function of increasing initial molecular weight, which is the expected result if indeed the reaction is to proceed via an active chain end mechanism.

Dependence of rate constant (k) on reaction temperature (T)

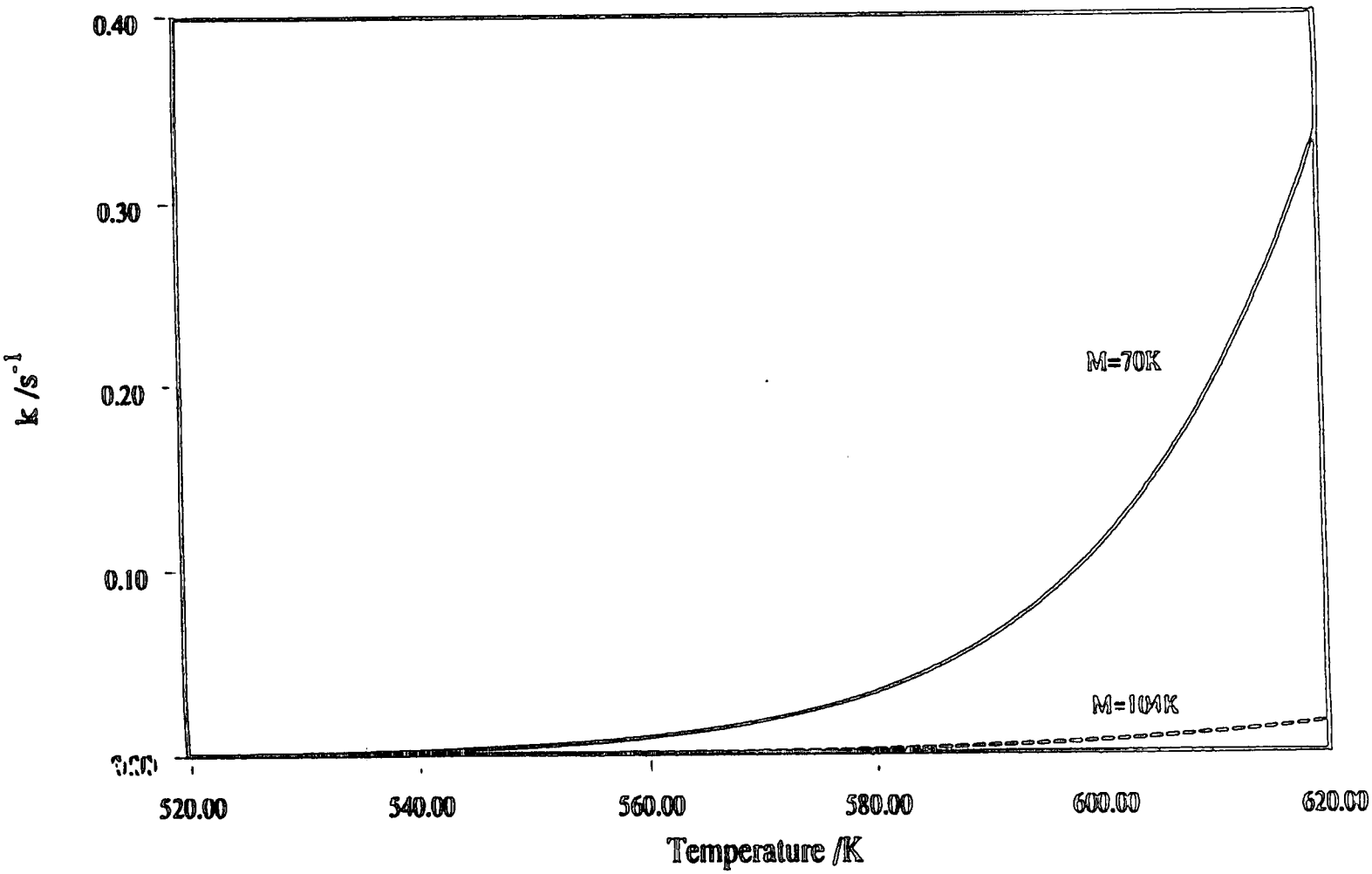

Figure 5.18

5.6 *References*

(1) Flory, P. J., *J.Am. Chem. Soc.* 58 1877 (1936)

(2) Flory, P. J., *Chem. Rev.* 39 139 (1946)

(3) Flory, P. J., *J. Am. Chem. Soc.* 62 1057 (1940)

(4) Flory, P. J., *J. Am. Chem. Soc.* 64 2205 (1942)

(5) Kotliar, A. M., *J. Polym. Sci. Polym. Chem. Ed.*8 11 1157 (1973)

(6) Patai. S., *The Chemistry of Carboxylic Acids and Esters*, Interscience, New York (1969)

(7) Davis, T., in *Chemical Reactions of Polymers, High Polymers. Vol XIX*, E. E. Fettes; Ed, Interscience, New York p. 501 (1964)

(8) Korshak, V. V. and Frunxe, T. M., *Synthetic Hetero-Chain Polyamides*, Monson, Jerusalem p.258 (1964)

(9) Bostic, E. E in *Chemical Reactions of Polymers, High Polymers, Vol XIX*, E.E. Fettes, Ed. Interscience, New York p.528 (1964)

(10) Kotliar, A. M., *J. Polym. Sci. Macrom. Rev.*, 16 367 (1981)

(11) Kursanov, D. N, Korshak, V. V. and Vinogradova, S.V., *12V. Akad, Nauk SSSR Otd, Khim. Nauk*, 140 *Chem. Abstr.* 48 3912g (1954)

(12) Charch, W. H. and Shivers, J. C., *Text. Res. J.* 29 536 (1959)

(13) Kresser, P. Faserforsch, *Textiltech.* 11 353 (1960)

(14) Tippetts, E. A. and Zimmermann, J., *J. Appl. Polym. Sci.* 8 2465 (1964)

(15) Ramjit, H. G. and Sedgivick, R. D., *J Macromol. Sci. Chem*, 10 815

(16) Dorozhkin, V. P., Averko-Antonovich, Yu, O., and Kirpichnikov, P. A., *Tr. Ratan. Kim. Tekhnol. Inst.*, 46 4 (1971), *Chem. Abstr.*, 78 4720t

(17) Lenz, R. W. Ohata, K and Funt, J., *J. Polym. Sci. Polym. Chem. Ed.* 11 2273 (1973)

(18) Lenz, R. W. and Go, S., *J. Polym. Sci. Polym. Chem. Ed.* 11 2927 (1973)

(19) Lenz, R. W. and Schuler, A. N., *J. Polym. Chem. Ed*, 12 1 (1974)

(20) Lenz, R. W. and Schuler, A. N., *J. Polym. Sci. Polym. Symp.*, 63 343 (1978)

(21) Kugler, J. Zachmann, H. G. and Fischer E. W. et al., *Macromolecules*, 20 1116 (1973)

(22) Benoit, H. C., Fischer, E. W. and Zachmann, H.G., *Polymer*, 30 379 (1989)

(23) Willis, B. T. M., '*Chemical Applications of Thermal Neutron Scattering*', Oxford University Press, Oxford (1973)

(24) Bacon, G., *Neutron Diffraction* 3rd edn. Clarendon Press, Oxford (1975)

(25) Kostorz, G., '*Treatise on Materials Science and Technology*' 15 Neutron Scattering; ed. H. Herman, Academic Press, New York (1979)

(26) Lovesey, S. W., '*Theory of Neutron Scattering from Condensed Matter*' Vol. 1, Clarendon Press, Oxford (1984)

(27) Richards, R. W., Chpt. 6 '*Determination of Molecular Weight*', Ed. Cooper, A. R., J. Wiley and Sons Inc. (1989) (28) Sadler, D. M., *Compr. Pol. Sci.* Vol. 1 p. 731, Pergamon Press (1989)

(29) Richards, R. W., *Compr. Pol. Sci.* Vol. 1 p. 133, Pergamon Press (1989)

(30) Newton, R. G., '*Scattering Theory of Waves and Particles Texts and Monographs in Physics*', Springer-Verlag, Berlin (1982) (31) Nowak, E., *Z. Phys.* B45 265 (1982)

(32) McLenaghan, A. D. W., *Ph. D. Thesis*, University of Strathclyde (1991)

(33) Kostorz, G., '*Physical Metallurgy*' Ch. 12. R. W. Cahn and P. Haasen(eds) Elsevier Science Publishers, New York (1983)

(34) De Gennes, P. G., '*Scaling Concepts in Polymer Physics*' Cornell University Press (1979)

(35) Debye, P., *Technical Report CR637*, Office of Rubber Reserve (1945)

(36) Benoit, H. C., *J. Polym. Sci.*, 11 507 (1953)

(37) Leibler, L., *Macromolecules*, 13 1602 (1980)

(38) Leibler, L and Benoit, H. C., *Polymer*, 22 195 (1981)

(39) Benoit, H. C. Wu, W. Benmouna, M., Mozer, B., Bauer, B. and Lapp, A. *Macromolecules*, 18 986 (1985)

(40) Benoit, H. C. and Hadziioannou, G., *unpublished results*

(41) Desiraju, G. R., Curtin, D. Y., Paul, I. C., *J. Org. Chem.* 42(25) 4071 (1977)

(42) Komiyama, M., Hirai, H., *J. Am. Chem. Soc.* 106 174 (1984)

(43) *GB Patent 8700922* ICI Dispersion Polymerisation Process

(44) Lenz, R. W., Jin, J. I., Feichtinger, K. A., *Polymer*, 24 327 (1983)

(45) Heenan, R. K., *LOQ Users Manual*, Rutherford Appleton Laboratories, Oxon (1988)

(46) McLenaghan, A. D .W., MacDonald, W. A., Richards, R. W., *(submitted for publication to Macromolecules)* (1991)

Chapter 6

Crystallisation-Induced Reorganisation

6.1 *Introduction*

Several references report on the preparation of polyester block copolymers by means of the limited transesterification of a blend of two polyester homopolymers at elevated temperatures (1-4). Initially ester-interchange takes place leading to the formation of large segments, however as the reaction proceeds, the interchange process continues and the segments become increasingly shorter until finally, at equilibrium, a random copolyester is formed. The structures of the block copolymers formed are very difficult to control and the resultant system is usually a blend of homopolymers or copolymers of extremely high polydispersity. Ester-interchange reactions are discussed in greater detail in section (5.1). Lenz and co-workers have explored an unusual route to the preparation of block copolymers from polyesters via a process termed crystallisation-induced reorganisation (CIR). This process is based on the transesterification reaction (section (5.1)) and involves the thermal treatment of random copolyesters near their initial melting temperature in the presence of an active ester-interchange catalyst.[5] Under these conditions crystallisation-induced chemical reorganisation occurs, converting equilibrated random copolymers to non-equilibrium blocky structures. The process is therefore, anti-entropic. The proposed driving force for this reaction is the placement of additional units on the ends of the crystallisable blocks and their subsequent removal from the reaction zone by crystallisation, hence rendering these blocks inaccessible to further transesterification. Analyses showed that the melting points and crystallinity of the initial copolyesters increased during the reaction.[5] These results, supported by NMR data on sequence distribution,[6] confirmed that the overall blockiness had increased. Muhlebach et al[7] discuss the effect of transesterification on blending polyhydroxybenzoic acid (poly(HBA)) and polyhydroxynaphthoic acid (poly(HNA)) in the anisotropic melt. The samples were compression moulded at 450°C at pressures of up to 8kpsi.

The tendency for isotropic melts of two polyesters to undergo ester-interchange producing random copolyesters is well documented in the literature.[8] However in the

study by Muhlebach et al, due to the time constraints imposed by degradation of the homopolymers at the temperature studied, as well as the fact that processing is carried out in the anisotropic, as opposed to the isotropic state; the reaction gave rise to a number of possible products. These products could be in the form of a phase-separated system, a random copolymer, or a block copolymer, as a result of the moulding process. From the results obtained, the homopolyesters transesterified very rapidly leading to the formation of a random copolyester. The pressures applied during moulding did not have a significant effect on the transesterification process. There is speculation as to whether the rapid conversion to a copolyester, observed in under 90 seconds, may be accounted for by standard transesterification kinetics, or whether this behaviour is unique to the nematic melt; these hypotheses were considered. Several reports in the literature[9-12] have proposed that the kinetics of transesterification are governed by an Arrhenius process with an activation energy (Ea) in the range 130-160KJmol^{-1}. The kinetic parameters of transesterification in LCP were determined using SANS techniques and are discussed fully in Chapter 5. Arrhenius behaviour was assumed and an activation energy of 170KJmol^{-1} was calculated.[13] Kugler and co-workers[9] showed, also using SANS techniques, that polyethylene terephthalate (PET) and its deuterated equivalent, undergo transesterification during melting. The results of this process yield an activation energy of 152KJmol^{-1}. Muhlebach and co-workers[7] assumed Arrhenius behaviour for the transesterification reaction involving poly(HBA) and poly(HNA). From their results, they proposed that the homopolymers undergo transesterification rapidly in the isotropic melt to produce a random copolymer in a manner reported for PET in the anisotropic melt.[9]

Continued studies by Lenz and co-workers show that crystallisation induced reactions occur in the anisotropic melt for selected liquid crystalline copolyesters[14,15] as well as below and within the isotropic melt, demonstrated in earlier studies. These reports, which suggest a tendency to order in the nematic melt, appear to contradict the results published by Muhlebach et al where, in their study, random copolyesters were produced in the nematic melt. However, Lenz's results could be interpreted on the basis that the

liquid crystalline copolyesters studied, have a distribution of ordered units even though the sequence appears to be random. It is proposed that the longer strings of ordered units have the potential to exist as higher melting nuclei, above the anisotropic melt.[15] This process competes effectively with the tendency for randomisation at temperatures above the crystal-nematic transition.

Other relevant points worth noting in an attempt to find a solution as to why the transesterification processes considered here should lead to such vastly different structural forms, include the CIR process reported by Lenz which starts from a random copolymer and requires long time periods to develop any significant amount of ordering. In the disordering process reported by Muhlebach, neither of these conditions hold and an entropic process dominates to produce a random copolyester.

Both processes outlined above are feasible. The aim of the present study is to establish whether a crystallisation induced reorganisation process (CIR) can occur in random LCP to produce a more blocky structure or whether the copolyester simply continues to randomise further due to transesterification in the melt. From a detailed study of the literature, the CIR process is proposed to be the more likely reaction for LCP due to the structural nature of the polymer. The possibility of this reaction occurring has been investigated both in the solid state and in the anisotropic melt.

This chapter discusses Lenz's work in detail, the experimental procedure carried out on LCP in an attempt to promote the CIR reaction and finally, the results obtained. From these results the nature of the reaction was determined and a thorough quantitative analysis of the structure of the treated LCP sample was performed using a wide range of techniques.

6.2 *Lenz's Theory*

In his early studies,[16,17] Lenz proposed that the process termed crystallisation-induced reorganisation was based on the well-known procedure of forcing an equilibrium reaction to higher conversions through removal of one of the products. Via this reaction, a random copolyester is converted to a more ordered structure. Lenz proposed that the following requirements concerning the copolymer and the experimental conditions must be met for this process to succeed:[18]

a) the copolymer's repeating units must be capable of undergoing a reversible isomerisation, rearrangement or reorganisation reaction at a moderate rate, and at a temperature below the melting point of the copolymer or at least below that at which the crystalline phase will develop;

b) at the temperature of reaction, either only one of the repeat unit species can exist in a stable crystalline form or a new, more stable crystalline structure is created, composed of a different repeating unit from the original copolymer (for example that of an alternative copolymer structure);

c) the structural constraints, or accessibility of the units of the crystalline phase, will permit either only the amorphous phase to react, or alternatively, the repeating units of the expanding crystalline phase are such that they are far less reactive than the units in other phases; and

d) either a nucleus of the growing crystal phase is present at the start of the reaction or there is a chance of nucleation occurring spontaneously once the critical sequence length for crystallisation is achieved during reorganisation. Alternatively, the changes in composition due to isomerism produce a statistical copolymer containing sufficient crystallisable units. In the event that these requirements are reached, allowing the incorporation of new units into the crystalline phase, as they may become available, then crystallinity will increase and longer blocks of that unit will be created in the copolymer. Such a reaction will result in either a change in the repeating unit structure or a

reorganisation of the repeating units without a change in composition. In either case the final copolymer will possess a more ordered sequence distribution, than that of the initial random copolymer, of identical composition.

Later investigations indicated that reorganisation reactions were not only possible at elevated temperatures in the solid state but were also effective above the melting point in the anisotropic state, for several thermotropic liquid crystal polymers.[14,15]

6.3 *Crystallisation-Induced Reorganisation Reactions*

The reorganisation of semi-crystalline copolyesters via ester-interchange, from random to block copolymers at temperatures just below their initial melting points has been found to occur in a range of copolyesters. One of the earliest observations of this type of process may perhaps have been by Gilkey and Caldwell in 1959.[1] They observed the formation of both block copolyesters and homopolymers whilst carrying out a high temperature melt polymerisation reaction involving m- and p-acetoxybenzoic acid, in an attempt to prepare copolymers of these mixtures.

From the literature another possible example of such a process may be that reported by Schulken, Boy and Cox,[19] who observed the formation of unusually high melting point copolymers of cis/trans-1,4-cyclohexylenedimethylene terephthalate on heating the polymer in the presence of an active catalyst at temperatures both above and below the melt. The observed blockiness in the treated polymers was attributed to the difference in reactivity between the two monomers, however the possibility of a CIR process occurring under their reaction conditions should not be ruled out.

In 1969, Lenz and co-workers prepared linear poly(ester-acetals) for both the cis and trans forms and from a mixture of the dioxolanyl geometric isomers of the glycerol acetal of methyl azelaaldehydate.[16] The resultant polymers, synthesised using basic condensation catalysts, retained the structural and geometric form of the monomer, however when prepared using lead acetate as the catalyst, as well as polycondensation occurring, structural rearrangement took place yielding polymers of unusually high dioxolanyl isomer content as well as higher crystallinity. The isomerisation reaction occurred at elevated temperatures and also surprisingly, at room temperature after considerable time periods. The driving force for this process was thought to be crystallisation of the dioxolanyl units by a phenomenon termed a "crystallisation-induced reaction." Further work studied the effects of isomerisation of 5 and 6 membered acetal rings in copolyesters composed of such functional groups along the polymer backbone.[17] Reactions were carried out both in the melt and in the semi-crystalline

solid state. Isomerisation was observed to occur at temperatures just below the melt in an apparently opposite direction to that anticipated from the equilibration data for the acetal ring. The explanation behind this proposed anti-equilibrium process was based upon the assumption that the 5-membered ring units are removed continuously by crystallisation throughout the reaction. Hence the reaction is being driven in the direction governed solely by the ability of the unit to crystallise, regardless of the actual thermodynamic properties of the process.

Further detailed investigations were carried out on reversible isomerism reactions, after which Lenz and co-workers directed their studies towards other possible applications of the crystallisation-induced reaction in polymers. The principles of this process appeared to be applicable to a reversible reorganisation reaction; the ester-interchange of copolyesters.[5,6]

Lenz et al extended their primary qualitative investigations into a much more detailed examination of the effect of reaction variables on the progression of the reorganisation. The effects of variables such as copolymer composition, reaction temperature, reaction time, catalyst type and amount, molecular weight and degree of crystallinity were studied.[7] These investigations were directed towards determining which reaction parameters exerted a controlling influence on the extent of the CIR process. The results obtained proved that the chemical reaction rate is not the sole controlling factor. The reaction temperature appeared to have significant influence on the nature of the resulting polymers. At temperatures greater than 15°C below the melting point of the initial copolyesters, parameters which influence the chemical reaction rate primarily control the extent of reorganisation. Thus the correct choice of catalyst, catalyst concentration, molecular weight, time and temperature of reaction, in this temperature range, all exert major effects on the extent of the reaction. However at temperatures closer to the melting point, the chemical reaction rate did not appear to be the controlling factor, since samples of widely differing molecular weight using varying catalyst concentrations both with or without temperature programmed treatments, exhibited comparable extents of reorganisation. The results verify that as the melting point is approached, a change in the

rate-controlling mechanism occurs. A detailed investigation into the effects of altering the above-mentioned parameters, the associated structural changes and the proposed reasoning behind these changes is given in the literature.[20]

Further quantitative investigations based on the ester-interchange reorganisation of polyethylene terephthalate-co-2-methyl succinate were carried out using high resolution NMR, to determine the sequence length distributions.

Extended heating of these random copolyesters at temperatures below the melting point, resulted in vast changes in the polymers' crystalline melting points and solubilities. The resulting polyesters appeared to have properties almost identical to those of the block copolyesters suggesting that the heat treatment did indeed lead to a reorganisation and ordering of the initial copolymers. The effects of parameters such as copolymer composition, crystalline properties and polymer structure were related to the sequence length distribution determined by high resolution NMR.[15]

It appeared of interest to determine whether an effectively irreversible CIR reaction could occur above the melting point in the liquid crystal melt, as well as below it since there is some degree of mobility in the nematic melt and the likelihood of a crystallisation process occurring is feasible. Lenz et al[15] investigated the possibility of CIR reactions occurring in a series of terephthalate based copolymers in the liquid crystal state. The initial liquid crystal copolymers formed a mixture of soluble and insoluble products on completion of the reaction and the latter were believed to be multiblock crystalline units.

6.4 *Experimental*

6.4.1 *Sample Preparation*

a) *Purification*

The copolyester, LCP, as supplied by ICI plc, was purified by centrifugation as described in section (3.3.2(a)), followed by reprecipitation in an excess volume of methyl ethyl ketone to remove any residual catalyst. The polymer samples tested, were taken from the same polymerisation batch therefore all samples should have identical molecular weights. The polymer was recovered by vacuum filtration, and dried in vacuo at ambient temperatures for 48 hours. The product, a white "ribbon-like" material, was then finely ground in a mortar and pestle with dry ice to pass a 40 mesh sieve.

b) *Catalyst Re-impregnation*

The interchange catalyst selected for the CIR reaction was potassium acetate. This material seemed the obvious choice since it is the catalyst used in the industrial polymerisation of LCP. Furthermore, from Lenz's studies, acetates have proven to be very effective interchange catalysts for the CIR process.[15]

The catalyst was re-impregnated into the purified LCP using the following procedure. Potassium acetate (2.5g) was dissolved in freshly distilled methanol (25cm^3) and added to a solution of the finely powdered copolyester after which the sample was immersed in an ultrasonic bath to aid in the complete wetting of the particles and in gas removal. The dispersion mixture was then immersed in a water bath at a temperature a few degrees below the boiling point of the methanol (64.6°C) and a stream of nitrogen was passed over the surface of the dispersion. On complete evaporation of the solvent, the product was dried under vacuum at room temperature for 24 hours. The resultant polymer contained 50% w/w potassium acetate.

c) *CIR Process*

Approximately 0.2g of the reimpregnated LCP was placed in a Carius tube, fitted with a Young's tap and the contents were finely ground using a glass rod. The tube was then evacuated to a pressure of 0.3mm Hg, purged with purified nitrogen several times and finally evacuated again to 0.3mm Hg. The Carius tube was sealed using a natural gas/oxygen torch and placed inside a reinforced steel sheath which was then placed in a furnace at the selected reaction temperature and time (section (6.4.1(d)). On completion of the heating cycle, the tube was removed from the furnace, opened and the contents were again ground using a glass rod. The polymer was purified by soxhlet extraction with methanol for 12 hours after which the sample was dried in a vacuum oven at 40°C. Analysis by X-ray Fluorescence techniques (XRF) indicated that no traces of potassium remained in the LCP samples confirming that the catalyst had been removed successfully.

The above procedure was repeated a further 8 times for catalyst-containing LCP and 3 times for LCP containing no catalyst, for a range of selected reaction temperatures and times.

d) ***Reaction Conditions***

All polymer samples were annealed at the following temperatures: 250°C, 290°C and 300°C for times ranging between 12 and 72 hours. These conditions were selected both on the basis of Lenz's work and from knowledge of the thermal behaviour of LCP. A standard DSC thermogram (Figure (5.1)) illustrates the thermal transitions occurring in LCP. The onset of melting occurs at 270°C and hence the effect (if any) of the CIR process below the melt (250°C) is studied, both in the presence and absence of the interchange catalyst. From microscopy results (section (3.4.1)) LCP is observed to be in the melt phase at 280°C, and at 300°C to have reached its liquid crystalline phase. The

effects of the presence of the interchange catalyst were studied for the latter two reaction temperatures also. Transesterification, the process on which the CIR reaction is based, is known to occur very rapidly at 280°C and 300°C (<60s) (section (5.5.3)). The results showed that this process did not occur at 250°C however, in the present study, the fact that the reaction is carried out over a much longer time period than in the previous studies (ie. a maximum reaction time of 72 hours as opposed to 3 minutes), as well as the fact that an ester-interchange catalyst is used, must be taken into consideration. Such conditions could enable the transesterification process to proceed at this low temperature (250°C).

The quantity of catalyst used in the CIR process was selected again on the basis of Lenz's results.[20] In his studies the concentration of catalyst was varied between 2 and 20% w/w. In the majority of cases the variation of concentration did not have any significant effect on the extent of the CIR reaction, hence an arbitrary concentration of 5% w/w catalyst was impregnated into the LCP sample.

6.4.2 *Experimental Techniques Used in the Structural Analysis of Treated LCP Samples*

a) *Differential Scanning Calorimetry*

A brief study of the practical aspects of Differential Scanning Calorimetry (DSC) is given in section (3.5.1). In the present chapter this technique is used in conjunction with the succeeding analytical techniques to determine the phase behaviour and thermal transitions occurring in the reorganised LCP samples. The experiments were carried out using a Perkin-Elmer DSC7 connected to a TAC7/PC Thermal Analysis Controller. The DSC was calibrated using both indium and zinc standards. Corrections were made for baseline drift. An approximate mass of 3-8 mg polymer was sealed in an aluminium pan and a standard heating rate of 20°C min^{-1} was used for each run. In the majority of cases, samples were analysed over the temperature range: 90-450°C. Values of melting

temperatures and heats of fusion of the resultant polymers were determined directly using this technique. In general, the results for heats of fusion, were reproducible to ±1.5 Jg^{-1} for the samples studied.

b) *Polarising Optical Microscopy*

The theory and practice of Polarising Optical Microscopy are dealt with briefly in section (3.2.1) and (3.2.2). In the present study this technique is used purely on a qualitative basis to observe any initial and subsequent birefringence in the reorganised LCP samples as a function of temperature and to observe the temperature and nature of the melting transition, establishing whether or not a liquid crystalline phase exists and if so, the temperature range over which it remains stable. These properties as well as other parameters such as degradation are identified with the aid of the results obtained from DSC analysis.

A heating rate identical to that used in DSC analysis (20°C min^{-1}) was employed and the phase behaviour was observed over the temperature range: 25-450°C. The powdered samples were mounted between two glass cover slips and placed inside the hot-stage. Where a liquid crystalline phase existed, the birefringence was enhanced by shearing the sample, achieved by applying gentle pressure to the upper cover-slip. Optical micrographs illustrating the mesophases were obtained for each sample studied.

c) *Wide-Angle X-Ray Scattering*

The general theoretical and experimental aspects of Wide Angle X-Ray Scattering (WAXS) are discussed in section (4.2). In the present study WAXS techniques are used in the quantitative and qualitative analysis of the LCP samples. Quantitative investigations involve the calculation of the % crystallinity of the samples, both as a function of temperature and time, as the CIR reaction progresses. Evaluation of this parameter from the WAXS spectra, is achieved using the method described in section

(4.2.2). Qualitative studies are based on the comparison of the WAXS spectra obtained for untreated and annealed LCP samples (section (4.4.1)). From these spectra, changes in intensity and peak position are associated with changes in % crystallinity and structure in the polymer and in the case of peak position, its crystalline form.

Furthermore a comparison of the spectra obtained from the results of the CIR process, with those obtained for the homopolyester, poly HBA and the copolyester, poly HQ/IA (ie. the two possible block forms in which LCP could exist) will verify as to whether or not the CIR reaction has succeeded in converting the initially random LCP to a more ordered "blocky" structure.

The experiments were carried out using a Philips Scanning Diffractometer, a PW1730 Generator and PW1050/30 Goniometer with proportional detector, connected to a PW1710 CPV system. Scattered spectra were obtained using CuKα as the source radiation in transmission and a single nickel filter was used. The slit sizes selected were $^1/_6$", 4° and 4° where the former is the divergence slit and the latter two, the receiver slits, for the x-ray source. The LCP powdered samples were mounted into aluminium sample holders of 1mm thickness, between two sheets of polyimide film and placed inside the diffractometer sample holder. These samples were scanned over the range, 2θ = 4 - 40° with a step size of 0.1° and a count time of 6 seconds. The apparatus was calibrated using a $BaSO_4$ filled PET film. The resultant WAXS data were corrected and analysed, using the Philips Automative Powder Diffraction software package, APD1700. The percentage crystallinities of the treated samples were calculated with the aid of this software. The accuracy of the values obtained for % crystallinity are fairly low due to the difficulty in fitting the amorphous and crystalline curves, using the method described in section (4.2.2), in order to calculate this parameter. This fitting is carried out manually and the results obtained were found, in some cases, to vary up to ±12% for the same sample. However the calculated values provide a good idea of the changes in crystallinity as a function of reaction conditions and since these changes are, in most cases, fairly significant, these values are considered adequate for the present study.

6.5 *Results and Discussion*

6.5.1 *Differential Scanning Calorimetry Phase Behaviour and Determination of Heats and Temperatures of Transition*

a) *Introduction*

The thermal behaviour of "untreated" LCP is discussed in detail in sections (3.4.1) and (3.7.1). In brief, the untreated LCP sample is assumed to undergo crystallisation (T=160°C) immediately following the glass transition and becomes increasingly crystalline as a function of temperature. Multiple endothermic peaks, a common feature in random liquid crystalline polyesters, exist over the range: 270-335°C (Figure 6.1). Melting begins at 270°C and at around 300°C, a liquid crystalline phase is seen to develop. This phase remains stable to a temperature of 380°C, after which degradation ensues. This section compares the DSC thermograms for untreated LCP and LCP annealed over a range of selected temperatures in the presence of the ester-interchange catalyst, potassium acetate. The nature of the endothermic peaks will be referred to as: M ≡ normal or S ≡ singlet, throughout this work.

b) *CIR Reaction Below the Melt*

The thermograms obtained for untreated LCP and LCP samples annealed at 250°C, over a range of reaction times (t) are illustrated in Figure 6.2. The crystallisation exotherm observed in the initial heating run of untreated LCP, is no longer apparent for the annealed samples. There is a gradual change in the nature of the endothermic peaks observed. As reaction time increases, the number of peaks observed decreases until finally, at t = 72h, only one sharp endotherm is observed, typical of semi-crystalline materials. This observation, strengthened by the significant increase in the heats of

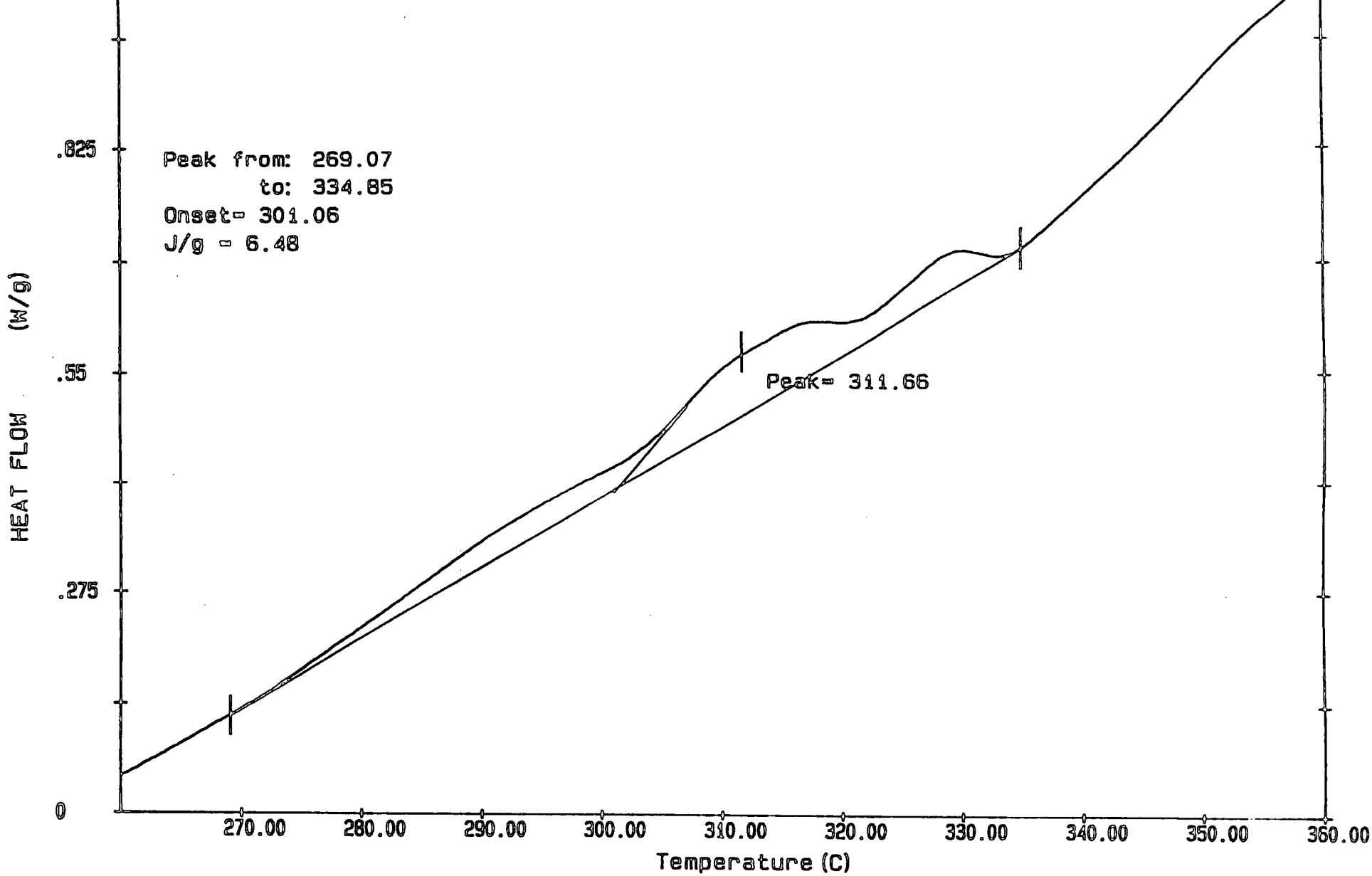
Peak from: 269.07
to: 334.85
Onset= 301.06
J/g = 6.48
Peak= 311.66
HEAT FLOW (W/g)
.825
.55
.275
0
270.00
280.00
290.00
300.00
310.00
320.00
330.00
340.00
350.00
360.00
Temperature (C)

Figure 6.1

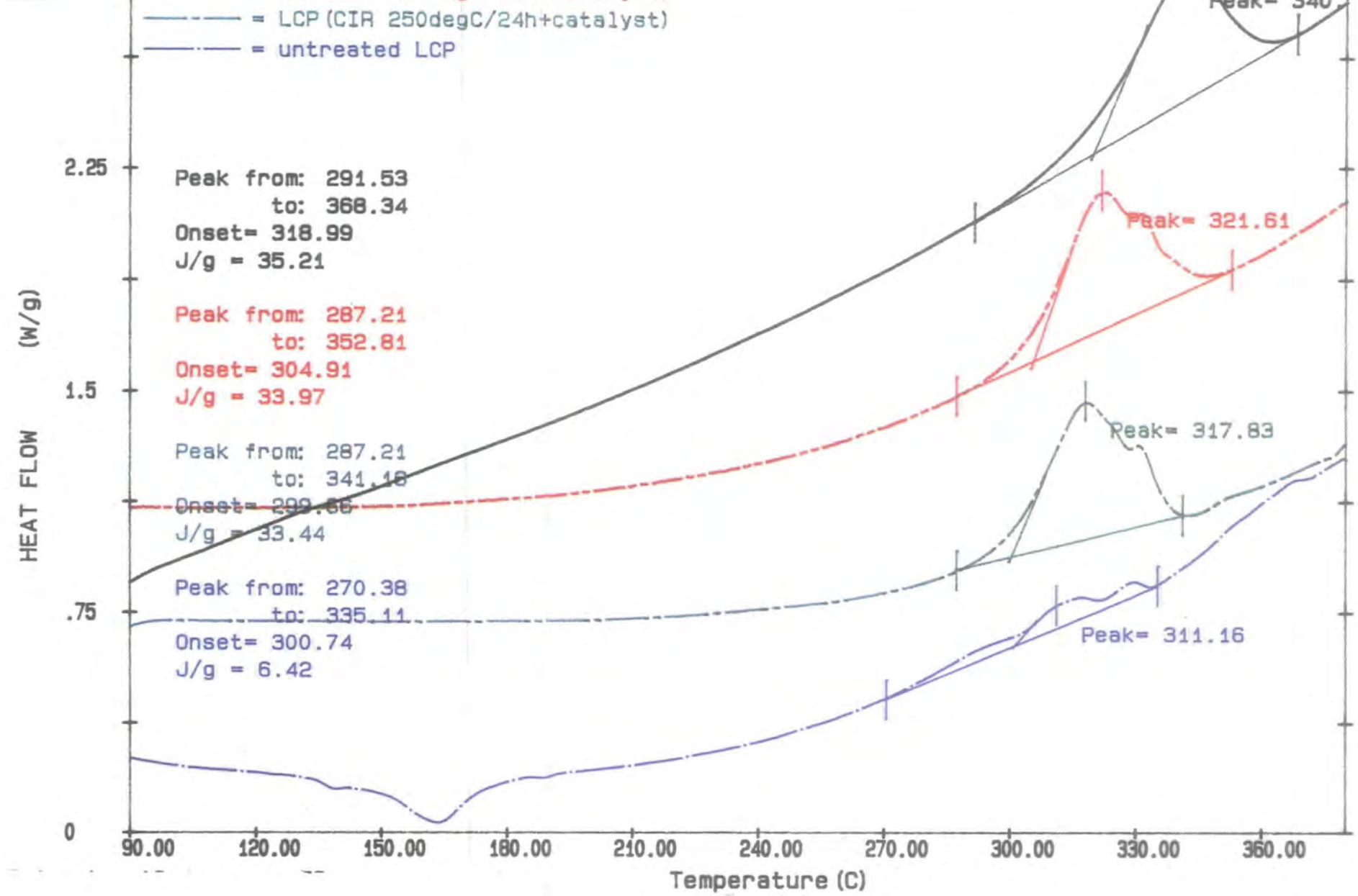
= LCP(CIR 250degC/24h+catalyst)
= untreated LCP
Peak= 340
Peak from: 291.53
to: 368.34
Onset= 318.99
J/g = 35.21
Peak from: 287.21
to: 352.81
Onset= 304.91
J/g = 33.97
Peak= 321.61
Peak from: 287.21
to: 341.18
Onset= 299.66
J/g = 33.44
Peak= 317.83
Peak from: 270.38
to: 335.11
Onset= 300.74
J/g = 6.42
Peak= 311.16
HEAT FLOW (W/g)
2.25
1.5
.75
0
90.00
120.00
150.00
180.00
210.00
240.00
270.00
300.00
330.00
360.00
Temperature (C)

Figure 6.2

fusion as a function of t and the increase in temperature of transition, suggests that LCP is becoming increasingly ordered with annealing time in the solid state. The thermal data for the LCP samples is given in Table 6.1.

Sample (reaction time)	$\frac{T_m}{°C}$	$\frac{\Delta H_m}{Jg^{-1}}$	$\frac{\Delta T_m}{°C}$	Nature of peak
LCP(0)	301	6	270-335	M
LCP(24)	300	33	287-341	M
LCP(48)	305	34	287-352	M
LCP(72)	319	35	292-368	S

Table 6.1 CIR reaction : 250°C (interchange catalyst present)

c) *CIR Reaction in the Melt*

DSC thermograms obtained for LCP samples annealed over the range 287-290°C in the presence of the ester-interchange catalyst are given in Figure 6.3. It was not intended that the reaction temperature should vary over the small range, but the furnaces used in the experiments proved difficult to control, however the accurate thermocouple temperature was recorded. There appears to be a controversy in the results. For the sample annealed at 287°C for t = 24h, a sharp single endotherm is observed. The values of heat and temperature of fusion have increased significantly, suggesting that LCP continues to order in the melt under these conditions. However for LCP samples annealed at 290°C for longer reaction times, the melting temperature increases with reaction time, as expected, but the heat of fusion appears to decrease with increasing reaction time. The latter observation contradicts the proposed increase in ordering of LCP as a function of reaction temperature and time. It is proposed that a limiting temperature is reached (ie. T = 290°C) where there is insufficient ordering present in the LCP samples to permit the development of crystalline regions due to melting. This

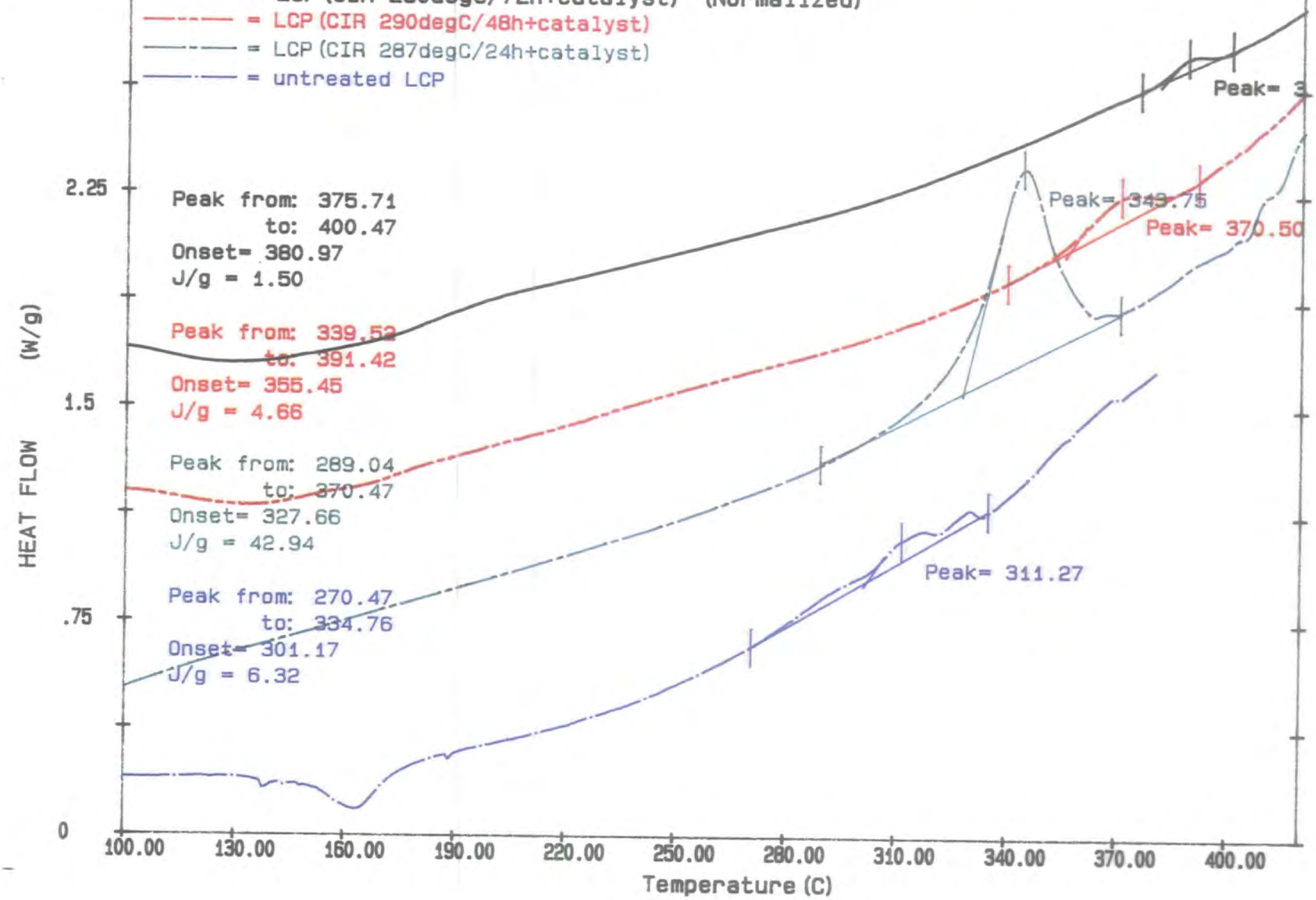
= LCP (CIR 290degC/48h+catalyst)
= LCP (CIR 287degC/24h+catalyst)
= untreated LCP
Peak= 3
Peak from: 375.71
to: 400.47
Onset= 380.97
J/g = 1.50
Peak from: 339.52
to: 391.42
Onset= 355.45
J/g = 4.66
Peak from: 289.04
to: 370.47
Onset= 327.66
J/g = 42.94
Peak from: 270.47
to: 334.76
Onset= 301.17
J/g = 6.32
Peak= 349.75
Peak= 370.50
Peak= 311.27
HEAT FLOW (W/g)
2.25
1.5
.75
0
100.00
130.00
160.00
190.00
220.00
250.00
280.00
310.00
340.00
370.00
400.00
Temperature (C)

Figure 6.3

proposal would explain the decrease in heats of fusion as a function of reaction time, however it does not explain why, if the samples are indeed randomising at this temperature, that the apparent melting point should continue to shift to higher temperatures as t increases; nor does it explain why only single melting peaks are observed, as opposed to the multiple peaks characteristic of random polymers. The thermal data for the LCP samples is given in Table 6.2.

Sample (reaction time)	Reaction Temperature / °C	T_m / °C	ΔH_m / Jg^{-1}	ΔT_m / °C	Nature of peak
LCP(0)	-	301	6	270-335	M
LCP(24)	287	328	43	289-370	S
LCP(48)	290	356	5	340-391	S
LCP(72)	290	381	2	376-400	S

Table 6.2 CIR reaction: 290°C (interchange catalyst present)

The behaviour of LCP under these conditions remains unclear, due to the slight variation in reaction temperature, which may or may not be affecting the results. It is also feasible that annealing time is playing the critical role in the polymer's behaviour under these conditions. Further studies are required in order to qualify these results.

d) ***CIR Reaction in the Liquid Crystalline Phase***

The thermogram obtained for untreated LCP is compared to those obtained for LCP which has undergone the CIR reaction (T = 300°C) for reaction times t = 24, 60 and 70h in the presence of the ester-interchange catalyst (Figure 6.4). From microscopy results (section 3.4.1), untreated LCP evidently exists in the nematic melt at this reaction temperature. Again, no crystallisation exotherm is present for the annealed samples.

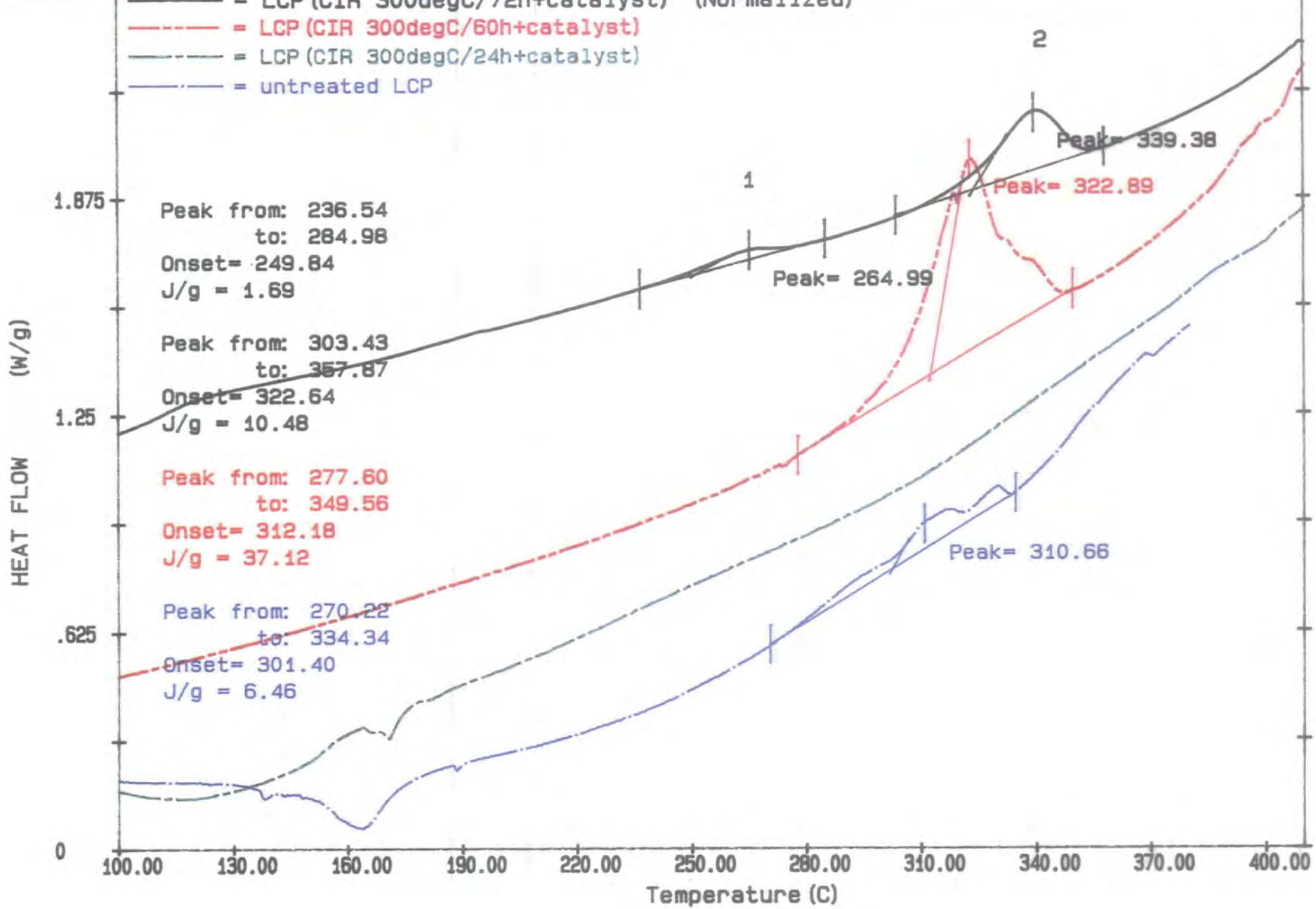
= LCP(CIR 300degC/72h+catalyst) (Normalized)
= LCP(CIR 300degC/60h+catalyst)
= LCP(CIR 300degC/24h+catalyst)
= untreated LCP
1
2
Peak= 339.38
Peak= 322.89
Peak= 264.99
Peak= 310.66
Peak from: 236.54
to: 284.98
Onset= 249.84
J/g = 1.69
Peak from: 303.43
to: 357.87
Onset= 322.64
J/g = 10.48
Peak from: 277.60
to: 349.56
Onset= 312.18
J/g = 37.12
Peak from: 270.22
to: 334.34
Onset= 301.40
J/g = 6.46
HEAT FLOW (W/g)
1.875
1.25
.625
0
100.00
130.00
160.00
190.00
220.00
250.00
280.00
310.00
340.00
370.00
400.00
Temperature (C)

Figure 6.4

This result is in agreement with the data obtained for the CIR reactions carried out at 250°C and 290°C. No transitions were observed during the DSC heating run for LCP annealed at t = 24h. The sample was in the form of a black powder after the reaction suggesting that the material had already undergone degradation. A multiple endotherm exists at elevated temperatures for LCP annealed at t = 60h and a single endotherm exists at an even higher temperature for t = 72h. A small, single endotherm is also evident for the latter sample, occurring over the range: 237-285°C. The presence of this peak cannot be attributed to melting as it occurs at a temperature lower than the onset of melting of untreated LCP. The thermal data for the LCP samples studied, is given in Table 6.3.

Sample (reaction time)	T_{m1} °C	T_{m2} °C	ΔH_{m1} Jg^{-1}	ΔH_{m2} Jg^{-1}	ΔT_{m1} °C	ΔT_{m2} °C	Nature of peak
LCP(0)	-	301	-	7	-	270-334	M
LCP(24)	-	-	-	-	-	-	-
LCP(48)	-	312	-	37	-	278-350	S
LCP(72)	250	322	2	11	237-285	303-358	S

Table 6.3 CIR reaction: 300°C (interchange catalyst present)

In general, the melting temperatures shift to higher values with increasing reaction time. No trends are apparent for the values of heats of fusion as a function of reaction time. Thus, from DSC analysis alone, no further conclusions can be drawn on the extent of ordering as the reaction progresses in the nematic melt. Further work is required in order to conclude on the polymer's behaviour under these conditions.

6.5.2 *POM: A Qualitative Study of the Phase Behaviour*

a) Introduction

The thermal behaviour of LCP powder, as determined by polarising optical microscopy

is discussed in detail in Chapter 3. In summary, LCP is almost completely amorphous at ambient temperatures however the birefringence, and thus the crystallinity increases progressively after the Tg (≈130°C) and at 270°C the material begins to flow due to melting consequently the field of view darkens momentarily. A liquid crystalline phase develops between 300-330°C (Figure 6.5) and the sample remains strongly birefringent until the material begins to degrade at 380°C.

b) CIR Reaction Below the Melt

The LCP samples were annealed under the same conditions as those specified in section (6.5.1(b)). At ambient temperatures the treated samples appear slightly more crystalline than untreated LCP. Crystallinity increases as a function of temperature and at T ≥180°C spherulites are visible (Figure 6.6) which increase in quantity and size until melting begins at 280°C. A schlieren pattern, characteristic of a nematic phase, develops between 350-355°C (Figures 6.7-6.9) and degradation begins at an approximate temperature of 400°C for each sample. The latter process is identified by the appearance of large voids in the sample.

c) CIR Reaction in the Melt

For LCP treated at 287°C (t = 24h) a significant amount of crystallinity is present in the sample when viewed under crossed-polars at ambient temperatures (Figure 6.10). Crystallinity increases as a function of temperature until melting begins at 380°C; a temperature significantly higher than that observed for untreated LCP. Degradation begins around 400°C. For LCP samples treated at extended reaction times (t = 48 and 72h) at 290°C, the levels of crystallinity are extremely low at ambient temperatures. Again crystallinity increases as a function of temperature. These samples melt at high temperatures (380-390°C) after which degradation occurs rapidly. A nematic phase is not observed for either of the samples (Figures 6.11).

FIGURE 6.5 Untreated LCP

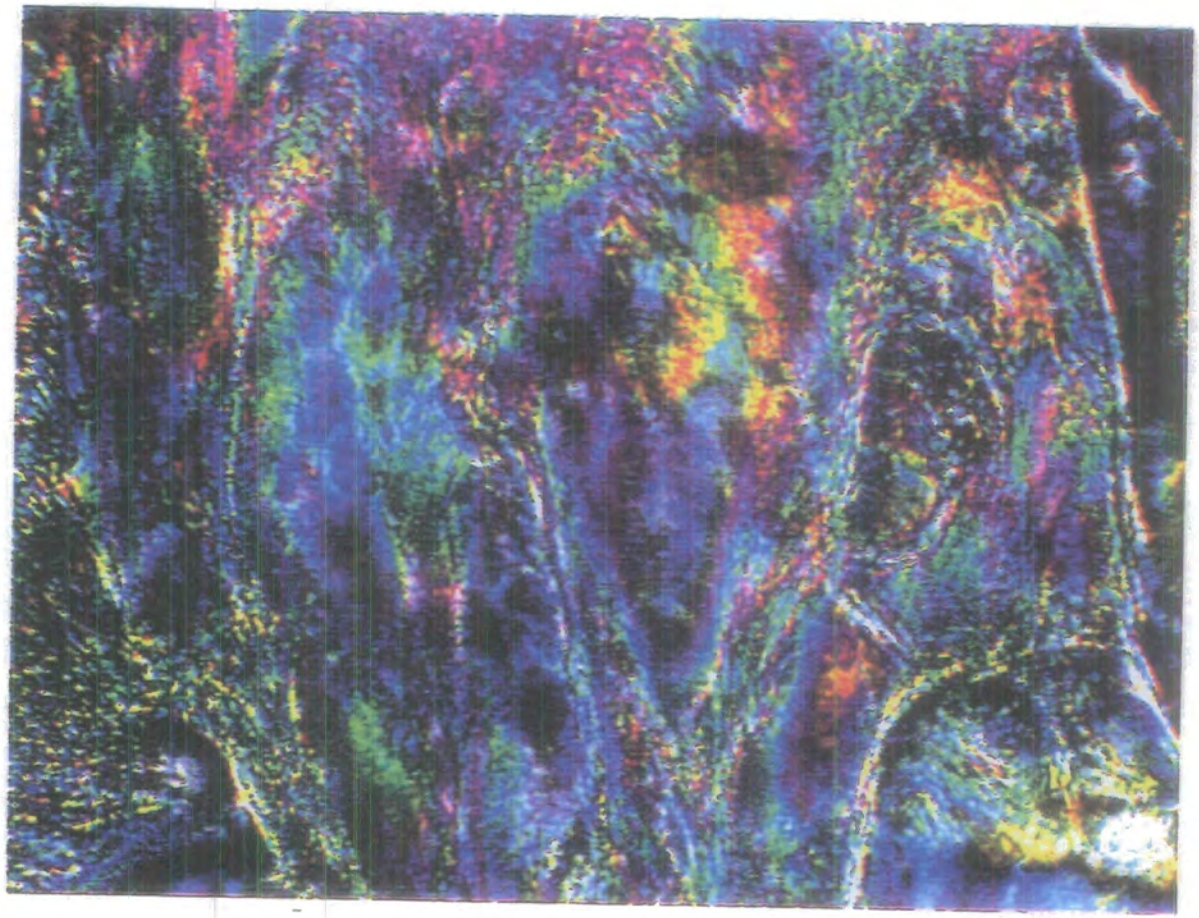

(x 400) crossed polars

L.C. PHASE @330degC

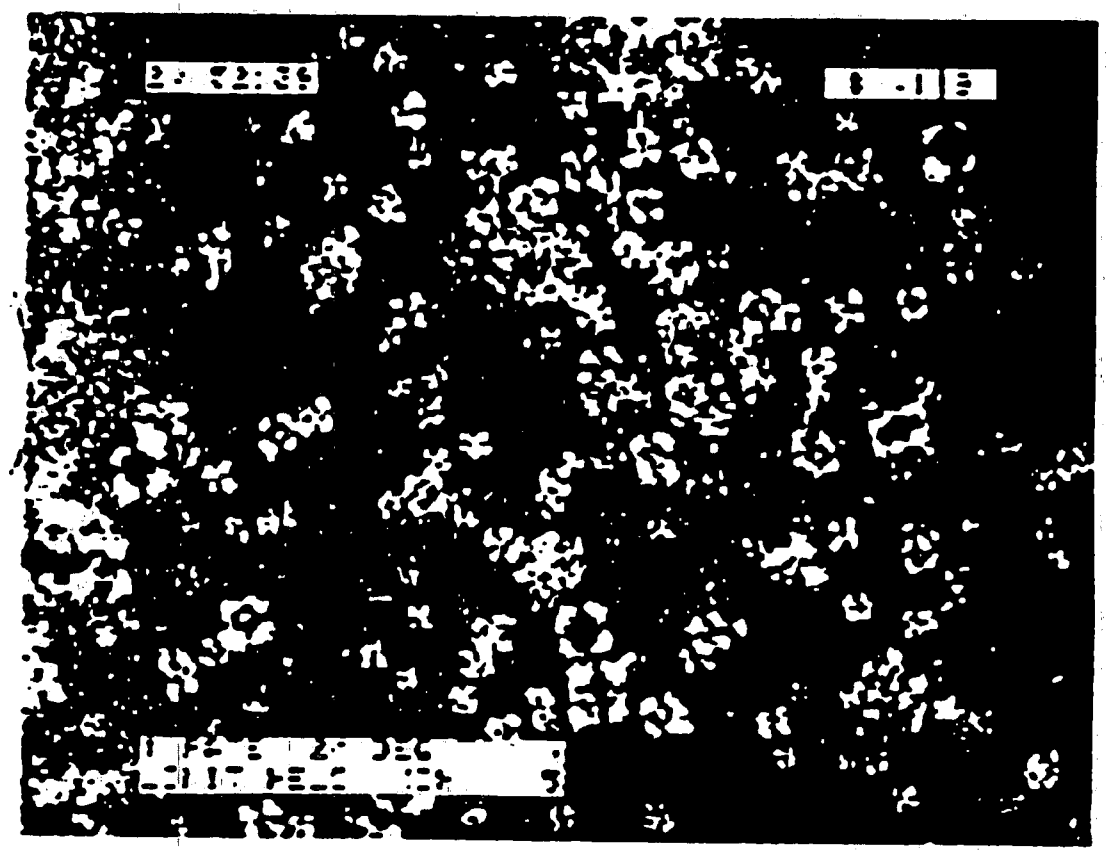

Figure 6.6 Spherulitic development in LCP @180 degC (x 400) crossed polars

FIGURE 6.7 LCP (CIR 250degC/24h) + catalyst

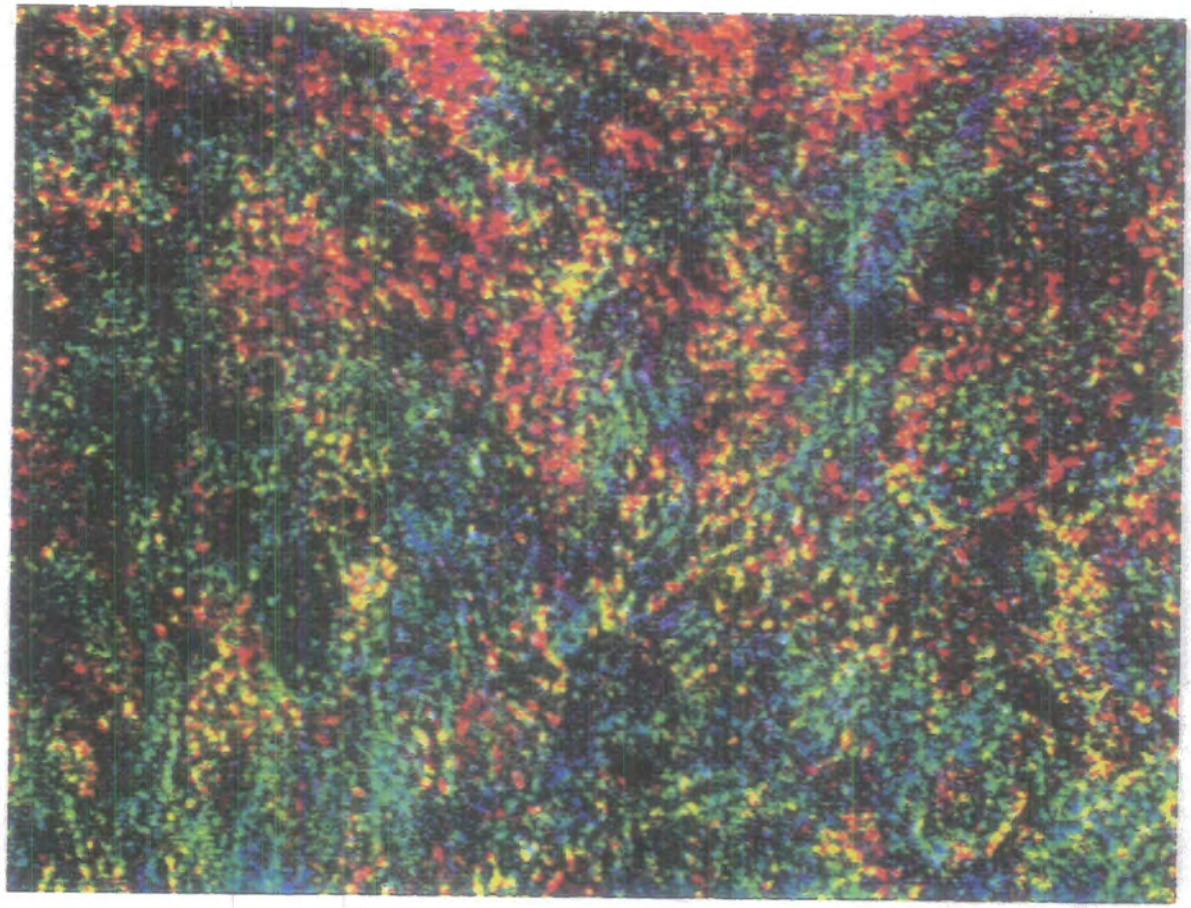

(x 400) crossed polars

L.C. PHASE @350degC

FIGURE 6.8 LCP (CIR 250degC/48h) + catalyst

(x 400) crossed polars

L.C. phase @355degC

FIGURE 6.9 LCP (CIR 250degC/72h) + catalyst

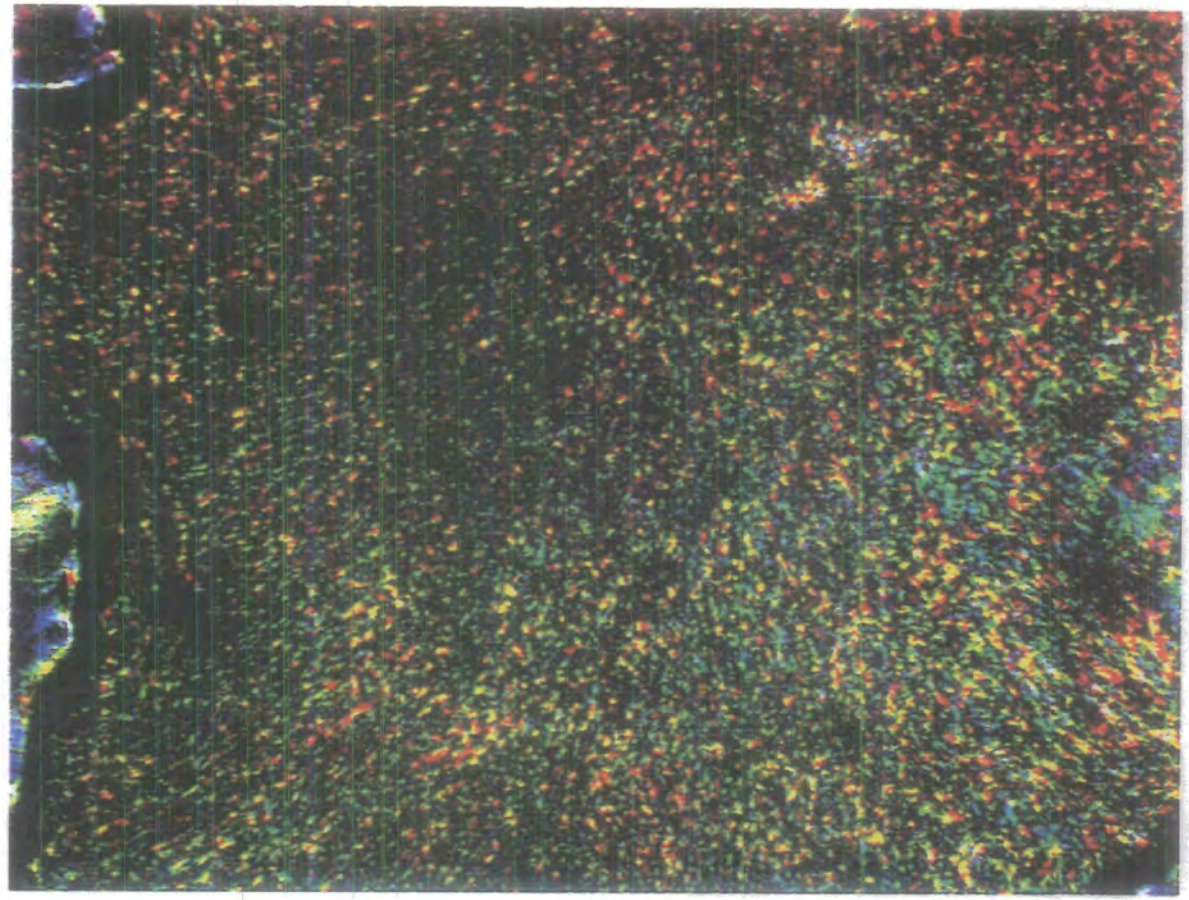

(x 400) crossed polars

L.C. phase @355degC

FIGURE 6.10 LCP (CIR 287degC/24h) + catalyst

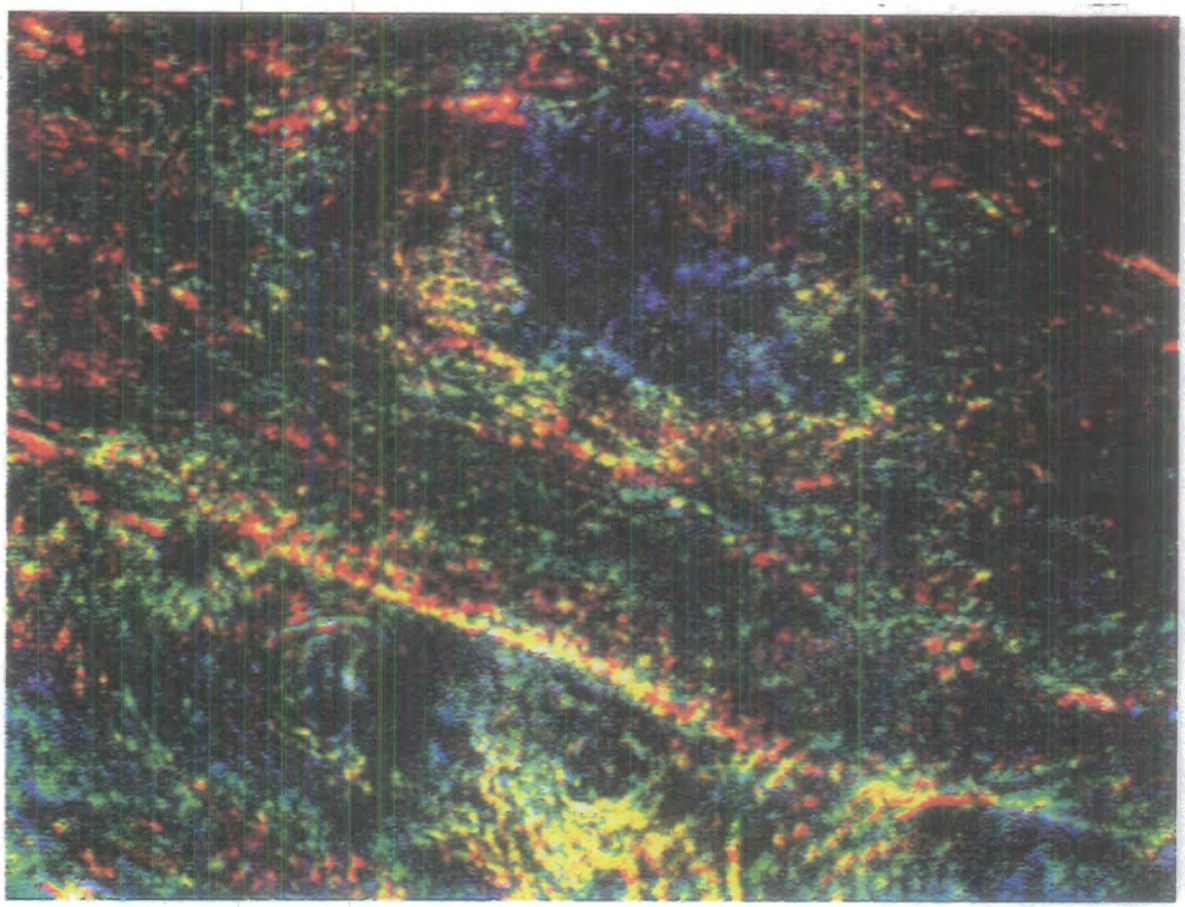

(x 400) crossed polars

L.C. phase @380degC

FIGURE 6.11 LCP (CIR 290degC/72h) + catalyst

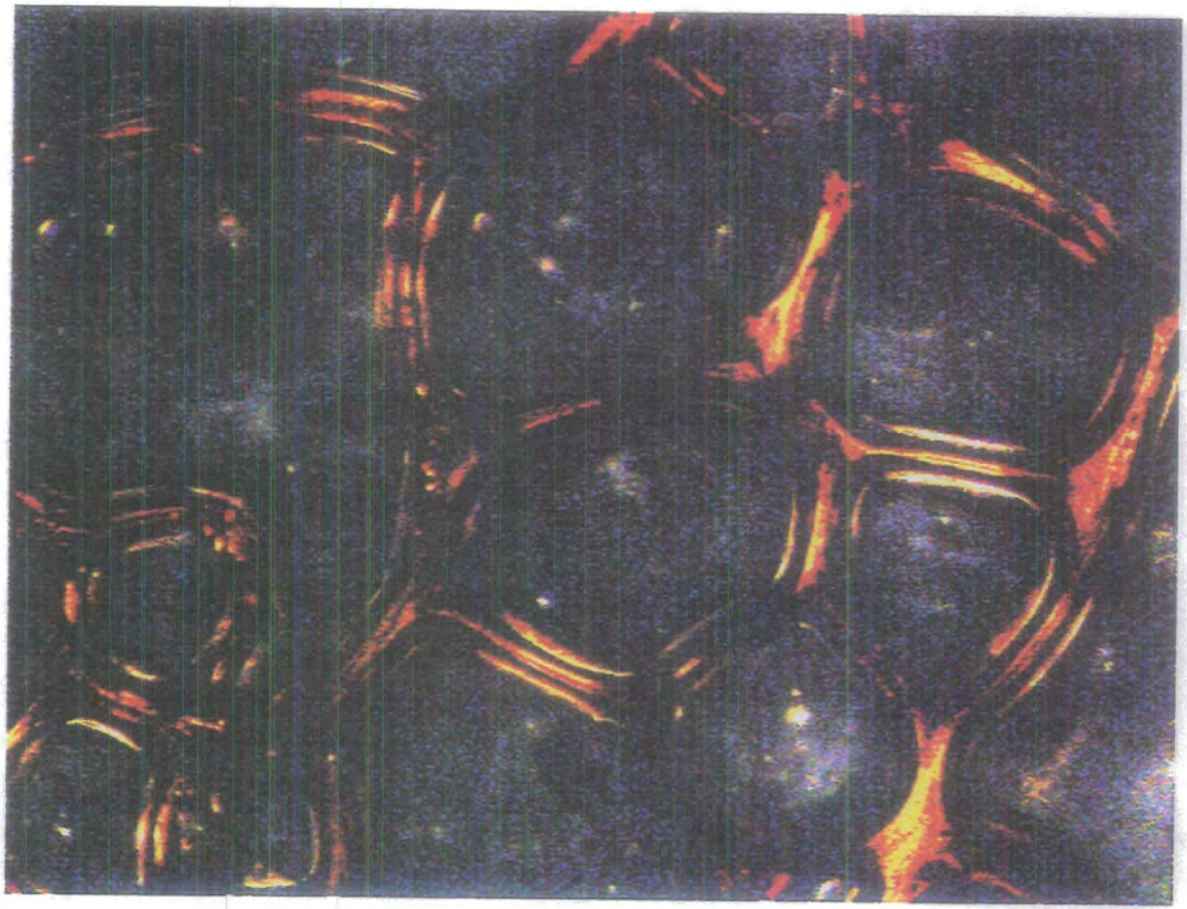

(x 100) crossed polars

No L.C. phase. Degrades on melting @390degC

In summary, the optical behaviour of the polymer samples annealed in the melt, does not appear to follow any trend as a function of reaction temperature. The fluctuation in reaction temperature is not considered to be accountable for the observed significant change in behaviour, as the temperature range is well within the limits of the oven temperature range.

d) CIR Reaction in the Liquid Crystalline Phase

The LCP samples were annealed as described in section (6.5.1(a)). At ambient temperature, the sample treated for t = 24h, appears completely dark between crossed-polars. No optical transitions occur whatsoever over the temperature range studied (25-500°C) (Figure 6.12). It would appear that degradation occurred during the CIR reaction. For LCP annealed for t = 60h, the slight degree of crystallinity observed at ambient temperatures increases as a function of temperature. Melting occurs around 360°C and at 370°C a nematic phase develops (Figure 6.13). The mesophase remains stable until degradation occurs at 400°C. For LCP annealed for t = 72h, a faint translucent orange colour is observed at ambient temperatures (Figure 6.14). The colour intensity increases and melting begins at 270°C. Degradation begins at 360°C. The initial presence of the birefringent intensity, characteristic of the mesophase, could be attributed to the liquid crystaline phase being "frozen in" during the CIR reaction and remaining in this form after cooling. The thermal behaviour of this sample remains unclear. No optical trends exist as a function of reaction time for the three samples studied.

6.5.3 *WAXS: Qualitative Structural Analysis and Determination of % Crystallinity*

a) Introduction

X-ray data was obtained for the LCP samples which have undergone the CIR reaction

In summary, the optical behaviour of the polymer samples annealed in the melt, does not appear to follow any trend as a function of reaction temperature. The fluctuation in reaction temperature is not considered to be accountable for the observed significant change in behaviour, as the temperature range is well within the limits of the oven temperature range.

d) CIR Reaction in the Liquid Crystalline Phase

The LCP samples were annealed as described in section (6.5.1(a)). At ambient temperatures, the sample treated for t = 24h, appears completely dark between crossed-polars. No optical transitions occur whatsoever over the temperature range studied (25-500°C) (Figure 6.12). It would appear that degradation occurred during the CIR reaction. For LCP annealed for t = 60h, the slight degree of crystallinity observed at ambient temperatures increases as a function of temperature. Melting occurs around 360°C and at 370°C a nematic phase develops (Figure 6.13). The mesophase remains stable until degradation occurs at 400°C. For LCP annealed for t = 72h, a faint translucent orange colour is observed at ambient temperatures (Figure 6.14). The colour intensity increases and melting begins at 270°C. Degradation begins at 360°C. The initial presence of the birefringent intensity, characteristic of the mesophase, could be attributed to the liquid crystalline phase being "frozen in" during the CIR reaction and remaining in this form after cooling. The thermal behaviour of this sample remains unclear. No optical trends exist as a function of reaction time for the three samples studied.

6.5.3 *WAXS: Qualitative Structural Analysis and Determination of % Crystallinity*

a) Introduction

X-ray data was obtained for the LCP samples which have undergone the CIR reaction

FIGURE 6.12 LCP (CIR 300degC/24h) + catalyst

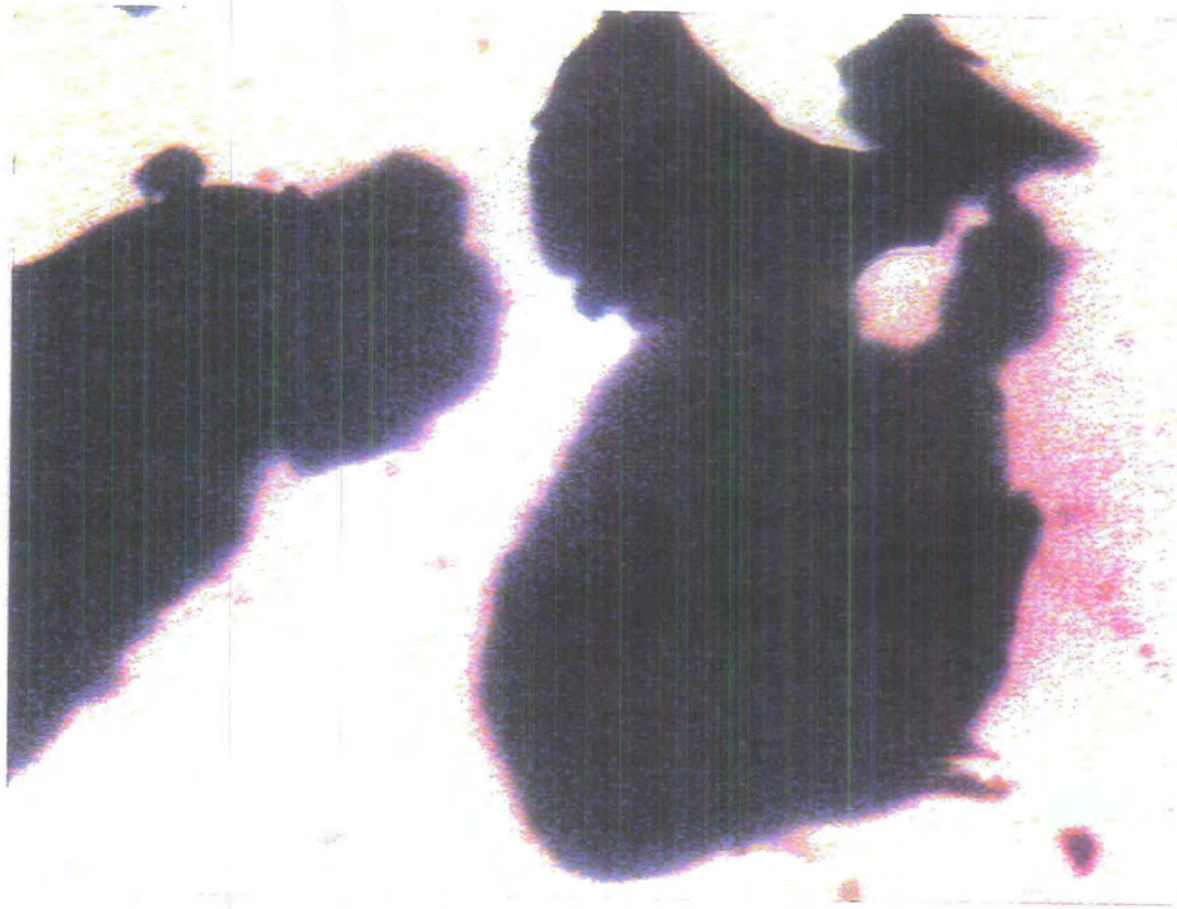

(x 100)

No optical transitions observed (25-500degC)

FIGURE 6.13 LCP (CIR 300degC/60h) + catalyst

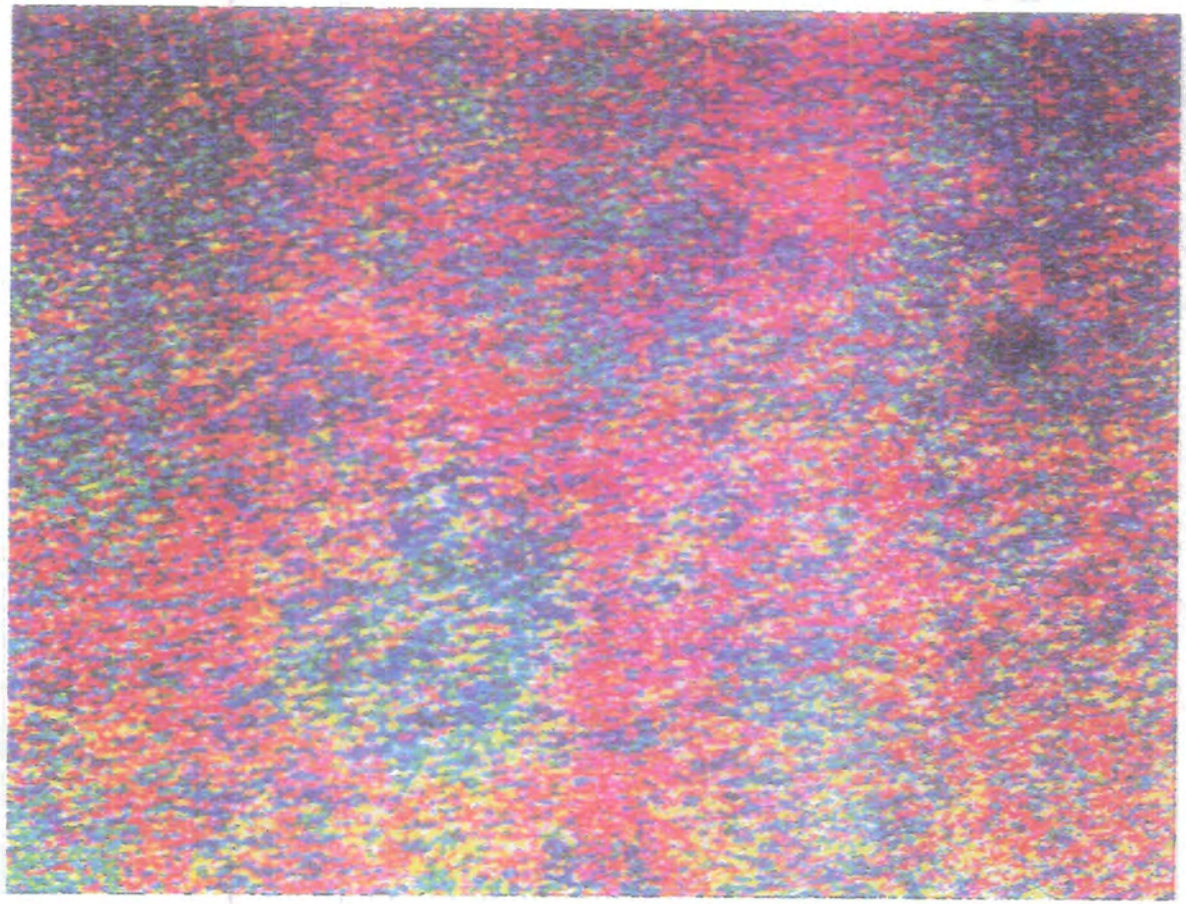

(x 400) crossed polars

L.C. phase @370degC

FIGURE 6.14 LCP (CIR 300degC/72h) + catalyst

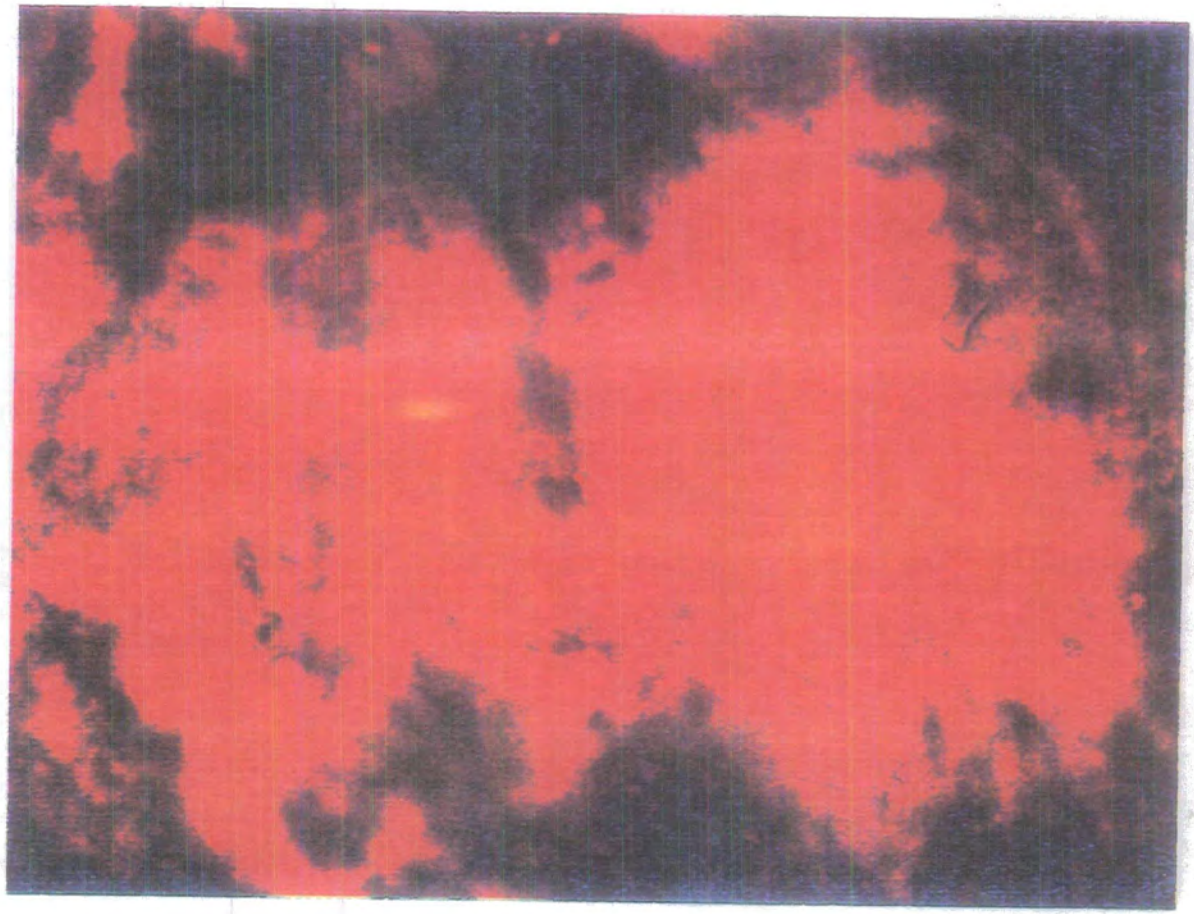

(x 100) crossed polars

Melt phase @270degC

and compared to the x-ray diffractograms obtained for untreated LCP and LCP samples annealed for very short time periods (Chapter 4).

This section covers two main areas:

i) a qualitative study of the x-ray diffractograms in order to conclude on any structural rearrangements resulting from the CIR reaction

ii) calculation of the percentage crystallinities for all LCP samples in order to provide a clear idea of the degree of ordering induced as a result of thermal treatment.

The diffractogram obtained for untreated LCP powder, illustrated in Figure (6.15) exhibits a halo characteristic of an amorphous material. The secondary curve represents LCP powder, annealed for several minutes in the melt phase. Again, an amorphous halo is observed, however the maxima exists at a higher angle than observed for untreated LCP powder. This shift is attributed to thermal effects. A computer simulation of the predicted crystalline pattern of LCP (Chapter 4, reference (27)) is given in Figure 6.16. The peak positions coincide with those exhibited for LCP films annealed at selected temperatures at t = 5 minutes (Figure 6.17). The peaks observed are "superimposed" onto a diffuse halo, typical of a slightly crystalline material and their relative intensities develop and increase as a function of t. The percentage crystallinities of the LCP samples were calculated as described in Chapter 4, whereby use of the computer software enables the amorphous halo, representative of the polymer in the melt phase to be fitted to the semicrystalline diffractogram of the annealed sample. Figure 6.18 illustrates the red curve representative of the intensity due to the crystalline regions only, obtained from subtracting the scattering intensity of the amorphous polymer from that of the semi-crystalline polymer. The percentage crystallinity is obtained from this data using equation (6.1)

$$x_{cr} = \frac{a_{cr}}{a_{am} + a_{cr}} \times 100 \qquad (6.1)$$

where a_{cr} represents the area under the subtracted curve and a_{cr} represents the area under the amorphous curve.

The calculated values of x_{cr} for the samples illustrated in Figure 6.17 are listed in Table

FIGURE 6.15 Amorphous LCP samples

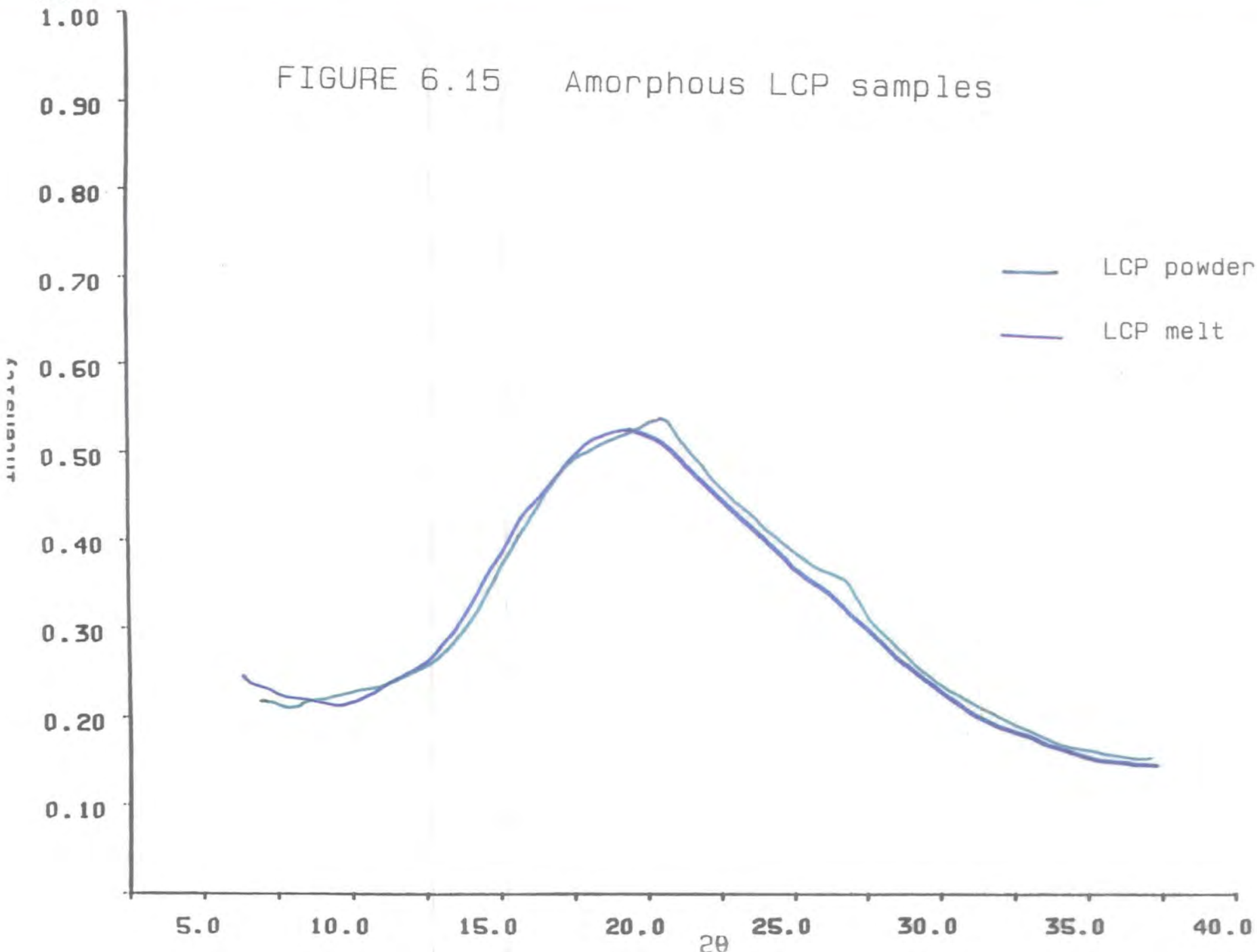

FIGURE 6.16 Simulation of crystalline LCP

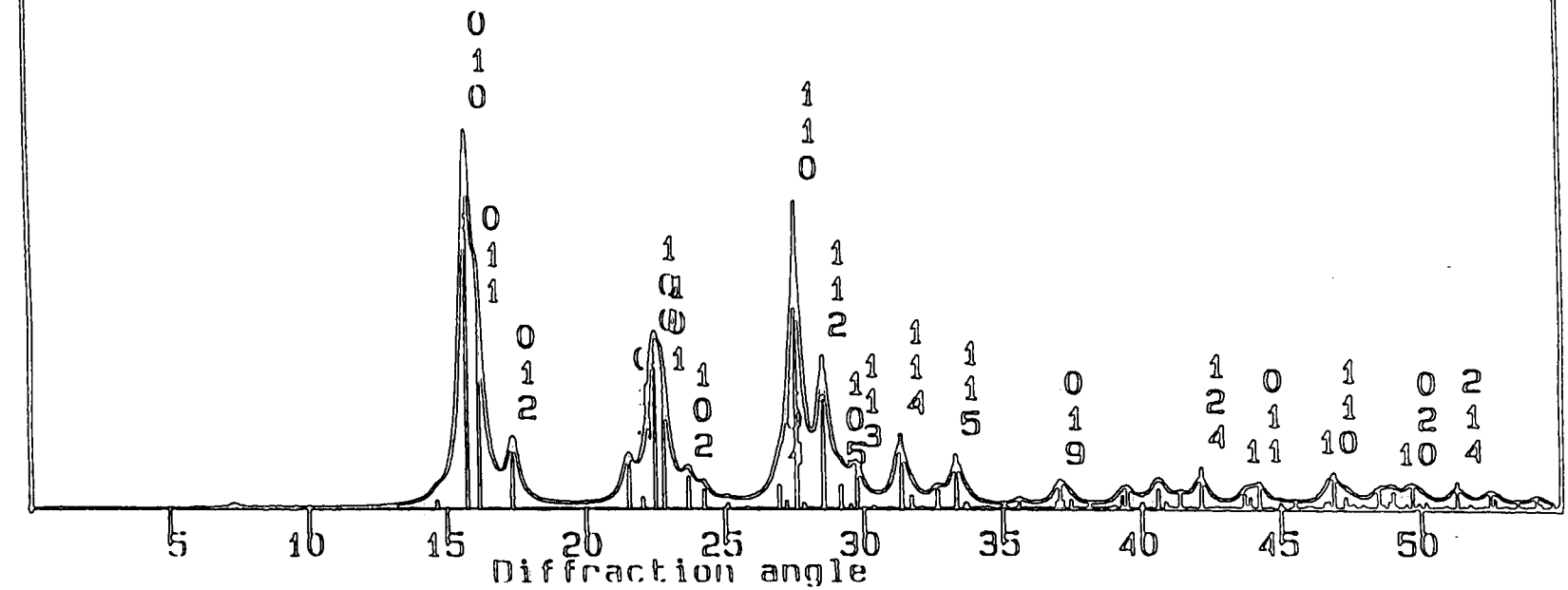

FIGURE 6.17 Annealed LCP films

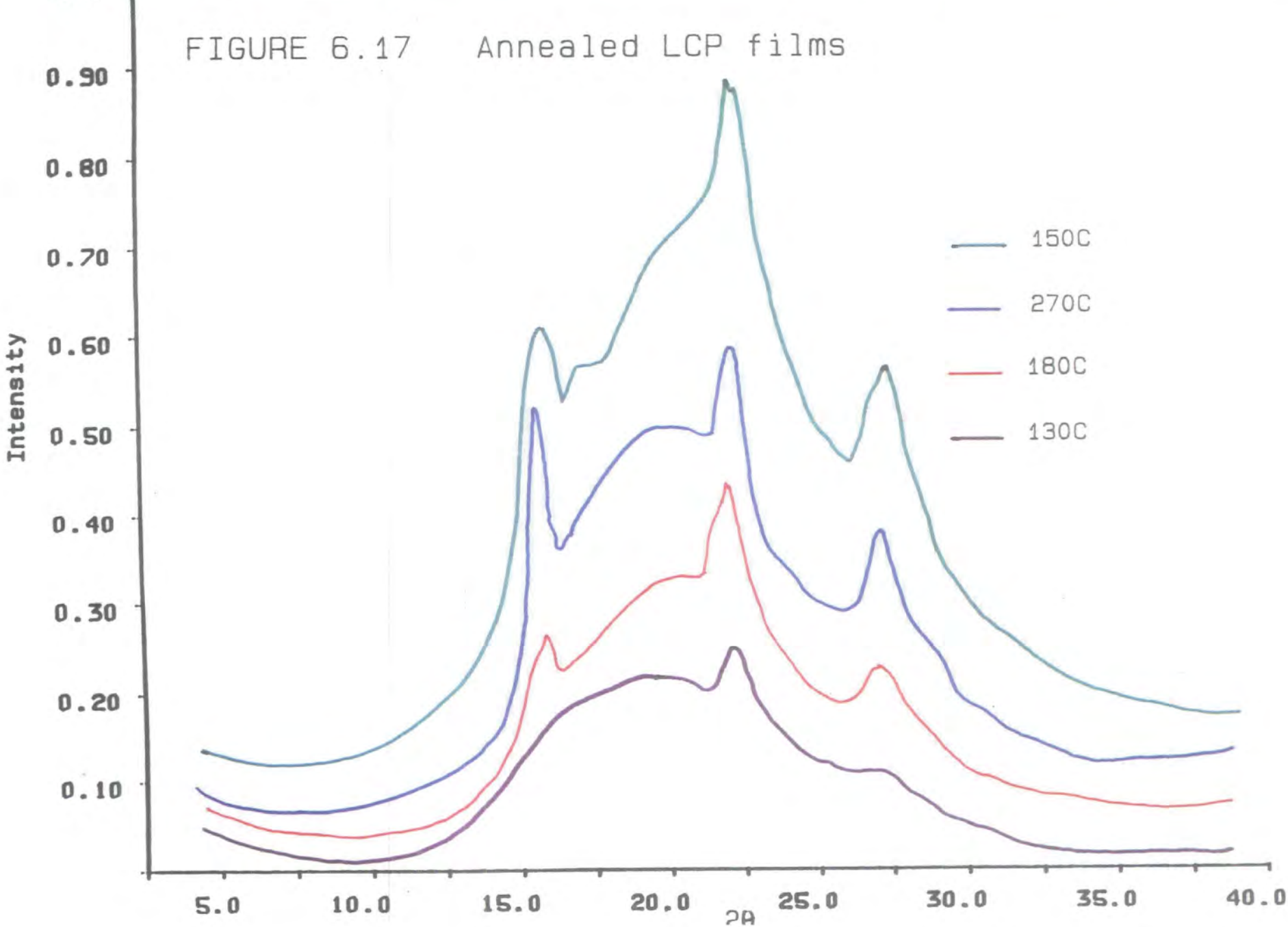

FIGURE 6.18 LCP Film (annealed@270degC)

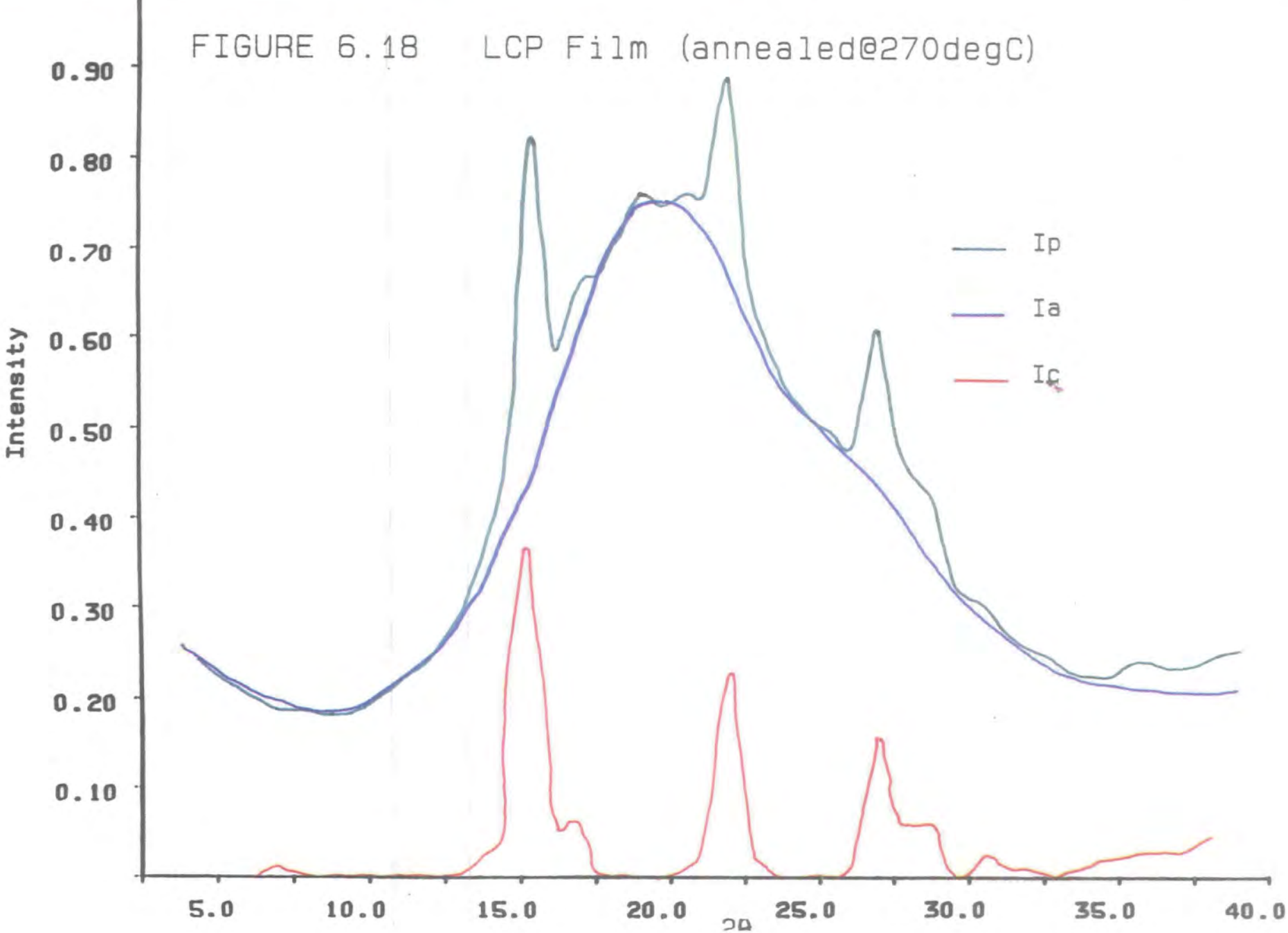

(6.4). The values increase with increasing annealing temperature, as expected.

Sample	T / °C	x_{cr} / %
LCP_{POWDER}	0	0
LCP_{FILM}	130	7
LCP_{FILM}	150	14
LCP_{FILM}	180	14
LCP_{FILM}	270	18

Table 6.4 LCP samples annealed for t = 5 minutes

b) CIR Reaction Below the Melt

The diffractometer scans for LCP samples annealed as described in section (6.5.2(b)) are given in Figure (6.19). For t = 24h, the 3 characteristic Bragg peaks observed for partially ordered LCP are present, however a further series of peaks have begun to develop for LCP annealed for t = 48h indicating that the sample is undergoing structural rearrangement. The characteristic peaks are still present, however they have increased in sharpness and intensity. For LCP annealed for t = 72h the diffraction pattern has changed dramatically. Again the characteristic peaks have increased further in sharpness and intensity however a significant number of new peaks have developed, indicating a change in ordering. Figure (6.20) illustrates the curves for LCP treated for t = 0, 24, 48 and 72h. From these observations, it is apparent that the degree of ordering increases significantly and that structural rearrangement is taking place with increasing annealing time. The calculated values of x_{cr} are given in Table (6.5). These values are significantly higher than the values listed in Table (6.4) for the annealed LCP films.

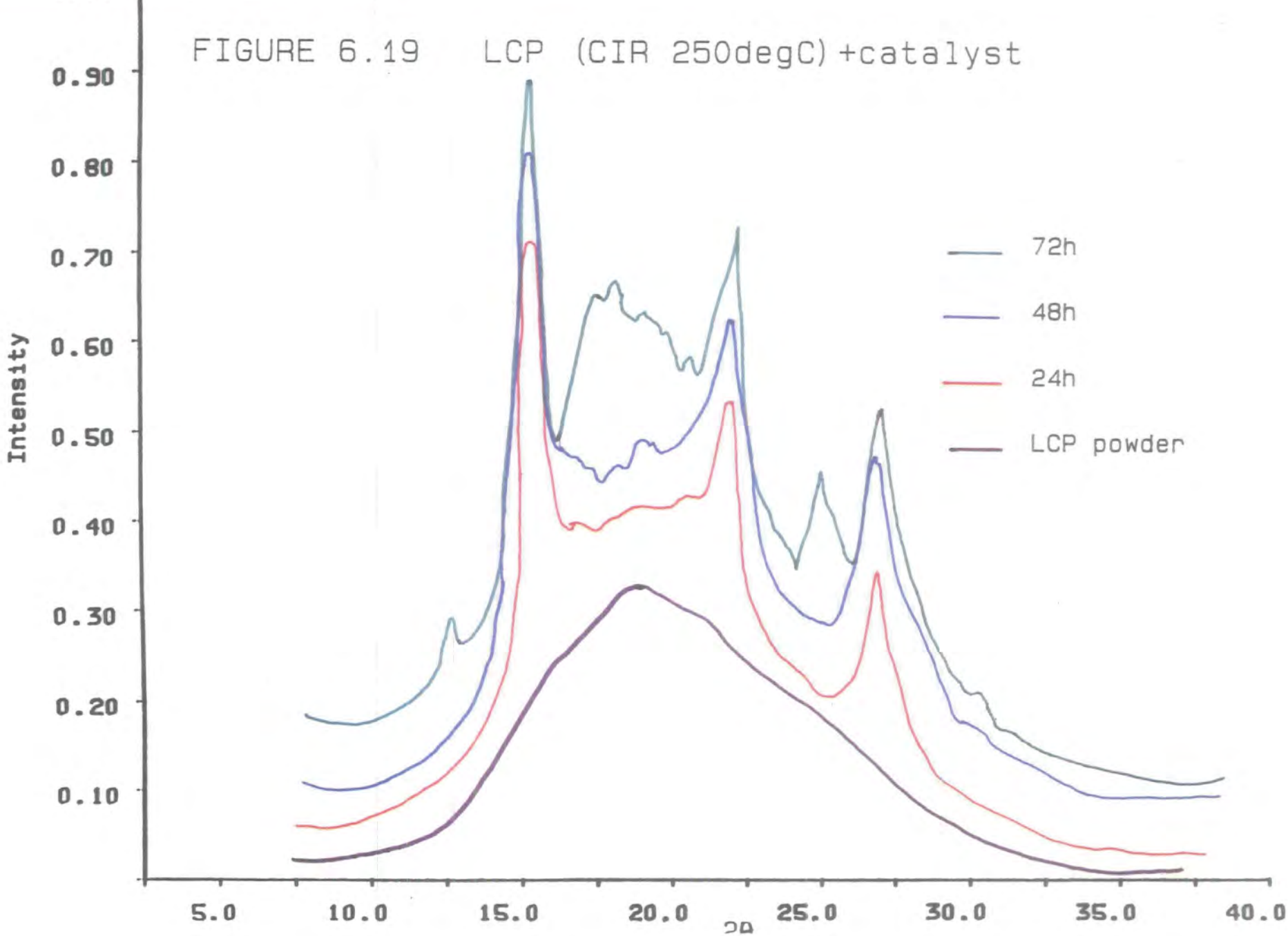
FIGURE 6.19 LCP (CIR 250degC) +catalyst
Intensity
0.90
0.80
0.70
0.60
0.50
0.40
0.30
0.20
0.10
5.0
10.0
15.0
20.0
25.0
30.0
35.0
40.0
72h
48h
24h
LCP powder

FIGURE 6.20 LCP (CIR 250degC/72h)+catalyst

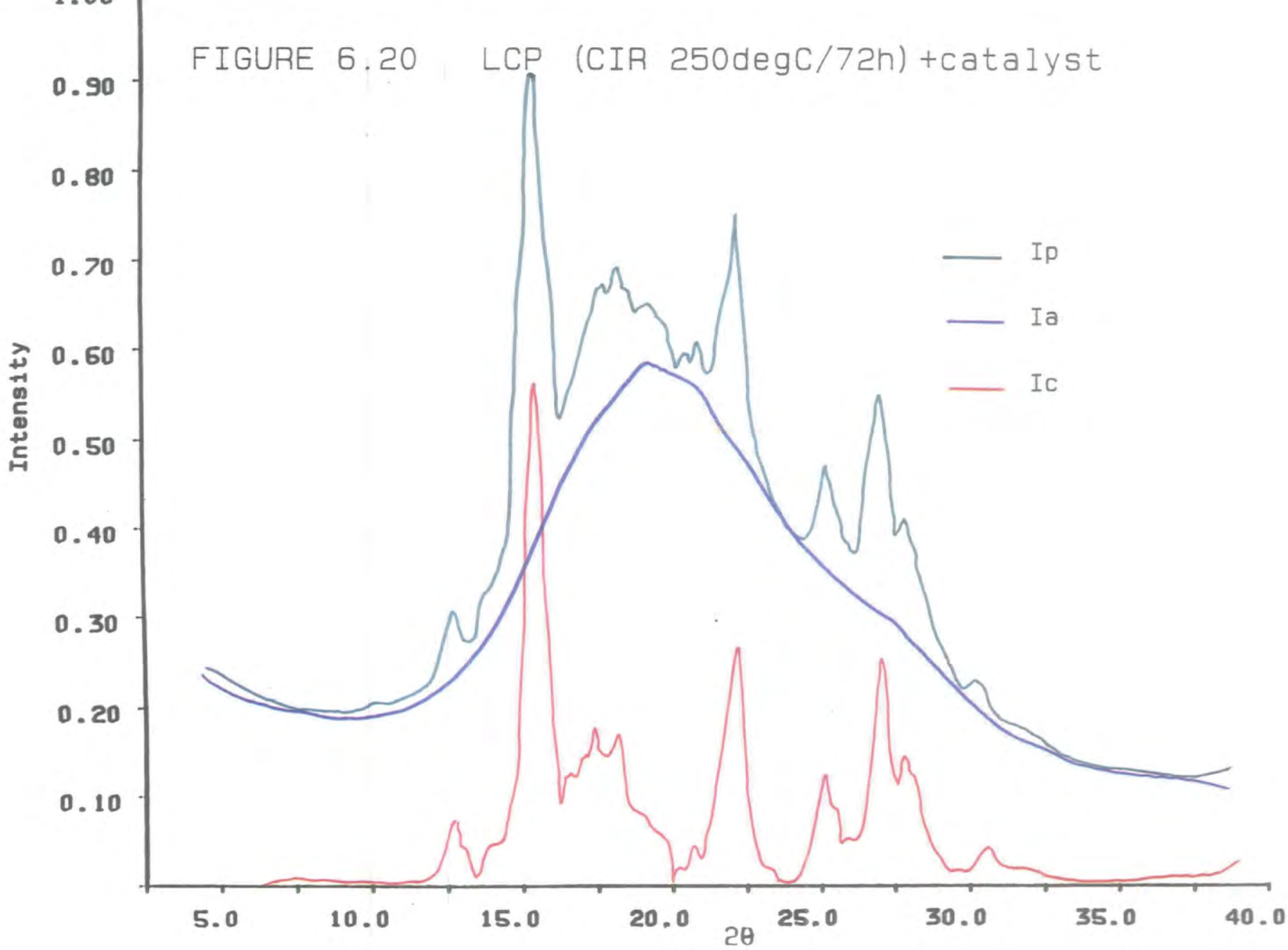

Sample	t / h	T / °C	x_{cr} / %
LCP	0	-	0
LCP	24	250	29
LCP	48	250	30
LCP	72	250	32

Table 6.5 CIR reaction below the melt

(c) ***CIR Reaction in the Melt***

Diffractograms of LCP samples annealed as described in section (6.5.1(c)) are given in Figure (6.21). For t = 24h, the characteristic peaks are present and the slight development of further peaks is apparent. For t = 48h, peaks are present at $2\Theta = 15.5°$ and 22°, characteristic of annealed LCP samples however the peak normally observed at $2\Theta = 27.5°$ is absent. The peak intensity is significantly lower than for the annealed films indicative of a reduction in order. Figure (6.22) gives the fitted curve for t = 48h. A solitary small peak exists at $2\Theta = 15.5°$ and the sample appears to be practically amorphous. The calculated values of x_{cr} are given in Table 6.6. From the results, the sample treated for t = 24h, has undergone structural rearrangement and the crystallinity level is comparatively high indicative of a high degree of order. Surprisingly the degree of order decreases with increasing t, suggesting that the polymer is disordering or indeed randomising in the melt.

FIGURE 6.21 LCP (CIR 290degC)+catalyst

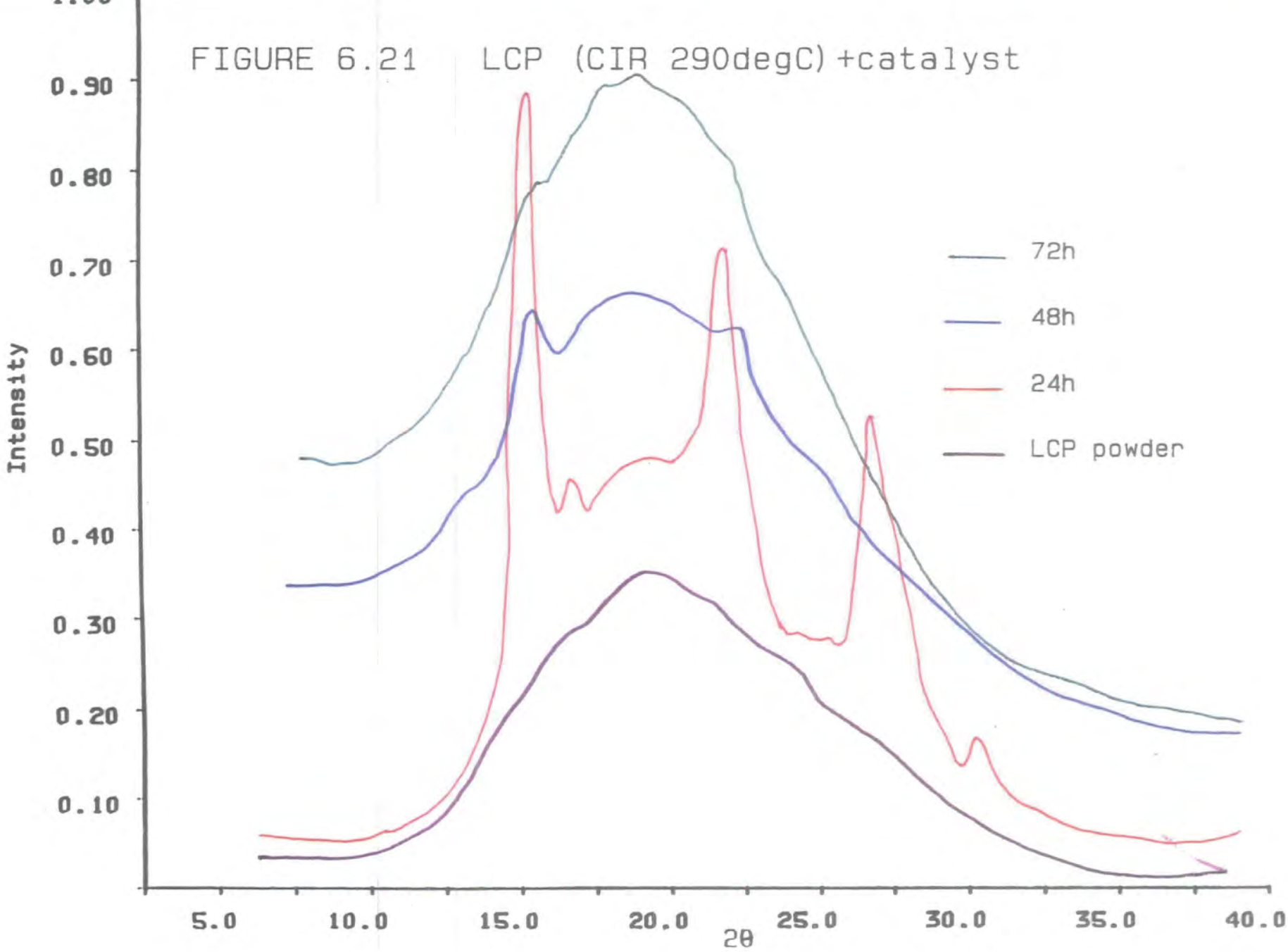

FIGURE 6.22 LCP (CIR 290degC/48h)+catalyst

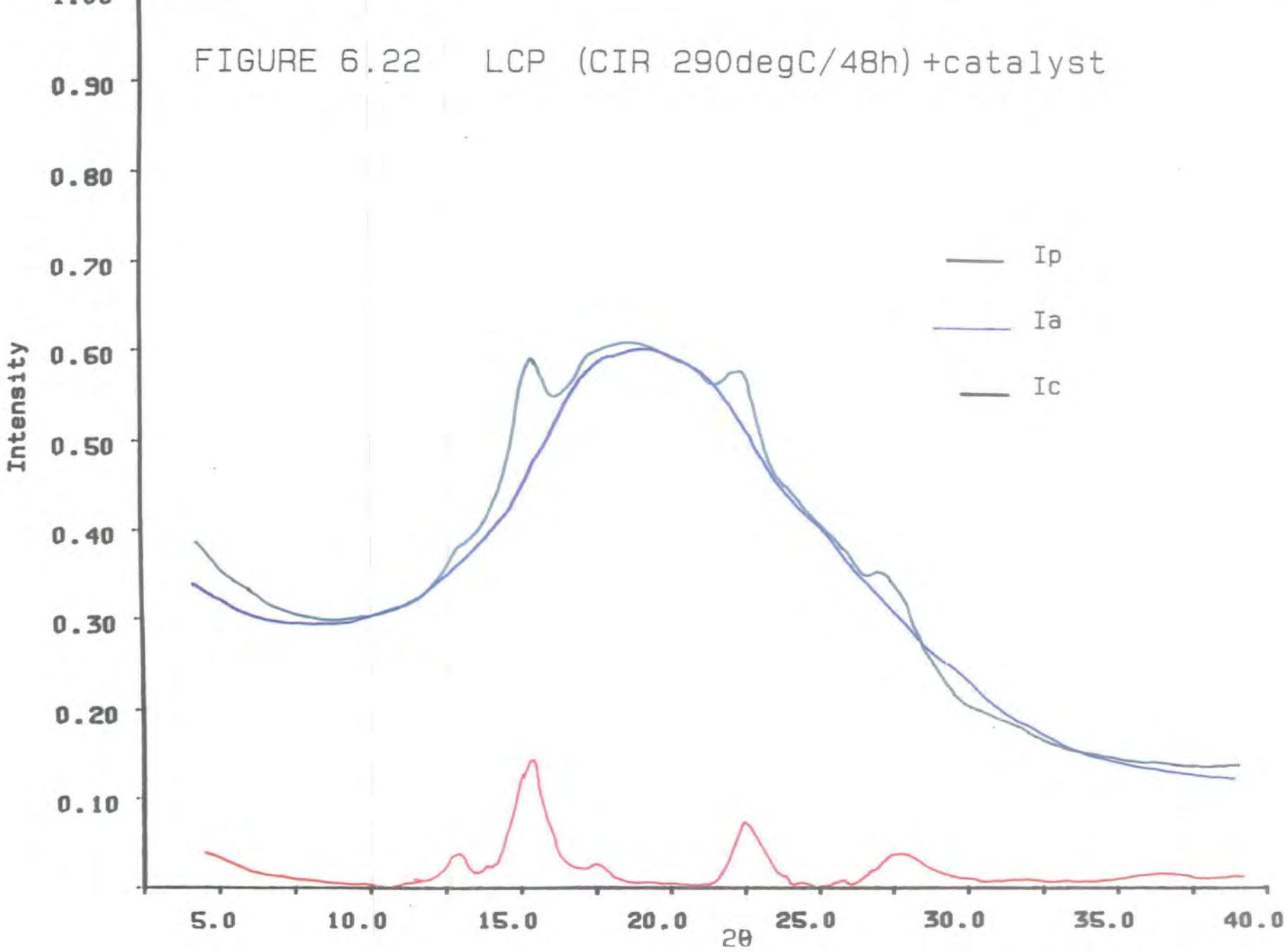

Sample	t / h	T / °C	x_{cr} / %
LCP	0	-	0
LCP	24	287	30
LCP	48	290	7
LCP	72	290	2

Table 6.6 CIR reaction in the melt

d) CIR Reaction in the Liquid Crystalline Phase

The LCP samples annealed as described in section (6.5.1(d)) are given in Figure 6.23. For LCP treated for t = 24h no crystalline peaks are present and a halo, characteristic of a completely amorphous polymer, is observed. For t = 60h, the characteristic LCP peaks exist. The intensity and sharpness of these peaks are significantly greater than observed for the annealed LCP films. For t = 72h, very small sharp peaks exist at $2\theta = 13°$, 17.5° and 26°. Thus the characteristic LCP peaks are completely absent indicating that the polymer structure has altered significantly. The low intensities of the new peaks suggests a low degree of ordering. The fitted curve for this sample is given in Figure (6.24) and the calculated values of x_{cr} are listed in Table (6.7). From the results obtained, no relationships exist between structural arrangement and annealing conditions.

Sample	t / h	T / °C	x_{cr} / %
LCP	0	-	0
LCP	24	300	0
LCP	48	300	30
LCP	72	300	8

Table 6.7 CIR Reaction in the Liquid Crystalline Phase

FIGURE 6.23 LCP (CIR 300degC) +catalyst

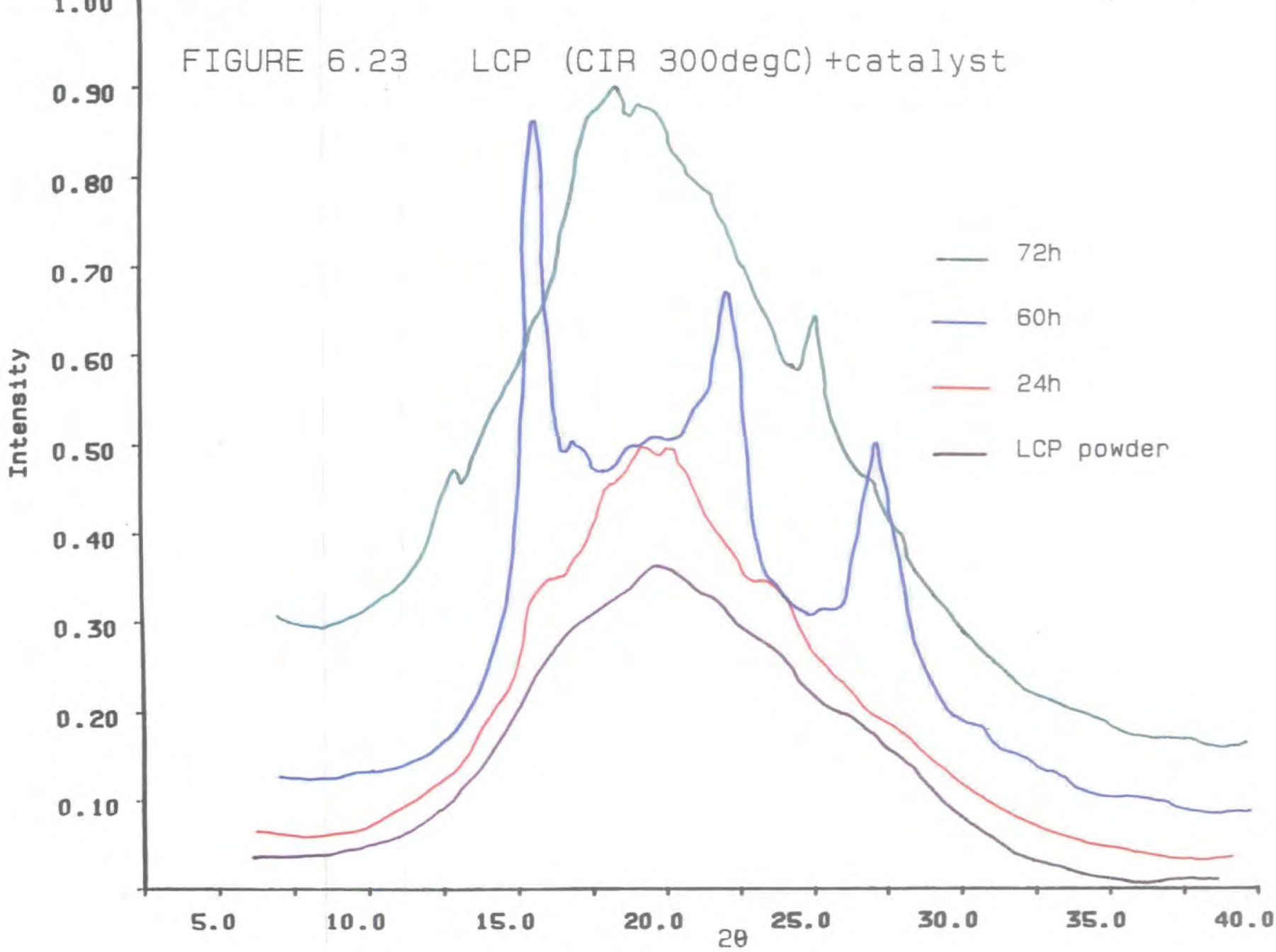

FIGURE 6.24 LCP (CIR 300degC/72h)+catalyst

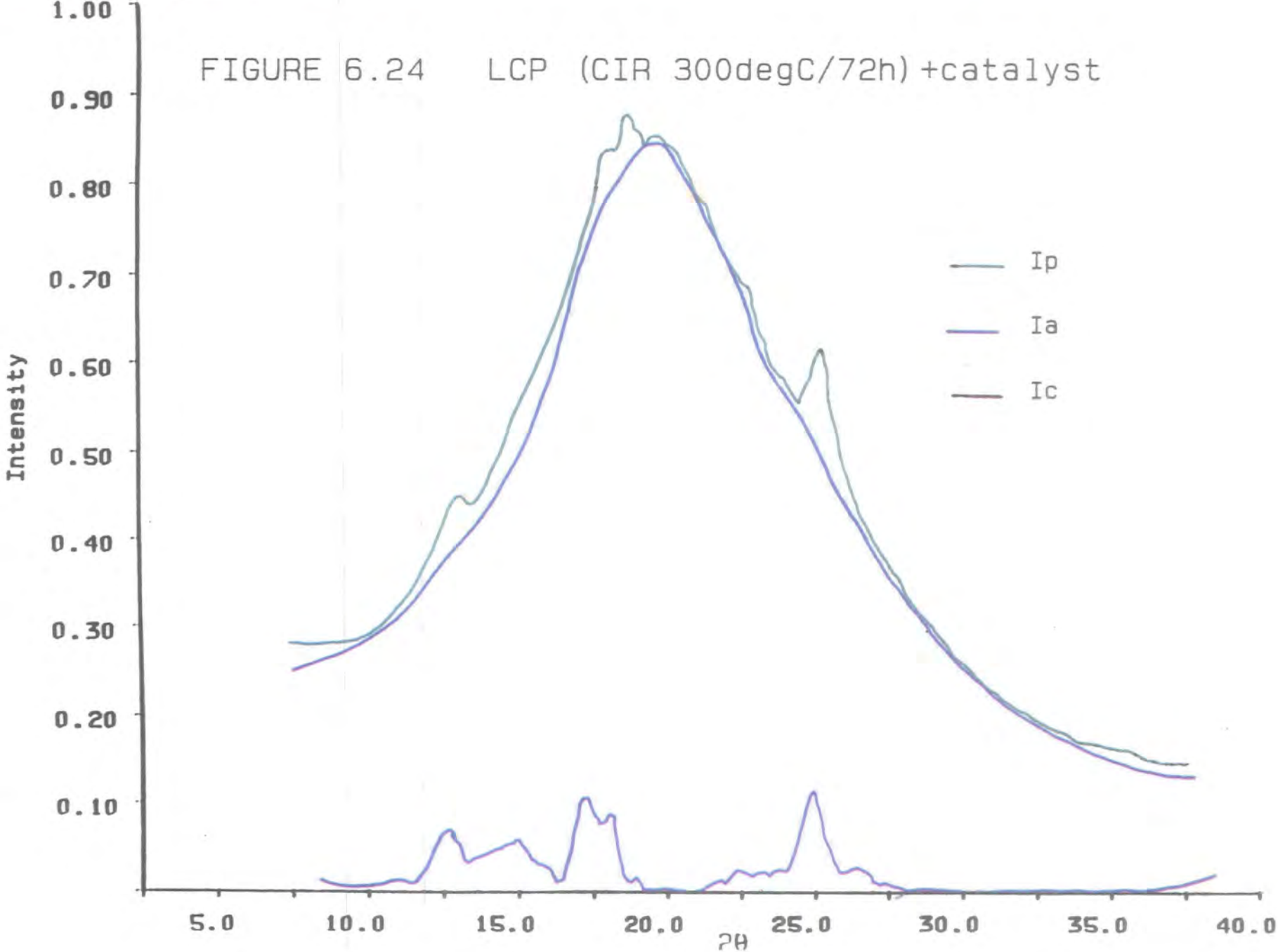

6.5.4 *CIR Reaction in the Absence of the Ester-Interchange Catalyst*

a) Introduction

LCP samples were annealed over the reaction time (t) = 48h at 3 selected temperatures: T = 250°C, 282°C and 300°C, in the absence of the ester-interchange catalyst. The main aim was to observe whether any significant effects in physical properties, resulting from the annealing of LCP, could be attributed solely to the presence of the interchange catalyst.

b) DSC

From the thermograms illustrated in Figure (6.25), no transitions are apparent before melting for each annealed LCP sample. A biphasic endotherm is exhibited for LCP annealed below the melt (T=250°C). For samples annealed at higher temperatures, sharp, single endotherms exist characteristic of semi-crystalline polymers. As T increases, the melting peaks shift to higher temperatures. In general, in addition to the melting peaks becoming sharper, the values of T_m and ΔH_f increase significantly as a function of reaction time. These parameters and the temperature ranges over which they exist are given in Table 6.8. The heats of fusion reach a maximum value of 40 Jg^{-1} at T = 282°C. This value is over 6 times higher than the heat of fusion observed for untreated LCP, a dramatic increase indicating that a significant amount of ordering has occurred.
In summary, the trends in the results illustrate that the CIR reaction occurs both above and below the melting temperature in the absence of the catalyst. It cannot be presumed from this data alone but it appears likely that ordering takes place in exactly the same way as for the catalyst reactions. Different samples of each annealed polymer were run and the results were found to be very reproducible.

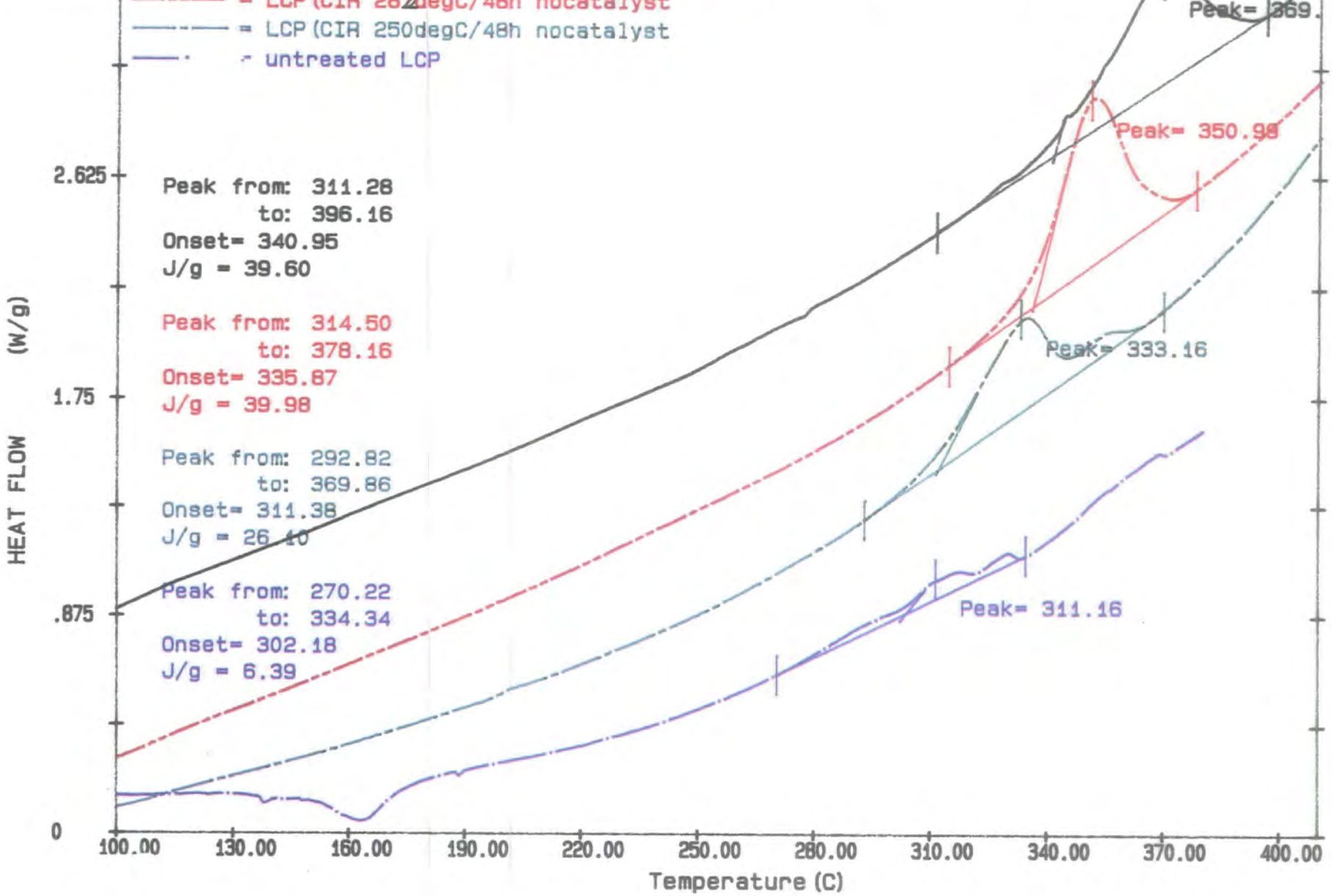
= LCP(CIR 250degC/48h nocatalyst
= untreated LCP
Peak= 369.
Peak= 350.98
Peak= 333.16
Peak= 311.16
Peak from: 311.28
to: 396.16
Onset= 340.95
J/g = 39.60
Peak from: 314.50
to: 378.16
Onset= 335.87
J/g = 39.98
Peak from: 292.82
to: 369.86
Onset= 311.38
J/g = 26.10
Peak from: 270.22
to: 334.34
Onset= 302.18
J/g = 6.39
HEAT FLOW (W/g)
2.625
1.75
.875
0
100.00
130.00
160.00
190.00
220.00
250.00
280.00
310.00
340.00
370.00
400.00
Temperature (C)

Figure 6.25

Sample t/h	T °C	T_m °C	ΔH_m Jg^{-1}	ΔT_m °C	Nature of peak
$LCP_{(0)}$	-	302	6	270-334	M
$LCP_{(48)}$	250	311	26	293-370	M
$LCP_{(48)}$	282	336	40	315-378	S
$LCP_{(48)}$	300	341	40	311-396	S

Table 6.8 CIR Reactions in the Absence of the Ester-Interchange Catalyst

c) P.O.M.

A slight amount of liquid crystallinity exists at ambient temperatures for each of the annealed LCP samples. This is illustrated from random areas of white, bright light visible between crossed-polars in the optical microscope. For samples annealed at T = 250°C (Figure 6.26) and T = 282°C (Figure 6.27) the nematic phases form at significantly higher temperatures than is observed for untreated LCP. The temperature of phase formation increases as a function of T. For reactions carried out at T = 300°C melting occurs just prior to degradation (Figure 6.28) and the nematic phase is not observed. Thus it can be concluded that either the LC phase exists above the degradation temperature, or that a semi-crystalline polymer has been formed as a result of the reaction. In general, ordering increases as a function of T.

d) WAXS

For samples annealed at T = 250°C, the characteristic LCP Bragg peaks are observed (Chapter 4). However, for LCP annealed at T = 282°C (Figure 6.30) further small peaks are present at 2Θ = 17° and 31°. For T = 300°C the characteristic LCP peaks are

FIGURE 6.26 LCP (CIR 250degC/48h) no catalyst

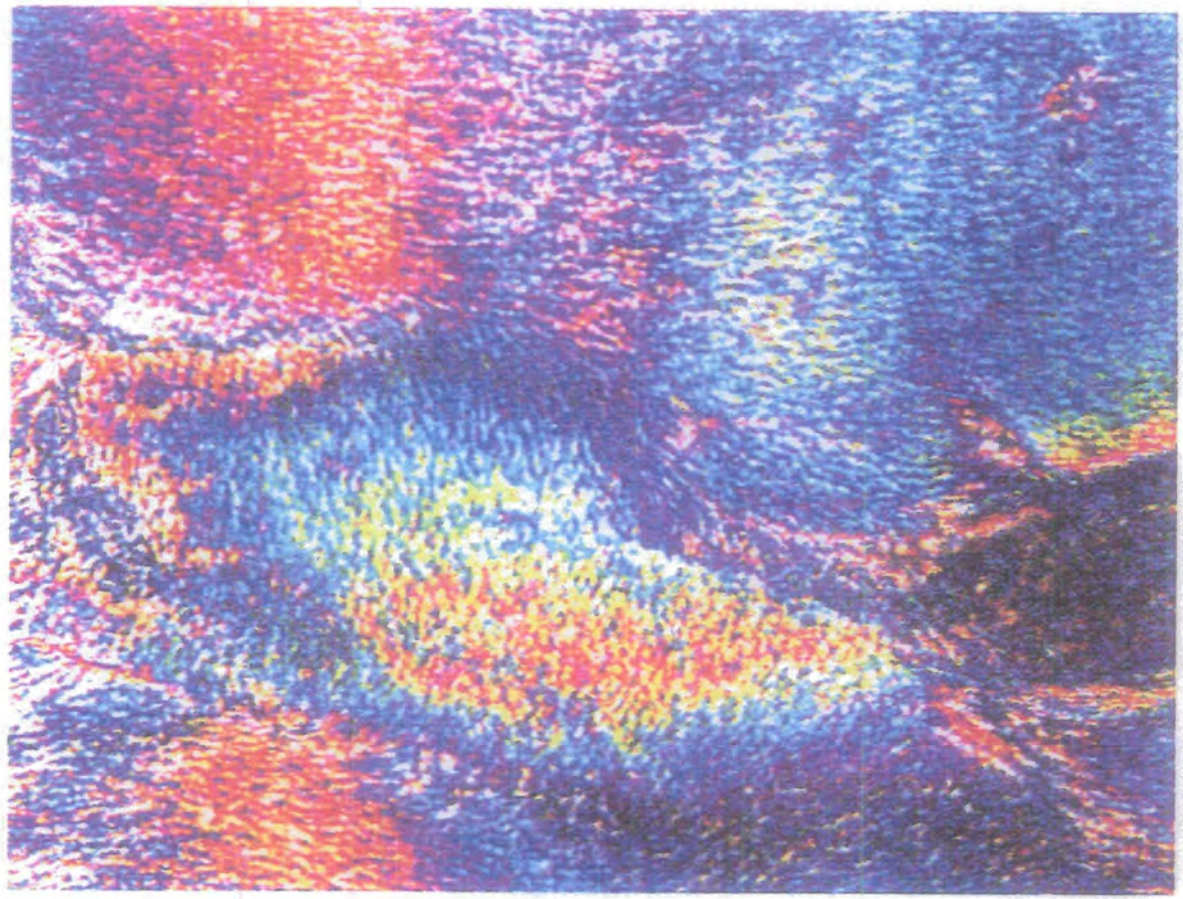

(x 400) crossed polars

L.C. phase @360degC

FIGURE 6.27 LCP (CIR 282degC/48h) no catalyst

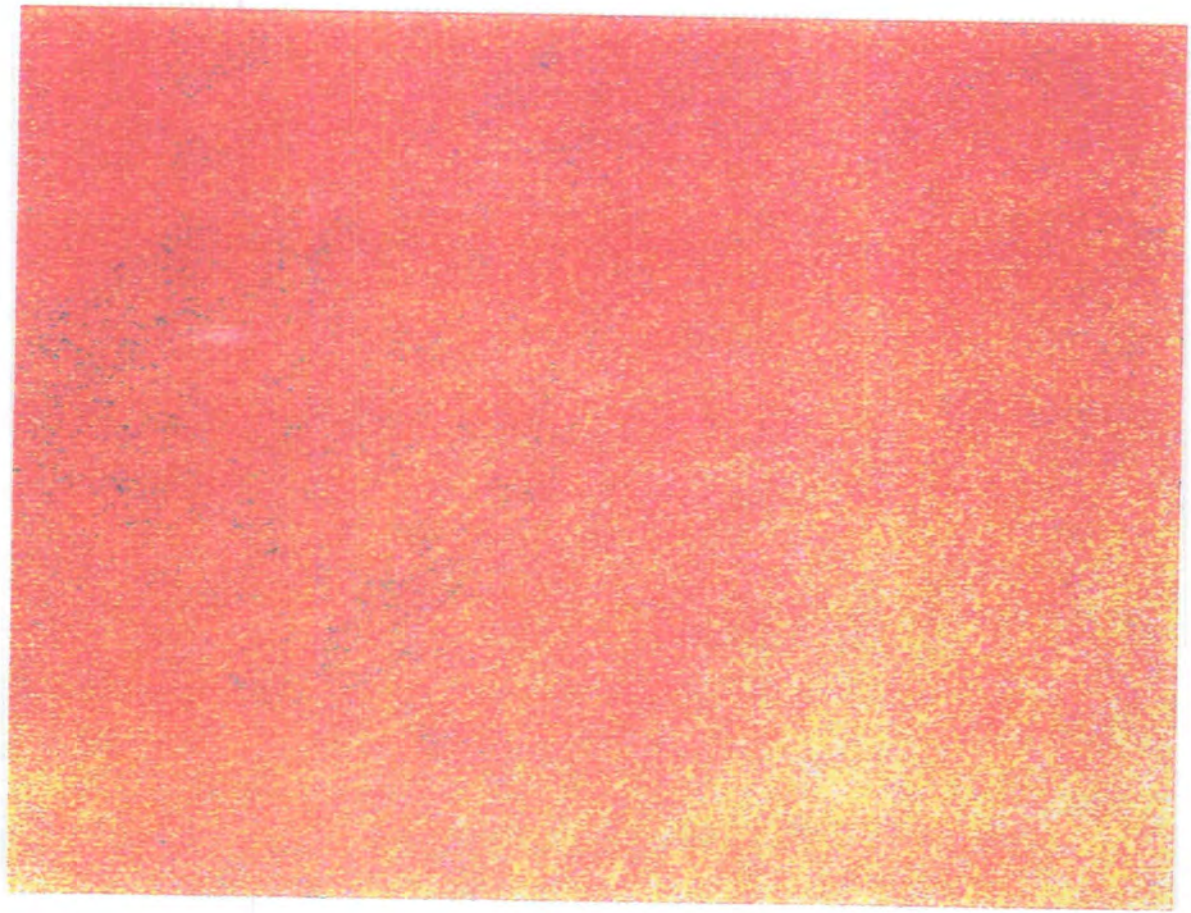

(x 400) crossed polars

L.C. phase @380degC

FIGURE 6.28 LCP (CIR 300degC/48h) no catalyst

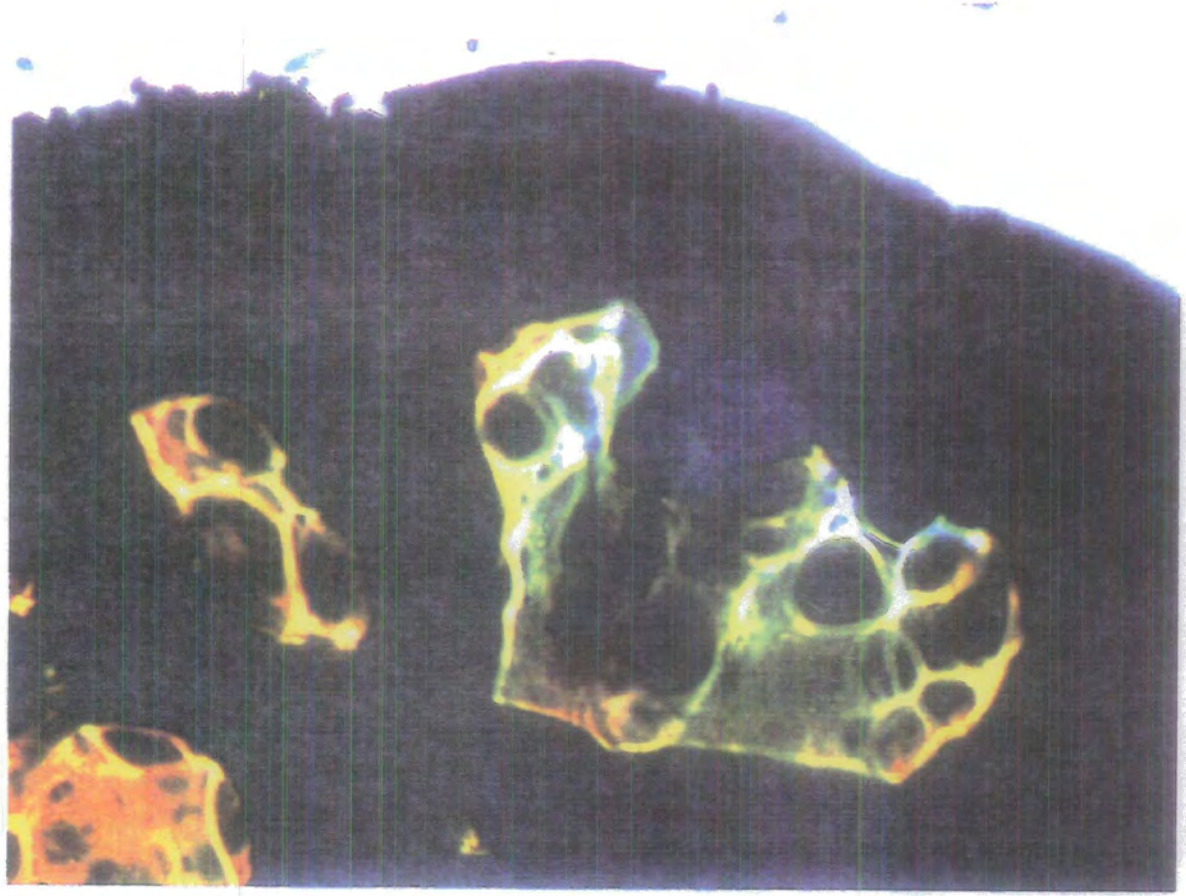

(x 100)

No L.C. phase. Degrades on melting @400degC

FIGURE 6.29 LCP (CIR 48h) +catalyst

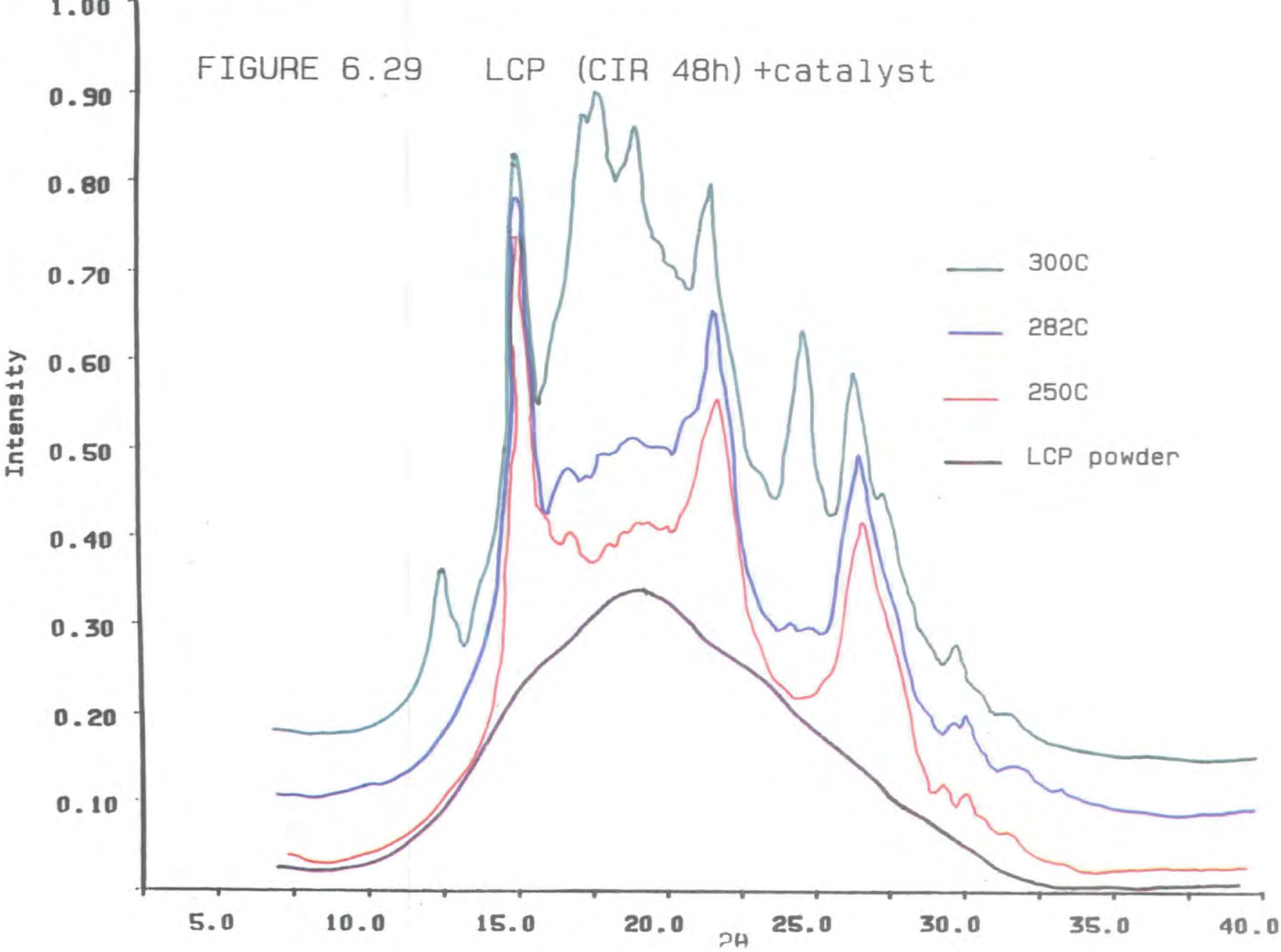

FIGURE 6.30 LCP (CIR 282degC/48h) no catalyst

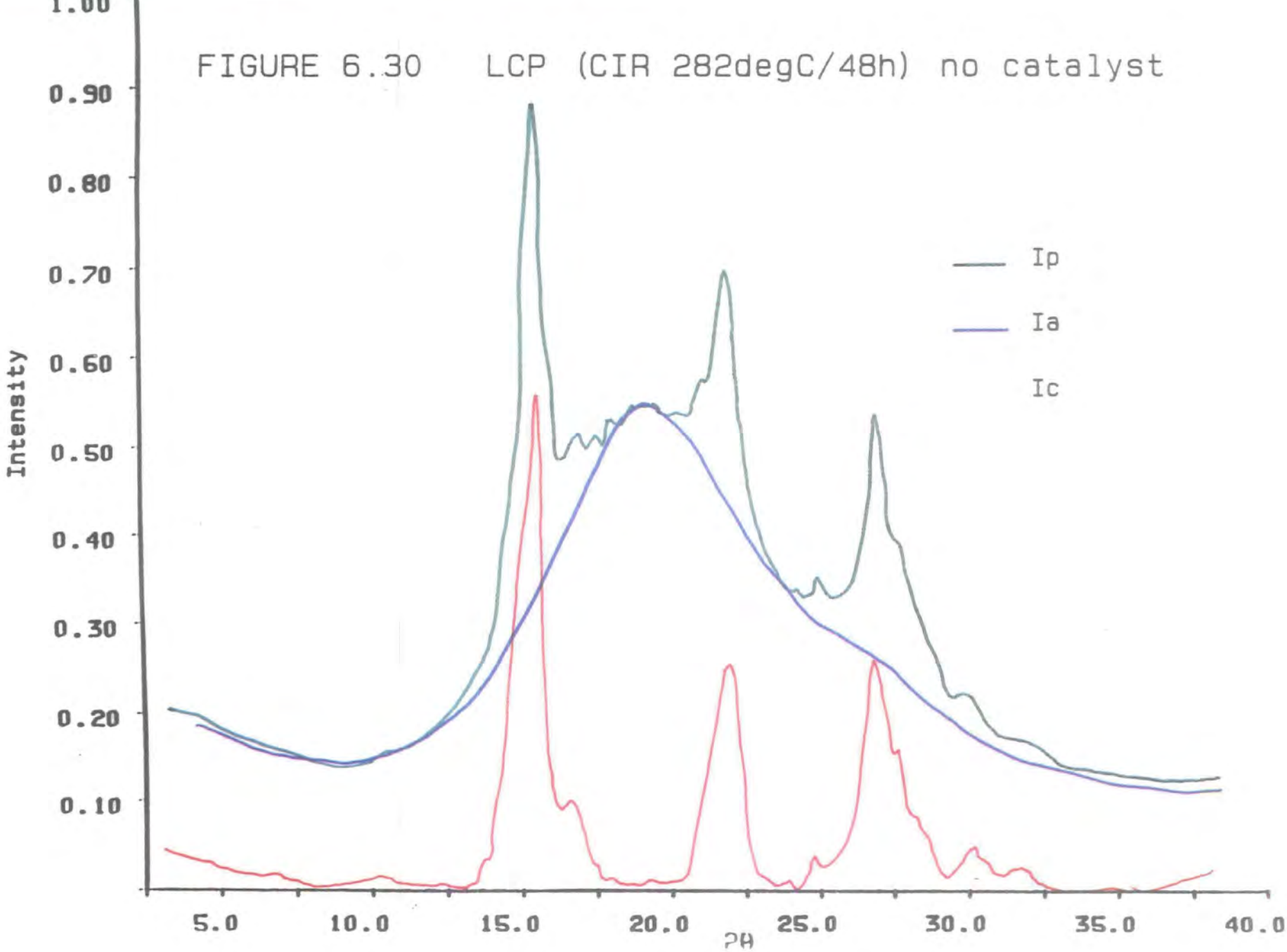

somewhat sharper and more intense than those observed for the samples annealed at lower temperatures. In addition, a significant number of peaks have developed at 2Θ = 13°, 17°, 20°, 25°, 28° and 31°. Thus a structural rearrangement has resulted from the reaction. The calculated % crystallinities (X_{cr}) of the samples are given in Table 6.9 and the WAXS diffractograms, in Figure (6.29). For LCP annealed at T = 300°C, the accuracy of this parameter is uncertain since the predicted theoretical curve for crystalline LCP cannot be applied to the sample, due to changes in the diffraction pattern. In general, the % crystallinity and peak sharpness increase as a function of T, which is in line with an increase in ordering. Pronounced structural rearrangement is confirmed by the development of new peaks, increasing in number and intensity with reaction time. The diffraction pattern for the highest diffraction pattern for the highest reaction time studied, illustrates a high degree of ordering which has taken place even in the absence of the catalyst.

Sample	t / h	T / °C	x_{cr} / %
LCP	0	-	0
LCP	48	250	28
LCP	48	282	29
LCP	48	300	30

Table 6.9 CIR Reactions in the Absence of the Ester- Interchange Catalyst

6.5.5 *Identification of Structures Formed by CIR*

Lenz's theory (section 6.2) shows that ultimately, block copolymers are formed as a result of the CIR process. LCP is composed of 3 monomeric units: HQ, IA and HBA. From the chemical structure of both IA and HQ, it is impossible for them to exist as single monomeric chains, however chains of HBA can exist. Hence if Lenz's theory

holds true for LCP and block structures result from the CIR reaction, then the following block structures are equally likely to develop:

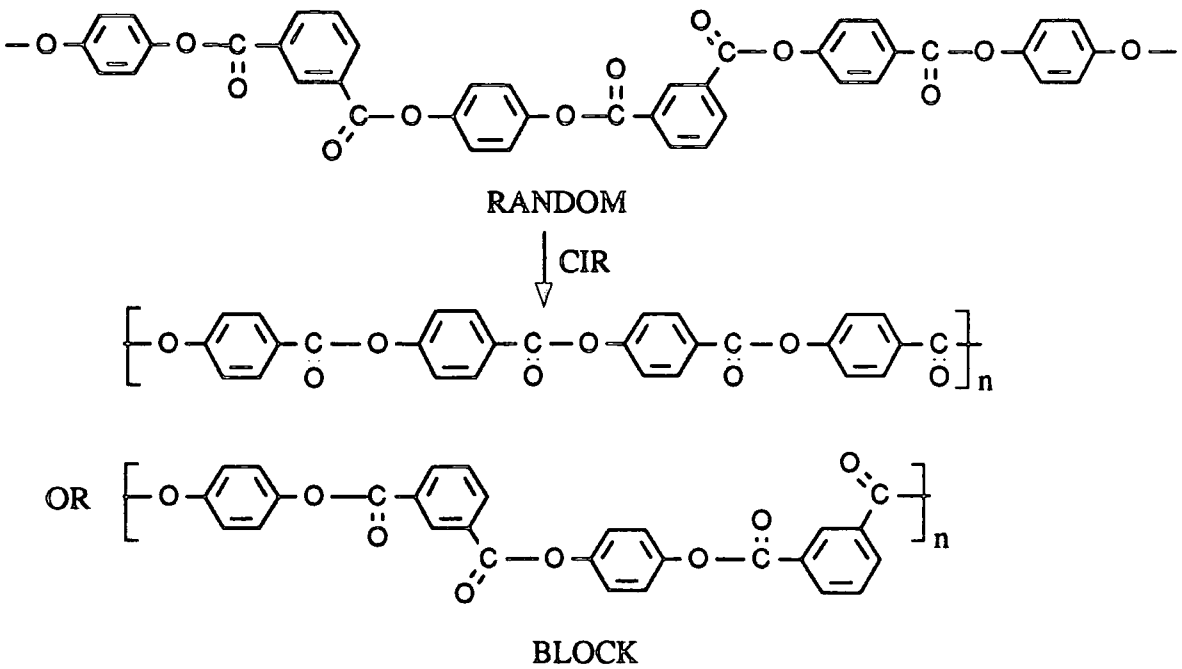

The block structures represent poly(HBA) and poly(HQ/IA) respectively. Samples of these polymers were obtained from ICI plc and a thermo-structural characterisation, equivalent to that applied to the CIR sample, was carried out for each. Thus a comparison of the data will reveal whether either of the block structures dominates as a result of the CIR reaction in LCP. From these limited studies, the CIR sample annealed at T = 300°C and t = 48h in the absence of the selected catalyst, has been chosen for comparison since it exhibits the highest degree of order. Neither the molecular weights of the CIR samples, nor the sequence distribution of block copolymers were determined due to their insolubility and unless their molecular lengths are very similar, no accurate comparison of the thermal transitions can be made. These transitions are known to vary with molecular weight which, based on Lenz's work, have been found to increase during reaction. It should not be overlooked that even if one block structure dominates, it is likely that the remaining LCP units occur randomly along the polymer chain which will result in lower thermal parameters than those observed for the pure block structures. A

brief review of the thermal behaviour of poly(HQ/IA) and poly(HBA) is however, included for completeness. The DSC thermograms for these polymers are given in Figure (6.31). From polarising microscopy, the endothermic peak for poly(HQ/IA) is due to melting and a liquid crystalline phase forms over the range 430-460°C (Figure 6.32).

From the heats of fusion calculated from DSC analysis, as anticipated, the value for poly(HQ/IA) is slightly higher than for the CIR sample, but in general they are both fairly comparable. Poly(HBA) does not appear to melt before decomposition at 590°C (Figure 6.33). A small endothermic transition is apparent over the temperature range 320-380°C. This is attributed to either a crystal-crystal[21] or a crystal-nematic transition.[22] From the present studies, it is considered to be due to the latter. For this study, the technique considered to be the most informative and the least ambiguous in the direct comparison of the structural behaviour of the polymers is WAXS. The diffractograms obtained for untreated LCP and the CIR sample are compared to that of Poly(HQ/IA) in Figure 6.34 and Poly(HBA) in Figure 6.35.

Referring back to the WAXS data for the CIR samples discussed in sections (6.5.3) and (6.5.(4d)), it is evident that peak sharpness and amplitude increase with increasing reaction temperature and time and in some cases, structural rearrangement occurs. Insufficient data has been obtained in order to conclude any trends with confidence and the selected catalyst does not appear to influence the rearrangement. The rearrangement does however favour the HQ/IA structure, apparent from the WAXS data. It is proposed that this structure formation is more favourable either kinetically or thermodynamically since it has a lower degree of order than poly(HBA). Specific features of the poly(HBA) structure are still apparent from WAXS studies and due to the presence of the diffuse halo, it is assumed that these units are scrambled at random amongst the predominant poly(HQ/IA) structure. From the limited results, neither the reaction mechanism nor the reasoning behind the preferential development of this structure can be explained.

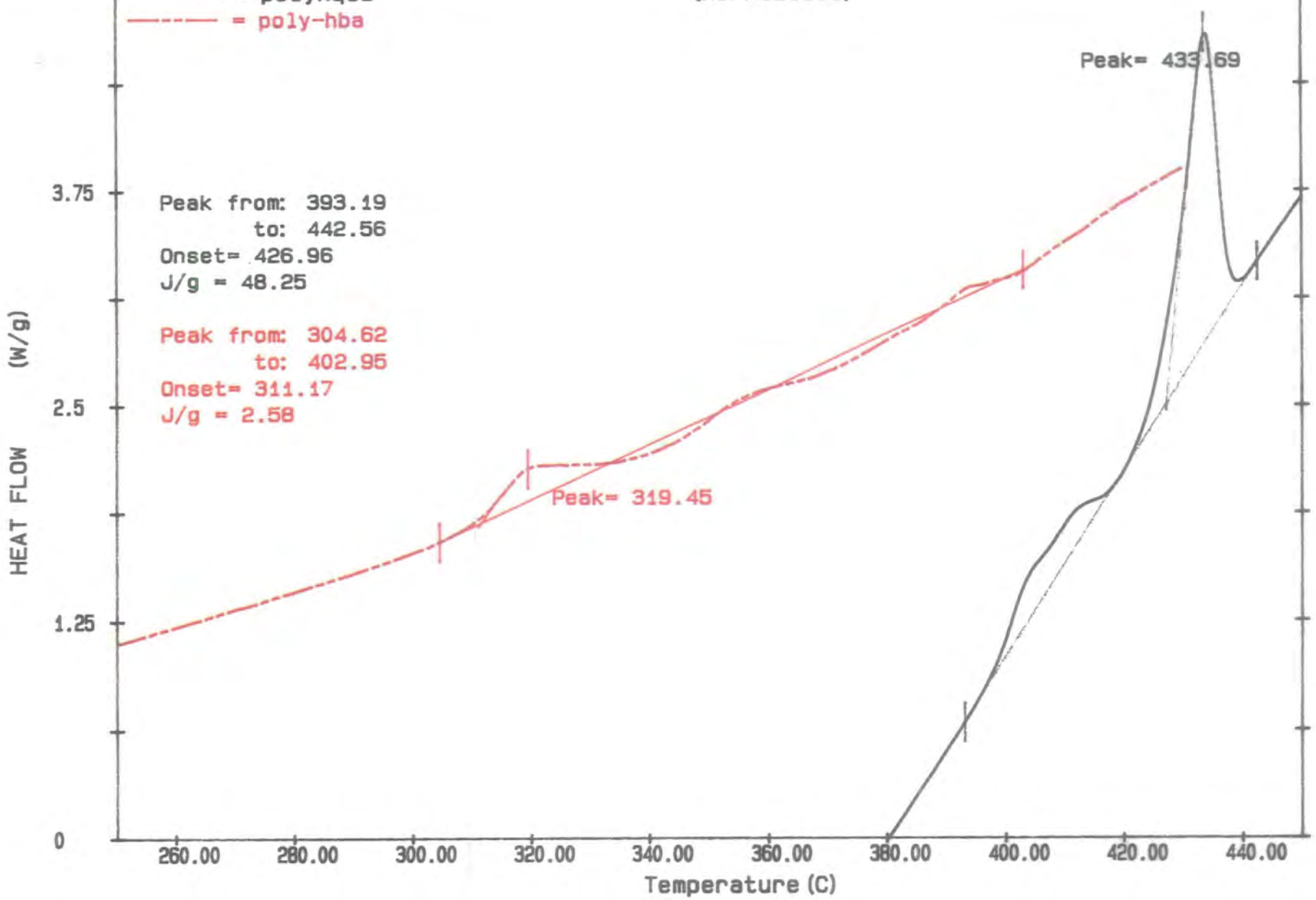
= poly-hba
Peak= 433.69
Peak from: 393.19
to: 442.56
Onset= 426.96
J/g = 48.25
Peak from: 304.62
to: 402.95
Onset= 311.17
J/g = 2.58
Peak= 319.45
HEAT FLOW (W/g)
3.75
2.5
1.25
0
260.00
280.00
300.00
320.00
340.00
360.00
380.00
400.00
420.00
440.00
Temperature (C)

Figure 6.31

FIGURE 6.32 Poly(HQ/IA) (heating run: 25-500degC)

25degC

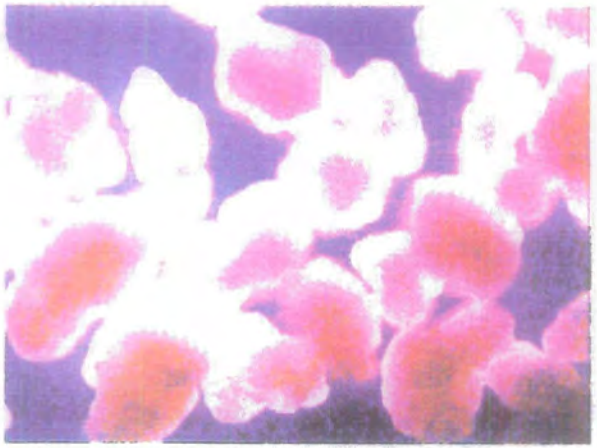

300degC

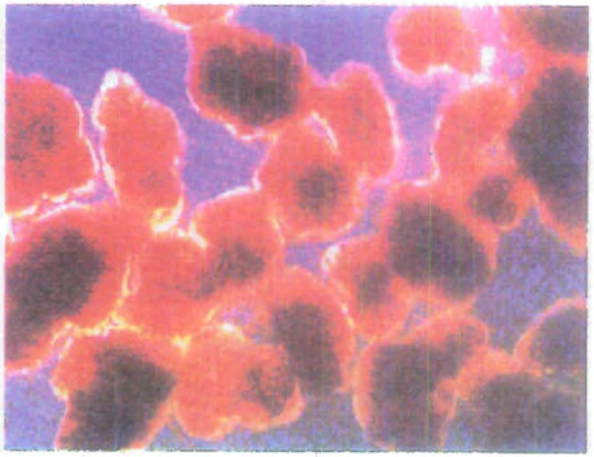

400degC

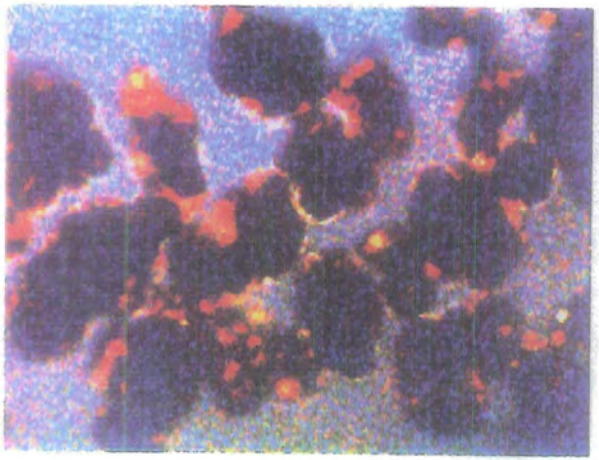

470degC

(x 100) crossed polars

FIGURE 6.33 Poly (HBA) (heating run: 25-600degC)

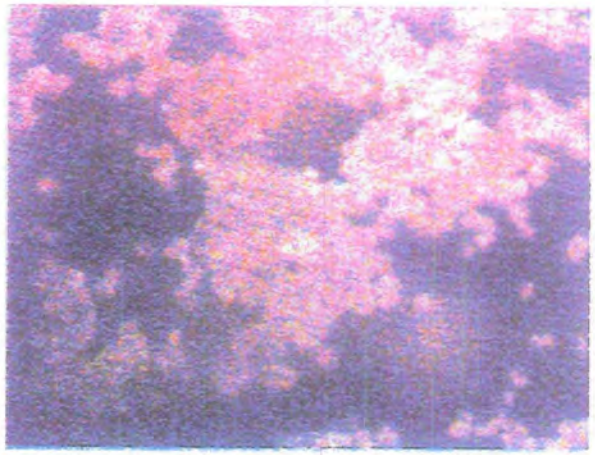

25degC

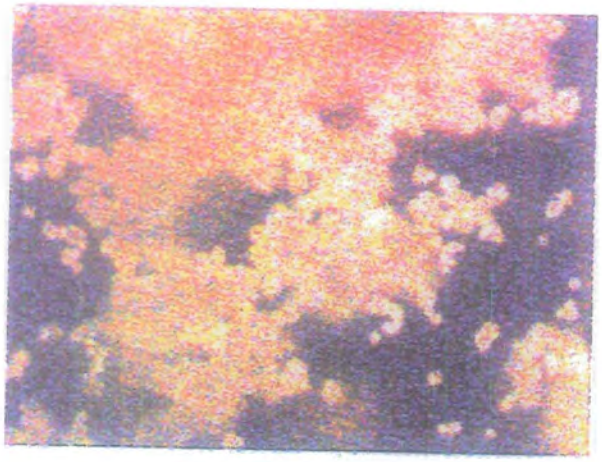

300degC

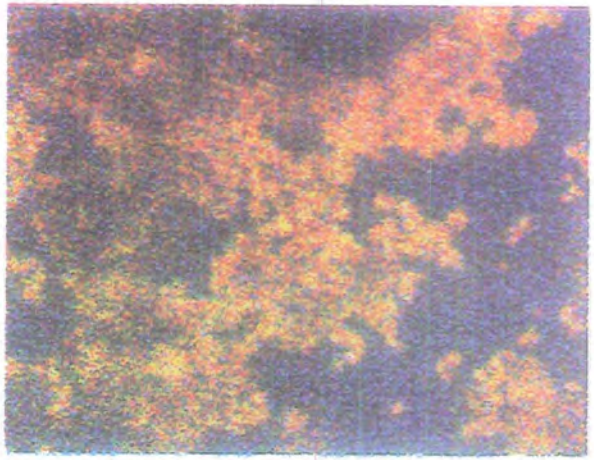

430degC

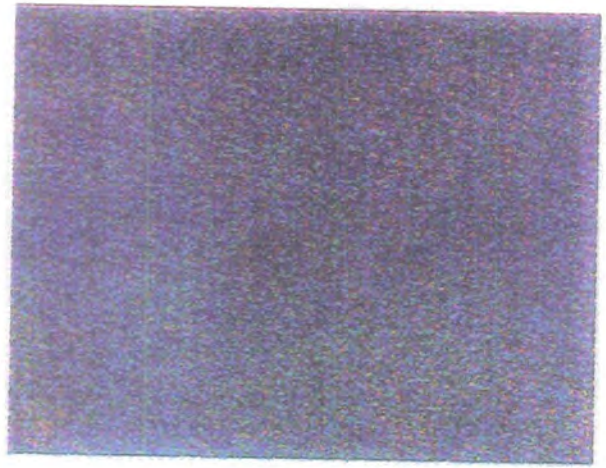

590degC

(x 100) crossed polars

FIGURE 6.34 Comparison of Poly(HQ/IA)

with LCP reorganised by CIR

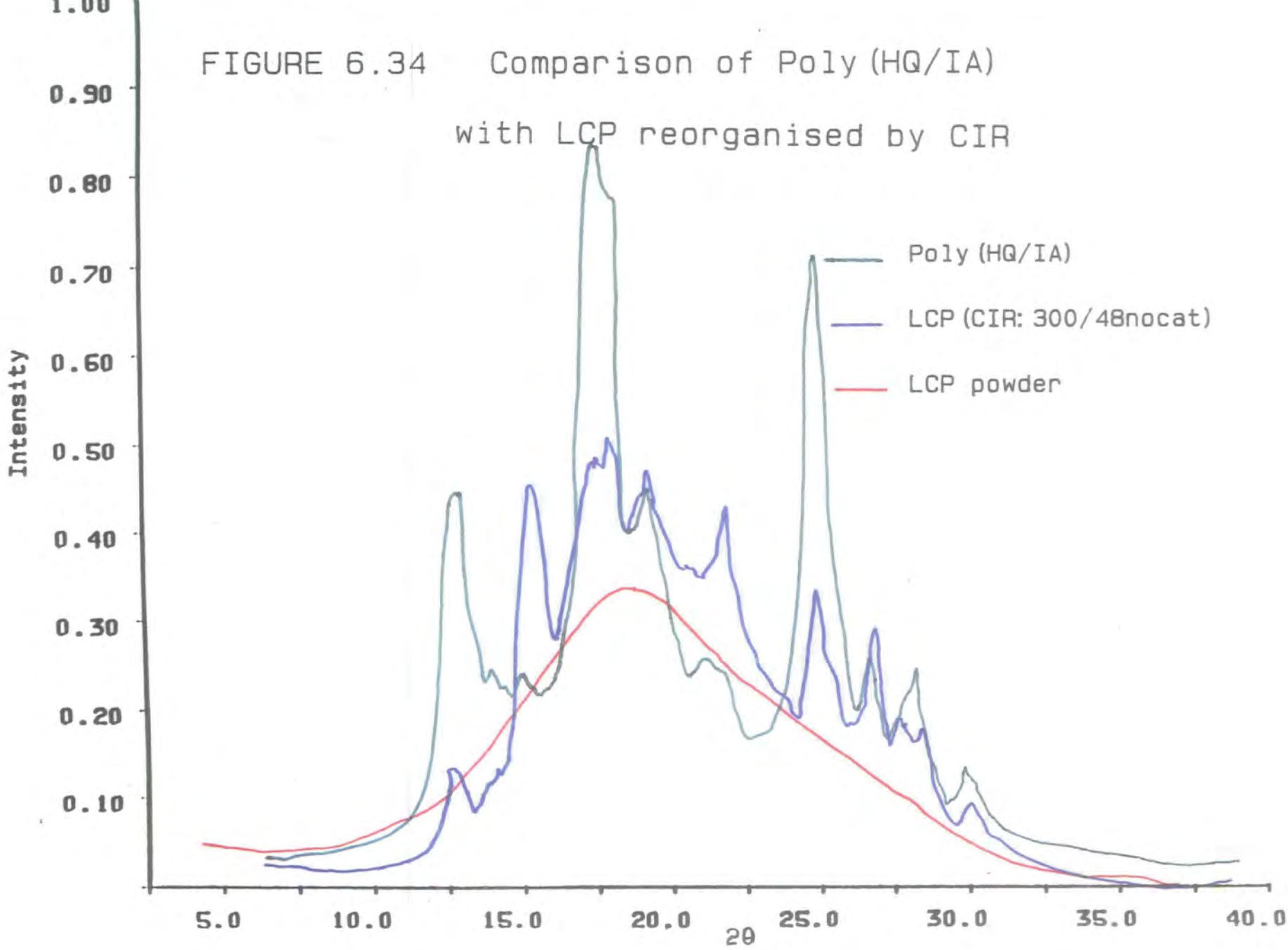

FIGURE 6.35 Comparison of Poly(HBA) with LCP reorganised by CIR

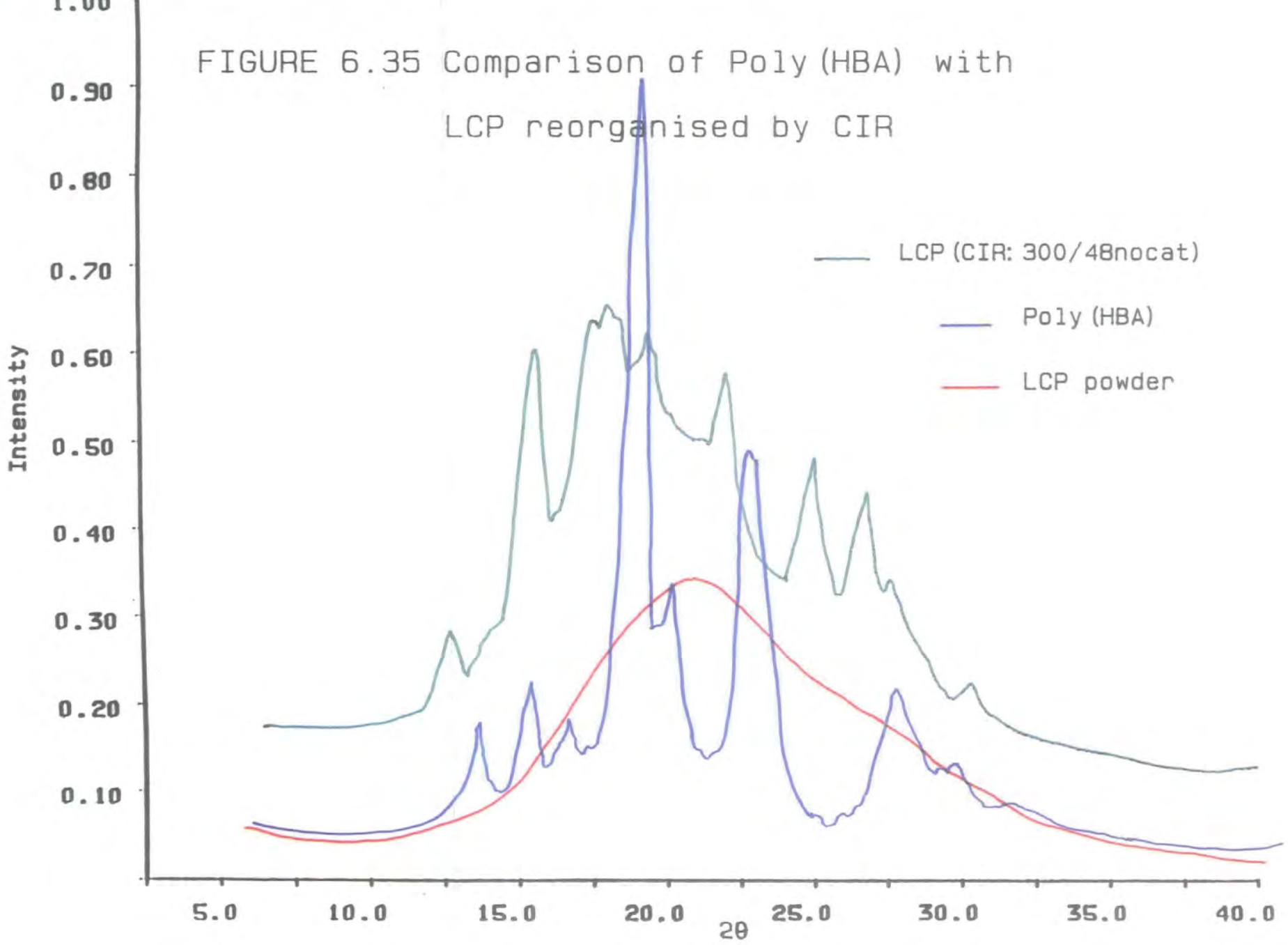

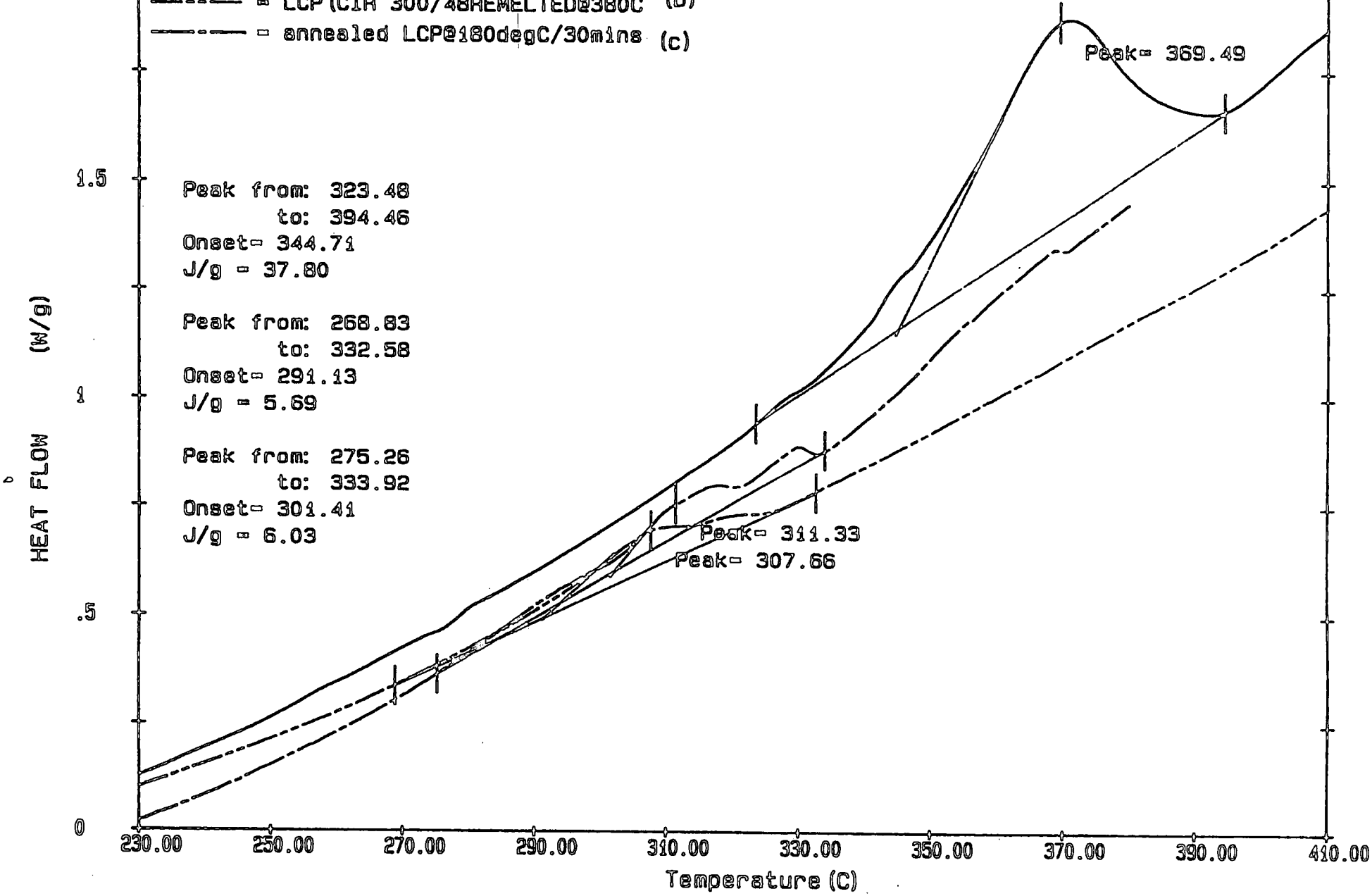
LCP(CIR 300/40REMELTED@380C (b)
annealed LCP@180degC/30mins (c)
Peak= 369.49
Peak from: 323.48
to: 394.46
Onset= 344.71
J/g = 37.80
Peak from: 268.83
to: 332.58
Onset= 291.13
J/g = 5.69
Peak from: 275.26
to: 333.92
Onset= 301.41
J/g = 6.03
Peak= 311.33
Peak= 307.66
HEAT FLOW (W/g)
0
.5
1
1.5
230.00
250.00
270.00
290.00
310.00
330.00
350.00
370.00
390.00
410.00
Temperature (C)

Figure 6.36

6.5.6 *Effects of Remelting LCP after Rearrangment via the CIR Reaction*

The effects of melting LCP which has undergone structural rearrangement as a result of the CIR process are studied. For continuity, the sample discussed is identical to that studied in section (6.5.5). However all samples were tested and similar conclusions were reached. In this study, due to the initial high degree of ordering, the effects due to remelting are magnified. DSC thermograms for the following samples are given in Figure (6.36)

(I) CIR sample

(II) CIR sample, annealed for 1 minute above its melting range (@380°C) and quenched to ambient temperatures

(III) untreated LCP, annealed at 180°C for 30 minutes.

From microscopy results discussed in section (6.5.2), (I) does not form a liquid crystalline phase prior to degradation however (II) forms a nematic phase at 330°C upon reheating. This behaviour is practically identical to that observed for untreated LCP (Chapter 3).

From DSC analysis, the temperatures and heats of fusion decrease significantly upon remelting. The resultant values are in line with those obtained for untreated LCP. In addition the sharp single endotherm, characteristic of a semi-crystalline material, disappears on remelting and is replaced by a multiple broad endotherm, again characteristic of random LCP. These observations are in line with those recorded for LCP which was remelted after annealing at 270°C for 30 minutes. WAXS diffractograms for (I), (II) and (III) are illustrated on Figure (6.37). The patterns for II and III are very similar and the reduction in % crystallinity on remelting is in line with the observed decrease in the heat of fusion. The quantitative data obtained from thermo-structural analysis is summarised in Table (6.10). It appears that the reorganised CIR sample reverts back to the original random LCP structure on remelting.

On the basis of these results a final experiment was carried out to observe the effects of

FIGURE 6.37 Effects of remelting after reorganisation by CIR

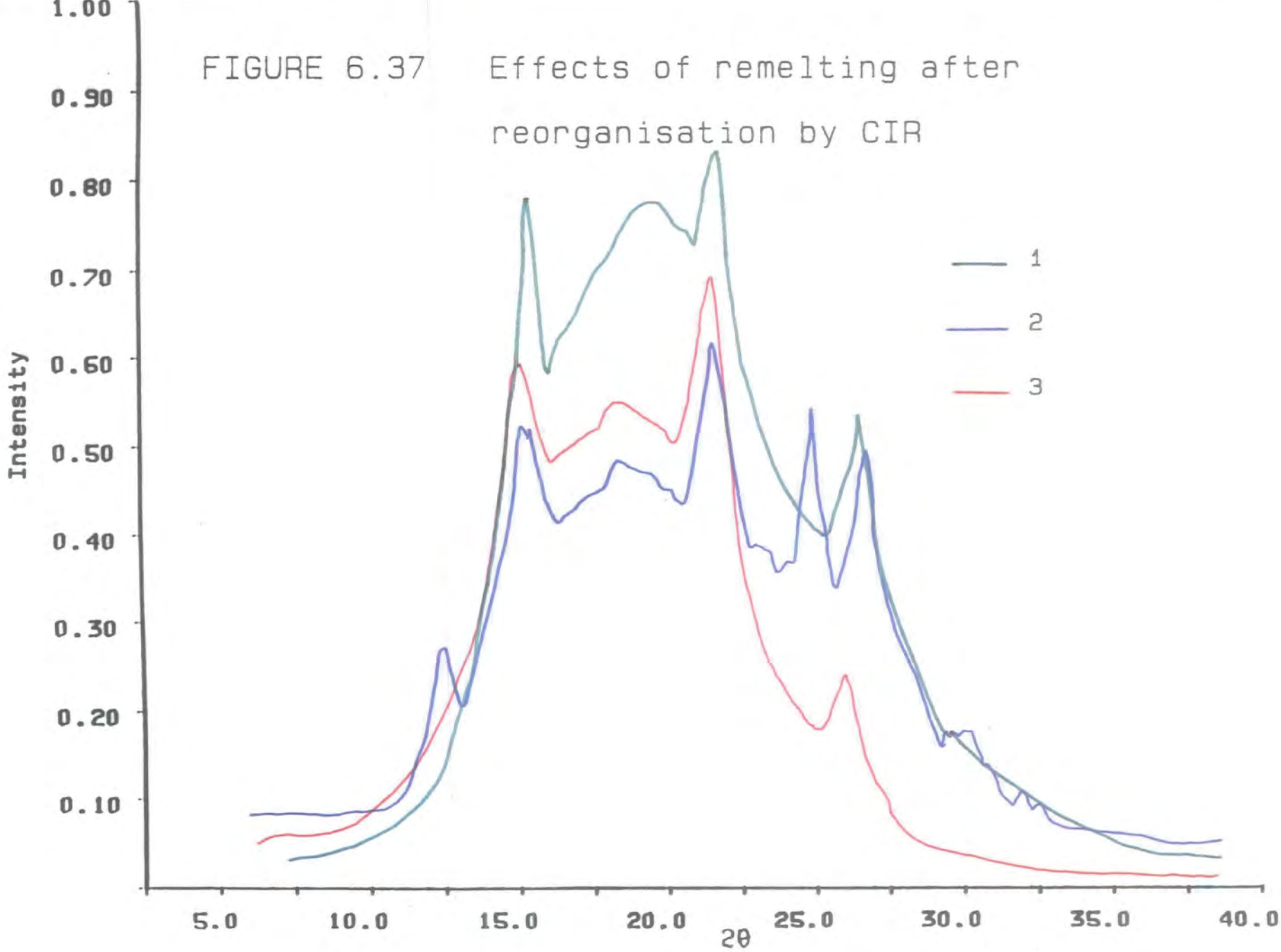

annealing (I) under the following conditions:

(IV) CIR sample annealed for 15 minutes below the melt (@330°C) and quenched to ambient temperatures.

The annealing process was carried out under isothermal conditions in the DSC cell.

From a comparison of the DSC scans for I and IV, the heats and temperatures of fusion have increased as a result of annealing. Microscopy studies confirm that no liquid crystalline phase is apparent and that degradation occurs immediately on melting. The quantitative results obtained are listed in Table (6.10). Unfortunately it was impossible to obtain a WAXS diffractogram of IV, however sufficient evidence exists to confirm that the extent of ordering I increases further as a result of annealing below the melt.

SAMPLE	T_m / °C	ΔH_f / Jg^{-1}	ENDOTHERM	L.C. PHASE	x_{cr} / %
I	345	37	s	x	30
II	300	8	m	√	18
III	292	5	m	√	14
IV	358	33	s	x	-

s ≡ single m≡ multiple

Table 6.10 Effects of Annealing LCP above and below the Melt after the CIR Reaction

6.6 *Conclusions*

LCP is observed to undergo the CIR reaction both above and below the melt. The presence of the selected interchange catalyst, potassium acetate does not influence structural development. Plausible explanations for the negligible catalytic effects could include: the incorrect choice of catalyst; an insufficient quantity of catalyst; or perhaps the kinetics of the rearrangement is not the major controlling factor.

No trends are apparent for CIR reactions carried out at the onset of melting however, from the limited results, LCP is thought to be randomising under these conditions as a function of time. These results are contradictory to those obtained for other reaction temperatures studied however, their accuracy is considered to be suspect due to the limited data and fluctuations in reaction temperature.

In general the degree of ordering increases as a function of reaction temperature both below the melt and in the anisotropic melt.

In particular, for reaction in the anisotropic melt and to a limited extent, reaction below the melt, structural rearrangement occurs for the higher reaction times studied, confirmed by significant increases in the heats and temperatures of transition and % crystallinities. Ultimately, as confirmed by thermal analysis and WAXS studies, a structure very similar to that of poly(HQ/IA) develops, indicating that the initial random polymer converts to a more ordered predominantly HQ/IA block structure.

As expected, where an increase in structural ordering is observed, the resulting LCP samples prove to be insoluble in any known non-degrading solvent system.

For CIR samples exhibiting the highest degree of ordering and rearrangement, no anisotropic phase was observed prior to degradation.

From the results given in Chapter 5, transesterification is known to occur extremely rapidly above the polymer melt which could consequently result in randomisation. Hence it is not surprising that annealing of the rearranged LCP samples above the melt leads to the reversion of the block structure to the initial random structure. In contrast,

order is enhanced further as a consequence of annealing rearranged LCP just below the melting temperature.

In summary, Lenz's theory holds for LCP samples annealed both in the solid state and in the anisotropic melt, irrespective of the presence of the selected interchange catalyst.

6.7 *References*

(1) Gilkey, R and Caldwell, J. R., *J. Appl. Polym. Sci.* 2 (5) 198, (1959).

(2) Charch, W. H. and Shivers, J. C., *Text. Res. J* 29 539 (1959).

(3) Kresser, P. Faserforsh. *Textiltech*, 11 353 (1960).

(4) Tippetts, E. A. and Zimmerman, J., *J. Appl. Polym. Sci.* 8 2465 (1964).

(5) Lenz, R. W. and Go, S., *J .Polym. Sci. Polym. Chem. Ed.* 11 2927 (1973).

(6) Lenz, R. W. and Go, S., *J. Polym. Sci. Polym. Chem. Ed.* 12 1 (1974)

(7) Muhlebach, A. Economy, J., Johnmson, R. L., Kams,T., and Lyeria, J., *Macromolecules* 23 1803, (1990)

(8) Jackson, W. J., Jr, Kuhfuss, H. F., *J. Polym. Sci. Polym. Chem. Ed.*, 14 2043 (1976)

(9) Kugler, J., Gilmer, J. W., Wiswe, D. W., Zachmann, H. G. K., Fischer, E. W., *Macromolecules* 20 1116, 1987

(10) Devaux, J., Godard, P., Mercier, J. P., *J. Polym. Sci. Polym. Phys. Ed.* 20 1901, 1982

(11) Ramjit, H. G., Sedwick, R. D., *J. Macromol. Sci. Chem.* A10 815 (1982)

(12) Kotliar, A. M., *J. Polym. Sci. Macromol. Rev.* 16 367 (1981)

(13) MacDonald, W. A., McLenaghan, A. D. W., McLean, G., Richards, R. W., King, S., *Macromolecules* (in press) (1991)

(14) Lenz, R. W., and Chen, G., *Polymer*, 26 1307 (1985)

(15) Lenz, R. W., Jin, J-I, Feichtinger, K. A., *Polymer*, 24 327 (1983)

(16) Lenz, R. W., Miller, W. R., and Pryde, E. H., *J. Polym. Sci.* A-1 (8) 429, (1970)

(17) Lenz, R. W., Martin, E., Schuler, A. A., *J. Polym. Sci. Polym. Chem. Ed. 11 2265* (1973)

(18) Lenz, R. W., O'Hata, K. and Funt, J., *J. Polym. Sci. Polym. Chem. Ed.* 11 2273 (1973)

(19) Schulken, R. M. Jr., Boy. R. E. Jr., Cox, R. H. *J. Polym. Sci. (C)* 6 17 (1964)

(20) Lenz, R. W. and Schuler, A. N., *J. Polym. Sci. Polym. Symp*: 63 343 (1978)

(21) Economy, J., Volksen, W., Viney, C., Geiss, R., Siemens, R., Karis, R., *Macromolecules*, 21 2777, (1988)

(22) Muhlebach, A., Lyeria, J., Economy. J., *Macromolecules*, 22 3741 (1989)

Chapter 7

General Summary and Suggestions For Further Work

To date an understanding of the fundamental physical properties of liquid crystal polymers in general, remains unexplained due partly to the fairly recent breakthrough in the discovery and design of these materials and the difficulties involved in their synthesis and characterisation. Thus the literature available on these materials is limited. This work provides another piece to the jigsaw in an attempt to build an understanding of the thermal behaviour of these materials.

As discussed in Chapter 2, wholly aromatic, para-linked polyesters can lead to the formation of crystalline polymers with melting points above their decomposition temperatures; hence the liquid crystalline phase will not be visible prior to decomposition. Consequently, these polymers are designed in such a way as to reduce their melting points significantly. LCP is composed of wholly aromatic units, but its design allows a stable liquid crystalline phase to be achieved by incorporating kinks in the otherwise linear chain via the use of the isophthalate unit and its random monomer sequence distribution.

In general, the synthesis of liquid crystal polymers is well established, where many are prepared via transesterification reactions leading to chemically disordered backbones. LCP falls into this category and hence it was felt important to understand how the chemical disorder along the chain influences phase structure in the fluid state, since the monomer sequence distribution has been found to be of significant importance in controlling the properties and to be a sensitive factor in the thermal behaviour of copolymers.

The primary aim of this work was to synthesise a chemically ordered version of LCP. From the literature, the synthesis of ordered-disordered chemical analogues of main-chain liquid crystal polymers proves extremely difficult due to either the problems associated with finding suitable polymerisation methods to synthesise ordered material

due to the insoluble nature of the chains or the inability to carry out a reaction at temperatures which are sufficiently low, to avoid transesterification and thus disruption of the monomeric sequence distribution in the chain. If successful, a back to back characterisation of both chemical analogues could be carried out. Chapter 2 discussed the attempted synthesis of an ordered version of LCP via two different routes, based on low temperature polymerisation reactions. Route 1 was based upon the interfacial polycondensation of a rigid, symmetric monomer with isophthaloyl dichloride. The stepwise synthesis of the monomer reached the stage where the increasing length and rigidity of the molecule rendered it insoluble, thus preventing further reaction. After exhaustive attempts at the synthesis, the experiment was terminated. Route 2 involved the synthesis of an asymmetric monomeric diol, which was to be reacted with isophthalic acid via a solution polymerisation to produce a partially ordered analogue of LCP. However due to numerous failed attempts at removing impurities from the monomer system, further reaction was inhibited and due to lack of time, the synthesis was again abandoned. The remainder of the present work, thus concentrated on the characterisation of random LCP only.

Molecular and configurational studies have been carried out previously on LCP (Chapter 5, reference 32) and a very limited thermal calorimetric study was undertaken in order to deduce vital study regions. From these limited studies it became obvious that the thermal behaviour of LCP was unique and far from simple, hence the major aim of this work was established; a thorough study of the thermal behaviour of LCP under various conditions. A simultaneous study of the structural changes in LCP as a function of temperature and time was carried out.

Polymers in general are extremely difficult to characterise due to the insolubility of these materials in common, non-degrading solvents, thus the use of standard characterisation techniques is restricted and often impossible. In addition, the thermal behaviour of many main-chain liquid crystal polymers is complex, due to their semi-crystalline nature.

Chapters 3-6 concentrate on the thermal treatment, consequent behaviour and characterisation of LCP using a range of diverse techniques. Since the thermal behaviour of polymers has been found to be extremely sensitive to thermal history, rate of heating/cooling and annealing, these parameters were studied under selected conditions.

The thermal transitions and mesophase texture were identified using hotstage microscopy and quantified using DSC. In summary LCP powder, as purified, is practically amorphous at ambient temperatures. The polymer begins to crystallise above the glass transition (T_g = 130°C) and crystallisation continues as a function of temperature until melting begins at 270°C. A nematic phase develops around 300-330°C. Thus LCP is classified as a thermotropic, nematic polyester. The nematic structure which develops upon melting is retained on quenching. This explains why the crystallisation exotherm observed after the glass transition in the initial heat disappears on reheating the sample. Thus the polymer retains some of the order developed in the mesophase. Experiments confirm that annealing below the melt does not appear to influence the thermal behaviour of LCP. In contrast, annealing at the onset of melting increases the degree of crystallinity in LCP due to sufficient mobility allowing the chains to order. However, annealing above the melt results in the ordered polymer reverting back to its random structure. This observation is attributed to rapid ester-interchange occurring at elevated temperatures and is confirmed by the results obtained from the interchange studies in Chapter 5. The highest annealing time used in these studies was 60 minutes. Microscopy results reveal that solvent-cast LCP films are slightly more crystalline than LCP powder at ambient temperatures suggesting that a small extent of ordering occurs on solvent addition. This finding coincides with the absence of the crystallisation exotherm, present in the DSC thermograms of LCP powder and from WAXS studies, again comparing 2Θ scans of LCP powders and films, as discussed in Chapter 4.

From microscopy, films exhibit nematic melts at equivalent temperatures to the powder.

DSC studies on the LCP films were abandoned due to the irreproducibility of the thermograms obtained. LCP fibres drawn from the melt are highly ordered due to the high degree of crystallinity observed from DSC and microscopy studies. WAXS studies confirm that the fibres are highly oriented in the draw direction.

The work in Chapter 4 was instigated by the data obtained from the annealing studies in Chapter 3. In general, LCP films were annealed at temperatures and times judiciously selected from thermal analysis results. Chapter 3 confirmed that the thermal behaviour of LCP could be altered significantly via annealing over comparatively short time periods (0-120 minutes). The main aim of this work was to observe any structural changes in LCP as a result of thermal annealing over selected conditions, using WAXS techniques.

In polymer science, x-ray diffraction is a powerful technique used frequently to provide information on the arrangement and form of packing of molecules. In this study WAXS is used to carry out a qualitative study on phase identification and any structural rearrangement or developments as well as the quantitative evaluation of crystallinity, as a function of annealing conditions, using both flat film camera and diffractometer techniques. For the majority of samples studied, the degree of crystallinity was evaluated. These values are of significant importance in the investigation of LCP's morphology and coincide with the changes in crystallinity deduced from the heats of transition obtained by DSC in Chapter 3.

Essentially, WAXS analysis of LCP complements the thermal analysis study and consequently leads to a thorough understanding of the thermo-structural behaviour of LCP.

WAXS photographs confirmed the mesophase type to be nematic, the random orientation present in LCP and the ability of melt-drawn fibres to form highly oriented structures. The limited quantitative studies undertaken confirmed that in general, the % crystallinities of the LCP samples increased as a function of temperature and time. The

crystallinity of unannealed LCP powder was practically negligible whereas the unannealed film demonstrated up to 14% crystallinity. An amorphous melt was observed at 330°C however ordering occurred as a function of time, confirmed by the development of Bragg peaks and thus an increase in crystallinity. A maximum crystallinity of 24% was evaluated for LCP annealed in the region of the crystallisation exotherm at T = 180°C for 60 minutes. In summary, although ordering increased as a function of annealing conditions, no significant structural rearrangement was observed.

The results obtained correlate well with those obtained in Chapter 3, however these studies are far from complete due to limited usage of the WAXS apparatus and failed attempts to gain access to further desired scattering facilities. The present work leads to a number of suggestions and unanswered questions, as well as forming a firm foundation for future work. These suggestions are summarised below:

1) DSC/WAXS studies: Daresbury Laboratories, U.K.

Experiments using these facilities were proposed for July 1990 but unfortunately were unable to be scheduled. Use of this apparatus would facilitate the study of any variations in structural/transition behaviour of LCP as a function of annealing temperature and time. The following questions could be resolved from such studies.

a) What is the significance of heating rate on structural development?

b) How do the crystalline peaks develop as a function of time under isothermal conditions?

c) Could the degree of order be increased even further by annealing the LCP samples for extended times?

d) What are the relationships between crystallinity, enthalpy and entropy? Do these values vary considerably as a function of annealing temperature or time?

2) Further studies involving greatly extended annealing times could help resolve the obvious structural developments already observed under mild annealing conditions and may provide a significant link to the full understanding of the crystallisation induced process which LCP experiences under severe annealing conditions, where blocky

structures are observed to develop as discussed in Chapter 6.

SANS has proven to be an excellent technique in the structural determination of condensed matter including polymers. The main unique property of this technique is the vast difference in scattering observed between deuterium and hydrogen. In addition, due to the chemical similarity of these molecules, the changes in physical properties due to mixing are negligible. The importance of the ester-interchange reaction has been stressed throughout this work. Transesterification is defined as the interchange reaction occurring between esters, where the number of chain ends cleaved is equal to the number of chain ends recombined, thus the overall molecular weight of the polymer remains unchanged. The transesterification process and the resultant types of polymers formed, have been studied in depth in the literature, however few publications exist on the kinetics and mechanism of the reaction. Limited studies have been carried out on PET, a semi-flexible polymer, hence it was thought relevant to carry out similar studies on rigid LCP in order to deduce whether or not, the nature of the polymer backbone influences the kinetics of transesterification.

The work in Chapter 5 aims to carry out a complete study of the mechanism and kinetics of transesterification in LCP using SANS techniques. Of significant interest to the work in this thesis, was to observe whether this reaction takes place in the solid phase; the temperature range over which it occurs and the rates of the reaction under selected conditions. As discussed in Chapter 5, Kugler studied the kinetics of transesterification in PET using a combination of SANS and light scattering techniques. He established that the reaction followed Arrhenius behaviour and from his analysis, the kinetic parameters were calculated. Benoit proposed an alternative theoretical analysis of data obtained solely from the SANS spectra. The data could then be used to interpret the kinetics of the reaction. Benoit's theory was applied to the study of transesterification in LCP. A partially deuterated LCP of equivalent molecular weight to the hydrogenous version was synthesised. Previous studies (Chapter 5, reference 23) showed that

transesterification occurred within the temperature range: 523-603K. From these results and those obtained by DSC as discussed in Chapter 3, suitable annealing conditions were selected. The polymers were blended and films were prepared and annealed for use in the SANS diffractometer. The transesterification process leads to the formation of hydrogenous/deuterated copolyesters. During this reaction, the molecular weight of the isotopically labelled LCP appears to decrease as a function of temperature and time. From analysis of the scattering data, the activation energy of transesterification is calculated. This value is in line with that obtained for PET from Kugler's studies, confirming that the mechanism for the transesterification reaction is identical for both the flexible and the rigid polymers.

Benoit proposed that transesterification could be initiated by active chain ends, where the active end is transferred from one chain to another, and further reaction continues. The rate constant for this mechanism is dependent upon the concentration of chain ends present and thus the overall initial molecular weight of the polymer. Consequently, the higher the initial molecular weight, the lower the number of active chain ends and the lower the rate constant. The rate constants were calculated for two LCP samples of differing initial molecular weights and these were compared directly to the rate constant obtained for low molecular weight PET at a selected temperature. This comparison presumes that the transesterification mechanism is identical for both polymers, which is proposed to be the case from the activation energies calculated.

The results demonstrate the rate constant to be a decreasing function of increasing initial molecular weight suggesting that transesterification does indeed proceed via an active chain end mechanism. Further work studying a range of flexible, semi-flexible and rigid polymers using both identical conditions and analytical methods would confirm these feasible observations.

The literature discusses the formation and behaviour of a vast number of polymers prepared via ester-interchange reactions. Several publications report on the initial formation of block copolymers via transesterification of a blend of two or more homopolymers at elevated temperatures. However, as the reaction proceeds, the polymer chains become increasingly shorter until finally at equilibrium, a random copolyester is formed. In contrast Lenz and co-workers have explored a unique route to the formation of highly blocky structures via a process termed, CIR. This process is based on the transesterification reaction and involves the thermal annealing of selected copolyesters close to their melting points in the presence of an ester-interchange catalyst. Consequently, non-equilibrium blocky polymers are formed. Analyses demonstrates that both the melting points and crystallinity of the initial copolyesters increased during the reaction. These observations, supported by NMR data on monomer sequence distribution, confirmed that the overall blockiness had increased. More recent studies by Lenz, demonstrated that the CIR process could occur in the anisotropic melt of selected liquid crystalline polyesters.

The present study aimed to establish whether the CIR process could occur in random LCP leading to the development of a blocky structure or whether the copolyester simply continues to randomise due to ester-interchange in the melt. Chapter 6 attempts to mimic Lenz's work in the study of LCP powder samples. The possibility of these reactions occurring in LCP were studied both below and at the onset of melting as well as in the anisotropic melt over extended reaction times. The annealing temperatures were selected from thermal analysis data and the reaction times were selected from Lenz's work, ranging from 0-72 hours. The interchange catalyst selected was potassium acetate (the catalyst used in the polymerisation of LCP) used at a concentration of 5%. This value was chosen at random based on Lenz's observations. LCP was observed to undergo the CIR process both above and below the melt. The presence of the catalyst did not have any influence on structural development. This could be due to either an

insufficient amount, or an incorrect choice of catalyst; or simply the possibility of the kinetics not being an influencing factor on the process. In general, the degree of ordering increases as a function of reaction temperature, suggesting that thermodynamics plays a significant role in the reaction.

WAXS, DSC and microscopy techniques were used to characterise the CIR samples for selected reactions carried out both below the melt and in the anisotropic melt. Structural rearrangement takes place for the higher reaction times studied, confirmed by significant increases in the heats and temperatures of melting and % crystallinities. Crystallinities of up to 32% were observed for selected CIR samples; a factor of 2-3 times greater than those achieved via the thermal annealing, discussed in Chapter 4.

Thermal analysis and WAXS studies confirmed that a structure very similar to HQ/IPA develops indicating that the initial random polymer converts to a more ordered, predominantly HQ/IA block structure. These results coincide with those proposed by Blundell (Chapter 4 reference (27)).

The CIR samples which exhibit the highest degree of ordering fail to display an anisotropic melt and prove to be completely insoluble in any known non-degrading solvent. Chapter 5 demonstrated that transesterification in LCP is extremely rapid above the melt which could lead to randomisation and therefore explain why annealing the rearranged, highly ordered samples well above their melting point, leads to the reversion of the block structure to the initial random structure. In contrast, order is enhanced further by annealing the rearranged LCP just below its melting temperature. A proposed explanation for this observation is that the energy input is sufficient to promote limited mobility of the polymer chains leading to ordering below the melt, but insufficient to promote randomisation. In summary LCP undergoes the crystallisation-induced reaction both in the solid state and in the anisotropic melt, irrespective of the presence of the selected interchange catalyst.

The present work was merely an initial study of the ability of LCP to undergo the CIR

process; the scope for further studies is extensive.

In order to achieve a greater understanding of which parameters control the reaction rate and to observe any definite trends in the extent of ordering as a function of reaction temperature and time, further studies are essential. Furthermore, it would be advantageous to measure the effects of varying the type and amount of interchange catalyst in order that the optimum, most effective catalytic conditions (if any) in the conversion of a random to a "blocky" structure may be evaluated. Finally a study of the monomer sequence distribution of the resultant samples using solid state NMR was considered in this study however, it was considered to be pointless due to the close similarity of the monomeric units of LCP, rendering them indistinguishable from one another. Further studies could include ^{13}C labelling of one of the monomers in order to accumulate supporting data to confirm the formation of a block copolymer resulting from the CIR process.

Due to the diverse and complex nature of the work presented, the structure of this thesis was chosen to provide a comprehensive, unambiguous study of the liquid crystal polymer (LCP). Consequently an overall discussion of the results obtained was not included. This chapter attempts to rectify this foresight by providing a general summary of the observations made and the results obtained. This proved challenging due to the volume of work and the diverse and individual aspects studied. It is hoped that this summary demonstrates the reasons for carrying out each aspect of the work, in addition to illustrating that that the results prove complementary to one another and ultimately to the overall understanding of polymer's behaviour. The results obtained are far from complete and in some cases the conclusions drawn remain speculative, but as "the Boss" used to preach, "research never stops, but at some stage it is necessary for you to do so" and I did.....eventually!

Index to Appendices

Appendices A and B include ^{1}H NMR, IR and visible spectra of the reagents synthesised in the attempted preparation of a chemically ordered LCP. The spectra are numbered 1-9 and for simplicity, the numbers refer to the same reagent in both appendices. The spectra included are referred to in Chapter 2.

Appendix A/B

1) bis(4-formylphenyl)isophthalate

2) tetrabutylammonium permanganate

3) bis(4-carboxyphenyl)isophthalate

4) bis(4-chloroformylphenyl)isophthalate

5) monocarbobenzoxyhydroquinone

6) p-carbethoxybenzoic acid

7) 4-hydroyphenyl-4-carbethoxybenzoate (section 2.4.3.2(ii))

8) 4-chloroformylphenyl-4-carbethoxybenzoate

9) 4-hydroxyphenyl-4-carbethoxybenzoate (section 2.4.3.2(iv))

Appendix A

^{1}H NMR spectra

1

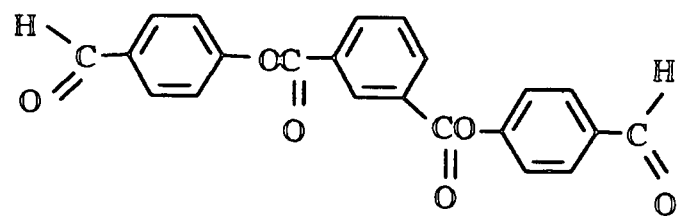

F1= 11.78353
F2= -.18630

#	CURSOR	FREQUENCY	PPM	INTEGRAL	INTENSITY
1	6099	1831.055	7.3204	.001	.435
2	6145	1822.649	7.2868	-.000	.334
3	6164	1819.177	7.2729	.077	24.488
4	6228	1807.481	7.2262	.001	.488
5	11563	832.563	3.3285	-.000	.328
6	11572	830.919	3.3219	.000	.321
7	11670	813.010	3.2504	.167	2.064
8	11786	791.812	3.1656	.000	.327
9	13015	567.225	2.2677	.000	.324
10	13132	545.844	2.1822	-.000	.323
11	13138	544.748	2.1779	.002	.699
12	13858	413.175	1.6518	.199	2.123
13	14125	364.384	1.4568	.114	2.250
14	14162	357.622	1.4297	.064	2.212
15	14263	339.165	1.3560	-.000	.343
16	14696	260.039	1.0396	.093	4.186
17	14733	253.278	1.0126	.117	7.737
18	14771	246.334	.9848	.056	3.473
19	14832	235.186	.9403	.001	.397
20	14838	234.090	.9359	.000	.326
21	14846	232.628	.9300	-.000	.313
22	14855	230.983	.9235	.003	.461
23	14863	229.521	.9176	.001	.362
24	16119	.000	.0000	.001	.616

3.RE FTD?

$((C_4H_9)N_4)MnO_4$

2

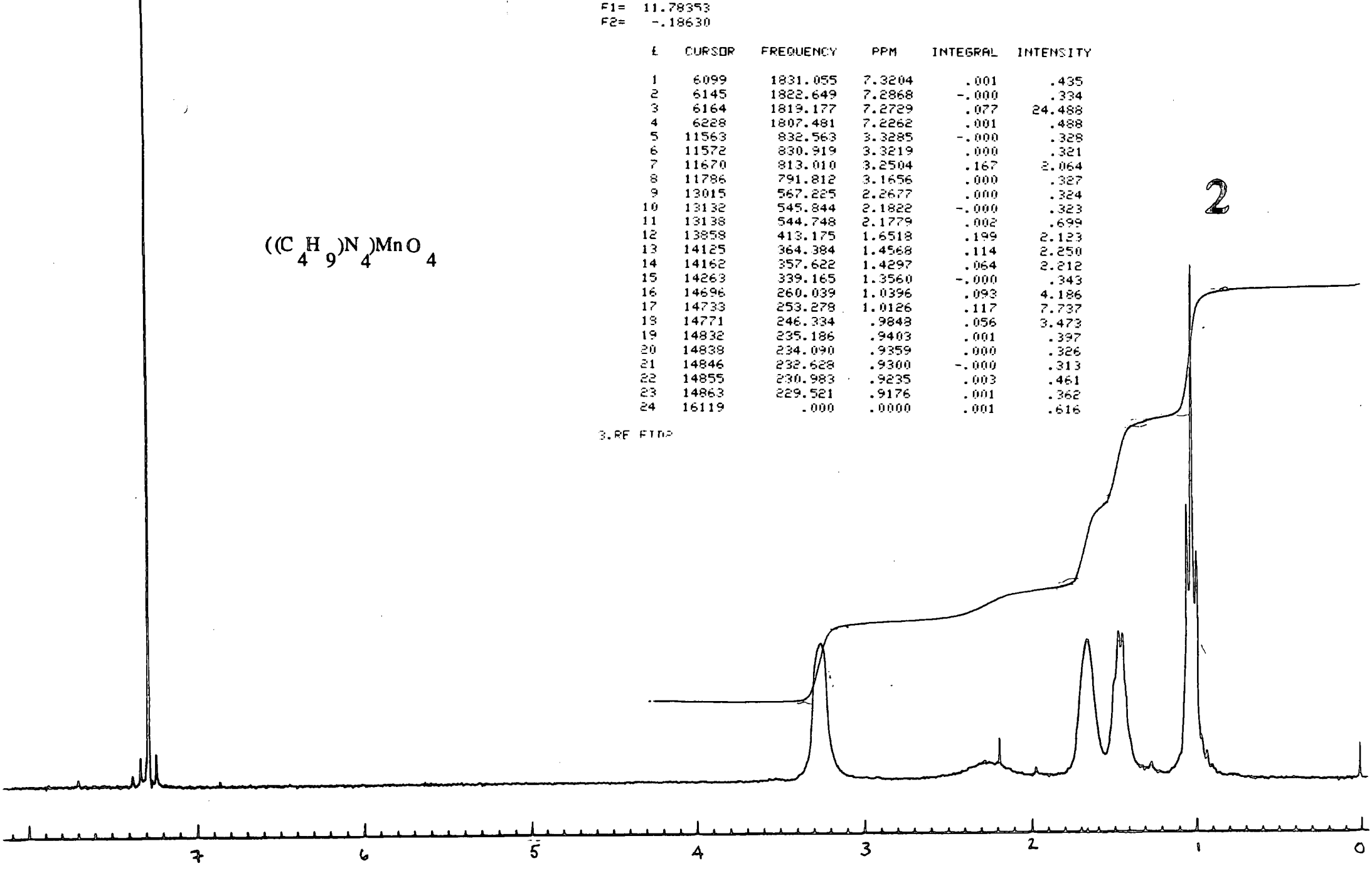

FREQUENCY	PPM	INTEGRAL	INTENSITY
2193.380	8.7690	.152	7.341
2122.335	8.4849	.071	6.648
2120.871	8.4791	.052	6.398
2114.767	8.4547	.074	7.149
2113.058	8.4478	.056	7.129
2016.134	8.0603	.302	16.666
2007.589	8.0262	.319	18.995
1971.701	7.8827	.070	2.930
1963.889	7.8515	.078	4.730
1956.076	7.8202	.032	2.256
1871.603	7.4825	.302	17.880
1862.814	7.4474	.306	16.421
624.533	2.4968	.031	2.377
622.824	2.4900	.026	3.206
621.115	2.4832	.022	2.416

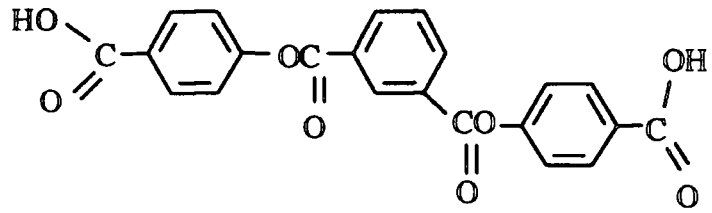

3

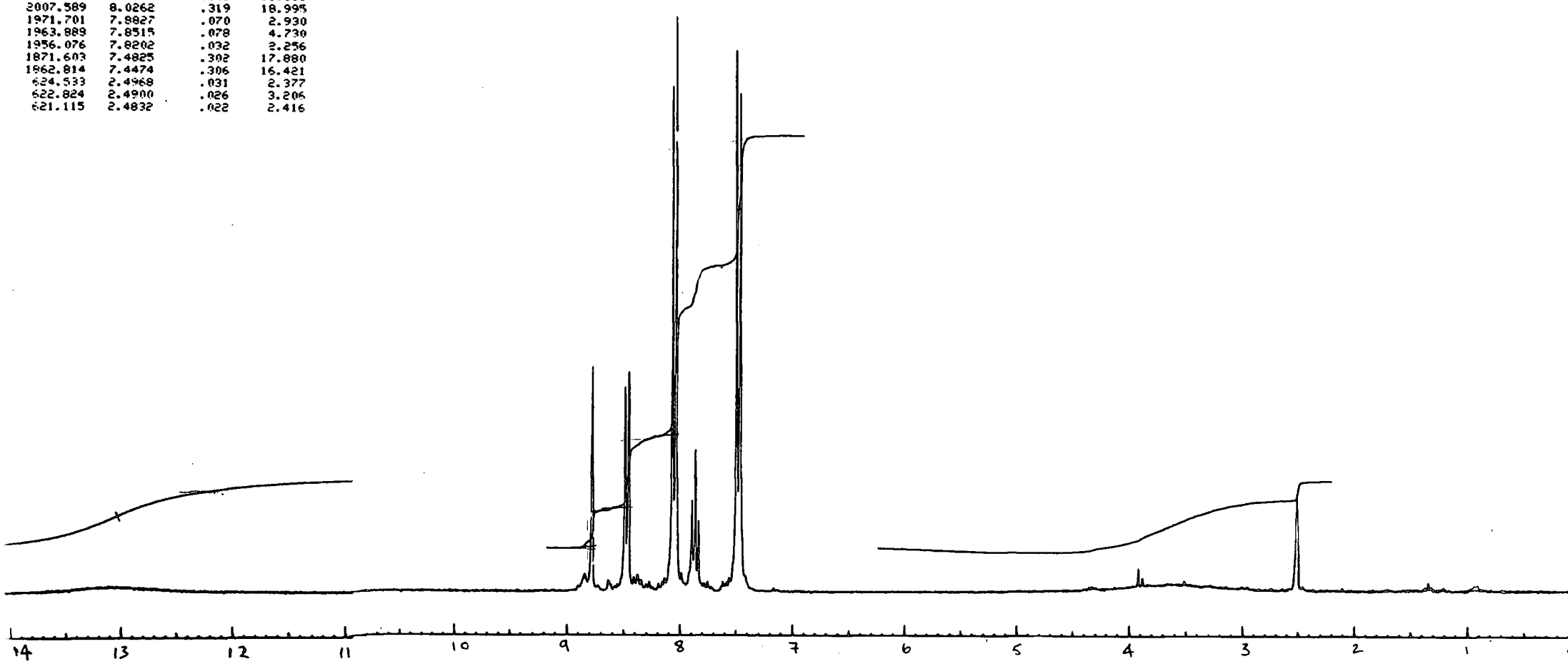

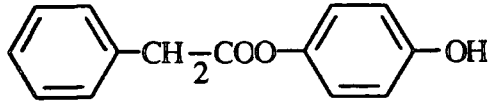
CH2COO
OH

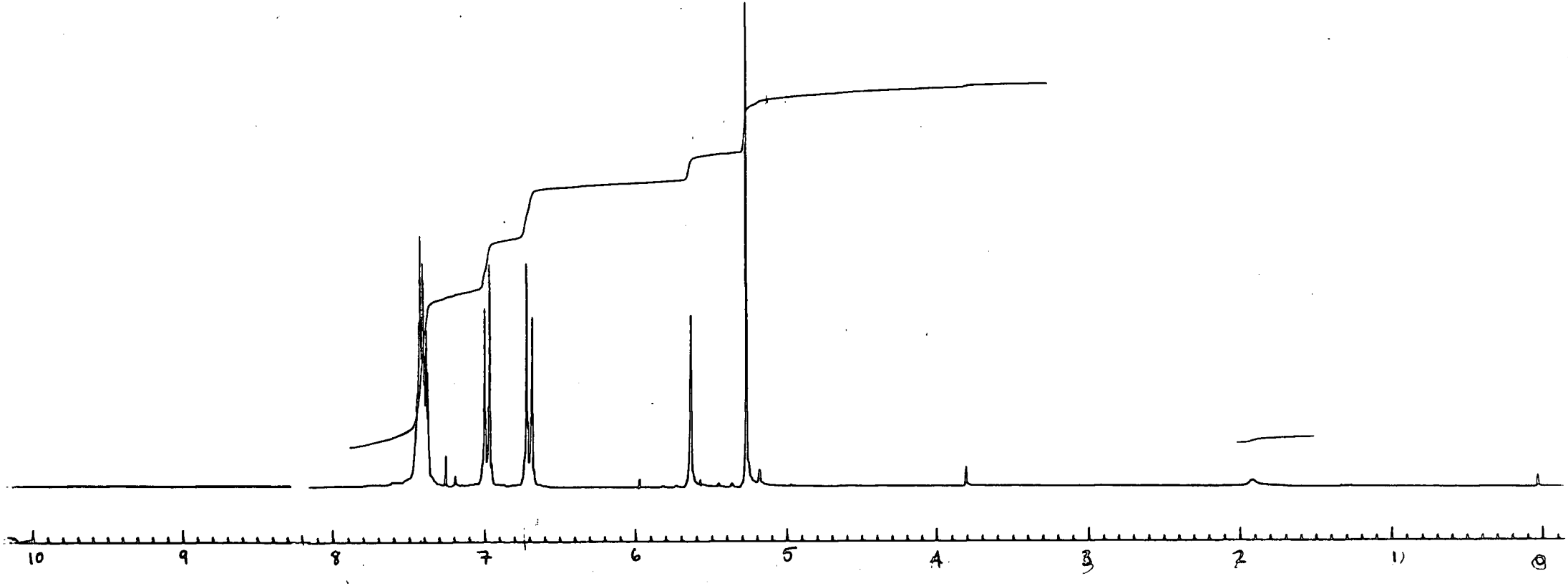
10
9
8
7
6
5
4
3
2
1
0

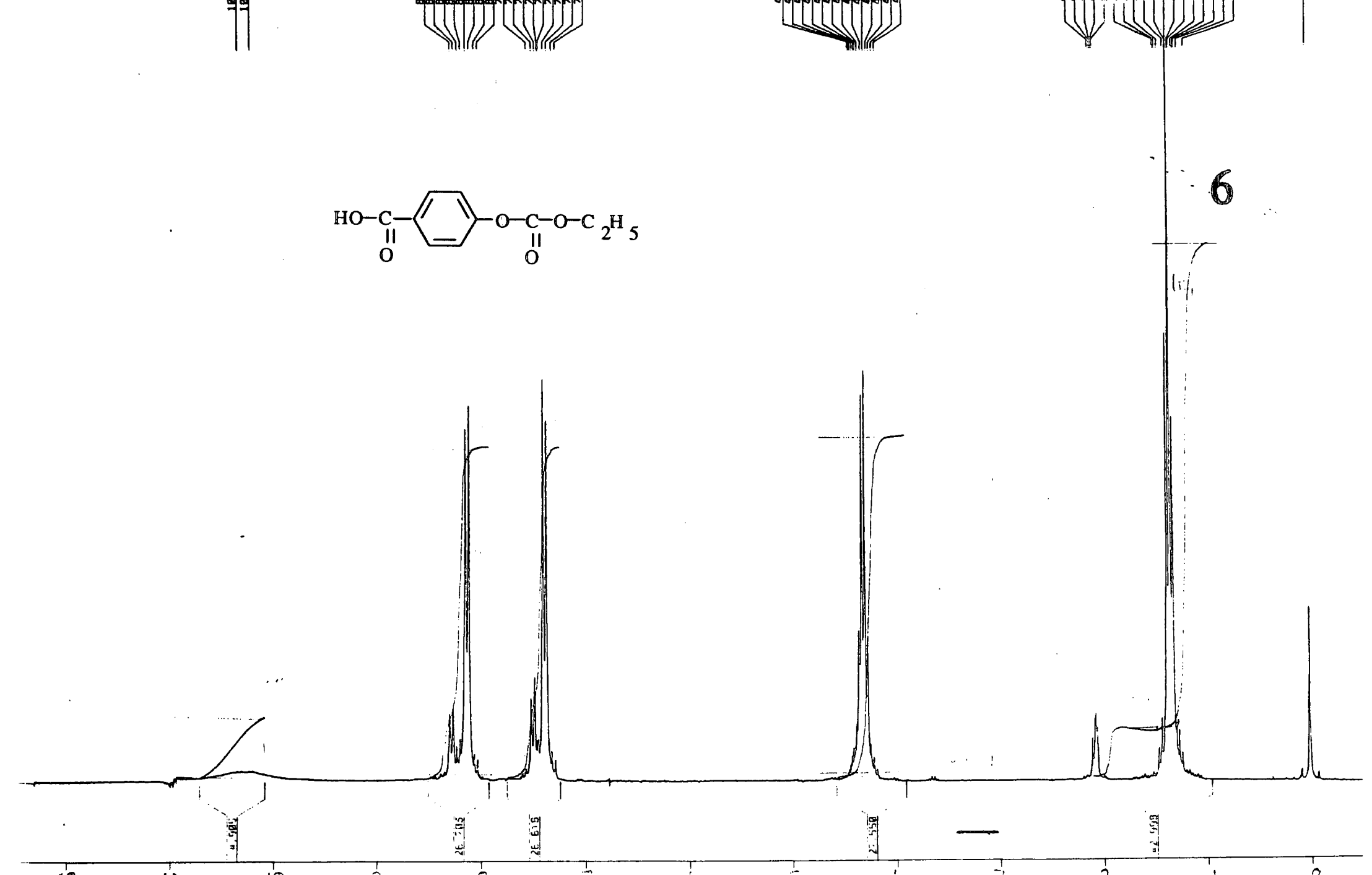
HO–C
O
O–C–O–C 2H 5
O
6

8.390
290.133
4089.000
8192
2994.012

1.000
16

3200.000
53L PO

0.0
CM .239
2885.11

9

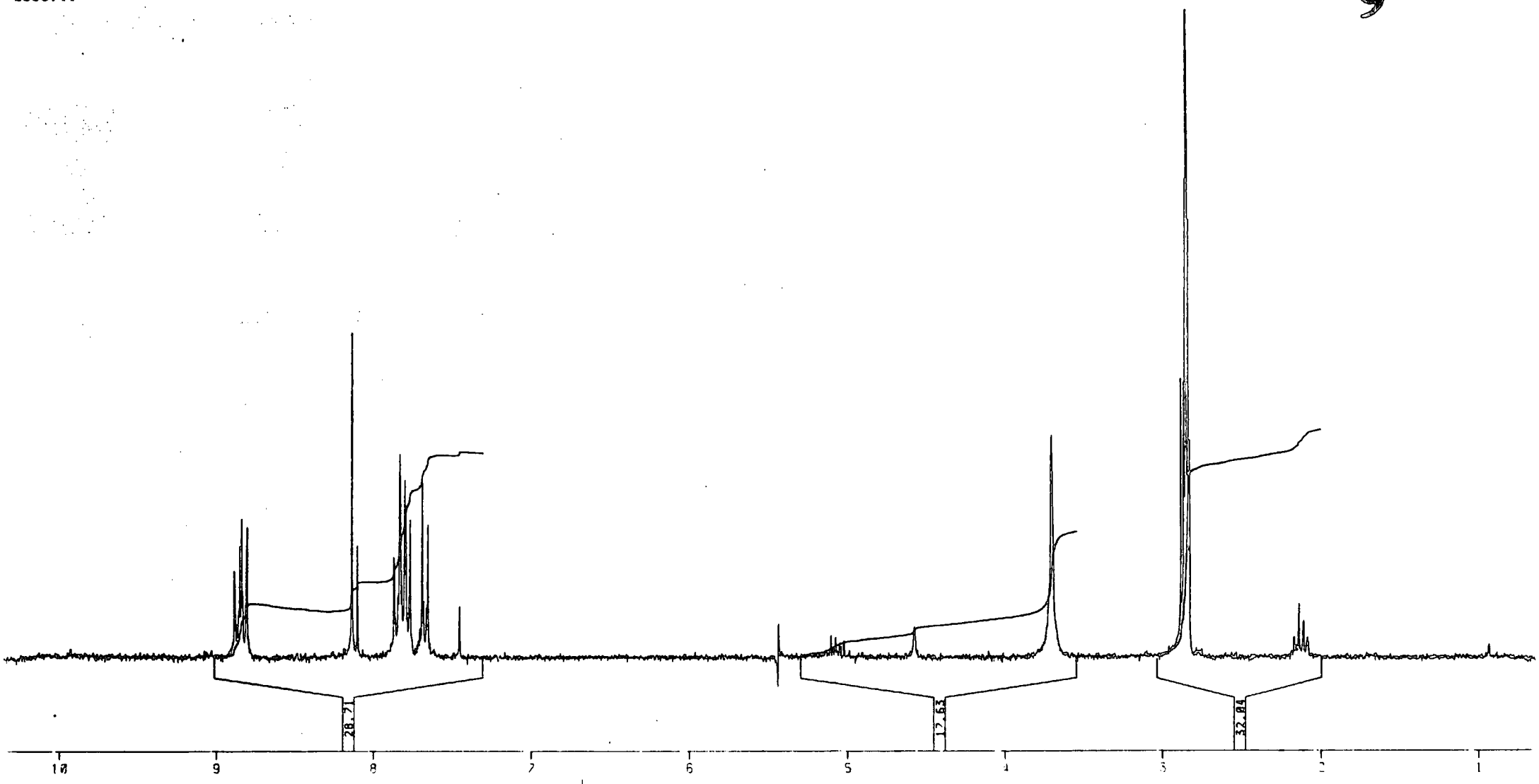

Appendix B

IR/UV/Visible Spectra

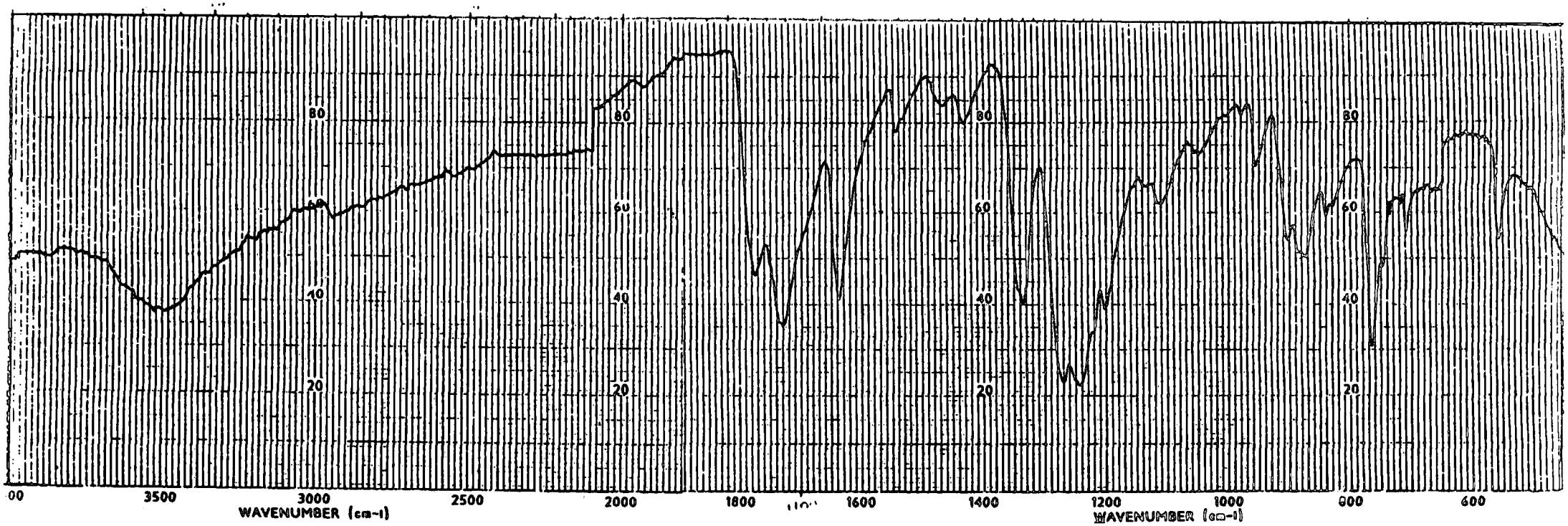
80
60
40
20
3500
3000
2500
2000
1800
1600
1400
1200
1000
800
600
WAVENUMBER (cm-1)

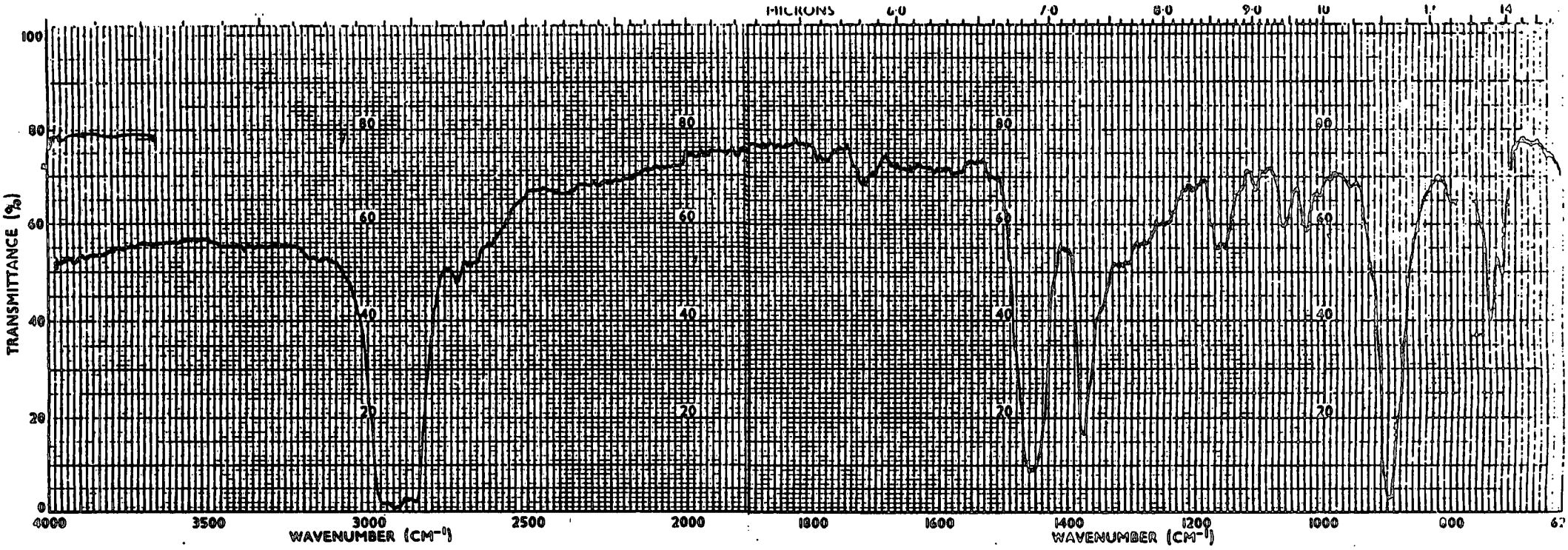
MICRONS
6·0
7·0
8·0
9·0
10
TRANSMITTANCE (%)
100
80
60
40
20
0
4000
3500
3000
2500
2000
1800
1600
1400
1200
1000
WAVENUMBER (CM⁻¹)
WAVENUMBER (CM⁻¹)

2 (a)

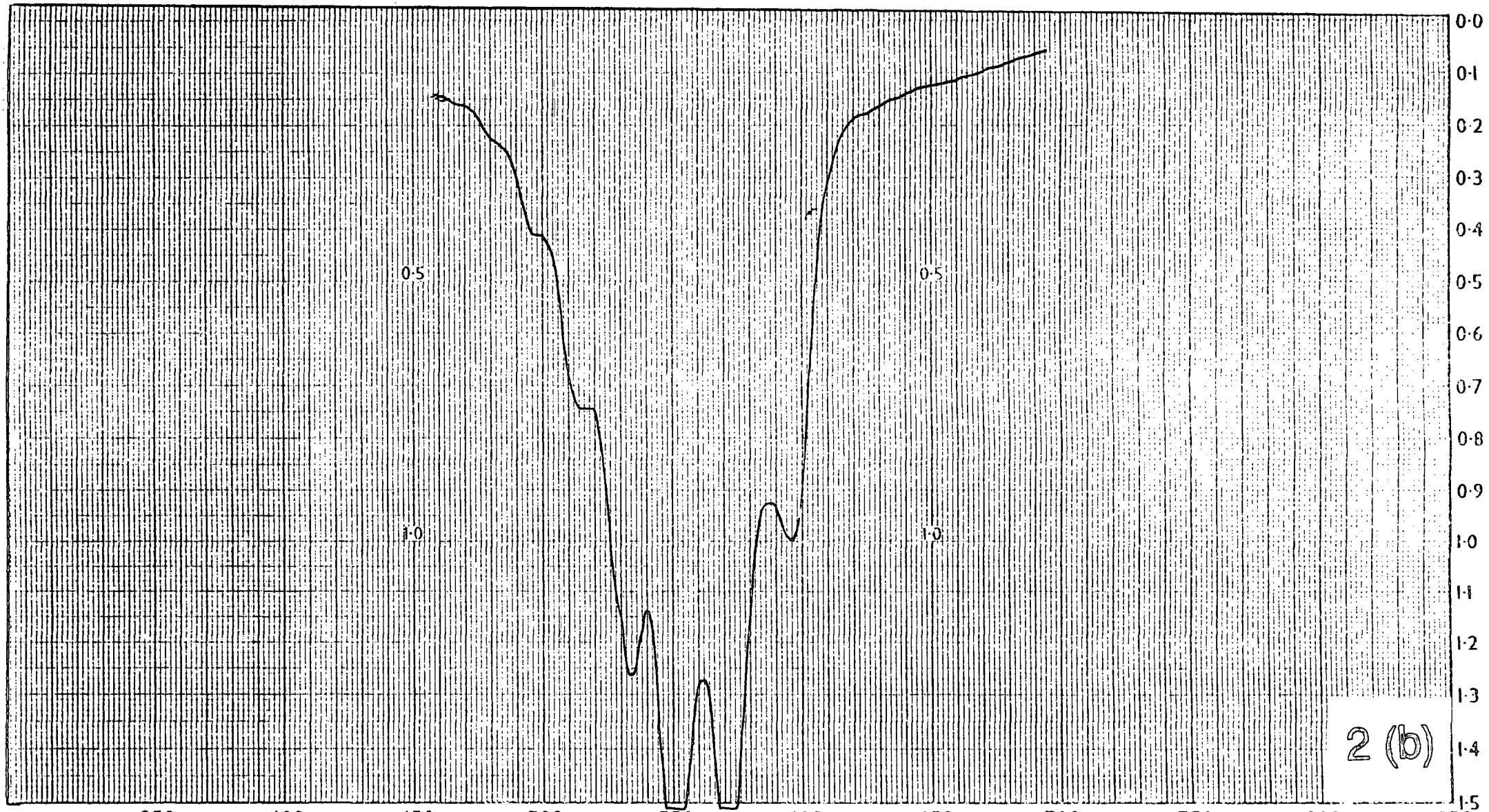
0·0
0·1
0·2
0·3
0·4
0·5
0·6
0·7
0·8
0·9
1·0
1·1
1·2
1·3
1·4
1·5
0·5
1·0
0·5
1·0
350
400
450
500
550
600
650
700
750
800
850
2 (b)

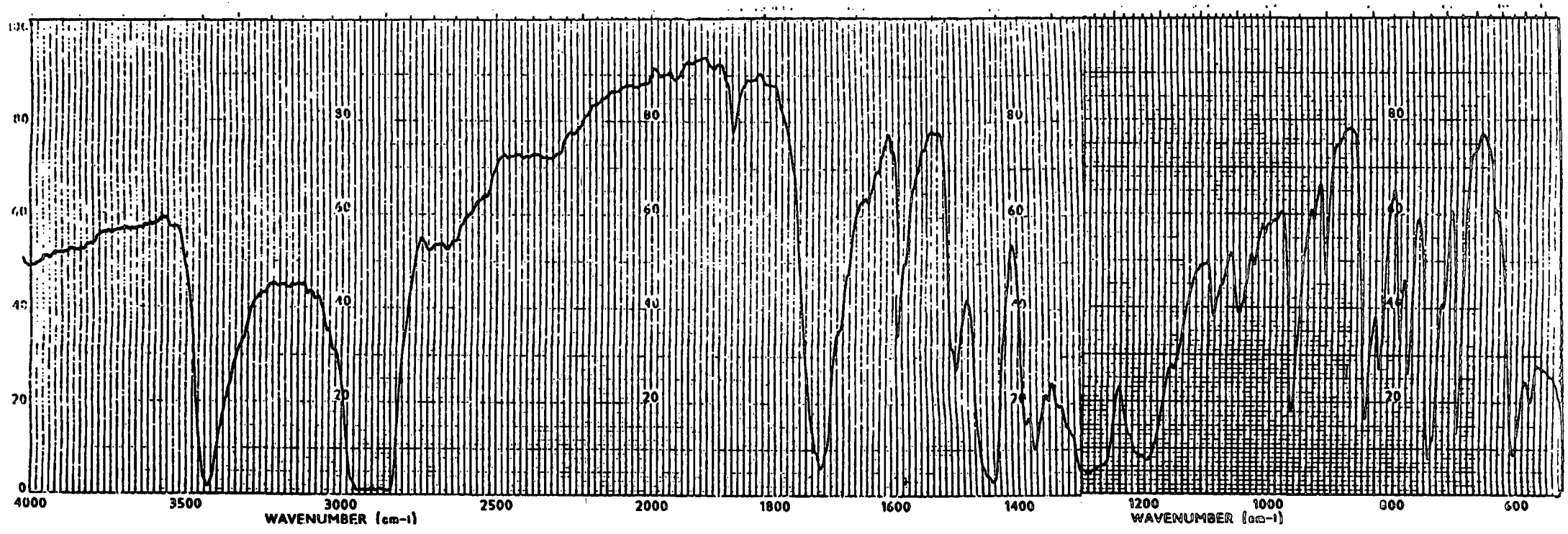
100
80
60
40
20
0
4000
3500
3000
2500
2000
1800
1600
1400
1200
1000
800
600
WAVENUMBER (cm-1)
WAVENUMBER (cm-1)

3

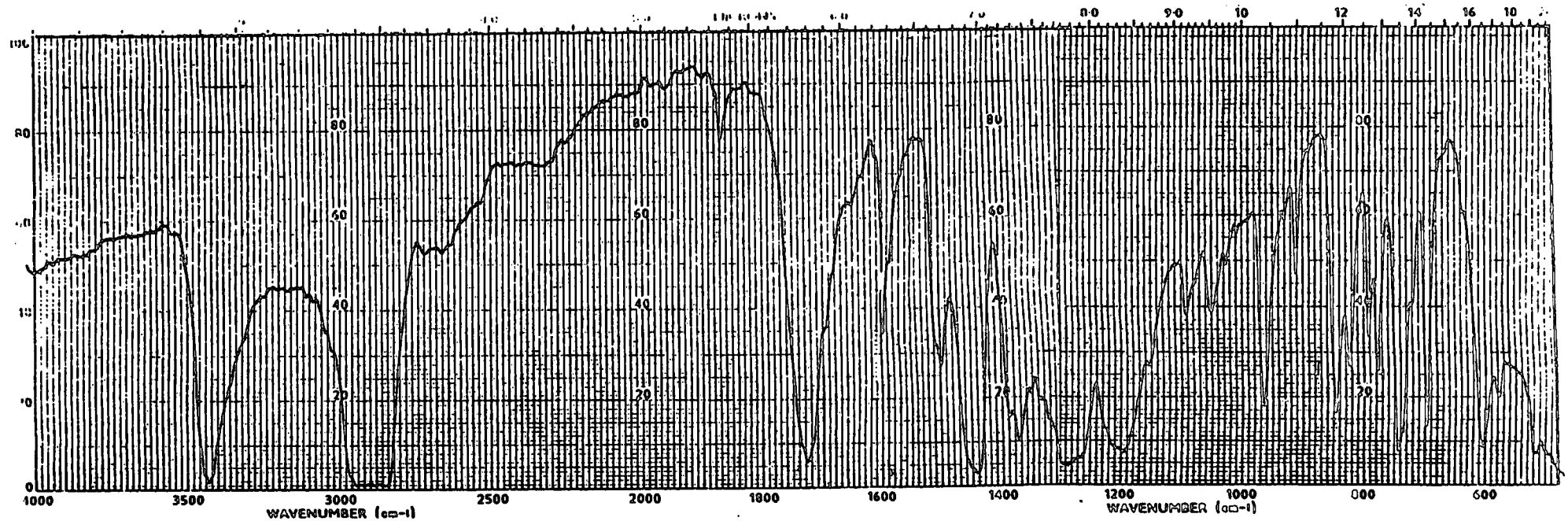
WAVENUMBER (cm-1)
WAVENUMBER (cm-1)

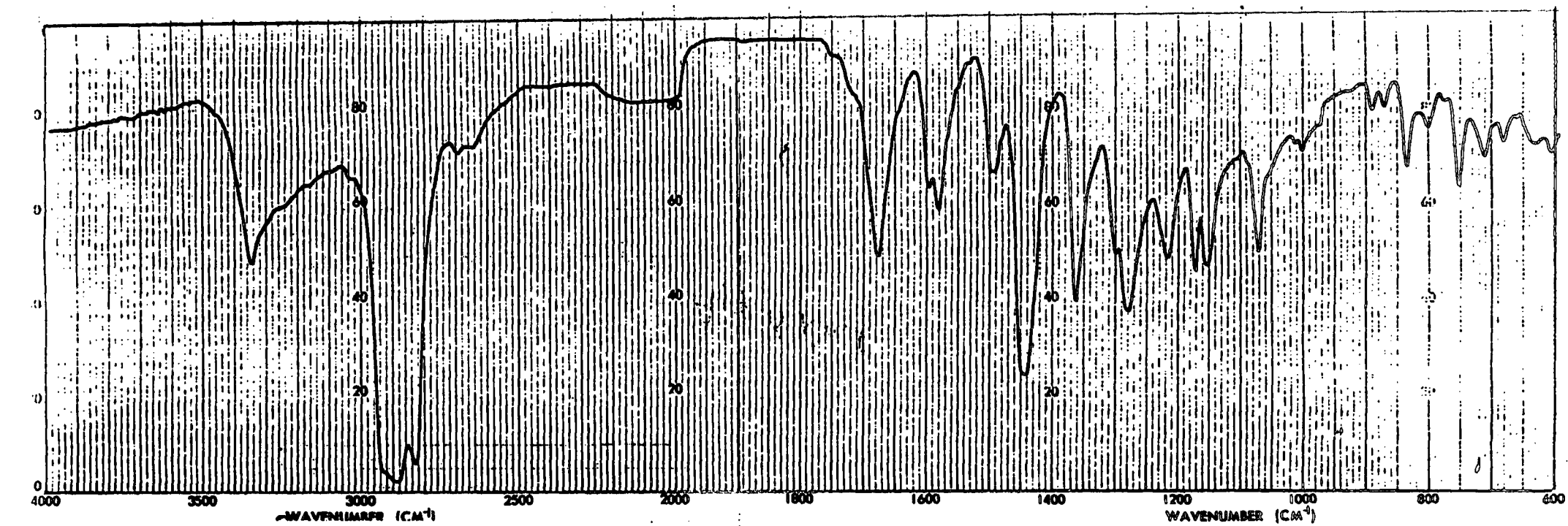
4000
3500
3000
2500
2000
1800
1600
1400
1200
1000
800
600
WAVENUMBER (CM⁻¹)
WAVENUMBER (CM⁻¹)
80
60
40
20

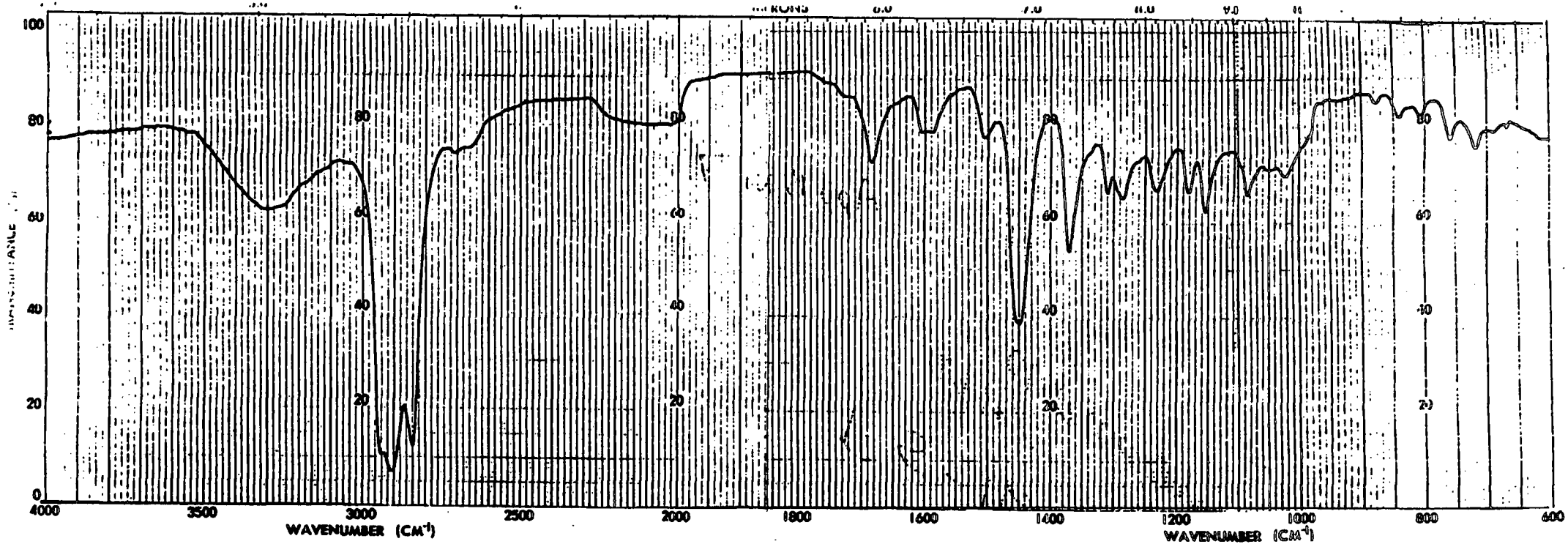
100
80
60
40
20
0
4000
3500
3000
2500
2000
1800
1600
1400
1200
1000
800
600
WAVENUMBER (CM⁻¹)
WAVENUMBER (CM⁻¹)

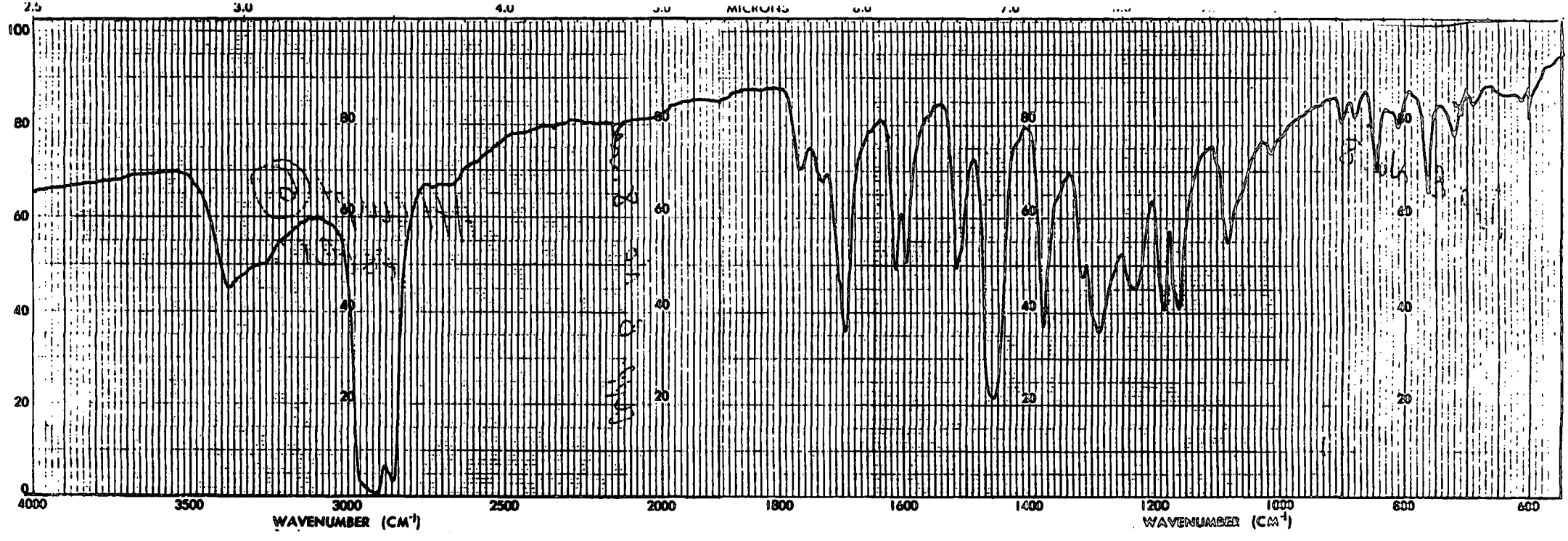
MICRONS
WAVENUMBER (CM⁻¹)
WAVENUMBER (CM⁻¹)
4000
3500
3000
2500
2000
1800
1600
1400
1200
1000
800
600
100
80
60
40
20
0

Appendix C

Research Colloquia, Conferences, Seminars and Symposia

The Board of Studies in chemistry states that each postgraduate research thesis will include an appendix listing the following:

a) all research colloquia, lectures and seminars arranged by the Department of Chemistry during his/her period of study

b) All research conferences and symposia attended by the author during his/her period of study

a) Colloquia, Lectures and Seminars given by invited speakers (October 1989 - September 1991)

Lectures attended by the author are denoted by *

UNIVERSITY OF DURHAM

Board of Studies in Chemistry

COLLOQUIA, LECTURES AND SEMINARS GIVEN BY INVITED SPEAKERS 1ST AUGUST 1989 TO 31ST JULY 1990

YAL, Dr. J.P.S. (Durham University) Breakthoughs in Heterogeneous Catalysis	1st November, 1989
HER, Dr. J. (Odense University) Synthesis of New Macrocylic Systems using Heterocyclic Building Blocks	13th November, 1989
CAW, Prof. J.E. (California Institute of Technology) Synthetic and Mechanistic Approaches to Ziegler–natta Polymerization of Olefins	10th November, 1989
ASDALE, Dr. C. (Newcastle University) The Mode of Action of some Anti–tumour Agents	21st February, 1990
MAN, Prof. J.M. (Emory University) Fitting Experiment with Theory in Ar–OH	23rd March, 1990
LER, Dr. A. (St. Andrews University) The Discovery of Penicillin: Facts and Fancies	7th December, 1989
ETHAM, Dr. A.K. (Oxford University) Chemistry of Zeolite Cages	8th March, 1990
K, Prof. D.T. (ICI Wilton) patially Resolved Chemistry (using Natures's aradigm in the Advanced Materials Arena)	22nd February, 1990
–HAMILTON, Prof. D.J. (St. Andrews University) ew Polymers from Homogeneous Catalysis	29th November, 1989
MBIE, Prof. L. (Nottingham University) he Chemistry of Cannabis and Khat	15th February, 1990
, Dr. U. (Glaxo) ynthesis and Conformation of C–Glycosides	31st January, 1990
IANI, Prof. C. (University of Lausanne, Switzerland) olecular Aggregates – A Bridge between omogeneous and Heterogeneous Systems	25th October, 1989
IAN, Prof. L.S. (USSR Academy of Sciences – Moscow) ew Syntheses in Fluoroaliphatic Chemistry: ecent Advances in the Chemistry of Fluorinated xiranes	9th July, 1990
AM, Dr. D. (B.P. Reserch Centre) ow Proteins Absorb to Interfaces	4th December, 1989
NWOOD, Prof. N.N. (University of Leeds) ovel Cluster Geometries in Metalloborane	9th November, 1989

OLLOWAY, Prof. J.H. (University of Leicester) Noble Gas Chemistry	1st February, 1990
UGHES, Dr. M.N. (King's College, London) A Bug's Eye View of the Periodic Table	30th November, 1989
UISGEN, Prof. R. (Universität München) Recent Mechanistic Studies of [2+2] Additions	15th December, 1989
LINOWSKI, Dr. J. (Cambridge University) Solid State NMR Studies of Zeolite Catalysts	13th December 1989
ANCASTER, Rev. R. (Kimbolton Fireworks) Fireworks – Principles and Practice	8th February, 1990
UNAZZI, Prof. L. (University of Bologna) Application of Dynamic NMR to the Study of Conformational Enantiomerism	12th February, 1990
ALMER, Dr. F. (Nottingham University) Thunder and Lightning	17th October, 1989
ARKER, Dr. D. (Durham University) Macrocycles, Drugs and Rock 'n' roll	16th November, 1989
ERUTZ, Dr. R.N. (York University) Plotting the Course of C–H Activations with Organometallics	24th January, 1990
LATONOV, Prof. V.E. (USSR Academy of Sciences – Novosibirsk) Polyfluoroindanes: Synthesis and Transformation	9th July, 1990
OWELL, Dr. R.L. (ICI) The Development of CFC Replacements	6th December, 1989
OWIS, Dr. I. (Nottingham University) Spinning off in a huff: Photodissociation of Methyl Iodide	21st March, 1990
OZHKOV, Prof. I.N. (USSR Academy of Sciences – Moscow) Reactivity of Perfluoroalkyl Bromides	9th July, 1990
ODDART, Dr. J.F. (Sheffield University) Molecular Lego	1st March, 1990
TTON, Prof. D. (Simon Fraser University, Vancouver B.C.) Synthesis and Applications of Dinitrogen and Diazo Compounds of Rhenium and Iridium	14th February, 1990
OMAS, Dr. R.K. (Oxford University) Neutron Reflectometry from Surfaces	28th February, 1990
OMPSON, Dr. D.P. (Newcastle University) The role of Nitrogen in Extending Silicate Crystal Chemistry	7th February, 1990

UNIVERSITY OF DURHAM

Board of Studies in Chemistry

COLLOQUIA, LECTURES AND SEMINARS GIVEN BY INVITED SPEAKERS
1ST AUGUST 1990 TO 31ST JULY 1991

ALDER, Dr. B.J. (Lawrence Livermore Labs., California) — 15th January, 1991
Hydrogen in all its Glory

BELL†, Prof. T. (SUNY, Stoney Brook, U.S.A.) — 14th November, 1990 ✡
Functional Molecular Architecture and Molecular Recognition

BOCHMANN†, Dr. M. (University of East Anglia) — 24th October, 1990
Synthesis, Reactions and Catalytic Activity of Cationic Titanium Alkyls

BRIMBLE, Dr. M.A. (Massey University, New Zealand) — 29th July, 1991
Synthetic Studies Towards the Antibiotic Griseusin-A

BROOKHART, Prof. M.S. (University of N. Carolina) — 20th June, 1991
Olefin Polymerizations, Oligomerizations and Dimerizations Using Electrophilic Late Transition Metal Catalysts

BROWN, Dr. J. (Oxford University) — 28th February, 1991 ✡
Can Chemistry Provide Catalysts Superior to Enzymes?

BUSHBY†, Dr. R. (Leeds University) — 6th February, 1991 ✡
Biradicals and Organic Magnets

COWLEY, Prof. A.H. (University of Texas) — 13th December, 1990
New Organometallic Routes to Electronic Materials

CROUT, Prof. D. (Warwick University) — 29th November, 1990
Enzymes in Organic Synthesis

DOBSON†, Dr. C.M. (Oxford University) — 6th March, 1991
NMR Studies of Dynamics in Molecular Crystals

GERRARD†, Dr. D. (British Petroleum) — 7th November, 1990 ✡
Raman Spectroscopy for Industrial Analysis

HUDLICKY, Prof. T. (Virginia Polytechnic Institute) — 25th April, 1991
Biocatalysis and Symmetry Based Approaches to the Efficient Synthesis of Complex Natural Products

JACKSON†, Dr. R. (Newcastle University) — 31st October, 1990
New Synthetic Methods: α-Amino Acids and Small Rings

KOCOVSKY†, Dr. P. (Uppsala University) — 6th November, 1990 ✡
Stereo-Controlled Reactions Mediated by Transition

LACEY, Dr. D. (Hull University) Liquid Crystals	31st January, 1991
LOGAN, Dr. N. (Nottingham University) Rocket Propellants	1st November, 1990
MACDONALD, Dr. W.A. (ICI Wilton) Materials for the Space Age	11th October, 1990
MARKAM, Dr. J. (ICI Pharmaceuticals) DNA Fingerprinting	7th March, 1991
PETTY, Dr. M.C. (Durham University) Molecular Electronics	14th February, 1991
PRINGLE†, Dr. P.G. (Bristol University) Metal Complexes with Functionalised Phosphines	5th December, 1990
PRITCHARD, Prof. J. (Queen Mary & Westfield College, London University) Copper Surfaces and Catalysts	21st November, 1990
SADLER, Dr. P.J. (Birkbeck College London) Design of Inorganic Drugs: Precious Metals, Hypertension + HIV	24th January, 1991
SARRE, Dr. P. (Nottingham University) Comet Chemistry	17th January, 1991
SCHROCK, Prof. R.R. (Massachusetts Institute of Technology) Metal-ligand Multiple Bonds and Metathesis Initiators	24th April, 1991
SCOTT, Dr. S.K. (Leeds University) Clocks, Oscillations and Chaos	8th November, 1990
SHAW†, Prof. B.L. (Leeds University) Syntheses with Coordinated, Unsaturated Phosphine Ligands	20th February, 1991
SINN†, Prof. E. (Hull University) Coupling of Little Electrons in Big Molecules. Implications for the Active Sites of (Metalloproteins and other) Macromolecules	30th January, 1991
SOULEN†, Prof. R. (South Western University, Texas) Preparation and Reactions of Bicycloalkenes	26th October, 1990
WHITAKER†, Dr. B.J. (Leeds University) Two-Dimensional Velocity Imaging of State-Selected Reaction Products	28th November, 1990

† Invited specifically for the postgraduate training programme.

b) Conferences and Symposia Attended

(* denotes paper presentation)

(# denotes poster presentation)

1)# "Macro Group UK Meeting - Aspects of Contemporary Polymer Chemistry"
University of Lancaster, 26th - 28th March 1991

2)* "North East Graduate Symposium"
University of Newcastle upon Tyne, 15th May 1991

3)# "IRC in Polymer Science and Technology Industrial Club Seminar"
University of Durham, 17-18th September 1991